i.a.

SEISMIC HAZARD ANALYSIS: IMPROVED MODELS, UNCERTAINTIES AND SENSITIVITIES

by

Rodrigo Araya

and

Armen Der Kiureghian

Report to the National Science Foundation

Report No. UCB/EERC-90/11
Earthquake Engineering Research Center
College of Engineering
University of California at Berkeley

March 1988

50272-101

REPORT DOCUMENTATION PAGE	1. REPORT NO. NSF/ENG-90005	2.	3. PB92-193010

4. Title and Subtitle
Seismic Hazard Analysis: Improved Models, Uncertainties and Sensitivities

5. Report Date
March 1988

6.

7. Author(s)
R. Araya and A. Der Kiureghian

8. Performing Organization Rept. No.
UCB/EERC-90/11

9. Performing Organization Name and Address
Earthquake Engineering Research Center
University of California, Berkeley
1301 So. 46th Street
Richmond, Calif. 94804

10. Project/Task/Work Unit No.

11. Contract(C) or Grant(G) No.
(C)
(G) ECE-8416518
CES-8618905

12. Sponsoring Organization Name and Address
National Science Foundation
1800 G. Street, N.W.
Washington, D.C. 20550

13. Type of Report & Period Covered

14.

15. Supplementary Notes

16. Abstract (Limit: 200 words)

Refined models are rarely used in seismic hazard analysis, since they require data which is usually not available and since with the conventional methods of analysis they pose formidable computational problems. The main objective of this study is to develop a new methodology for assessing earthquake hazards that allows the use of refined models of earthquake occurrences, sources, attenuation laws, and measures of intensity, the full incorporation of model uncertainties in the seismic hazard estimation, and the analysis of sensitivities of the seismic hazard with respect to variables and model parameters. The availability of this improved methodology enables the seismic hazard analyst to employ refined earthquake source models and associated attenuation laws, including the effects of source geometry, rupture directivity and propagation of seismic waves, in the assessment of seismic hazard. The proposed methodology facilitates the analysis of sensitivities of the computed seismic hazard to various sources of uncertainties and to various model parameters. Such analyses can be used to determine areas where further refinements and collection of data can be more effective in reducing the dispersion in the estimated seismic hazard. A simple method to estimate the dispersion of the calculated seismic hazard is also presented, that takes advantage of the solution procedure developed. Examples and applications are presented to illustrate the versatility of the procedure and to examine the accuracy of the solution technique.

17. Document Analysis a. Descriptors

b. Identifiers/Open-Ended Terms

c. COSATI Field/Group

18. Availability Statement	19. Security Class (This Report)	21. No. of Pages
Release Unlimited	unclassified	165
	20. Security Class (This Page) unclassified	22. Price

ABSTRACT

The field of seismic hazard analysis has achieved maturity both in its theoretical development and in application. The probabilistic approach provides a logical and consistent framework for incorporating geological, geophysical and historical data, combined with judgment derived from professional experiences in the assessment of seismic hazard. Lack of complete understanding of the earthquake phenomenon, its causes, characteristics and effects lead to significant uncertainties in the prediction of the seismic threat in many regions. Refined models are rarely used in seismic hazard analysis, since they require data which is usually not available and since with the conventional methods of analysis they pose formidable computational problems.

The main objective of this study is to develop a new methodology for assessing earthquake hazards that allows the use of refined models of earthquake occurrences, sources, attenuation laws, and measures of intensity, the full incorporation of model uncertainties in the seismic hazard estimation, and the analysis of sensitivities of the seismic hazard with respect to variables and model parameters. The availability of this improved methodology enables the seismic hazard analyst to employ refined earthquake source models and associated attenuation laws, including the effects of source geometry, rupture directivity and propagation of seismic waves, in the assessment of seismic hazard. The proposed methodology facilitates the analysis of sensitivities of the computed seismic hazard to various sources of uncertainties and to various model parameters. Such analyses can be used to determine areas where further refinements and collection of data can be more effective in reducing the dispersion in the estimated seismic hazard. A simple method to estimate the dispersion of the calculated seismic hazard is also presented, that takes advantage of the solution procedure developed. Examples and applications are presented to illustrate the versatility of the procedure and to examine the accuracy of the solution technique.

ACKNOWLEDGEMENTS

Financial support from a Fulbright Grant is gratefully acknowledged. Partial support was also provided by the University of Chile and by the U.S. National Science Foundation under Grants No. ECE-8416518 and CES-8618905.

Table of Contents

LIST OF TABLES

LIST OF FIGURES

Chapter 1

INTRODUCTION

1.1. Background

The last 20 years have seen a rapid increase in the demand for earthquake-resistant design of structures not only in highly seismic regions but also in areas with less active seismicity. This is because the engineering profession is being involved in a wide range of projects that require earthquake-resistant design and construction, even if there is a low probability of such construction ever experiencing a devastating earthquake. The social or economic losses produced by the failure of certain structures is so considerable as to make their design under seismic loads of relatively large return periods (of the order of thousands of years or more for nuclear power plants) a necessity. The offshore and, especially, the nuclear industry have become increasingly conscious of the earthquake threat and now require seismic risk assessment of their facilities, even when sited in low seismicity regions. The techniques and applications of seismic risk assessment for of nuclear power plants (NPPs) have evolved rapidly over the past ten years. Probabilistic risk assessment (PRA) studies of NPPs are performed routinely nowadays to assess the seismic safety of such facilities. These procedures integrate the results from seismic hazard analysis with results from dynamic analysis of structural and/or mechanical systems, component fragilities, and the plant systems response. The field of seismic hazard analysis, being the main component of PRA studies, has profited greatly from this development.

1.2. Objectives of the Present Study

The purpose of a seismic hazard evaluation is to arrive at earthquake ground motion parameters for use in evaluating sites and facilities for future seismic loading conditions. A probabilistic earthquake hazard assessment involves obtaining the level of a ground motion parameter that has a specified probability of being exceeded during a specified time interval. The ground motion parameter can be used to define a uniform hazard design spectra or a complete acceleration time-history.

The conventional computational procedures for the probabilistic estimation of seismic hazard are somewhat limited. They can only accommodate simple models of earthquake sources, occurrences and attenuation of seismic waves. They are incapable of accounting for the variability of a great number of parameters thus restricting the generality of the results. If analyses of sensitivities or confidence intervals for the hazard estimate are required, then hundreds or perhaps thousands of repeated computer runs are required to perform such analysis by standard statistical methods.

A new methodology that recognizes that the formulation of earthquake hazard assessment and structural reliability problems are analogous is introduced to overcome the above mentioned shortcomings. Making use of efficient techniques of integration available from the reliability field, a very general formulation of the seismic hazard problem is considered. This formulation enables the analyst to improve the modeling of seismic sources and attenuation of seismic waves and to incorporate uncertainties in the analysis without substantially increasing the cost and complexity of the solution. As a byproduct of the analysis, the sensitivities of the hazard estimate with respect to different variables involved in the analysis are obtained. These sensitivity measures are used to compute the standard error of the hazard estimate.

Thus, the objectives of the current research are:

1. To develop this new methodology for assessing seismic hazard which allows: (a) the use of refined models of earthquake occurrences, sources, and attenuation laws, (b) the full incorporation of model uncertainties in the hazard estimation, (c) the analysis of sensitivities of the hazard with respect to model parameters and (d) the estimation of the standard error of the computed hazard.
2. To examine refined source models and associated attenuation laws, including the effects of source geometry, rupture directivity, propagation of seismic waves and amplification of ground motion due to local geology, and to incorporate such models in the hazard estimation. Existing models are the basis for this study.
3. To illustrate how the analysis of sensitivities to models and parameters can be used in seismic hazard to determine areas where further refinements and data are needed.

1.3. Scope and Organization

Chapter 2 is devoted to a review of the current state-of-the-art in probabilistic seismic hazard analysis. Each of the different components involved in the procedure is examined, discussing their main features and the information required to characterize them, and providing bibliography for the interested reader. They include the modeling in time and space of earthquake occurrences, earthquake magnitude recurrence models and the description of attenuation of ground motion intensity. Methods of seismic hazard computation, analysis of uncertainties and estimation of confidence intervals for the assessment are also covered. Finally, for completeness, a survey of the currently available computer codes for seismic hazard computation is presented.

The new formulation for seismic hazard assessment that takes advantage of the efficient integration schemes from the structural reliability field is presented in Chapter 3. An introduction to structural reliability methods, including the first- and second-order reliability methods and various simulation methods, is included in this chapter. In addition, procedures to perform sensitivity analysis and to obtain the standard error of the estimate are discussed.

Taking advantage of the full probabilistic formulation presented in Chapter 3, improved earthquake source modelings are developed in Chapter 4. Two general source models are described and refined attenuation relationships associated with the two models are presented.

Numerical examples are presented in Chapter 5. The first two are devoted to testing the accuracy of the proposed approximate methods. Other examples are included to illustrate the versatility of the procedure and its potential for improved applications in seismic hazard analysis.

A summary of the study is presented in Chapter 6 with conclusions and recommendations for future work.

Chapter 2

PROBABILISTIC SEISMIC HAZARD ANALYSIS: A REVIEW

2.1. Introduction

The design of structures or facilities in regions of potential seismic activity should consider the likelihood of occurrence of various levels of earthquake intensity at the site of interest. The definition of the level of ground motion intensity for design purposes must include an assessment of the likelihood of exceedance of the defined level at the site during a specified exposure time. The time of occurrence, location, size and other characteristics of future earthquakes are unpredictable. Therefore, to properly account for the vast uncertainties involved, such an assessment should be based on a probabilistic approach. The procedure for such analysis is called probabilistic seismic hazard analysis (PSHA).

The general basis for PSHA was first established in 1968, in the seminal work of Cornell [54]. The works of other researchers soon followed [75 , 76 , 133 , 55]. Since then, important advances have been made in the analytical modeling of the earthquake phenomenon, in the technical methodologies used, and in the computer codes available. In the past ten years, the number of applications of probabilistic earthquake hazard assessment has grown substantially.

In this chapter, a detailed literature review of methods for PSHA is presented. Each of the elements involved in the procedure and some of the improvements suggested in the literature are discussed. At the end of the chapter, a brief description of computer programs available for PSHA is presented.

2.2. Formulation of PSHA

A probabilistic seismic hazard assessment involves obtaining, the probability of exceedance of a specified ground motion intensity level at a given site and during a specified time interval. As displayed in Fig. 2.1, the PSHA procedure involves the following elements:

1. Probabilistic modeling of earthquake occurrences in time and space, including geometric descriptions of the sources of future earthquakes and estimates of their activity rates.
2. Description of the recurrence relationship that provides information on the relative frequency of occurrence of earthquakes of different magnitudes, and determination of the probability distribution of earthquake parameters, such as seismic moment, rupture length, slip rate, etc.
3. A description of the attenuation of ground motion with distance from the earthquake source, as a function of the earthquake magnitude and other parameters that characterize the energy release at the source and the propagation of seismic waves to the site.
4. Evaluation of the probability of exceedance for various levels of the intensity of shaking.

Each of the above elements involves uncertainties that should be modeled and analyzed through probabilistic methods. The details of the PSHA procedure are well documented in Ref. 165. Other extensive reviews can be found in Refs. 140 , 178 and 92.

The probability of exceedance of a ground motion intensity level for a given earthquake occurrence is computed by use of the total probability theorem:

$$P(Y>y) = \int P(Y>y\,|\mathbf{x}) f_{\mathbf{X}}(\mathbf{x})\, d\mathbf{x} \tag{2.1}$$

where P indicates probability, Y is the earthquake intensity, y is the intensity level for which the exceedance probability is sought, $\mathbf{X}$ is a vector of random variables that influence the outcome of Y, and the integration is performed over all possible outcomes of $\mathbf{X}$. To determine the probability of exceedance of the specified intensity level during a given interval of time, the above probability should be combined with a model of earthquake occurrences in time. The resulting estimate can be plotted as an annual probability of exceedance versus the intensity level as, for instance, depicted in step 4 of Fig. 2.1. The common choice of variables for $\mathbf{X}$ is the magnitude, M, and distance, R, of the earthquake. Assuming that these two variables are independent, Eq. 2.1 is expressed as,

$$P(Y>y) = \int_{R}\int_{M} P(Y>y\,|m,r) f_M(m) f_R(r)\, dm\, dr \tag{2.2}$$

which is the familiar expression for computing the seismic hazard.

Results from PSHA are used for different purposes, e.g., probabilistic risk assessments, definition of design response spectra, and determination of seismic hazard maps. The details of these applications are beyond the scope of this study.

2.3. Modeling in Time of Earthquake Occurrences

The earthquake generation is a complex phenomenon that is not yet completely understood. Due to inherent randomnesses, the occurrence of these events cannot be predicted in a deterministic way. Therefore, earthquake occurrences in time should be modeled as stochastic processes. Several such models have been proposed over the years, based on assumptions regarding the generation mechanism or based on records of past events. For a review of these models, see Refs. 171 , 172 , 77 , 174 and 106.

Stochastic models used to represent the occurrence of earthquakes in time include the Poisson model, Poisson-related models, renewal models, and Markov and Semi-Markov models. The simplest stochastic model is the Poisson model. This model has been used extensively in seismic hazard studies [54 , 98 , 61 , 56 , 66 , 149] due to its simplicity both in formulation and in application. A brief review of the various stochastic models is presented below.

2.3.1. The Poisson Model

The Poisson model is based on the following assumptions:

(i) An event can occur at random and at any time.

(ii) The number of occurrences within a given time interval is independent of the occurrences in other nonoverlapping intervals.

(iii) The probability of occurrence of an event in a small interval Δt is proportional to Δt and is given by $\nu\Delta t$, where ν is the mean rate of occurrence of the events (assumed to be constant); and the probability of two or more occurrences in Δt is negligible (is of higher orders than Δt).

The first two assumptions imply that an occurrence at an instant in time is not affected by past occurrences nor does it affect any future occurrences. These assumptions imply the basic *lack of memory* or *complete independence* property of the Poisson process.

The probability distribution of the process is given by

$$P(N_t = n) = \frac{e^{-\nu t}(\nu t)^n}{n!} \qquad n = 0,1,2... \tag{2.3}$$

where N_t is the number of occurrences in time interval $[0, t)$ and ν is the mean occurrence rate; that is, the average number of occurrences per unit time. Let T_1 denote the time to the first occurrence of the event. We observe that $T_1 > t$ means that no event occurs in time t. Hence,

$$P(T_1 > t) = P(N_t = 0) = e^{-\nu t} \tag{2.4}$$

Since occurrences of events in nonoverlapping intervals are statistically independent, it can be shown that T_1 is also the recurrence time or the time between two consecutive occurrences of the event [60]. Thus, the distribution function of the time interval (waiting time), T, between two consecutive events is,

$$F_T = P(T \leq t) = 1 - e^{-\nu t} \tag{2.5}$$

which is the exponential distribution with parameter ν.

Statistical data shows that the Poisson model often is a reasonable assumption when aftershocks are removed from observed earthquake sequences, specially for large shocks [80 , 119]. To check the goodness of fit of the model, several statistical tests are available (See, for example, Refs. 79 , 144 and 77).

Since the Poisson model assumes independence between the occurrences of events, it is unable to describe earthquakes as events caused by the sudden release of gradually accumulated strains in the Earth's crust, nor is it able to describe foreshocks and aftershocks that precede or follow major earthquakes. This shortcoming makes the Poisson model inappropriate for problems in earthquake prediction. However, for applications in seismic hazard analysis, where the distribution of the ground motion intensity level from earthquakes occurring within the lifespan of a structure is of interest, the simple Poisson model is a reasonable approach for most situations. This conclusion was confirmed in a study by Cornell and Winterstein [58], where the potential influence of non-Poissonian models on *practical* hazard estimates (defined as future time windows of about 50 years and annual probabilities of exceedance of 10^{-3} or less) was analyzed. The study concluded that the Poisson model is not satisfactory for engineering purposes only when the seismic hazard is controlled

by a single tectonic feature satisfying two conditions: (a) the time since the last significant event has exceeded the mean inter-event time; and (b) the feature has a strong "characteristic-time" behavior. For other situations of engineering interest the Poisson model is a valid assumption.

The simple Poisson process is also deficient in describing the clustering of earthquake events in time, which is often triggered by a large main shock. This phenomenon has been addressed by statisticians and seismologists, since "clusters" (e.g., foreshocks and aftershocks) have little interest in engineering applications. Variations of the simple Poisson model, including clustering, branching and so-called trigger models have been proposed in the specialized literature [151 , 171 , 87 , 153 , 173].

2.3.2. The Non-Homogeneous Poisson Model

This model is based on the same assumptions as the Poisson process, except that the mean rate of occurrence is now a function of time. For a more detailed description of this process, see Ref. 60. The expected number of events until time t is,

$$a(t) = E[N_t] = \int_0^t \nu(t)\,dt \tag{2.6}$$

and the probability distribution of the process is given by

$$P(N_t = n) = \frac{e^{-a(t)}a(t)^n}{n!} \qquad n = 0,1,2... \tag{2.7}$$

The time differences between consecutive events are measured by the interarrival times $\tau_n = T_n - T_{n-1}$, where $\tau_1 = T_1$. The distribution of the interarrival times is given by [120]

$$F_{\tau_n}(s) = P(T_n - T_{n-1} \le s) = 1 - \int_0^\infty \frac{\nu(t)\,a(t)^{n-2}}{(n-2)!} e^{-a(t+s)}\,dt \tag{2.8}$$

One of the functions proposed in the literature for $\nu(t)$ is the so-called "cyclic Poisson" by Vere-Jones and Ozaki [173] where $\nu(t) = \nu_o \exp[\rho \sin(\omega_o t + \theta)]$. In this model, ν_o is a measure of the temporal average rate of occurrence of the process, ρ determines the amplitude of the cyclic fluctuations, and ω_o and θ describe the frequency and phase of the cyclic term, respectively. The advantage of the non-homogeneous over the homogeneous Poisson model is that it can incorporate certain features observed in earthquake sequences, such as cyclic behavior in the occurrence rate. The trade-off for

this improvement is a larger number of parameters that need to be estimated, thus requiring more seismic data. This is also true for most non-Poissonian models. Several other Poisson-related models have been proposed to model the occurrence of earthquakes in time.

2.3.3. Renewal Models

If the interarrival times of a sequence of events are assumed to be independent and identically distributed (i.i.d.), then the sequence forms a renewal process. The homogeneous Poisson process has independent, exponentially distributed interarrival times and, therefore, is a special case of the renewal process.

Several renewal models have been proposed to describe the occurrences of earthquakes in time. Esteva proposed the gamma distribution for the interarrival times [76]

$$f_T(t) = \frac{\nu}{\Gamma(k)}(\nu t)^{k-1}e^{-\nu t} \tag{2.9}$$

where $\Gamma(.)$ is the gamma function. The above equation reduces to the exponential distribution when $k = 1$. If $k < 1$, short intervals are more frequent and the coefficient of variation is greater than that in the Poisson model; if $k > 1$, the reverse is true.

Kameda and Ozaki [101] define a "double Poisson" renewal process model for earthquake occurrences based on the catalogue of historical earthquakes in Kyoto, Japan. The model assumes the expected number of earthquake occurrences is a step function in time. The mean rate of events assumes two constant values depending on whether the time to the next event is greater or smaller than a threshold value t_o. If the time to the next event is smaller than t_o, then the mean rate of occurrence is ν_1; for times $t \geq t_o$, i.e., when no earthquakes occur for a time t_o, the occurrence rate jumps from ν_1 to ν_2.

The Weibull distribution has been used frequently to model the distribution of interarrival times [83 , 147 , 58]. The main reason is that for this model the hazard rate increases with time since the last event, which is consistent with the theory that describes earthquake occurrences as the sudden release of accumulated energy due to stress build up since the last large event. The Weibull distribution hypothesis has been tested for a series of large historical earthquakes on the Southern

portion of the San Andreas fault [36].

Cornell and Winterstein [58] define the interarrival distribution as

$$F_T(t) = 1 - \exp\left[-\left(\frac{V_\tau! \, t}{E[\tau]}\right)^{1/V_\tau}\right] \tag{2.10}$$

where τ is the interarrival time between significant events, $V_\tau = (\mathrm{Var}[\tau])^{\frac{1}{2}}/E[\tau]$ is the coefficient of variation, which is commonly between 0 and 1 ($V_\tau = 1$ for the Poisson model), and $V_\tau! = \Gamma(V_\tau + 1)$ $\approx 1 - 0.5\,V_\tau(1 - V_\tau)$ in that range of values. Numerical comparisons of the seismic hazard obtained for this and other models, including the Poisson model, are presented in their study. In their analysis, the seismic hazard is defined as the probability of exceeding a magnitude level in the next T years on a given seismic feature.

2.3.4. Markov and Semi-Markov Models

The main feature of Markovian processes is the memory of successive events which is used to describe the dependence of future events on the occurrence of the last event. A description of the Markov process can be found in any textbook on stochastic processes, for example Ref. 60.

Both spatial and temporal memory can be represented with Markov models; however attempts to model spatial memory so far have been unsuccessful. Applications of Markov processes to model the temporal dependence of earthquake events can be found, for example, in Refs. 168 , 154 , 139 , 107 and 5. Refs. 142 , 49 and 50, employ semi-Markov models for the same purpose.

Special cases of the Markov model are the "time-predictable" [150] and "slip-predictable" [41] models. The first model assumes positive correlation between the inter-event time and the size of the preceding event, whereas the second model assumes positive correlation between the current inter-event time and the size of the next event. A combined time-slip predictable model that permits both correlations to be non-zero is presented in Ref. 58.

Although Markov models have not yet had an impact on the practice, the discipline is moving fast towards a stage where these models can be applied with advantage. The main roadblock at the current time appears to be the lack of sufficient data. Thus, there is a demand for simple models

which are consistent with the physics of earthquake generation and that can be applied in situations where only scarce data is available. It is claimed [58] that the Poisson model, despite its apparent contradiction with physical notions of strain accumulation and release, provides a reasonable approximation for most applications of seismic hazard analysis.

2.4. Modeling in Space of Earthquake Occurrences

A fundamental step in probabilistic earthquake hazard analysis is a delineation of seismic source zones and identification of seismically active faults. Seismic source zones define areas that share common seismological, tectonic, and geologic attributes and that can be described by a unique magnitude-frequency relation. In terms of PSHA, a seismic source represents a region of the Earth's crust in which future seismicity is assumed to follow specified probability distributions for occurrences in time, earthquake sizes, and locations in space.

Definition and classification of seismic sources is a subject that encompasses expertise from: seismic geology, seismology and statistics. An insightful discussion on the topic is presented in a recent paper by Thenhaus [158]. According to his classification, four types of seismic zones can be recognized:

1. **Seismotectonic Zones.** A seismotectonic zone is a seismic source zone in which a causal relationship has been established between a geologic structure (usually a fault) and earthquakes. For such zones, processes of earthquake mechanism and generation can be studied from both a structural geologic viewpoint and a seismological viewpoint.

2. **Paleoseismic Zones.** A paleoseismic zone is a zone having an important Quaternary-Holocene structural history that indicates the possibility of seismic activity in the future. These zones usually lack seismic history.

3. **Seismogenic Zones.** A seismogenic zone lacks the development of a clear history relating the contemporary seismic activity to a geologic structure. For such zones, critical gaps in the Quaternary geologic history preclude direct evidence of active faulting.

Seismogenic zones are, by far, the most common type of source zone employed in probabilistic

hazard analysis. Commonly, seismogenic zones are area sources, but the zone type applies also to inferred associations of seismicity with individual faults.

4. **Seismicity Zones.** Seismicity zones are seismic source zones that are defined with no consideration of their relation to geologic structures. They are defined solely based on the spatial distributions of the seismic history, and their use and reasonableness can only be judged relative to the intended use of the final hazard estimate.

Additional references on the seismic source definition and its related topics can be found, for example, in Refs. 112 , 156 , 48 , 51 , 179 , 170 and 169. A descriptive analytical definition of seismic source models for use in PSHA is presented by Der Kiureghian [66 , 65]. Four source models are defined: (1) well known fault; (2) area with preferred fault orientation; (3) area with unknown faults; and (4) uniform seismicity region. These models are depicted in Fig. 2.2.

Case studies on the effect of different source models on the estimates of seismic hazard for some regions of the United States and the world are presented in Refs. 141 , 132 , 13 and 111. In a recent paper, Bender [18] analytically examines the problem of defining source boundaries in seismic hazard analysis. When the boundaries are crisp, steep changes are observed in the computed levels of intensity for sites located near the boundaries. A more realistic situation is obtained with a fuzzy model of the seismic source boundaries. Such modeling is obtained by defining a non-uniform distribution of earthquake occurrences in space within the seismic region.

A crucial step in the spatial modeling of earthquakes is the definition of the characteristics of the earthquake source. In the early works, simplifying assumptions were made with respect to the geometry of the source but increasing levels of sophistication have since been introduced. A description of geometric models of the earthquake source developed over the years is presented below.

1. **Point Source** [54 , 55]. It is assumed that the energy release during an earthquake is concentrated at a point. This assumption is acceptable for small-magnitude earthquakes or in certain cases for large-magnitude earthquakes at far distances. However, this model neglects the possibility that, during a major earthquake, a site that is far from the epicenter could well be close to the energy release zone if the fault break runs close to or even through the site.

2. **Line-Rupture** [8 , 73 , 66]. In this model it is assumed that an earthquake originates at the focus and propagates as an intermittent series of line ruptures or slips in the ruptured zone of the Earth's crust, and that the maximum intensity of ground shaking at a site is determined by the segment of the slip that is closest to the site. The length of the rupture is assumed to be a function of the size of the earthquake.

3. **Area-Rupture** [135]. The representation of the earthquake source is modeled more realistically by a 2-dimensional rupture. Two shapes are postulated to represent the rupture area, i.e., a rectangular and an elliptical shape. The length and width of the rupture area are considered to be functions of the size of the earthquake.

Modeling earthquake ruptures as points is an acceptable approximation for small events and for medium events at far distances. In all other situations, explicit inclusion in the analysis of at least one of the dimensions of the rupture is necessary. Otherwise, the analysis may yield unconservative estimates of the seismic hazard, especially for high levels of the ground motion intensity. (See Refs. 66 and 16).

2.4.1. Relations for Earthquake Source Parameters

There are both empirical and theoretical reasons to expect a direct relationship between the rupture dimensions and the size of the earthquake. Tocher [161] was the first to relate the observed surface fault rupture L with magnitude M using ten California and Nevada earthquakes. He fitted a relationship of the form

$$M = a + b \log_{10} L \tag{2.11}$$

Subsequently, refinements on the regressions of M on $\log L$ [93 , 94 , 177 , 124 , 156 , 157 , 92] and of $\log L$ on M [4 , 29] have been developed, in which the set of observations of rupture lengths has been subdivided into fault types, geological regions, and so on. In addition, similar regression relations with the magnitude have been worked out for the fault slip ($\log D$) [47 , 157] and for products like DL [161 , 93 , 94 , 177 , 104 , 47 , 30] based on various physical models of the earthquake rupture phenomenon. Regressions of the magnitude with the rupture area have been investigated [167 , 176 , 155 , 30]. However, to the author's knowledge, no regression between the magnitude and the

rupture width has been performed.

A listing of the relationships between source parameters and the earthquake size that are available in the literature would be too long to include in this study. The reader is referred to the above cited references for values of the regression parameters and estimates of their dispersion. In particular, the paper by Bonilla et al. [30] presents the most up-to-date and thorough study on the subject.

When the rupture width in terms of magnitude is needed, the usual procedure is to obtain it indirectly from the existing relations of rupture area, A, and length, L, with the magnitude. For that purpose, an assumption regarding the shape of the rupture is required to estimate the width. The most simple hypothesis, and hence the most used, is a rectangular rupture where the width is given by $W(M) = A(M)/L(M)$. Similar formulas can be derived for other assumed shapes, such as the elliptical rupture area [135]. In Ref. 135, the regression of M on $\log A$ was incorrectly used to estimate the rupture area from magnitude.

To obtain the regression of M on $\log A$, Bonilla et al. [30] determined the rupture area of twenty two earthquakes by first estimating the rupture length and width and then obtaining A as their product. Since the rupture widths are reported in their paper, it is unnecessary to go through the rupture area relation to obtain the width. A simple regression analysis of their data yields, without incorporating measurement errors in the independent variable,

$$\log_{10} W = -0.20 + 0.18M \tag{2.12}$$

where W is the rupture width in kilometers, and M is the surface wave magnitude. The standard deviation of the estimate about the regression line is $s = 0.131$ and the correlation coefficient is $r^2 = 0.423$. The error in the regression equation is usually assumed to have the lognormal distribution. The list of data used for the regression is included in Table 2.1, and the data and the regression line are plotted in Fig. 2.3. The relationship satisfies Wyss's [176] proposal of selecting $5 \leq W \leq 20$ km for vertical strike slip and normal faults for the range $5 \leq M \leq 8.3$.

The correlation between the estimated rupture width and surface length is examined using the data and regressions reported in Ref. 30. The regression equation

$$\log_{10} L = -2.77 + 0.619M \tag{2.13}$$

relating the surface rupture length, L, to the surface wave magnitude, M, is used. To derive this expression, data from surface rupture lengths available for all types of faults worldwide was used, as it was to obtain Eq. 2.12. The standard deviation of this regression relation is $s = 0.286$ and the correlation coefficient is $r^2 = 0.438$.

The estimated correlation coefficient between $\log_{10}W$ and $\log_{10}L$ for the data in Ref. 30 is $\rho_{\log_{10}W \log_{10}L} = -0.6546$. The negative correlation implies that, for a given magnitude, when the rupture length is longer than the average, then it is more likely that the corresponding rupture width is narrower than the average. A negative correlation is expected, since the magnitude of the earthquake is expected to directly depend on the area of the rupture. If the area is assumed to be constant for a given magnitude, departures from the average length will be associated with departures in the width that keep the area constant. The estimated correlation value is rather significant and should be included in seismic hazard analysis whenever the source model is described as a rupture area.

It has been pointed out [122] that it is incorrect to use regressions of $\log L$ on magnitude M to predict a magnitude given a fault rupture length. It is also incorrect to interpret values of magnitude estimated from maximum rupture length at a fault as maximum rather than most likely values. Another deficiency in the applications of regression models is the lack of consideration of errors in both variables, dependent and independent, in the formulation [26 , 123]. Most studies conducted after 1979 incorporate these concepts (in particular, Refs. 155 and 30).

2.5. Earthquake Magnitude Recurrence Models

The seismic and tectonophysical behaviour of seismic regions is characterized by their frequency-magnitude relations. These relations are basic elements in estimating the earthquake recurrence times and hazard. Thus, there has been a continued interest in the seismology and engineering communities in the issue of determining the appropriate expression for the frequency-magnitude relation and in inferring the parameters incorporated in the postulated relations from observational samples, i.e., from seismic catalog data.

The first attempts to model the earthquake magnitude recurrence were made by Ishimoto and Iida [95] and by Gutenberg and Richter [82], who independently proposed a linear relation between the logarithm of the frequency and the magnitude. This model is currently known as the Gutenberg-Richter (GR) law. The equation that describes this model is expressed as

$$\log N(m) = a - b\,m \tag{2.14}$$

where $N(m)$ is the number of earthquakes with magnitude greater than or equal to m in a given region and specified time period, 10^a is the total number of earthquakes with magnitude greater than zero and b is the slope. This equation is usually written in the form

$$N(m) = \exp[\alpha - \beta m] \tag{2.15}$$

where $\alpha = 2.3a$ and $\beta = 2.3b$.

Assuming earthquakes with magnitudes smaller than m_0 have no engineering importance, the cumulative distribution of magnitudes is given by

$$\begin{aligned} F_M(m) &= P(M < m \mid M \geq m_0) \\ &= \frac{N(m_0) - N(m)}{N(m_0)} = 1 - e^{-\beta(m - m_0)} \qquad m \geq m_0 \end{aligned} \tag{2.16}$$

The corresponding probability density function is

$$f_M(m) = \frac{d}{dm} F_M(m) = \beta\, e^{-\beta(m - m_0)} \qquad m \geq m_0 \tag{2.17}$$

The parameter a provides a measure of the overall occurrence rate of earthquakes in the region considered and is the zero magnitude intercept of Eq. 2.14 on a semilog paper. The parameter b or β has received considerable attention from seismologists, geologists and earthquake engineers. This parameter is significant in that it defines the relative likelihood of earthquakes of various magnitudes occurring in a specific region. The b value has an inverse relation with the likelihood, so that the likelihood of larger magnitudes relative to small magnitudes diminishes as the b value increases. Methods to estimate b from a set of observed magnitudes and their adequacy are discussed in Refs. 175 and 15.

Several other laws, based on physical as well as observational grounds, have been suggested that differ from the GR model, especially at the high magnitude levels (see e.g., Refs. 166 , 143 , 118 ,

22 , 81 , 121). However, only a few of the available relations have been used in seismic hazard assessments. In addition to the GR law [54], the relations used include a truncated version of the GR law [57 , 66], a quadratic law [131], a bilinear law [149] and a nonlinear law [92]. A brief description of these magnitude recurrence laws is presented below.

1. The truncated GR law.

The existence of a maximum regional magnitude has been recognized for quite some time. Many researchers have used formulas for the frequency-magnitude relation that incorporate this concept (e.g., Ref. 59). The first application of a formula of this kind in PSHA is due to Cornell and Vanmarcke [57] in 1969 and is of common use nowadays. The formulation of this relation follows.

If an upper bound m_1 for the magnitude is assumed in the GR law, then

$$F_M(m) = P(M < m \mid m_0 \le M \le m_1) = \frac{1 - e^{-\beta(m-m_0)}}{1 - e^{-\beta(m_1-m_0)}} \qquad m_0 \le m \le m_1 \tag{2.18}$$

is the modified cumulative distribution function for M and the corresponding density function becomes

$$f_M(m) = \frac{\beta e^{-\beta(m-m_0)}}{1 - e^{-\beta(m_1-m_0)}} \qquad m_0 \le m \le m_1 \tag{2.19}$$

Using a point-source model, Cornell and Vanmarcke [57] concluded that the seismic hazard was seldom sensitive to the upper bound magnitude m_1. However, in a later paper, Der Kiureghian and Ang [66] disagreed with this conclusion. Using a more realistic model of the earthquake source, i.e., a line instead of a point, Der Kiureghian and Ang [66] showed that the upper bound magnitude m_1 is an important factor in the assessment of seismic hazard, especially for high intensity levels (see Figs. 6 and 7 of their paper).

2. The quadratic law.

Although proposed earlier by seismologists [152], a quadratic frequency-magnitude law was introduced in Cornell's analytical approach for PSHA in 1973 by Merz and Cornell [131]. The relationship they considered is of the form,

$$\log N(m) = \begin{cases} a & m < m_0 \\ a + b_1(m - m_0) + b_2(m - m_0)^2 & m_0 \le m \le m_1 \\ 0 & m > m_1 \end{cases} \tag{2.20}$$

The corresponding cumulative density function is,

$$F_M(m) = \begin{cases} 0 & m < m_0 \\ k^* \{1 - \exp[\beta_1(m - m_0) + \beta_2(m^2 - m_0^2)]\} & m_0 \le m \le m_1 \\ 1 & m > m_1 \end{cases} \quad (2.21)$$

where

$$k^* = \{1 - \exp[\beta_1(m_1 - m_0) + \beta_2(m_1^2 - m_0^2)]\}^{-1} \quad (2.22)$$

$$\beta_1 = 2.3 b_1 \quad (2.23)$$

$$\beta_2 = 2.3 b_2 \quad (2.24)$$

and the probability density function is,

$$f_M(m) = \begin{cases} 0 & m < m_0 \\ k^* \{-(\beta_1 + 2\beta_2 m) \exp[\beta_1(m - m_0) + \beta_2(m^2 - m_0^2)]\} & m_0 \le m \le m_1 \\ 0 & m > m_1 \end{cases} \quad (2.25)$$

In their paper, Merz and Cornell examine the influence of the quadratic magnitude-frequency law on the seismic hazard for a simple fault-site configuration. The parameters selected for Eq. 2.20, taken from Ref. 152, were fitted from data for North and Central America obtained during 1963 to 1968. Therefore, their conclusions are somewhat limited. They conclude that the use of a quadratic law instead of a linear law in PSHA is significant for high intensity levels, with the hazard curve falling off faster in the case of the quadratic law. This result is due to the fact that, in their example, the quadratic law predicts less events of high magnitudes than the linear law. To the writer's knowledge, no comparison has been reported between these two models when the line-rupture model is incorporated in the analysis.

3. The bilinear law.

Relationships of this kind have been used by the group of Stanford University researchers for the seismic hazard studies of several countries, after their study for Nicaragua [149]. They justify the use of a bilinear regression curve on the basis that it reduces the bias due to incomplete small magnitude data. In such cases, they claim, a single line overestimates the frequency of large magnitudes and, consequently, the hazards tend to be greatly overestimated, particularly at distances away from the seismic zone. Comparisons between hazard estimates based on the two models are not reported in their studies.

4. The characteristic earthquake model.

It has been observed recently that certain discrepancies exist between earthquake recurrence estimates based on historical seismicity and based on geologic data for specific seismic regions. Recurrence intervals for large-magnitude earthquakes inferred from geological studies are found to be much smaller than those predicted from historical seismicity data. Several recurrence models have been proposed to account for this pattern. Among them, the so-called "characteristic earthquake model" [148] is gaining increasing attention and acceptance.

Basically, this model uses Eq. 2.14 for the magnitude range m_0 to an intermediate magnitude, m_i, with the slope based on the historical seismicity. The intermediate magnitude is taken to be much smaller than the maximum magnitude, m_1, that the fault or seismic feature is capable of producing. The recurrence of m_1, or earthquakes with magnitudes slightly lower, is determined from the geologic data. The recurrence relation between the intermediate and maximum magnitude values is constructed as a straight line consistent with Eq. 2.14. The slope of this segment is usually much smaller than that for the magnitude range m_0 to m_i.

The influence of this earthquake recurrence model on the estimates of the seismic hazard was examined for two sites in Southern California [92]. Two recurrence models were used for the main seismic feature of the region (the southern portion of the San Andreas fault) to compare the results: (1) a GR law with the *b*-value obtained from geological data (e.g., the slip rate of the fault); and (2) the characteristic earthquake model as described above. The final conclusion reached in the study was that the average return period for a given intensity level significantly increased when the characteristic earthquake model was used.

A probability density function for magnitudes corresponding to a simplified version of the characteristic earthquake model was developed by Youngs and Coppersmith [180]. In this model, magnitudes are exponentially distributed up to the magnitude $m' = m_1 - 1/2$. Above this magnitude lies the characteristic earthquake which is uniformly distributed in the magnitude range of $(m_1 - 1/2)$ to m_1.

As it can be noted from the above discussions, the major issue in modeling the magnitude recurrence is to explain the behavior for large-magnitude earthquakes. (For a review of models see, for example, Ref. 143). The main problem encountered is the paucity of the observational data: the instrumental magnitude catalogs cover customarily a period of 40-80 years, much shorter than the return period of large earthquakes. It is, therefore, clear why it is often difficult to prove or disprove any one of the relations proposed in the literature, as they all appear consistent with the available seismicity catalogs.

Tied with the recurrence model is the determination of the maximum magnitude earthquake m_1 for a specified seismic region or feature. A good discussion on this subject can be found in Ref. 92. Six different approaches to estimate maximum earthquake magnitude are discussed, namely, magnitude determination based on: (1) rupture length; (2) rupture area; (3) total displacement; (4) seismic moment; (5) slip rate; and (6) historical seismicity.

2.6. Modeling of Ground Motion Attenuation

The severity of ground motion at points away from the earthquake source is called the intensity of ground motion. Normally, intensity increases with increasing size of the event and decreasing distance, although significant fluctuations may occur due to geologic or soil inhomogeneities. Furthermore, other parameters can be recognized as also affecting the intensity of ground motion, namely, the azimuth of the site with respect to the direction of the fault rupture, the velocity of propagation of the rupture, the type of faulting, the frequency of the propagating waves, the stress drop, etc.

Several measures of ground motion intensity have been used including the Modified Mercalli intensity scale; peak and various definitions of *effective* ground motion parameters, such as acceleration, velocity or displacement; duration of significant shaking; frequency content of the motion, by means of the ordinates of the Fourier amplitude spectrum; and response spectral values. At this point it is difficult to establish a ranking of importance of these proposed measures since the appropriateness of their use depends on the specific situation under study.

The functional description of the dependence of a ground motion intensity on a number of variables is called an **intensity attenuation law.** Usually, the law describes the average behavior of

the intensity of ground motion as a function of distance from the source of energy and of the size of the earthquake. Attenuation laws can be obtained empirically, by fitting a curve to a set of observations. By far, this has been the most popular approach when defining intensity attenuation laws.

A comprehensive review of attenuation relationships developed before the 1979 Imperial Valley, California, earthquake is given in Ref. 91. The 1979 Imperial Valley earthquake marked a major change in the strong-motion data base by providing many more near-source data points or observations than had been available previously. A more recent review can be found in Ref. 44.

Theoretical earthquake models have also been used to predict the intensity of ground motion in regions where strong-motion recordings are scarce or nonexistent. Basically, these models can be separated into three categories [44]. The first type uses kinematic and dynamic models of the fault-rupture mechanism to generate deterministic predictions of the ground motion. The second category of theoretical models uses stochastic simulation of ground motions based on simple seismological source models (sometimes in conjunction with random vibration theory) to produce random predictions of strong ground motion. The third type of model uses simple seismological source models (sometimes calibrated empirically) to deterministically predict strong ground motion. Extensive references on this topic are given in the review by Campbell [44].

When it comes to model selection, the general form chosen by most investigators is characterized by the expression

$$Y = Z_y \, f(M, R, P_i) \tag{2.26}$$

where Y is the strong motion parameter to be predicted (dependent variable); Z_y is a random variable representing the uncertainty in Y for a given earthquake; R is a measure of the *significant* distance from the earthquake to the site; M is the magnitude, specified in any scale, that describes the size of the earthquake; and P_i are a set of parameters characterizing the earthquake source, the wave propagation path, and the local site conditions.

One of the most common forms for Eq. 2.26 is

$$Y = Z_y \frac{c_1 e^{c_2 M}}{(R + c_4)^{c_3}} \tag{2.27}$$

where $c_1 - c_4$ are parameters obtained through regression.

As mentioned before, the random variable Z_y accounts for the scatter observed in the data and represents the uncertainty in the values predicted. It is usually assumed to be lognormally distributed, though this is not a requirement in most regression procedures. Care should be exercised with such an assumption since it predicts an unbounded value for Y.

The effect of the attenuation uncertainty on PSHA has received attention since the early works. But it is only recently that the problem of imposing an upper bound to the distribution of Z_y has been addressed. The notion of the existence of an upper limit to the ground motion intensity is based on physical grounds. Zemell [181] presents a methodology to incorporate in the Cornell approach a particular bounded distribution for the parameter Z_y and an upper bound y_{max} to the ground motion intensity. The significance of both restrictions is more evident at low hazard levels, as expected, since the changes affect the tails of the distribution of Z_y. In a more extensive study, Bender [17] concludes that if the variability of ground motion intensity is included in the analysis the hazard estimate at low intensities decreases, while that at high intensities increases.

Two types of attenuation uncertainty are differentiated in Ref. 63, one for which the values of Z_y at various occurrences are statistically independent and the other for which they are perfectly correlated. Analytical procedures to incorporate these uncertainties in the analysis of seismic hazard are discussed in that reference. Sources of attenuation uncertainty of the first kind are the inherent randomness in the mechanism of earthquake generation and the characteristics of wave propagation paths. Variabilities in the subsoil and geologic conditions at the recording sites and the overall variability in the geologic characteristics of various seismic regions produce attenuation uncertainties of the second type. However, the usual scarcity of data in general would prevent a clear separation of the uncertainties due to the various items.

The effect of different distributions for the uncertainty parameter Z_y on the estimation of seismic hazard was studied in Ref. 113. Their results are summarized in Fig. 2.4 which illustrates, for a specific situation, the effect on the seismic hazard of including a bounded or unbounded uncertainty distribution in the attenuation law. They concluded that for very low probabilities of

exceedance, distributions that consider limiting values of ground motion intensity provide a more realistic assessment of the hazard. Some of the PDF's for the variable Z_y proposed in the literature are included in Table 2.2.

2.7. Evaluation of Seismic Hazard

A general procedure for the calculation of seismic hazard is presented below. We assume that the seismic region surrounding the site of interest consist of n potential sources. Let ν_i denote the mean rate of occurrence of earthquakes in source i with magnitudes equal to or greater than m_0, where m_0 represents the lower bound magnitude for earthquakes of engineering interest. The mean total occurrence rate in the region is

$$\nu = \sum_{i=1}^{n} \nu_i \tag{2.28}$$

For an earthquake occurring randomly in the region, the intensity Y at the site is obtained in a functional form as

$$Y = g(\mathbf{X}) \tag{2.29}$$

where $\mathbf{X}$ is the vector of random variables that define the attenuation of seismic intensity. Then for a given earthquake, the probability of exceeding the intensity level y at the site is given by

$$P(Y > y) = \sum_{i=1}^{n} \frac{\nu_i}{\nu} \int_{g(\mathbf{X}) \geq y} f_{\mathbf{X}}(\mathbf{x})\, d\mathbf{x} \tag{2.30}$$

where $f_{\mathbf{X}}(\mathbf{x})$ is the joint probability density function (PDF) of $\mathbf{X}$ and the integration is performed over all values of $\mathbf{X} = \mathbf{x}$ for which the computed intensity from Eq. 2.29 exceeds y. In order to compute the seismic hazard for a specified interval of time, T, the above probability has to be used in conjunction with a stochastic model of the earthquake occurrences in time. For example, if the Poisson model is used

$$P(Y_T > y) = 1 - e^{-\nu TP(Y>y)} \approx -\nu TP\,(Y > y) \tag{2.31}$$

where the approximation is valid only for small values of $\nu TP\,(Y > y)$. It can be shown [35] that this approximation provides an upper bound on the unconditional seismic hazard, i.e., that which is independent of the information on past events. For other models, bounds for the seismic hazard are

given in Ref. 35.

When other models of earthquake occurrences in time have been used, the seismic hazard is usually expressed as the probability of exceeding a certain magnitude, m_c, in a specified period of time. The mathematical tool available to handle more sophisticated models of earthquake occurrences in time associated with a measure of intensity is that of marked point processes [35].

For the case of Y depending only on magnitude and distance (ignoring the variability Z_y), Eq. 2.30 can be written as

$$P(Y>y) = \sum_{i=1}^{n} \frac{\nu_i}{\nu} \int_M \int_R P(Y>y \mid m,r) f_{R|M}(r,m)\, dr\, f_M(m)\, dm \tag{2.32}$$

Also the return period associated with the intensity level y is

$$\bar{T}_y = \frac{1}{\nu P(Y>y)} \tag{2.33}$$

Different approaches to computing Eq. 2.32 have been proposed in the past. Closed form solutions can be obtained when simplifying assumptions are made on the formulation. In the Cornell approach, for instance, due to the point modeling of earthquake source, the distance R is independent of magnitude M and hence, Eq. 2.32 is reduced to its simplified version given by Eq. 2.2. This equation is solved to obtain the cumulative density function (CDF) of Y directly and hence the computation of the probability of exceedance is analytical.

If some of the restrictive assumptions are released it becomes more difficult and some times impossible to obtain a closed form solution for the probability of exceedance. In most of these cases, Eq. 2.30 (or its better known version, Eq. 2.32) is solved numerically. The addition of each new random variable to **X** is equivalent to adding a new fold to the integral in Eq. 2.32. This restricts the number of random variables that can be considered in the analysis.

To compute the above mentioned multi-fold integral, current methods of seismic hazard analysis employ simplifying assumptions and impose restrictions on the modeling of the source mechanism and the attenuation law. The explicit inclusion of model uncertainties in the analysis has also been limited. The analysis of sensitivities, when done, is usually performed in a crude and costly fashion; i.e., by repeated analysis, where parameters are perturbed one at a time. It is clear,

therefore, that an alternative approach is necessary to deal with refined models in seismic hazard analysis.

A new method based on first- and second-order structural reliability techniques has been recently proposed [67 , 134]. The procedure suggested can accommodate refined modeling of the earthquake process. A more detailed description of this methodology is presented in Chapter 3.

2.8. Analysis of Uncertainties and Estimation of Bounds

In the process of estimating the seismic hazard the inclusion of uncertainties is sometimes overlooked. At this point, it is useful to differentiate the various types of uncertainties that are relevant:

(i) *Inherent variability* is the natural or irreducible variation, from the nature of physical processes. It cannot be reduced with the collection of additional data since the stochastic nature of the phenomenon will remain unchanged.

(ii) *Statistical uncertainty* is that component of uncertainty due to a limited sample size that precludes the exact evaluation of model parameters. This source of uncertainty can be reduced or, in concept, completely eliminated with the collection of additional data since model parameters can be estimated with increased accuracy.

(iii) *Model uncertainty* is attributed to the limitations of the analyst and models to represent the *real* world. In principle this source of variability can be reduced or eliminated with the improvement in our understanding of physical phenomena and the development of more refined models.

Although the field of earthquake prediction has undergone considerable development, the occurrence of earthquakes remains intrinsically unpredictable. This is primarily due to the inherent variability in the mechanism of earthquake generation. Uncertainties in the occurrence of earthquakes, therefore, belong to the first type of uncertainty described above.

Errors in estimating the parameters a and b of the relationship between rupture length and earthquake magnitude given by Eq. 2.11, as estimated by Bonilla et al. [30] in Eq. 2.13, that arise from the smallness of the sample size, correspond to the second type described above. Another

example of this type of uncertainty is the error in estimating the parameters of the probability distribution of earthquake magnitudes due to a limited earthquake catalog. Several other examples of uncertainties of this kind can be found in seismic hazard analysis.

As mentioned before, the third class of uncertainty arises from the use of idealized mathematical models to describe complex phenomena. This model uncertainty can be due to lack of understanding of the phenomenon itself and/or due to the use of simplified models. The definition of seismic sources influencing the hazard at a given site and the selection of ground motion attenuation models incorporate uncertainties in the analysis associated with this third class.

In recent years, in PRA studies of NPPs, there has been a tendency to separate the contribution of modeling uncertainties to seismic hazard from the contribution of variables perceived to represent inherent variabilities. The separation is often difficult and arbitrary since it generally involves judgement, and the benefits in the analysis of such separation are not always clear. One possible advantage is that with the distinction between types of uncertainty, the analyst knows where and to what degree the seismic hazard estimate can be improved, either through collection of additional statistical data or through the use of refined models to reduce errors of simplification.

In the literature, several approaches have been presented to deal with all three types of uncertainties. Inherent variability or "randomness", as it is usually called, can be modeled by considering the uncertain parameter as a random variable with its corresponding probability distribution. Examples of this kind are M, R, and that part of Z_y that is due to inherent randomness in earthquake generation mechanism, propagation path, etc.

To incorporate the other two types of uncertainties in the analysis, several procedures have been proposed: combination of multiple experts' opinions [14], Monte Carlo simulation [21], logic tree methods [114 , 52] and other approximate procedures (Ref. 130 , for example). Studies at the Lawrence Livermore National Laboratory (LLNL) [21] were the first to address the multiple expert problem. A more recent study conducted for the Electric Power Research Institute (EPRI)[74] has also addressed this problem.

In one of the methodologies proposed (Refs. 114 and 52) the treatment of uncertainty is based

on the use of logic tree methods. Basically, the analyst is required to assign discrete probabilities to all possible values of uncertain parameters and models. Several cases are run considering all possible combinations, and the results are combined to obtain the mean and variance of the hazard estimate. Bounds for the estimate are obtained from these values by assuming a distribution (normality is often assumed) for the results. This approach limits the description of uncertainty in the inputs (models and parameters) since the analyst is restricted to specifying a small number, usually 2 or 3, of alternative values for each parameter. Otherwise, this procedure can be extremely costly, especially when a large number of parameters and models are to be considered in the analysis.

The LLNL methodology presents a similar drawback. Their approach is to model uncertainties by associating a probability (uncertainty) distribution to each of the inputs. A number of runs are performed where, the values of the inputs are obtained through Monte Carlo simulation. The computational effort required to compute all combinations of cases can be enormous. As an example, for a study involving ten sites, 2,750 such cases where generated for each site, bringing the total number of runs to 27,500.

Thus, it is desirable to obtain an estimate of the dispersion in the estimated hazard due to estimation and model uncertainty with only one or a few runs, without significantly increasing the computational effort. An approach that satisfies this requirement is presented in Section 3.4.

2.9. Available Computer Programs

Many computer programs are available to perform the computation of the seismic hazard. The most widely known are due to McGuire [125 , 126], but others are currently available in the literature [6 , 19 , 46].

The program EQRISK [6], developed at the University of Southern California, is aimed at computing uniform hazard spectra (UHS) of strong ground motion. The formulation of the seismic hazard procedure follows that of Cornell [54], incorporating some modifications as described by Anderson and Trifunac [7].

SEISRISK II [19] is a revised and improved version of the original undocumented program SEISRISK I [2] developed at the U. S. Geological Survey to create the 1976 national earthquake

hazard maps [1]. The program has been used recently to produce the seismic hazard maps of the contiguous United States [3] and of California, Alaska, and the outer continental shelf [159 , 160].

The program STASHA [46] was developed at Stanford University during seismic hazard studies for California [108] and several other countries [149 , 137 , 110 , 138 , 109].

Some of the characteristics of these programs are outlined below.

1. **McGuire's 1976 Program.** Calculations in this program are represented by the basic form of Eq. 2.2. The integration over distance r is computed numerically and the remaining integral is computed analytically. For certain situations, the integration over magnitude m is also performed numerically.

Seismic source areas are specified as a set of arbitrarily shaped quadrilaterals. Larger sources can be divided into subsources which are strings of quadrilaterals. Faults are modeled as narrow source areas.

The truncated exponential distribution in Eq. 2.19 is used to model the recurrence of earthquakes. The program can use any form of attenuation law and associated residual distribution. A tabulated attenuation law can also be used. The program includes a feature useful to obtain seismic hazard maps, i.e., the capability of performing the computation for a grid (or grids) of sites.

Some of the shortcomings of the program are discussed elsewhere [19].

2. **FRISK.** The name stands for Fault **RISK.** The main difference between this program and the preceding one is that it incorporates the length of the rupture in the analysis. Earthquake sources are modeled as faults composed of series of line segments.

The length of the rupture is taken as a function of earthquake magnitude (see discussion in Section 2.4) and the distance r in Eq. 2.2 is defined as the closest distance between the site and the rupture zone.

Other capabilities of the program are the inclusion of uncertainty in the rupture-length relationship and in the upper bound magnitude m_1. In addition, the program is capable of repeated calculations, so that PSHA for several ground motion intensity measures and for several sites can be performed with only one execution of the program.

Distributions for the random variables involved in the analysis are provided in the program. However, other distributions can be substituted if desired.

3. **EQRISK.** This program is intended for computing UHS of strong ground motion. The UHS are obtained by computing the seismic hazard curves independently in several frequency bands. From these curves, a complete spectrum is defined such that it has a uniform probability of being exceeded in the specified time interval. The program includes a library of attenuation relations for Fourier amplitude, absolute acceleration, pseudo-velocity and relative velocity spectra.

Earthquakes are modeled as point or line ruptures. Geometrical models of seismic sources used in the code are points, lines (in general, not straight), areas, and dipping planes. Line ruptures are only allowed in linear sources.

The output of the program is spectral amplitudes at eleven selected periods for the UHS desired.

4. **SEISRISK II.** The main objective of this computer code is for use in seismic hazard mapping. It was designed for efficient computation for a large number of sites and seismic sources.

In the program, earthquakes are modeled as points within source zones and as finite-length ruptures along faults. Source zones are modeled as seismically homogeneous areas enclosed by one or more arbitrary quadrilaterals, connected or disjoint. Fault zones consists of one or more seismically homogeneous faults, each of which is composed of several connected straight line segments. Variability in the rupture-length and in the intensity attenuation relations can be included.

The authors claim that the program is three times faster that the earlier version, SEISRISK I, for a certain grid spacing of sites, and of the order of 10-100 times faster than McGuire's programs previously discussed.

SEISRISK III [20], a revised version of this program has recently become available. The principal difference between this new version and the previous is that, although it retains the concept of seismic source zones, it allows earthquakes within a zone to be normally rather than uniformly distributed. A precise definition of seismic source boundaries is rarely possible and the above assumption incorporates the uncertainty present in the modeling of these boundaries. The result is that

calculated earthquake intensity levels vary more smoothly at sites near a seismic source boundary. Other differences are related to the computation procedures aimed at increasing the efficiency.

5. **STASHA.** The program consists of three basic stages: (i) data treatment, (ii) seismic source modeling and (iii) seismic hazard computation. The first step of the analysis consists of storing the information on past seismic events. Missing data is completed based on judgement or using random number simulation.

In the second stage, modeling of seismic sources is facilitated by plotting an epicentral map of the region. The parameters of the earthquake recurrence relationship can be obtained for two different models, truncated and bilinear GR.

The computation of the seismic hazard is performed in the third stage. The program includes two models, "classical" and "probabilistic". Only the second, more general one, will be described here.

Source geometry in this model includes broken lines, areas and dipping planes where earthquakes are modeled as line ruptures. Attenuation uncertainty is included in the analysis using a log-normal distribution. The Poisson model is used to represent earthquake occurrences in time. A Bayesian formulation of the Poisson model is also included.

Output options include seismic hazard estimates or probabilistic response spectra for a site or for a grid of sites and seismic hazard maps (the program does not do the contouring).

Many other unpublished programs are currently in use, both in research and engineering practice. The direct integration of Eq. 2.30 for some of the examples presented in Chapter 5, was performed with the program **SRAP** developed by Der Kiureghian [64]. This program follows the procedure developed by Der Kiureghian and Ang [66] whereby earthquake ruptures are modeled as lines. Its formulation is based on the following idealizations and assumptions: (1) Earthquake occurrences in time constitute a simple Poisson process; (2) Earthquake occurrences in space are events uniformly distributed in source regions modeled in accordance to any of the four seismic source idealizations depicted in Fig. 2.2; (3) The earthquake magnitude recurrence follows a truncated GR law and thus, the magnitude density function is given by Eq. 2.19. Two types of

attenuation laws are incorporated in the program. The first is given in a tabular form, relating the earthquake intensity, Y, with the magnitude and shortest distance to the earthquake rupture, M and R. The second is the usual form given by Eq. 2.27. Uncertainty in the attenuation law is explicitly considered by the random variable Z_y (Eq. 2.27), which is assumed to have a truncated lognormal distribution. The integration over this variable is truncated at a number (specified by the user) of standard deviations above and below the mean of $\ln Z_y$.

The output of the program consists of return periods and exceedance probabilities associated with selected levels of intensity. Seismic hazard values corresponding to selected intervals of time (up to five) may be obtained. The contribution from any or each source to the total seismic hazard can be printed.

This program shares the same limitations of the computer codes described above. One of them is that it incorporates only a few random variables in the analysis. For SRAP, the three random variables considered in the analysis are: magnitude, M, location on the seismic source (that determines the shortest distance from the earthquake rupture to the site), X, and attenuation uncertainty, Z_y. Another of these shared limitations is that the program is restricted to attenuation equations of the form discussed above. Cases for which some of the parameters c_1 to c_4 are functions of the magnitude [43] or distance [72 , 71] are not accounted for in the solution procedure. This limitation can be circumvented by providing the attenuation law in a tabular form. No uncertainty is included in the relationship between rupture length and magnitude (Eq. 2.11) nor on any of the parameters involved in the modeling, like maximum magnitude, m_1, or parameter β of the magnitude distribution function. The computer programs described above also fail to account for these uncertainties, except in a limited way, like the program SEISRISK [19], that accounts for the uncertainty in the rupture length-magnitude relation and the program FRISK [126] that, in addition to the uncertainty in that relation, incorporates the uncertainty in the upper bound magnitude m_1.

Table 2.1. Earthquake Magnitude and Rupture Width Data [1]

Event No.	Yr.Mo.D.	Country	Fault Type [2]	Magnitude [3]	Width Downdip [4]
5	1906.04.18	U.S.A.	E	8.32	13
7	1927.07.07	Japan	E	7.65	16
14	1930.11.25	Japan	E	7.28	12
21	1940.05.19	U.S.A.	E	7.17	8
23	1943.09.10	Japan	E	7.42	13
26	1945.01.12	Japan	B	6.84	14
29	1951.11.24	China	D	7.44	17
30	1952.07.21	U.S.A.	B	7.66	15
32	1954.07.06	U.S.A.	A	6.34	14
33	1954.08.24	U.S.A.	A	6.95	14
34	1954.12.16	U.S.A.	C	7.24	14
36	1956.02.09	Mexico	D	6.94	15
38	1959.08.18	U.S.A.	A	7.57	15
41	1967.07.22	Turkey	E	7.41	15
42	1968.04.09	U.S.A.	E	6.83	11
44	1968.10.14	Australia	B	6.89	10
48	1971.02.09	U.S.A.	D	6.53	18
50	1975.05.31	U.S.A.	E	5.30	3
51	1976.02.04	Guatemala	E	7.46	13
54	1978.09.16	Iran	B	7.48	17
55	1979.10.15	U.S.A.	E	6.66	8
58	1980.10.10	Algeria	B	7.25	16

(1) Taken from Bonilla, Mark and Lienkaemper [30]

(2) Five principal types of faults are defined: A, normal slip; B, reverse slip; C, normal oblique slip; D, reverse oblique slip; and E, strike slip.

(3) Surface wave magnitude, M_s.

(4) Measured in kilometers.

Table 2.2. Uncertainty Distributions for Earthquake Intensity Attenuation Relations

Name	PDF, $f_{Z_y}(z_y)$	Parameters	Reference	Notes
Lognormal	$\frac{1}{\sqrt{2\pi}\zeta z_y} e^{-\frac{1}{2}\left(\frac{\ln z_y}{\zeta}\right)^2}$; $0 < z_y$	ζ	Esteva [75]	1
Truncated	$\frac{k^*}{\sqrt{2\pi}\zeta z_y} e^{-\frac{1}{2}\left(\frac{\ln z_y}{\zeta}\right)^2}$; $0 < z_y \le z_u$	ζ, z_u	Kulkarni [113]	2
Censored	$\frac{1}{\sqrt{2\pi}\zeta z_y} e^{-\frac{1}{2}\left(\frac{\ln z_y}{\zeta}\right)^2} + k^* \delta(z_y - z_m)$; $0 < z_y \le z_m$	ζ, z_m	Kulkarni [113]	2,3
Constrained	$\frac{(\ln z_y - a)^{q-1}(b - \ln z_y)^{r-1}}{z_y B(q,r)(b-a)^{q+r-1}}$; $0 < e^a \le z_y \le e^b$	a, b, q, r	Kulkarni [113]	4
Bounded	$\frac{15}{16\sqrt{7}\zeta z_y}\left[1 - \left(\frac{\ln z_y}{\sqrt{7}\zeta}\right)^2\right]^2$; $e^{-\sqrt{7}\zeta} \le z_y \le e^{\sqrt{7}\zeta}$	ζ	Zemell [181]	1

Notes

1. $\zeta^2 = \mathrm{Var}[\ln z_y]$
2. $k^* = \left[1 - \Phi\left(\frac{\ln z_y}{\zeta}\right)\right]^{-1}$
3. $\Phi(x) = \frac{1}{\sqrt{2\pi}} \int_{-\infty}^{x} e^{-\frac{u^2}{2}} du$ is the standard normal cumulative probability.
4. $\delta(.)$ is the Dirac delta function
5. $B(q,r) = \frac{\Gamma(q)\Gamma(r)}{\Gamma(q+r)}$ is the beta function.

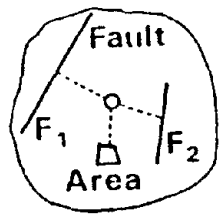

STEP 1: Earthquake Sources

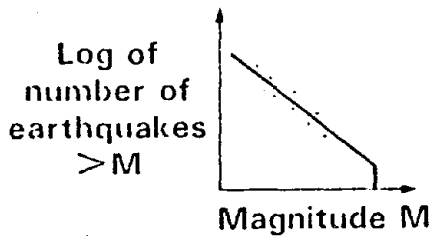

STEP 2: Magnitude Recurrence

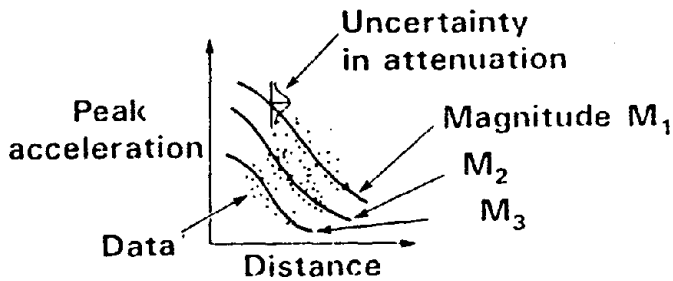

STEP 3: Intensity Attenuation Relationship

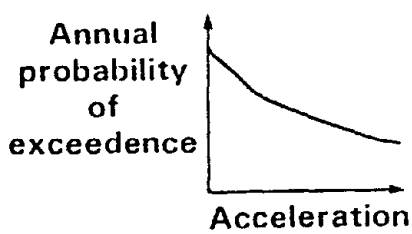

STEP 4: Evaluation of the Hazard Curve

Fig. 2.1. Probabilistic Seismic Hazard Analysis Procedure

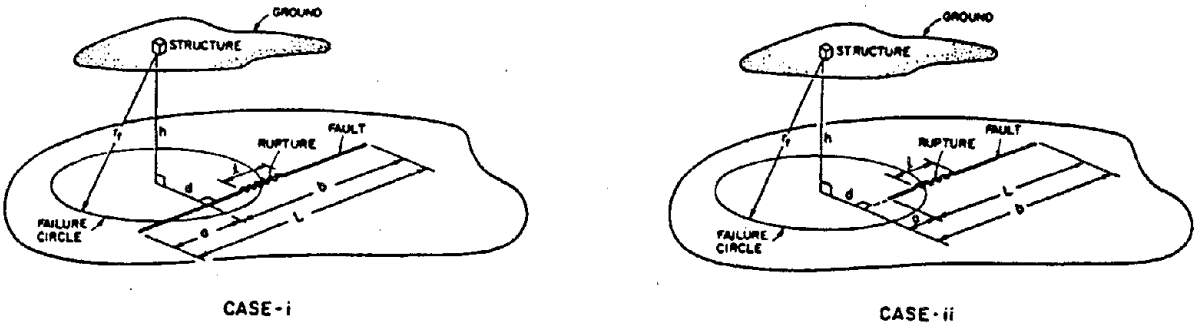

Model for Well Known Fault

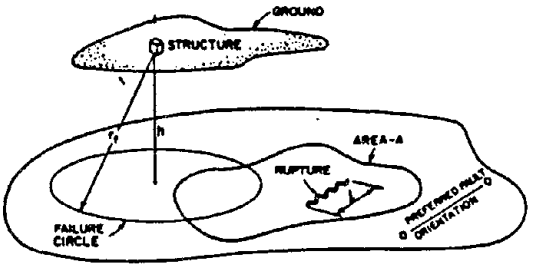

Model for Area with Preferred Fault Orientation

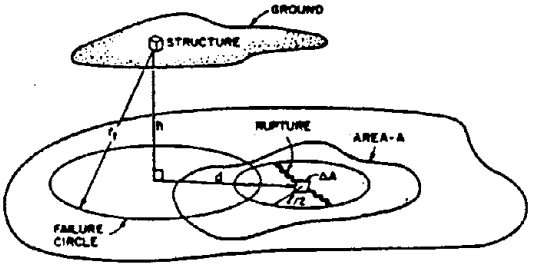

Model for Area with Unknown Faults

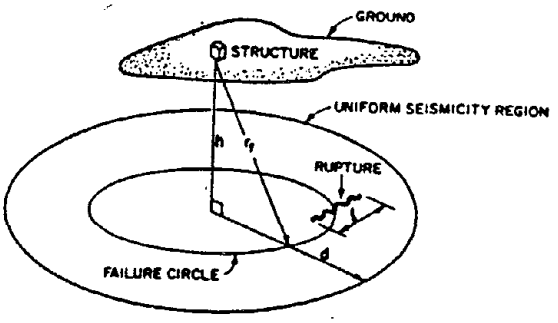

Model for Uniform Seismicity

Fig. 2.2. Idealized Earthquake Source Models (Ref. 65)

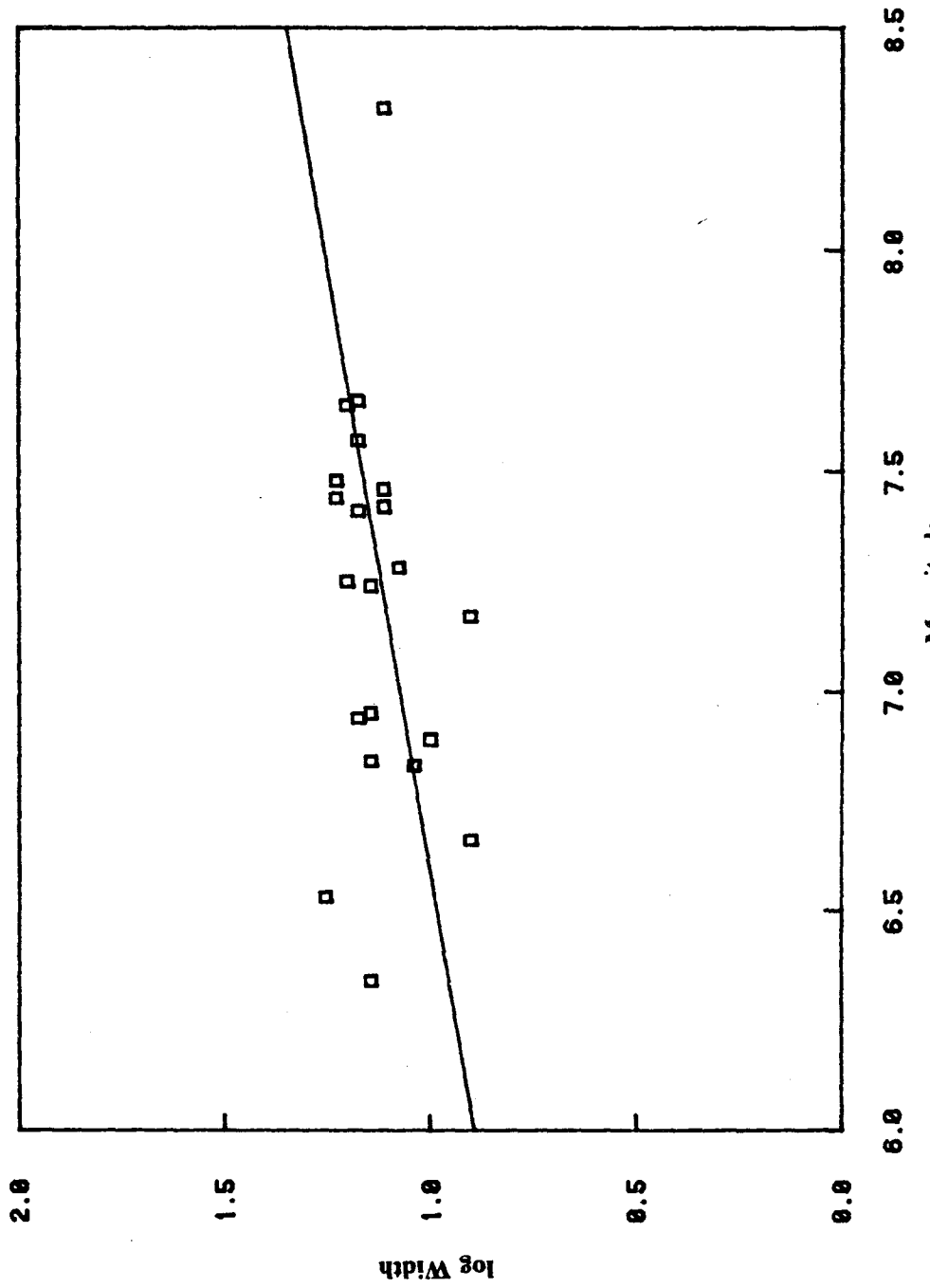

Fig. 2.3. Surface-wave Magnitude versus Rupture Width, with Regression of Log Width on Magnitude

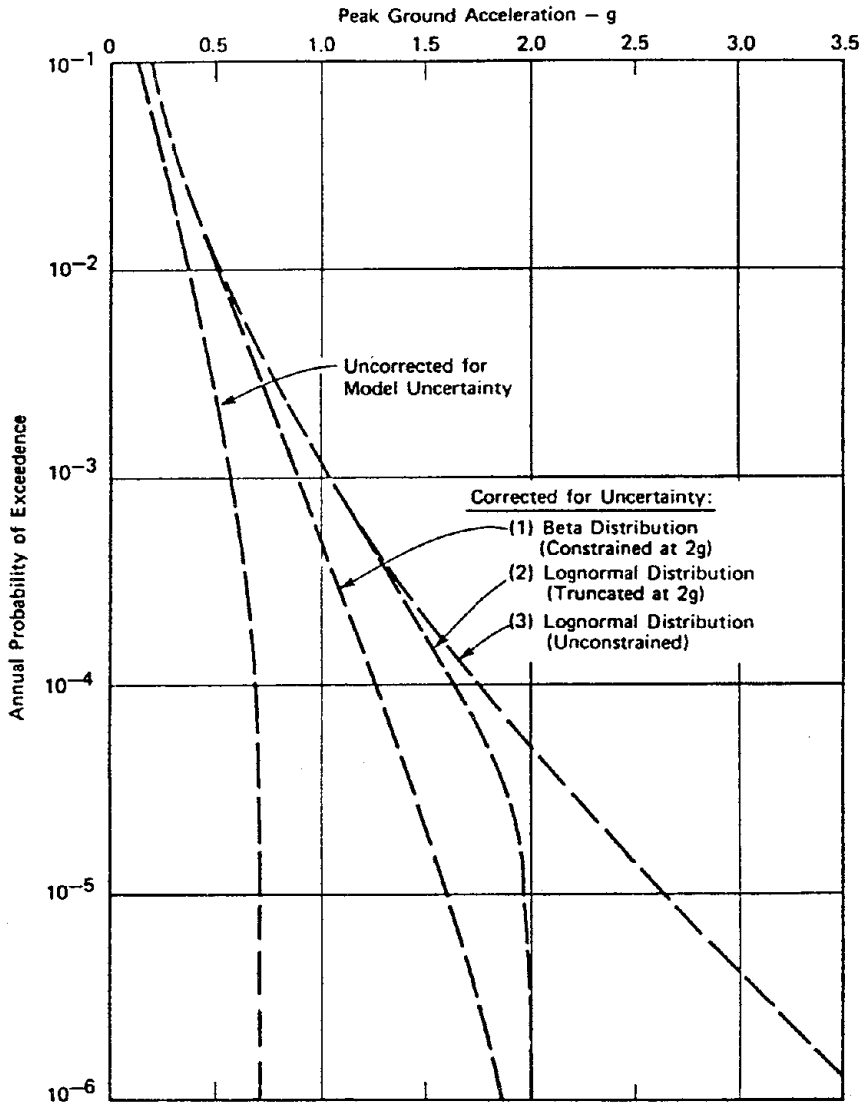

Fig. 2.4. Effect of PGA Uncertainty Distribution on Seismic Hazard Example (Ref. 113)

Chapter 3

A NEW FORMULATION FOR ASSESSMENT OF SEISMIC HAZARD

3.1. Introduction

A full probabilistic method for assessing seismic hazard is presented in this chapter. In addition to inherent variabilities, the method explicitly takes into account uncertainties in the analysis which arise due to estimation errors and model imperfections, and provides measures of uncertainty on the computed hazard. These measures are given in terms of standard error of estimation on the computed seismic hazard. Also provided are sensitivity factors which show the effect and importance of each variable and parameter on the computed hazard. The information they provide is of vital interest in the analysis to delineate areas where further refinements and data collections would help reduce the dispersion in the computed hazard.

The method is based on numerical and efficient procedures available from the field of structural reliability. In particular, first- and second-order reliability methods (FORM and SORM) are examined and compared with results obtained from "exact" numerical integration and from several simulation procedures (basic Monte-Carlo, antithetic variates and directional simulation). Examples to illustrate these procedures are presented in Chapter 5.

3.2. Definitions of Seismic Hazard

Conventional PSHA is based on the attenuation of one ground motion parameter, usually the peak ground acceleration (PGA), that is believed to adequately describe the intensity of ground motion at the site of interest. It is current knowledge, however, that the destructive potential of earthquakes is better represented by two or more parameters of the ground motion, or even by a combination of them. In particular, in recent years the idea of damageability index of ground motion for a specific class of structures has become popular (e.g., Ref. 103). Such an index is generally expressed as a function of several ground motion parameters, such as PGA or root-mean-square acceleration (RMSA), duration of strong motion, and parameters describing the frequency

content. An example of such is the *PD* factor defined in Ref. 11 as proportional to $A^2 S / \omega_c^2$, where A^2 is the peak mean square value of ground acceleration, S is the strong motion duration, and ω_c, the characteristic frequency of the earthquake ground motion. This index was obtained from the analysis of the response of elastoplastic hysteretic structures subjected to severe earthquake motions. In such instances, a multivariate hazard analysis methodology that considers the joint occurrences of the parameters describing the damageability index is needed. The idea for such analysis was first introduced by Der Kiureghian [65]. The following formulation is based on this notion.

Let a damageability index be expressed as a function $I(\mathbf{Y})$ of ground motion variables $\mathbf{Y} = (Y_1, \ldots, Y_m)$, and assume these variables are given in terms of a set of basic variables $\mathbf{X} = (X_1, \ldots, X_n)$ that characterize the earthquake event. The latter variables may include the characteristics of the earthquake source, its location, and variables describing the characteristics of the wave propagation path and local site effects. The relation between $\mathbf{Y}$ and $\mathbf{X}$ is expressed as

$$\mathbf{Y} = \mathbf{A}(\mathbf{X}) \tag{3.1}$$

where $\mathbf{A}$ is a function vector of $\mathbf{X}$ with elements $A_i(\mathbf{X})$. Given such ground motion representation, the seismic hazard for a given site can be defined in several ways. We define *marginal hazard* for the i-th intensity parameter Y_i as the probability of Y_i exceeding a level y_i in a given earthquake event, i.e.,

$$h_i = P\,(Y_i > y_i) = \int_{A_i(\mathbf{x}) > y_i} f_{\mathbf{X}}(\mathbf{x})\, d\mathbf{x} \tag{3.2}$$

which is basically the same equation as Eq. 2.30 for a single seismic source. This formulation is useful when several ground motion parameters are to be considered simultaneously and independently, as is done in the programs FRISK and SRAP.

We define *union hazard* as the probability of exceedance of any of several ground motion parameters above their respective thresholds in a given earthquake event. Union hazard is expressed as

$$H_U(\mathbf{y}) = P\,(\bigcup_{i=1}^{k} Y_i > y_i) = \int_{\bigcup_{i=1}^{k} A_i(\mathbf{x}) > y_i} f_{\mathbf{X}}(\mathbf{x})\, d\mathbf{x} \tag{3.3}$$

where $H_U(.)$ denotes the total hazard and y is a vector with elements y_i. There are many practical situations where the union hazard is of interest. One example is when the failure of a structure (collapse, damage or serviceability), is defined as the exceedance of any of the ground motion parameters $\mathbf{Y} = (A, V, D, S)$, above the levels $\mathbf{y} = (a, v, d, s)$, where A is peak acceleration, V is peak velocity, D is peak displacement, and S is strong ground motion duration. In a similar way, *intersection hazard* is defined as the probability of simultaneous exceedance of each intensity parameter Y_i above the respective threshold y_i, i.e.,

$$H_I(\mathbf{y}) = P\left(\bigcap_{i=1}^{k} Y_i > y_i\right) = \int_{\bigcap_{i=1}^{k} A_i(\mathbf{x}) > y_i} f_{\mathbf{X}}(\mathbf{x})\, d\mathbf{x} \tag{3.4}$$

This definition of hazard is useful for a complex structure with several lines of defense or components whose joint failure produces the global failure of the structure. A tall building whose system to withstand earthquake lateral forces is composed by shear walls and a peripheral moment-resisting frame is an example of such a redundant structural system.

A more comprehensive formulation of the seismic hazard is specified by the *generalized hazard*, defined as

$$H(\mathbf{y}) = P\left(g(\mathbf{Y}) \le 0\right) = \int_{g(\mathbf{A}(\mathbf{x})) \le 0} f_{\mathbf{X}}(\mathbf{x})\, d\mathbf{x} \tag{3.5}$$

where $g(.)$ is a selected function of the random variables Y. The three cases defined above are special cases of this generalized hazard. For instance, the marginal hazard for the i-th component of Y is obtained by defining $g(\mathbf{Y}) \equiv y_i - Y_i$. Furthermore, $g(\mathbf{Y}) \equiv \min_i (y_i - Y_i)$ defines the union hazard and $g(\mathbf{Y}) \equiv \max_i (y_i - Y_i)$ defines the intersection hazard.

The generalized hazard formulation is used to compute the hazard associated with the exceedance of the damageability index, $I(\mathbf{Y})$, above a threshold i. To do this, we define $g(\mathbf{Y}) = i - I(\mathbf{Y})$. As an example, consider the earthquake destructive potential factor PD defined earlier. For that case, the function g takes the form

$$g(\mathbf{Y}) = pd - 262\frac{A^2 S}{\omega_c^2} \tag{3.6}$$

where $\mathbf{Y} = (A^2, S, \omega_c)$, is the vector of parameters that characterize the earthquake destructive potential, A^2 is measured in cm^2 sec^{-4}, S in sec and ω_c in rad/sec, and pd is the specified threshold, measured in cm^3 sec^{-2}.

When the surface defined by $g(\mathbf{Y}) = 0$ is smooth, the computation of the integral in Eq. 3.5 is similar to that of the marginal hazard from Eq. 3.2. If $g(\mathbf{Y})$ is not a simple function, as in the cases of union and intersection hazard presented above, more complex procedures that also involve the computation of the marginal hazards should be used. These methods will be discussed later in this chapter. In both cases, a multifold integral must be computed. A general form of this function corresponding to a non-smooth case is $g(.) = \bigcup_k \bigcap_{i \in C_k} g_i(.) \leq 0$, where C_k denotes a collection of components whose joint failure constitute the failure of the system.

The integral in Eq. 3.5 (or that in Eq. 3.2) poses two problems: One is the formulation of the joint PDF of $\mathbf{X}$ when many dependent variables are involved, and the second is the evaluation of the multifold integral over the subspace of $\mathbf{X}$ for which $g(\mathbf{Y}) \leq 0$ (or $A_i(\mathbf{x}) > y_i$ in the latter case). These topics are discussed in the following two sections.

3.3. Models for Multivariate Distributions

For dependent variables joint distribution models are needed. Multivariate distribution models are limited for use in direct statistical estimation [96]. Two families are particularly useful: (a) joint distribution models formulated through conditional distributions; (b) joint distribution models formulated by marginal distributions and joint statistics, for example, covariances or coefficients of correlation.

The first family of multivariate distribution models is formulated by repeated use of the definition of conditional probability density function (conditional PDF),

$$f_{\mathbf{X}}(\mathbf{x}) = f_{X_n}(x_n | x_1, \cdots, x_{n-1}) \cdots f_{X_2}(x_2 | x_1) f_{X_1}(x_1) \tag{3.7}$$

where $f_{X_i}(x_i | x_1, \ldots, x_{i-1})$ denotes the conditional PDF of X_i given $X_1 = x_1, \ldots, X_{i-1} = x_{i-1}$. By selecting appropriate distributions for the conditional PDF's, a variety of multivariate distributions can be developed. This model is useful when information is available in terms of the conditional

distributions. One example of this kind is the distribution of shortest distance from a site to the rupture area in a defined fault, which can be formulated conditional on the dimensions of the source (i.e., rupture length, width, etc.). Another example is the distribution of residuals in a regression analysis, such as the distribution of rupture length for a given magnitude.

The second family of distributions is constructed based on the knowledge of marginal distributions and the second-moment joint statistics of the variables. This model is obtained by use of marginal transformations of the variables into standard normal variates and the assumption of joint normality of the standard variates [96 , 116]. According to this model, the joint PDF of **X** is

$$f_{\mathbf{X}}(\mathbf{x}) = \phi_n(\mathbf{z},\mathbf{R}_o)\frac{f_{X_1}(x_1)\cdots f_{X_n}(x_n)}{\phi(z_1)\cdots\phi(z_n)} \tag{3.8}$$

where $f_{X_i}(x_i) = d[F_{X_i}(x_i)]/dx_i$ is the marginal PDF of X_i; $z_i = \Phi^{-1}[F_{X_i}(x_i)]$ in which Φ^{-1} is the inverse of the cumulative standard normal probability; $\phi(.)$ is the standard normal PDF; and $\phi_n(\mathbf{z},\mathbf{R}_o)$ is the n-dimensional normal PDF of zero means, unit standard deviations, and correlation matrix $\mathbf{R}_o$. The elements $\rho_{o,ij}$ of $\mathbf{R}_o$ are obtained from relations given in Ref. 116 in terms of the original correlation coefficients ρ_{ij} and the marginal distributions of i and j. The above model is valid as long as each marginal CDF $F_{X_i}(x_i)$ is continuous and strictly increasing and $\mathbf{R}_o$ is positive definite. This conditions are satisfied in nearly all situations of practical interest.

3.4. Methods for Computation of Seismic Hazard

In the current methods of earthquake hazard assessments the integral in Eq. 3.5 is computed numerically, except for some trivial cases. Thus, the number of random variables to be incorporated in the analysis is limited to only a few (usually less than four), since the addition of each new variable adds a new fold to the integral. The modeling of the earthquake process is necessarily simplified to accommodate this restriction. This certainly poses a serious limitation to the formulation of the seismic hazard problem.

As an example, in the program SEISRISK II [19] a maximum of four random variables can be incorporated directly in the analysis, namely, magnitude, M, distance, R, uncertainty in the attenuation law, Z_y, and uncertainty in the rupture-length relationship, Z_l. The effects of variability in

other parameters, such as the seismicity parameter b, or the maximum magnitude m_1, are either ignored or are examined by repeated analysis, with different values for the parameter. The ability of computing the integral from Eq. 3.5 defines the degree of complexity, or *realism*, that can be incorporated in the modeling. For instance, when that integral is solved analytically, as in the Cornell approach, not more than three random variables can be used to characterize the problem: magnitude M, distance from the site to the earthquake, R, and uncertainty in the attenuation relation, Z_y. The zone of earthquake energy release can only be modeled as a point and the attenuation relation used is of the form of Eq. 2.27.

Numerical integration, on the other hand, although it permits a somehow improved earthquake modeling has its limitations. The number of variables to incorporate in the modeling and the degree of complexity of the intensity attenuation relationship are often restricted. However, this is the approach in the current procedures of seismic hazard analysis. Most, if not all, computer programs for seismic hazard perform a numerical calculation of Eq. 3.5 (see section 2.9 of Chapter 2).

In this last case, the release of energy from the earthquake is usually modeled as occurring along a line rupture, the length of this rupture being a function of earthquake size. Explicit uncertainty in the ground motion intensity and rupture-length relationships is often incorporated in the formulation. However, inclusion of uncertainty in other parameters is not considered except for indirect procedures that demand repeated computations of Eq. 3.5. The use of complex modeling of the attenuation of earthquake intensity, such as that described in Ref. 10 to represent the azimuthal effect of intensity attenuation, is also cumbersome from the computational standpoint.

Even when the distribution of the random variables is specified, the computation of the integral in Eqs. 3.2, 3.3, 3.4, or 3.5 can be difficult. A direct numerical evaluation of the integral is often impractical because of the large dimension. However, integrals of this kind have been of interest in structural reliability for a long time and efficient techniques for their evaluation are now available [9 , 120]. Basically, these techniques consist of two steps: (1) Transformation of the variables into the standard normal space; (2) Replacement of the boundary of the integration domain in the standard space with an approximating boundary for which the exact or approximate solution of

the integral exists. A detailed description of this procedure and the solution alternatives is presented in the following sections.

The solution procedure outlined above enables the analyst to carry out a full probabilistic description of the earthquake hazard problem without limitation of the number of variables it can accommodate. Sensitivity factors, representing partial derivatives of the hazard with respect to various parameters, are byproducts of the analysis and are easily computed. They are measures of influence on the hazard of the variabilities arising from various random variables, and of various parameters included in the modeling. They are also used to estimate the standard error of the computed hazard. This methodology is described in section 3.5.

3.4.1. Structural Reliability Methods

Two classes of problems arise in structural reliability: structural component reliability problems, and structural system reliability problems. Solution approaches for both kinds of problems are addressed below.

3.4.1.1. Structural Component Reliability Methods

The component reliability problem deals with the computation of the multifold integral in Eq. 3.2, and Eq. 3.5 in certain cases. The technique for fast and efficient computation of this integral consists of two steps. The first step involves a one-to-one transformation of the basic variables such that

$$\mathbf{U} = \mathbf{T}(\mathbf{X}) \tag{3.9}$$

where U is a vector of uncorrelated and standardized normally distributed variables, i.e., with zero means and unit standard deviations. Examples for such transformations are available in the literature [90 , 69].

The simplest definition of the transformation T appears when the basic variables are mutually independent with CDFs F_{X_i} . Each variable can then be transformed separately with the transformation defined by the identities

$$\Phi(u_i) = F_{X_i}(x_i) \tag{3.10}$$

where $\Phi(.)$ is the cumulative standard normal distribution. The transformation is thus

$$\mathbf{T}: \quad u_i = \Phi^{-1}(F_{X_i}(x_i)) \qquad i = 1, \ldots, n \tag{3.11}$$

with the inverse transformation

$$\mathbf{T}^{-1}: \quad x_i = F_{X_i}{}^{-1}(\Phi(u_i)) \qquad i = 1, \ldots, n \tag{3.12}$$

For variables with joint PDF defined by Eq. 3.8, the transformation to the standard normal space is given by

$$\mathbf{T}: \quad \mathbf{U} = \mathbf{L_o}^{-1} \begin{bmatrix} \Phi^{-1}(F_{X_1}(x_1)) \\ . \\ . \\ \Phi^{-1}(F_{X_n}(x_n)) \end{bmatrix} \tag{3.13}$$

where $\mathbf{L_o}^{-1}$ is the lower-triangular decomposition of $\mathbf{R_o}$. When the basic variables are defined through the conditional distributions, the *Rosenblatt transformation* [145] has been suggested by Hohenbichler and Rackwitz [90] as a good choice. The transformation is defined by

$$\mathbf{T}: \quad \begin{aligned} u_1 &= \Phi^{-1}(F_1(x_1)) \\ u_2 &= \Phi^{-1}(F_2(x_2|x_1)) \\ &\cdot \\ u_i &= \Phi^{-1}(F_i(x_i|x_1, x_2, \ldots, x_{i-1})) \\ &\cdot \\ u_n &= \Phi^{-1}(F_n(x_n|x_1, \ldots, x_{n-1})) \end{aligned} \tag{3.14}$$

where $F_i(x_i|x_1, x_2, \ldots, x_{i-1})$ is the cumulative density function of X_i conditional upon $(X_1 = x_1, \ldots, X_{i-1} = x_{i-1})$. The transformation first transforms X_1 into a standardized normal variable, U_1. Then the conditional variable $X_2|X_1 = x_1$ is transformed into a standardized normal variable, and so forth.

The inverse transformation can be obtained in a stepwise manner as

$$\mathbf{T}^{-1}: \quad \begin{aligned} x_1 &= F_1{}^{-1}(\Phi(u_1)) \\ x_2 &= F_2{}^{-1}(\Phi(u_2|x_1)) \\ &\cdot \\ x_n &= F_n{}^{-1}(\Phi(u_n|x_1, \ldots, x_{n-1})) \end{aligned} \tag{3.15}$$

In most situations, and seismic hazard analysis is not an exception, the transformations T and its inverse $\mathbf{T}^{-1}$ must be determined numerically.

Unless specified otherwise, it will be assumed that $g(.)$ is a smooth function of the vector of intensity variables, **Y**. The integration domain in the transformed space is expressed by $g(\mathbf{T}^{-1}(\mathbf{u})) \leq 0$. Thus, the boundary of integration in Eq. 3.5 is defined now by $g(\mathbf{T}^{-1}(\mathbf{u})) = G(\mathbf{u}) = 0$ and the integral to compute is expressed as

$$H = \int_{G(\mathbf{u}) \leq 0} \phi(\mathbf{u})\, d\mathbf{u} \tag{3.16}$$

where $\phi(\mathbf{u})$ denotes the standard multinormal density of **u** and H represents the probability of exceedance of intensity level **y**. In the terminology of structural reliability, the function $G(\mathbf{u})$ is known as the *limit-state function*, the boundary of integration $G(\mathbf{u}) = 0$ as the *limit-state surface* and H as the *probability of failure*. A word of caution is necessary, since failure in this case does not necessarily mean actual failure of the structure or facility under study if level **y** is exceeded. It should be interpreted only in the binary meaning of "success" and "failure", when a certain condition is satisfied or not.

The reasons for the transformation defined in Eq. 3.9 are two useful properties of the standard normal space. One is that the probability density in that space is rotationally symmetric about the origin and decays exponentially with the square of the distance from it. The second property is that the probability contents for some simple subsets in arbitrary dimensions are available. These two properties are the bases for the efficient techniques of integration of Eq. 3.5 mentioned above, namely the First- and Second-Order Reliability Methods, FORM and SORM.

3.4.1.1.1. FORM Approximation

The first property states that in the uncorrelated standard normal space, equal probability density points are located on concentric hyperspheres with the center at the origin (mean point). Thus, in this space the point $\mathbf{u}^*$ on the integration boundary which has minimal distance to the origin has the highest probability density in the region of integration. This point is known as the *design point*.

The value of the integral in Eq. 3.16 can be obtained analytically only for some simple integration boundaries. One of the simplest case is when the boundary corresponds to an hyperplane, in which case the probability content of the subset of the standard normal space defined by such sur-

face, i.e., the approximation of Eq. 3.16, is

$$H_{FO} = \Phi(-\beta) \tag{3.17}$$

where H_{FO} is the first-order approximation of the hazard and β is the distance from the origin to the hyperplane. A first-order approximation for Eq. 3.16 is provided by Eq. 3.17, meaning that the integration boundary $G(\mathbf{u}) = 0$ is approximated by an hyperplane.

The issue becomes now where to approximate the boundary. It is sound to approximate the boundary at a point where its contribution to the total integral and that of its neighborhood is high. The design point satisfies this condition by definition. Additionally, and since the probability content decays exponentially with distance away from this point, the errors due to the departures between the "true" and "approximated" boundary will not be significant. Thus, the FORM approximation of Eq. 3.5 is given by Eq. 3.17 where β, the shortest distance between the design point and the origin, is defined as

$$\beta = \boldsymbol{\alpha}^T \mathbf{u}^* \tag{3.18}$$

in which

$$\boldsymbol{\alpha} = -\frac{\nabla_U G(\mathbf{u}^*)}{|\nabla_U G(\mathbf{u}^*)|} = \frac{1}{\beta}\mathbf{u}^* \tag{3.19}$$

is the vector of direction cosines along the axes u_i's. The value β so defined is known as the *reliability index.*

This approximation works well as long as the limit-state surface has only one minimal distance point and when it is nearly flat in the neighborhood of the design point.

3.4.1.1.2. SORM Approximation

When the surface is nonflat, which occurs when $G(\mathbf{u})$ and/or the transformation, $\mathbf{T}$, are/is nonlinear, a second-order approximation to H, denoted H_{SO}, is obtained by approximating the boundary of integration by a second-order surface at $\mathbf{u}^*$, usually a hyperparaboloid or a hypersphere.

Several approximations of H_{SO} have been derived in recent years. The simplest of these, based on a paraboloid fitting, is due to Breitung [34] which was later modified by Hohenbichler [88]

$$H_{SO} = \Phi(-\beta) \prod_{i=1}^{n-1} (1 + \psi(-\beta)\kappa_i)^{-\frac{1}{2}} \tag{3.20}$$

where n is the number of variables, κ_i are the main curvatures of the limit-state surface or an approximating hyperparaboloid at the design point, taken positive for a convex surface with respect to the origin, and $\psi(-\beta) = \phi(\beta)/\Phi(-\beta)$. For large β, $\psi(\beta) \to \beta$, and Eq. 3.20 tends asymptotically to Breitung's formula. Three other formulas have been developed later by Tvedt [163 , 164] based also on paraboloid fitting of the limit-state surface, which have been examined in Ref. 68. These first- and second-order approximations are conceptually illustrated in a two-dimensional space in Fig. 3.1.

The approximations generally work well, as long as the limit-state surface has only one minimal distance point. This is because, with only one such point most of the contribution to the probability of interest in the integral of Eq. 3.5 comes from the neighborhood of the point on the integration boundary which is nearest to the origin, where the limit-state surface is well approximated. When it has several local minimal distance points, approximate bounds on the probability integral may be obtained by fitting planar or parabolic surfaces at all such points [70].

The selection of the "best" hyperparaboloid to approximate the integration boundary has been a matter of recent study. The two main approaches proposed in the literature are: (1) the curvature-fitted paraboloid and (2) the point-fitted paraboloid. In both cases the hyperparaboloid is tangent to the boundary at the design point. The difference is that in the first case the hyperparaboloid maintains the main curvatures of the surface at the design point [34], whereas in the second it is fitted to selected points on the surface [68].

A considerable effort is spent computing the curvatures of the limit-state surface in the first case, hereafter called SORM-CF, since the full $n \times n$ curvature matrix at the design point is required. In the point-fitted case (SORM-PF) fewer computations are required to define the hyperparaboloid in most cases, since only the coordinates of the fitting points are required. In addition, with the curvature-fitted surface one has to either compute one or more determinants of order $n-1$ or solve an eigenvalue problem of the same order to compute H_{SO}. Such evaluations are not needed for the point-fitted surface since the principal curvatures are directly computed.

In this last case the approximating hyperparaboloid is defined by fitting to a set of discrete points selected on the limit-state surface at prescribed distances from the design point, $\mathbf{u}^*$. These *fitting points* are selected so as to provide a good fit over a large segment of the neighborhood of $\mathbf{u}^*$. An alternative method to the one presented in Ref. 68 to select these fitting points is presented below.

The point-fitted hyperparaboloid. Following Ref. 68, the second-order approximation is considered in a rotated standard space $\mathbf{U}'$ in which the u_n' axis coincides with the design point (see Fig. 3.2). The orthogonal transformation

$$\mathbf{U}' = \mathbf{R}\,\mathbf{U} \tag{3.21}$$

is used for that purpose, where the nth-row of $\mathbf{R}$ is selected to be $\mathbf{u}^*/(\mathbf{u}^{*T}\,\mathbf{u}^*)^{1/2}$.

The fitting points, $2(n-1)$ in number, are selected along the coordinate axes in the rotated space. Along each axis u_i', $i = 1, \ldots, n-1$, two points on the limit-state surface are selected such that their probability density is a specified ratio, γ_r, of the probability density at the design point, i.e.,

$$\gamma_r = \frac{\text{PDF of } \mathbf{u}_{\pm i}}{\text{PDF of } \mathbf{u}^*} = \frac{\phi(|\mathbf{u}_{\pm i}|)}{\phi(|\mathbf{u}^*|)} = e^{-\frac{1}{2}(\rho^2 - \beta^2)} \tag{3.22}$$

where $\mathbf{u}_{\pm i}$ are the fitting points on the positive and negative sides of the u_i' axis, and ρ is the distance from the fitting points to the origin. This condition, different from that imposed in Ref. 68 to select the fitting points, serves two purposes: (1) to ensure that the points exist in all situations, and (2) to make a consistent approximation for all situations.

In Ref. 68 the fitting points were selected such that their abscissa is a fixed fraction $\pm k$ of the distance β between the design point and the origin. The value of the parameter k was defined as

$$k = \begin{cases} 1 & \text{for } \beta \le 3 \\ \dfrac{3}{\beta} & \text{for } \beta > 3 \end{cases} \tag{3.23}$$

The rationale for this rule was that γ_r should not be too small because it would be undesirable to select fitting points with much lower probability density than the design point. However, this condition is not satisfied by just limiting the value of the abscissa of the fitting point in the standard

normal space. As a counter example, we examine the probability content of two points in the standard space, one with coordinates $(k\beta, 0)$ and the other, $(k\beta, \infty)$. Among all points with fixed abscissa $k\beta$, the first has the largest probability density ($\exp[-(k\beta)^2/2]$) whereas the second has the lowest (zero). Therefore, it is clear that using the rule specified in Ref. 68 the fitting points obtained are of uneven probability content, some comparable to that of the design point ($\exp[-\beta^2/2]$), others much lower. The approximation in some cases is appropriate whereas is inadequate in others, since the fitted paraboloid may not closely approximate the true surface in the vicinity of the design point.

There are other situations for which this procedure is not suited. As an example, if the limit-state surface in the rotated standard space tends asymptotically to a line parallel to the ordinate axis located at a distance less than $k\beta$, as depicted in Fig. 3.3, the fitting point is never reached. This can happen, for instance, when the transformation for any variable is highly nonlinear, say from exponential to normal distribution. Unfortunately, this is the case for several variables in seismic hazard analysis, where normality is hardly justified, such as depth of focus, location of epicenter on a finite fault, seismicity parameter b, magnitude M.

In the SORM-PF method, the principal directions of the approximating hyperparaboloid are selected to coincide with the coordinate axes in the rotated space, regardless of the orientation of the principal directions of the limit-state surface. The approximating n-dimensional paraboloid, thus, is defined by

$$u_n' = \beta + \frac{1}{2}\sum_{i=1}^{n-1} \tilde{\kappa}_i \, u_i'^2 \tag{3.24}$$

where $\tilde{\kappa}_i$ are the corresponding principal curvatures. These curvatures are determined in terms of the fitting points in the same manner as described in Ref. 68. For the example shown in Fig. 3.2 the curvature is given as

$$\frac{1}{\sqrt{1+\beta\tilde{\kappa}_i}} = \frac{1}{2}\left(\frac{1}{\sqrt{1+\beta\tilde{\kappa}_{+i}}} + \frac{1}{\sqrt{1+\beta\tilde{\kappa}_{-i}}}\right) \tag{3.25}$$

where $\tilde{\kappa}_{\pm i}$ are the curvatures of the two semiparabolas. The specific value of γ_r to be chosen for finding the fitting points is examined in Chapter 4 through numerical examples.

Algorithm for computing $\mathbf{u}^*$ and the fitting points. The main effort in the first- or second-order reliability method is in finding the minimum distance point, $\mathbf{u}^*$. This is formulated as a constrained optimization problem:

$$\begin{cases} \textit{minimize} & |\mathbf{u}| \\ \textit{subject to} & G(\mathbf{u}) = 0 \end{cases} \tag{3.26}$$

Standard solution algorithms for this problem are available [120 , 117]. Starting from a initial point $\mathbf{u}_0$, these algorithms typically generate a sequence of points $\mathbf{u}_1, \mathbf{u}_2, \ldots,$ which converge at a minimum-distance point, provided the algorithm is stable.

Any procedure for computing roots is suitable for finding the fitting points, provided that stability and convergence are satisfied. The secant rule, also suggested for the original point-fitting procedure [68], can be used for the modified version presented here. The search algorithm for the fitting points proceeds as follows:

(1) Compute the distance ρ that defines points in the standard space with specified ratio of probability γ_r with respect to the design point.

(2) Sweep along the circle of radius ρ, of equal probability density, until intercepting the limit-state surface. The secant method may be used for this purpose.

(3) If a solution is found, stop the procedure; if a solution is not found, i.e., the limit-state surface does not contain points with probability density γ_r times that of the design point, where $\gamma_r \ll 1$, then it means that $\mathbf{u}^*$ is not the actual design point. The above optimization algorithm will have to be resolved with a different starting point to obtain the correct solution for $\mathbf{u}^*$.

This procedure is depicted in Fig. 3.4.

3.4.1.2. System Reliability Methods

When the general formulation of the seismic hazard from Eq. 3.5 is used and the *g* function is non-smooth, as defined earlier, then a system reliability solution strategy is required. Methods of solution for systems reliability are discussed, for example, in Refs. 9 and 120. A brief description is presented in the following paragraphs.

Two special classes of systems can be recognized, which require different solution techniques: (a) *Series Systems*, where the failure of the system occurs when any component of the system fails; and (b) *Parallel Systems*, where the failure of the system occur when all components of the system fail. The first case can be recognized as a case of union hazard and the latter, of intersection hazard. Examples of both situations can be found in seismic hazard analysis, as discussed before.

For the case of union hazard (formulation equivalent to series system), if all limit states are positively correlated then the seismic hazard is bounded by [53]

$$\max_i h_i \leq H(\mathbf{y}) \leq 1 - \prod_{i=1}^{k}(1-h_i) \approx \sum_{i=1}^{k} h_i \tag{3.27}$$

where the approximation shown for the upper bound is valid for small probabilities only. This bounds are termed *Unimodal Bounds*. An improvement to these rather loose bounds is obtained with the *Bimodal Bounds* [70]

$$h_1 + \sum_{i=2}^{k} \max\left\{\left[h_i - \sum_{j=1}^{i-1} h_{ij}\right]; 0\right\} \leq H(\mathbf{y}) \leq h_1 + \sum_{i=2}^{k}[h_i - \max_{j<i} h_{ij}] \tag{3.28}$$

where $h_{ij} = P(Y_i > y_i \bigcap Y_j > y_j)$ and k is the total number of marginal hazards considered. First- and second-order approximations of h_i and h_{ij} can be computed, as discussed in Ref. 120. The bounds depend on the numbering of the failure modes, and different orderings may correspond to the largest lower bound (*infimum*) and the lowest upper bound (*supremum*). Practical experience recommends ordering the limit states in decreasing order of the probability of exceedance.

Combinations of the basic cases already discussed are sometimes found in practice. The solution approach should be examined separately for each case. Bounds for the case of intersection hazard (equivalent to parallel system formulation), although available are of little use. First- and second-order approximations and asymptotic expressions for the generalized seismic hazard are also available [120 , 89]. At the present time, there is little practical experience with these methods and their appropriateness should be assessed in each situation.

3.4.2. Simulation Methods

Under certain circumstances, neither numerical integration nor FORM/SORM methods are feasible or sufficiently accurate to use. One of these examples is the generalized seismic hazard case that involves intersections or unions of g functions or combinations thereof, similar to the general system reliability problem. Simulation methods are gaining interest for use in the assessment of system reliability. Efficient simulation methods have been suggested in recent years that can be easily applied to the seismic hazard problem. In some particular cases only a simulation approach will allow the analyst to obtain an accurate estimate of the seismic hazard. For instance, they may be used to examine the accuracy of results obtained by an approximate method. Hence, a brief description of these methods follows.

3.4.2.1. Basic Monte Carlo Simulation

Basically, Monte Carlo simulation is a sampling technique where the observations are artificially generated by a computer in accordance with the probability distributions of the random variables [146 , 9]. The results from Monte Carlo simulation can be treated statistically. It should be noted that, as in ordinary sampling, the results of a Monte Carlo simulation are not "exact" unless the simulated sample size is infinitely large. Additionally, errors in the Monte Carlo simulation method may arise from the underlying procedures for generating random numbers.

The results from the simulation procedure can be expressed statistically by its mean

$$\hat{\mu}_H = \frac{1}{N}\sum_{i=1}^{N} p_i \tag{3.29}$$

where N is the number of simulations and p_i is an indicator variable equal to one when $g(\mathbf{y}) \leq 0$ (success) and zero otherwise (failure). The variance of the estimation may be estimated by

$$\hat{\sigma}_H{}^2 = \frac{1}{N(N-1)}\sum_{i=1}^{N} (p_i - \hat{\mu}_H)^2 \tag{3.30}$$

Confidence intervals for the estimate can be obtained using the mean and standard deviation calculated from Eqs. 3.29 and 3.30. If N, the number of simulations, is sufficiently large the distribution of H can be assumed to be normal by the central limit theorem. The $(1-\alpha)$ confidence interval of the estimate then is

$$<H>_{1-\alpha} = (\hat{\mu}_H - \Phi^{-1}(1-\alpha/2)\,\hat{\sigma}_H \; ; \; \hat{\mu}_H + \Phi^{-1}(1-\alpha/2)\,\hat{\sigma}_H) \tag{3.31}$$

In seismic hazard analysis, the probability values of interest usually are of the order of 10^{-3} or less, for usual structures and facilities. This implies that N must be very large to obtain a reliable estimate of the seismic hazard since it takes in average $1/H$ simulations to obtain one outcome of X with $p_i = 1$, and at least 50 such *realizations* to obtain a reliable estimate.

A number of procedures are available to reduce the error (or variance) without increasing the number of simulations. One such procedure, which is employed in some of the examples in Chapter 5, is discussed below.

3.4.2.2. Simulation with Antithetic Variates

This method was developed in 1956 [84]. Basically, for each simulated vector **X** an additional outcome **X′** is computed, such that each pair of the corresponding random variables is negatively correlated, i.e., $\mathrm{Cov}(x_i, x_i') < 0$. The improvement in the accuracy of the estimator depends on the problem.

The procedure is described as follows: (1) a set of n uniformly distributed random numbers $u_1, u_2, \ldots, u_n$ is generated and transformed to obtain **X**; (2) the related set of random numbers $1-u_1, 1-u_2, \ldots, 1-u_n$ is transformed to obtain **X′** and the values of the indicator p_i; (3) each of these two realizations is treated independently to compute $g(\mathbf{X})$.

3.4.2.3. Directional Simulation

This method has been suggested as a tool for evaluating the multi-normal distribution function [62]. It is only recently that it has been applied to structural reliability problems [23]. The n-dimensional standard normal vector **U** is expressed as $\mathbf{U} = R\,\mathbf{V}$, with R positive. The random variable R^2 has a chi-square distribution with n degrees of freedom, and is independent of the random unit direction vector $\mathbf{V} = (V_1, V_2, \ldots, V_n)$ having a uniform distribution over the n-dimensional unit sphere Ω_n in the space of **U**. The seismic hazard is computed by conditioning on $\mathbf{V} = \mathbf{v}$

$$\begin{aligned} H(\mathbf{y}) &= \int_{\mathbf{v}\in\Omega_n} P\,(G(R\,\mathbf{V}) \le 0 \,|\, \mathbf{V}=\mathbf{v}) f_{\mathbf{V}}(\mathbf{v})\, d\mathbf{v} \\ &= \int_{\mathbf{v}\in\Omega_n} P\,(G(R\,\mathbf{v}) \le 0) f_{\mathbf{V}}(\mathbf{v})\, d\mathbf{v} \end{aligned} \tag{3.32}$$

where $f_{\mathbf{V}}(\mathbf{v})$ is the density of V on the unit sphere. The main idea in this method is to compute the conditional probability analytically and the integral by simulation. Since the conditional probability usually has a small value, high level of accuracy can be achieved with a relatively small number of simulations of V. The conditional probability is computed using the distribution of R. The values of r for which $G(r\,\mathbf{v}) \leq 0$ are usually given by the interval $[r_o, \infty)$, thus, the desired probability is given by

$$P\,(G(R\,\mathbf{v}) \leq 0) = P\,(R \geq r_o) = 1 - \chi_n^2(r_o^2) \qquad r_o \geq 0 \tag{3.33}$$

where χ_n^2 is the chi-square distribution function of n degrees of freedom, and r_o is the root of the equation $G(r\,\mathbf{v}) = 0$. Three special situations should also be considered: (1) the solution interval is $(0, r_o]$; (2) there are multiple roots for the equation; and (3) there is no solution. The first case corresponds to a situation where the probability of exceedance is rather large. This situation is not common in structural reliability but it might occur in seismic hazard analysis, especially when the complete seismic hazard curve is needed. In such a case, the probability from Eq. 3.33 is computed as

$$P\,(G(R\,\mathbf{v}) \leq 0) = P\,(R \leq r_o) = \chi_n^2(r_o^2) \qquad r_o \geq 0 \tag{3.34}$$

When there are multiple roots, the probability of interest can be computed exactly provided all the roots are identified. For that case the above-mentioned probability is computed as

$$P\,(G(R\,\mathbf{v}) \leq 0) = 1 - \sum_{i=0}^{l} I[0.5(r_i + r_{i+1})\mathbf{v}]\,[\chi_n^2(r_{i+1}^2) - \chi_n^2(r_i^2)] \tag{3.35}$$

where $r_0 = 0$, $r_{l+1} = \infty$, and $r_1, r_2, \cdots, r_l$ are the ordered positive roots of the limit-state equation $G(r\,\mathbf{v}) = 0$, and $I[.]$ is an indicator function defined by

$$I[r\,\mathbf{v}] = \begin{cases} 0 & r\,\mathbf{v} : \{G(r\,\mathbf{v}) \leq 0\} \\ 1 & \text{otherwise} \end{cases} \tag{3.36}$$

The root r_o (or roots r_j, $j = 1 \cdots l$ when more than one), corresponding to each vector $\mathbf{v}_i$ are found by any suitable procedure. In situations when the line defined by the direction $\mathbf{v}_i$ does not intercept the n-dimensional surface $G(r\,\mathbf{v}) = 0$, or when the value of r_o (or r_1 for the multiple roots case), is far too large to compute the probability in Eq. 3.33 or Eq. 3.34 (Eq. 3.35, in the latter case), the value of the conditional probability is approximated by zero.

The computation proceeds as follows:

(1) Generation of N outcomes $\mathbf{v}_1, \mathbf{v}_2, \cdots, \mathbf{v}_N$ of the unit vector V.

(2) For each outcome $\mathbf{v}_i$, determine the root or roots along the direction as defined above and compute the conditional failure probability p_i from Eq. 3.33, Eq. 3.34 or Eq. 3.35.

(3) Estimate the mean and variance of the probability and the confidence interval from Eqs. 3.29-3.31.

Mixing the antithetic variates method with the directional simulation procedure is also feasible. For each simulated direction vector $\mathbf{v}_i$, a corresponding antithetic direction vector, $\mathbf{v}_i' = -\mathbf{v}_i$, is computed. The procedure is then followed considering the vectors $\mathbf{v}_i$ and $\mathbf{v}_i'$ as independent simulations. The resulting variance is smaller than that using one direction and twice the number of simulations.

These simulation procedures can be combined with FORM and SORM for further improvement of the results. As an example, directional simulation combined with second-order approximations of the limit-state surface has been recently used [115] with considerable reduction of the computation effort.

3.5. Sensitivity Analysis and Analysis of Uncertainties

In the past the analysts of seismic hazard do not appear to have been overly concerned with the assessment of sensitivities and uncertainties in the estimate of seismic hazard. However, an estimate without a measure of the error is practically meaningless. Different methods have been recently used to provide an assessment of the dispersion of the probabilistic seismic hazard estimate (see Chapter 2 section 2.8). All of these methods require repeated analysis with different sets of parameters, with the results treated statistically to compute the mean, standard deviation and fractiles of the hazard estimate. From this information, confidence intervals can be defined under certain assumptions of the distribution of the computed hazard. No systematic methods for sensitivity analysis in seismic hazard evaluation have been developed yet. Such analysis can help identify areas where refinements in the modeling or in the parameter estimation will have greater influence in reducing the dispersion

in the estimated hazard. Systematic methods based on FORM and directional simulation for computing sensitivities and uncertainties of seismic hazard are described in this section.

3.5.1. Sensitivity Analysis

The reliability methods described in the preceding section present the additional advantage of providing measures of sensitivities of the computed probability to the different variables and parameters involved, with no or little extra effort. As a byproduct of the optimization algorithm to find the nearest point, a vector α (the normalized gradient vector at the design point) representing partial derivatives of the hazard with respect to variations in the components of the standard normal vector U, is obtained from Eq. 3.19. The values α_i are often referred to as the *sensitivity factors* in the terminology of structural reliability. They represent sensitivities of the first-order estimated hazard with respect to the design point. The transformed version of the preceding vector, γ , representing partial derivatives of the hazard with respect to the components of the original random vector X, can also be obtained

$$\gamma = -\frac{\nabla_X g(x^*)}{|\nabla_X g(x^*)|} \tag{3.37}$$

where $x^* = T^{-1}(u^*)$ is the design point in the original space. Similar sensitivity measures with respect to any desired model parameter (e.g., a parameter of the attenuation law or a parameter of the probability distribution of the magnitude M) can be readily computed in terms of α [120]. Apart from the sensitivity measures with respect to the basic random variables present in the formulation of the hazard, two additional sets of these measures can be obtained: (a) sensitivity measures with respect to *distribution parameters* and (b) sensitivity measures with respect to parameters in the *limit-state function*. Expressions for these measures are described below.

3.5.1.1. Sensitivity with respect to Distribution Parameters

Let the distribution of X, $F_X(x, \psi)$, be specified in terms of a set of parameters ψ. The vector ψ contains parameters that are used to describe the distribution, e.g., means, variances, and correlation coefficients. Thus, the transformation from Eq. 3.9 can be written as

$$\mathbf{U} = \mathbf{T}(\mathbf{X}, \Psi) \tag{3.38}$$

The partial derivatives of the reliability index β with respect to the components of the vector ψ are computed making use of the expression $\beta^2 = \mathbf{u}^{*T}\,\mathbf{u}^*$ obtained by replacing the expression of α from Eq. 3.19 in Eq. 3.18, as

$$\begin{aligned}\frac{\partial}{\partial\psi_i}\beta(\psi) &= \frac{1}{\beta}\mathbf{u}^{*T}\,\frac{\partial}{\partial\psi_i}\mathbf{u}^* \\ &= \frac{1}{\beta}\mathbf{u}^{*T}\,\frac{\partial}{\partial\psi_i}\mathbf{T}(\mathbf{x}^*, \psi)\end{aligned} \tag{3.39}$$

Replacing Eq. 3.19 in the above equation,

$$\frac{\partial}{\partial\psi_i}\beta(\psi) = \alpha^T\,\frac{\partial}{\partial\psi_i}\mathbf{T}(\mathbf{x}^*, \psi) \tag{3.40}$$

In vector form for all elements of ψ :

$$\nabla_\psi\beta = \alpha^T\,\mathbf{J}_{u^*,\psi} \tag{3.41}$$

where $\mathbf{J}_{u^*,\psi}$, the Jacobian of the transformation, is calculated with $\mathbf{x}^*$ fixed. Hence, sensitivities to the first-order failure probability estimate H is, according to Eq. 3.17,

$$\begin{aligned}\nabla_\psi H_{FO} &= \nabla_\psi\,\Phi(-\beta(\psi)) \\ &= -\phi(-\beta(\psi))\,\nabla_\psi\beta \\ &= -\phi(-\beta(\psi))\,\alpha^T\,\mathbf{J}_{u^*,\psi}\end{aligned} \tag{3.42}$$

This is the final expression to compute the sensitivities of the hazard H with respect to distribution parameters. During the process of solution, $\beta(\psi)$ and α are obtained and only the Jacobian needs to be computed additionally.

3.5.1.2. Sensitivity with respect to Parameters of the Limit-State Function

Let the limit-state function be specified in terms of a set of parameters η, i.e., $G(\mathbf{u},\eta)$. The partial derivatives of the reliability index β with respect to the components of the vector η are also computed making use of the expression for β given above

$$\begin{aligned}\frac{\partial}{\partial\eta_i}\beta(\eta) &= \frac{1}{\beta}\mathbf{u}^{*T}\,\frac{\partial}{\partial\eta_i}\mathbf{u}^* \\ &= \frac{1}{\beta}\left(-\beta\,\frac{\nabla_{u^*}G(\mathbf{u}^*, \eta)^T}{|\nabla_{u^*}G(\mathbf{u}^*, \eta)|}\right)\frac{\partial}{\partial\eta_i}\mathbf{u}^*\end{aligned} \tag{3.43}$$

From the total derivative of the limit-state function $G(\mathbf{u}^*, \boldsymbol{\eta})$ we have

$$\nabla_{u^*} G(\mathbf{u}^*, \boldsymbol{\eta})^T \frac{\partial \mathbf{u}^*}{\partial \eta_i} + \frac{\partial G(\mathbf{u}^*, \boldsymbol{\eta})}{\partial \eta_i} = 0 \tag{3.44}$$

Hence,

$$-\nabla_{u^*} G(\mathbf{u}^*, \boldsymbol{\eta}) \frac{\partial \mathbf{u}^*}{\partial \eta_i} = \frac{\partial G(\mathbf{u}^*, \boldsymbol{\eta})}{\partial \eta_i} \tag{3.45}$$

Combining Eqs. 3.43 and 3.45 yields

$$\frac{\partial}{\partial \eta_i} \beta(\boldsymbol{\eta}) = \frac{\dfrac{\partial G(\mathbf{u}^*, \boldsymbol{\eta})}{\partial \eta_i}}{|\nabla_{u^*} G(\mathbf{u}^*, \boldsymbol{\eta})|} \tag{3.46}$$

In vector form for all elements of $\boldsymbol{\eta}$

$$\nabla_{\eta} \beta = \frac{1}{|\nabla_{U} G(\mathbf{u}^*, \boldsymbol{\eta})|} \nabla_{\eta} G(\mathbf{u}^*, \boldsymbol{\eta}) \tag{3.47}$$

where the derivatives with respect to $\boldsymbol{\eta}$ are computed with $\mathbf{u}^*$ fixed. The sensitivities of first-order probability of exceedance or seismic hazard estimate, H_{FO}, according to Eq. 3.17, are obtained from:

$$\begin{aligned} \nabla_{\eta} H_{FO} &= \nabla_{\eta} \Phi(-\beta(\boldsymbol{\eta})) \\ &= -\phi(-\beta(\boldsymbol{\eta}))\, \nabla_{\eta} \beta \\ &= -\phi(-\beta(\boldsymbol{\eta})) \frac{1}{|\nabla_{u^*} G(\mathbf{u}^*, \boldsymbol{\eta})|} \nabla_{\eta} G(\mathbf{u}^*, \boldsymbol{\eta}) \end{aligned} \tag{3.48}$$

This is the final expression to compute the sensitivities of the hazard H with respect to parameters of the limit-state function. During the process of solution, only the partial derivatives of $G(\mathbf{u}^*, \boldsymbol{\eta})$ with respect to the components of $\boldsymbol{\eta}$ need to be computed additionally when these sensitivities are required. The expressions from Eqs. 3.42 and 3.48 are easily computed during the process of solution.

The above sensitivity measures can also be obtained when simulation procedures are used. In particular, sensitivities of the estimated seismic hazard (as given by Eq. 3.32) with respect to deterministic parameters of the limit-state function or to distribution parameters can be computed directly in the directional simulation scheme [24]. The vectorial form of these sensitivities is

$$\nabla_{\eta} H_{FO} = \int_{\mathbf{v} \in \Omega_u} \frac{2r}{\nabla_{\eta} G(\mathbf{u}^*, \boldsymbol{\eta})^T \mathbf{v}} \nabla_{\eta} G(\mathbf{u}^*, \boldsymbol{\eta})\, \kappa_n(r^2) f_{\mathbf{V}}(\mathbf{v})\, d\mathbf{v} \tag{3.49}$$

where κ_n is the chi-square density function of n degrees of freedom. Using this expression, the vector of sensitivities can be estimated by directional simulation in a similar way to the simulation of H.

These sensitivity measures, aside from the information they provide by themselves, can also be used to compute estimates of the standard error of the hazard. This is explained in the following section.

3.5.2. Analysis of Uncertainties

There exists a clear distinction between the different types of uncertainties discussed in section 2.8 of Chapter 2. They have been treated differently in seismic hazard analysis: integration is carried out over probabilistic variabilities to get a single hazard curve, whereas modeling uncertainties are expressed by multiple assumptions, hypothesis, or parameter values. These multiple interpretations result in a collection of hazard curves that are treated statistically.

The separation between inherent, statistical, and model uncertainty is difficult. As an example, let us examine the uncertainty in the earthquake intensity attenuation. Sources of inherent randomness that contribute to the total uncertainty arise from the mechanism of earthquake rupture, the propagation path of the seismic waves, and the properties of the medium of propagation. The details of the rupture process in time and space on the seismic source are random in nature and cannot be predicted in advance. The multiple reflections and refractions of the seismic waves as they travel across the earth are also unpredictable and contribute to the total uncertainty. The properties and characteristics of the propagating medium also influence the attenuation of seismic waves and contribute to the final uncertainty. They cannot be deterministically defined, not only because of the randomness in their distribution in space, but also due to the unpredictability of the propagating path of the seismic waves.

Modeling uncertainty arises since simple formulas such as those in Table 4.1 do not adequately model the complex phenomenon of earthquake generation and wave propagation. A part of this uncertainty can be eliminated by using more refined models which account for some of the parameters characterizing the phenomenon, such as the average properties of the medium, rupture directivity and velocity, etc. The problem with such refined models, however, is the difficulty in

estimating their parameters as sufficient data for such purposes is still not available.

The large scatter in observed data around attenuation laws represents the combined effect of inherent variabilities and model uncertainties. At this time, the contribution of each component can only be determined by judgement. Several approaches to incorporate model uncertainty are currently available, as mentioned in section 2.8 of Chapter 2.

In recent years, in PRA studies of nuclear power plants, there has been a tendency to separate the contribution of statistical and modeling uncertainties to seismic hazard from the contribution of variables perceived to represent inherent randomness. This is the approach of the methodology presented below, which allows the analyst to separate the two types of contributions. Inherent variability is incorporated in the probabilistic formulation as random variables with prescribed probability distribution. On the other hand, let the vector $\boldsymbol{\Theta}$ denote the set of parameters that define the models and distributions used in formulating the seismic hazard. Example elements of this vector are β, m_1, ν, parameters c_1, c_2, c_3 and c_4 of the attenuation model (Eq. 2.27), and parameters a and b of the rupture length-magnitude relationship.

Let $H(\boldsymbol{\Theta})$ denote the estimated hazard for intensity level $\mathbf{y}$ for a given set of parameters, $\boldsymbol{\Theta} = \boldsymbol{\theta}$. For each such set $\boldsymbol{\theta}$, $H(\boldsymbol{\Theta})$ is a point estimate of the hazard for level $\mathbf{y}$. In particular, for $\boldsymbol{\theta}$ equal to the mean of $\boldsymbol{\Theta}$, the estimated hazard may be regarded as a first-order estimate of the mean hazard, μ_H.

The problem is now to estimate the standard error of $H(\boldsymbol{\Theta})$, a complex function of $\boldsymbol{\Theta}$. A simple technique to use is linearization. From the Taylor series expansion in the neighborhood of the mean parameter values, $H(\boldsymbol{\Theta}) = H(\mathbf{M}_{\boldsymbol{\Theta}}) + \nabla_{\boldsymbol{\Theta}} H(\mathbf{M}_{\boldsymbol{\Theta}})(\boldsymbol{\Theta} - \mathbf{M}_{\boldsymbol{\Theta}})$, the variance of $H(\boldsymbol{\Theta})$ is

$$\hat{\sigma}_H^2 = \nabla_{\boldsymbol{\Theta}} H(\mathbf{M}_{\boldsymbol{\Theta}})\, \hat{\Sigma}_{\boldsymbol{\Theta}\boldsymbol{\Theta}}\, \nabla_{\boldsymbol{\Theta}} H(\mathbf{M}_{\boldsymbol{\Theta}})^T \tag{3.50}$$

where $\hat{\Sigma}_{\boldsymbol{\Theta}\boldsymbol{\Theta}}$ is an estimate of the covariance matrix of $\boldsymbol{\Theta}$ and $\nabla_{\boldsymbol{\Theta}} H(\mathbf{M}_{\boldsymbol{\Theta}})$ is the vector of partial derivatives of the hazard with respect to the components of $\boldsymbol{\Theta}$ evaluated at the mean point. This vector is available from the analysis of sensitivities and Eqs. 3.42 and 3.48 are used for its computation.

Since $\boldsymbol{\Theta}$ may include parameters from the distribution of $\mathbf{X}$ as well as parameters from the limit-state function, it is useful from the computational standpoint to partition the vector in two

segments: $\Theta^T = (\Theta_\psi^T, \Theta_\eta^T)$. The appropriate partial derivatives of the hazard obtained from Eq. 3.42 will form the upper part of the vector $\nabla_\Theta H(M_\Theta)$ whereas those obtained from Eq. 3.48 will form the lower part of it.

Measures of uncertainty associated with the seismic hazard assessments at various levels are key when decisions are to be properly made. Certainly, more information is provided if the distribution of the computed estimate is known, once its standard error is obtained. Confidence intervals and fractiles of the estimate are calculated from this information.

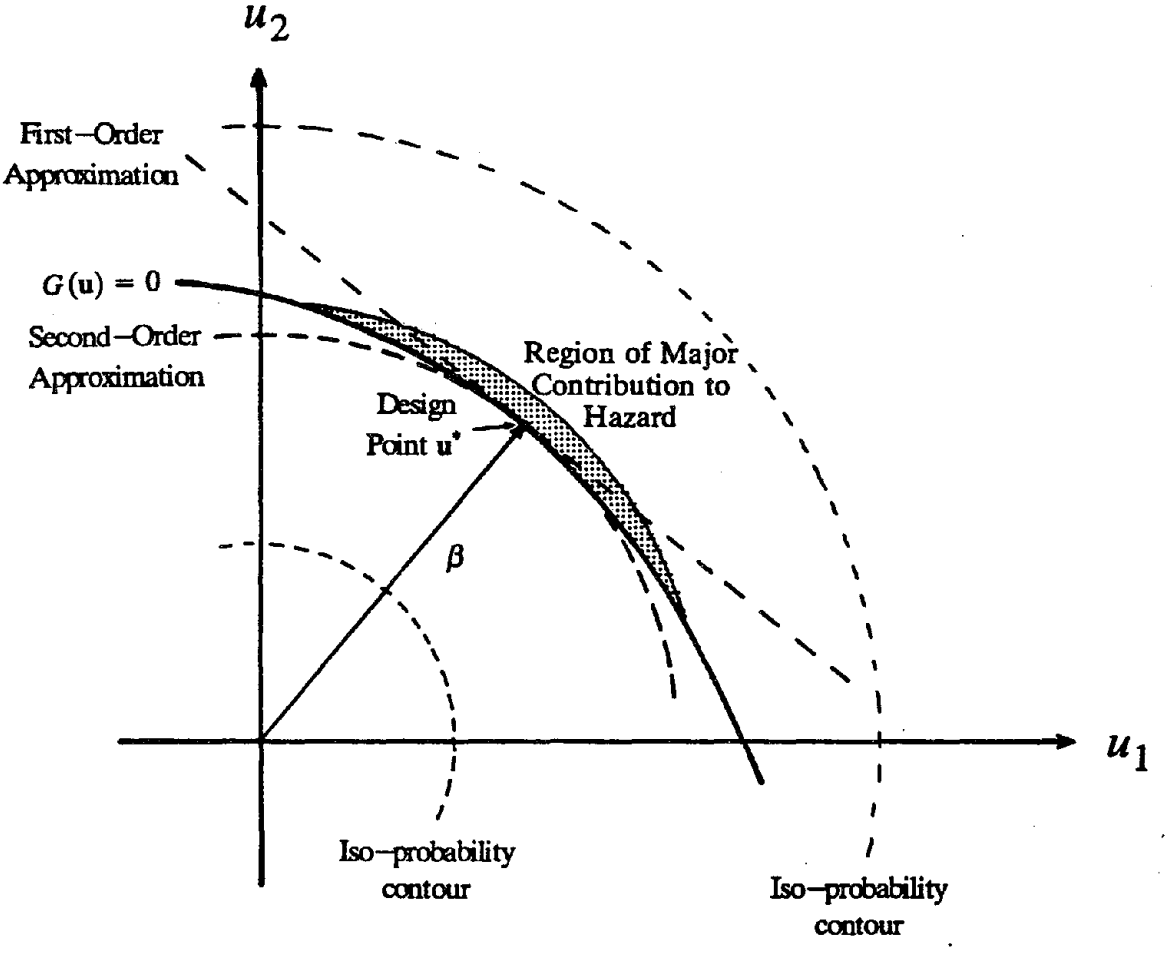

Fig. 3.1. Approximations in Standard Space

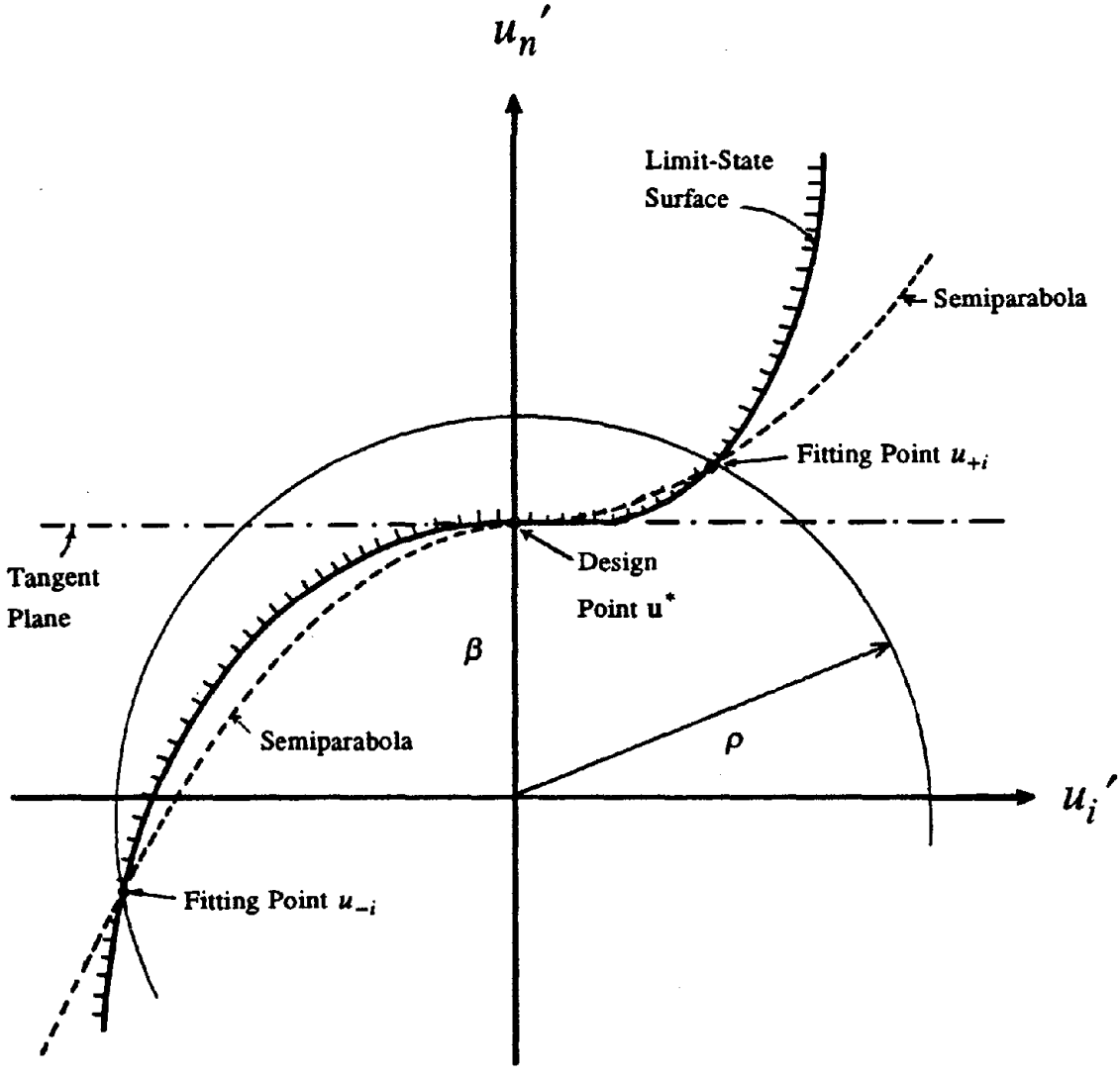

Fig. 3.2. Fitting of Paraboloid in Rotated Standard Space

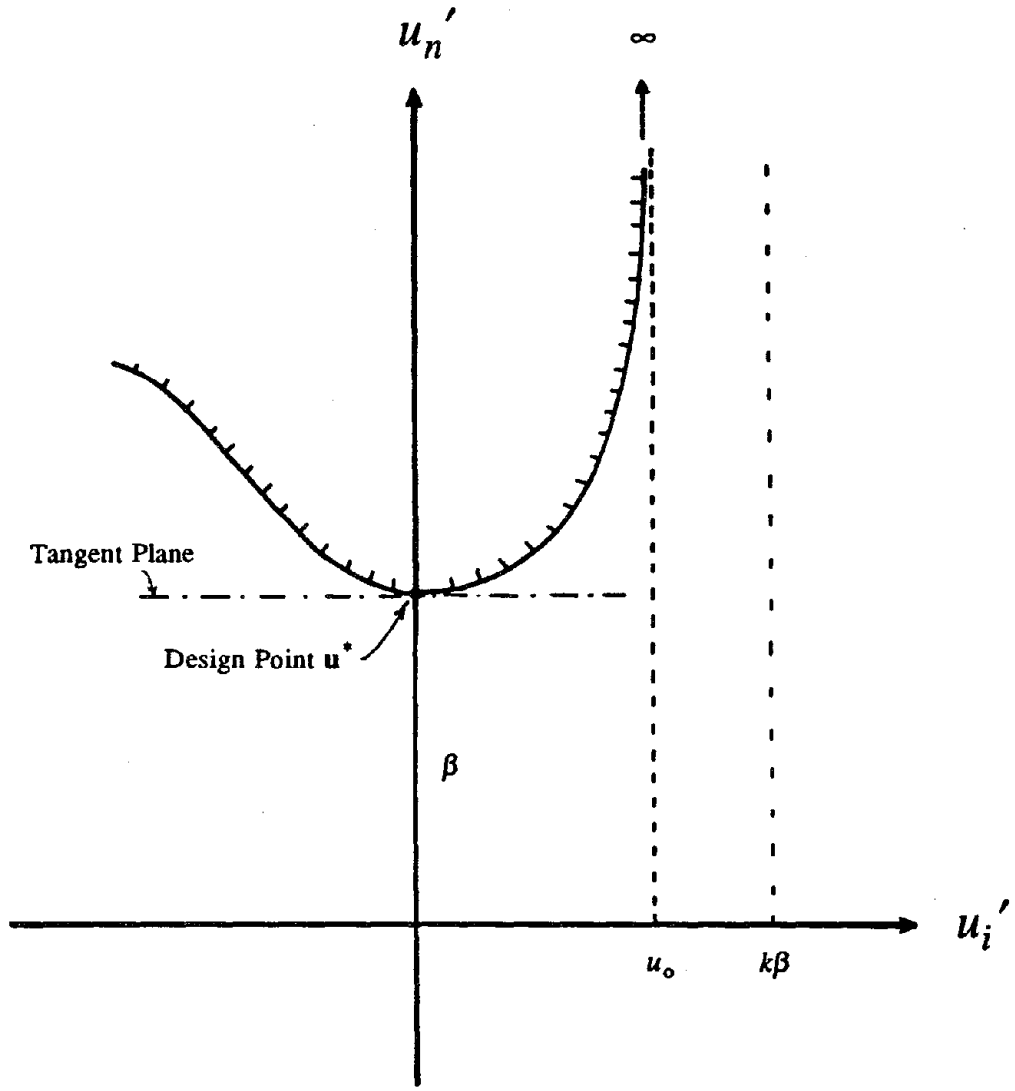

Fig. 3.3. Example Illustrating Failure of Procedure from Ref. 68 to Obtain Fitting Points

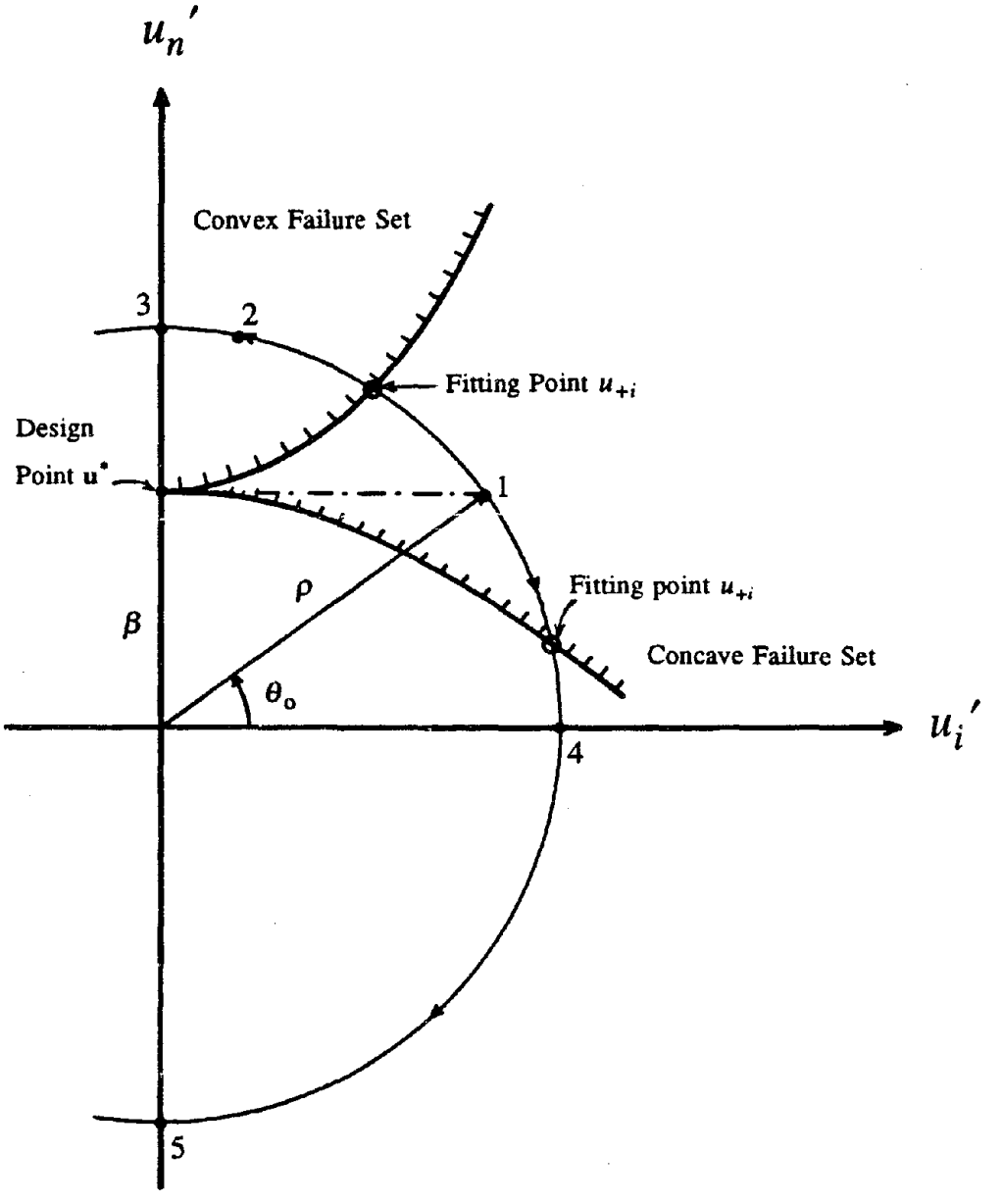

Fig. 3.4. Solution Strategy to Find the Fitting Points

Chapter 4

SEISMIC HAZARD WITH IMPROVED EARTHQUAKE MODELING

4.1. Introduction

This chapter presents a general formulation for seismic hazard analysis including the development of improved modeling of the earthquake rupture process and associated attenuation of seismic intensity. This formulation is especially suited for the solution approach presented in Chapter 3.

According to the formulation presented in Chapter 3, the seismic hazard can be expressed as the integral of the joint probability density of the random variables involved in the analysis over the domain defined by $G(\mathbf{u}) \leq 0$. In order to perform the integration, the function A_i from Eq. 3.2, i.e., the ground motion intensity descriptor in terms of the basic variables, X, needs to be specified. Several definitions of this function are examined in the following sections.

Two basic seismic source models are developed in this chapter. These models include a rather general geometric description of the earthquake source. Particular cases, such as the source models presented in Ref. 65, can be obtained as special cases of the general formulations presented here.

The models presented in this chapter are used in the numerical applications described in Chapter 5.

4.2. Improved Geometric Description of Earthquake Rupture Process

Potential sources of seismic threat for a site can be of various nature. Geologic faults are one of the most common source of seismic activity. In certain cases the geometry of the fault or system of faults is well defined, as it is the case for the San Andreas fault system in California. In other cases the geometry is rather uncertain or unknown, due to insufficient surveys or lack thereof. A review of current practice in evaluating faults for their earthquake hazard can be found in Ref. 112.

There are also seismically active areas without clearly defined features, as is the case for the seismicity zones defined in section 2.4 of Chapter 2. An example of such zone is the Charleston

region in the Eastern United States. For this reason, a comprehensive seismic hazard model must include potential sources with known, partially known and unknown fault geometry, as well as diffuse or area sources. In this study, two different source models are introduced: (a) general fault source and (b) general area source. A general formulation of these source models follows.

4.2.1. General Fault Source

This source model is basically defined as a linear fault with its main characteristics well or partially known. The uncertain characteristics of the fault may include its total length, l_f, strike, θ, and dip angle, ϕ, all of which are modeled as random variables. The position of the site with respect to the fault is assumed to be well defined.

As in Ref. 136, two alternative models of the extend of rupture along the fault are considered; namely, that the rupture may or may not extend beyond the known ends of the fault. The first situation arises when the fault ends are not well defined, or when there are reasons to believe that the rupture may propagate beyond the end points. Other example of this situation is found when fictitious ends are defined for a long fault when it is believed that events taking place beyond those points will not contribute to the hazard at the site.

The second situation is more reasonable to justify since it is believed that geologic features of this sort have definite limits. Additionally, there are specific situations when this model should be used. For instance, it is believed that bends in faults play a role in starting and stopping earthquake ruptures [105]. Thus, bends in a given fault must be defined as physical limits to ruptures occurring between them.

Since the location of the site is well defined, a set of local Cartesian coordinate system is established with its center at the site. The orientation of the axes is arbitrary but the analyst might wish to select the x-axis in the orientation of the north to make it compatible with the usual definition of the fault strike by geologists. The location of the fault is determined by the location of its end points, A and C (Fig. 4.1). Uncertainty in the length and orientation of the fault trace (defined as the projection of the fault onto the ground surface) is modeled by the random location in space of these points, the most general case being represented by the joint distribution

$f_{X_A Y_A X_C Y_C}(x_A, y_A, x_C, y_C)$.

This formulation provides maximum flexibility in modeling the uncertain geometry of a fault. For example, when the x-axis is parallel to the fault (y_A and y_C are deterministic and equal to each other), a modeling with joint distribution $f_{X_A X_C}(x_A, x_C)$ that includes a coefficient of correlation $\rho_{X_A X_C}$ near -1, will imply uncertainty only in the fault length. A joint distribution $f_{Y_A Y_C}(y_A, y_C)$ with a coefficient of correlation $\rho_{Y_A Y_C}$ near -1, and deterministic x_A and x_C can be used to model uncertainty in the fault orientation with respect to the site, and with $\rho_{Y_A Y_C}$ near 1 to model uncertainty in the distance of the fault from the site. Fault traces, although often represented as lines in maps, are actually zones of a finite width, usually of about a few kilometers. The latter modeling can be used to represent this physical situation. Obviously, many other practical situations can be represented by the aid of this formulation.

The geometric layout of this source model is depicted in Fig. 4.1. As mentioned before, the fault trace is limited by its end points A and C; ruptures may or may not be constrained by each of these ends points, as discussed before. Point B represents the perpendicular projection of the site on the fault trace. The center of the earthquake rupture is located on the fault plane (point H) and is completely defined by its horizontal distance s from the left end A of the fault trace, its depth z and the dip angle ϕ. The projection of the center of rupture on the fault trace is point F and its vertical projection onto the ground surface is point E. The position of the site with respect to the fault may be defined by the perpendicular distance from the site to the fault trace ($\overline{SB} = d$) and the lengths of the left ($\overline{AB} = l_1$) and right ($\overline{BC} = l_2$) segments of the fault defined by the projection point B. If the fault is located completely to the left of the site then l_1 is taken to be negative, if completely to the right then l_2 is taken to be negative. These distances are computed in terms of coordinates of the end points from

$$d = \frac{|(y_C - y_A)x_A - (x_C - x_A)y_A|}{\sqrt{(x_C - x_A)^2 + (y_C - y_A)^2}} = \frac{|(y_C - y_A)x_C - (x_C - x_A)y_C|}{\sqrt{(x_C - x_A)^2 + (y_C - y_A)^2}} \tag{4.1}$$

$$l_1 = \frac{|(y_C - y_A)y_A + (x_C - x_A)x_A|}{\sqrt{(x_C - x_A)^2 + (y_C - y_A)^2}} \tag{4.2}$$

$$l_2 = \frac{|(y_C - y_A)y_C + (x_C - x_A)x_C|}{\sqrt{(x_C - x_A)^2 + (y_C - y_A)^2}} \tag{4.3}$$

These definitions are similar to those used in Ref. 65 to characterize a well known fault. In addition to the coordinates of end points A and C, the dip angle ϕ is considered to be a random variable with distribution $f_{PH}(\phi)$.

The rupture is modeled as a rectangular area contained in the fault plane, as depicted in Fig. 4.1b. The rupture is defined by its center point H whose location on the fault trace and depth are random variables with joint PDF $f_{SZ}(s, z)$. The rupture can have any inclination with respect to the horizontal on the fault plane, as defined by its rake or plunge, ψ, which is also taken as a random variable with distribution $f_{\Psi}(\psi)$. The length, l_r, and width, w_r, of the rupture are expressed as functions of the earthquake magnitude, M,

$$l_r = Z_l \exp[a_l M - b_l] \tag{4.4}$$

and

$$w_r = Z_w \exp[a_w M - b_w] \tag{4.5}$$

where Z_l and Z_w are random variables that account for the uncertainty in the relations and a_l, b_l, a_w and b_w are coefficients obtained from regression analysis. The variables Z_l and Z_w are usually assumed to be lognormally distributed, which implies a possibility for an infinitely long or wide rupture. The use of truncated distributions, such as those from Table 2.2, for these variables seems to be more appropriate. As demonstrated in section 2.4 of Chapter 2, Z_l and Z_w are correlated variables. Therefore, a joint distribution model of the type in section 3.3 of Chapter 3 would be appropriate. Probability distribution models for M are discussed in Chapter 2.

A measure of distance is required for defining the attenuation law of the ground motion intensity. Several such measures have been proposed in the past, including the epicentral or hypocentral distance, the distance to the center of energy release, the shortest distance to the rupture zone or to its surface projection. Given the layout shown in Fig. 4.1, a number of such distance terms can be calculated. For this purpose, it is useful to consider the following distances: $\overline{BS'} = d\cos\phi$, $\overline{SS'} = d\sin\phi$, $\overline{BB'} = \overline{FH} = z\,\mathrm{cosec}\phi$, $\overline{BF} = \overline{B'H} = |s - l_1|$, and $\overline{EF} = z\cot\phi$.

(a) Shortest distance to the rupture:

$$R_f = \sqrt{[d\sin\phi]^2 + [\max\{0; \tilde{d}_p - w_r/2\}]^2 + [\max\{0; \tilde{d}_l - l_r/2\}]^2} \tag{4.6}$$

where $\tilde{d}_p$ and $\tilde{d}_l$ are the distances perpendicular and parallel to the rupture orientation, ψ, respectively, from the center of the rupture to the projection of the site on the inclined fault plane (Fig. 4.1b). They are given by

$$\begin{aligned}\tilde{d}_p &= \overline{S'D'} = \overline{S'B'}\cos\psi + \overline{B'H}\sin\psi \\ &= |\,|z\,\mathrm{cosec}\phi - d\cos\phi\,|\cos\psi + |s - l_1|\sin\psi\,|\end{aligned} \tag{4.7}$$

$$\begin{aligned}\tilde{d}_l &= \overline{D'H} = \overline{B'H}\cos\psi - \overline{S'B'}\sin\psi \\ &= |\,|s - l_1|\cos\psi - |z\,\mathrm{cosec}\phi - d\cos\phi\,|\sin\psi\,|\end{aligned} \tag{4.8}$$

Since the dip is measured as the smallest angle between the ground surface and the fault plane, the angle ϕ in Eqs. 4.7 and 4.8 must be replaced by $\pi - \phi$ when the plane dips away from the site.

The rupture should be constrained at least from above since it cannot extend beyond the free surface. The restriction that must be imposed is

$$z \geq [w_r/2\cos\psi + l_r/2\sin\psi]\sin\phi \tag{4.9}$$

If the rupture is constrained also from below, i.e., it cannot extend deeper than a certain depth z_m, the restriction is

$$z \leq z_m - [w_r/2\cos\psi + l_r/2\sin\psi]\sin\phi \tag{4.10}$$

When the rupture is modeled such that it is contained between the fault ends, then the random variable s is constrained by

$$l_f - [w_r/2\sin\psi + l_r/2\cos\psi] \geq s \geq [w_r/2\sin\psi + l_r/2\cos\psi] \tag{4.11}$$

The two constraints in Eq. 4.11 can be individually active or inactive, depending on whether the rupture is constrained at both ends, only at one end, or not constrained at all.

(b) Shortest distance to the projection of the rupture on the fault trace:

$$R_s = \sqrt{d^2 + [\max\{0; \hat{d}_l\}]^2} \tag{4.12}$$

where $\hat{d}_l$, the shortest distance from point B to the projection of the rupture on the fault trace is given by

$$\hat{d}_l = |s - l_1| - |l_r/2 \cos\psi| - |w_r/2 \sin\psi| \tag{4.13}$$

The same restrictions as in the previous case are imposed when the rupture is constrained within the fault end points.

(c) Distance to the center of rupture:

$$R_h = \sqrt{[d \sin\phi]^2 + [z \operatorname{cosec}\phi - d \cos\phi]^2 + [s - l_1]^2} \tag{4.14}$$

This distance may be regarded as the hypocentral distance when the dimensions of the rupture are ignored.

(d) Distance to surface projection of the center of rupture:

$$R_e = \sqrt{[d - z \cot\phi]^2 + [s - l_1]^2} \tag{4.15}$$

This distance may be regarded as the epicentral distance when the dimensions of the rupture are ignored.

The above general fault source model in special cases produces models previously used by other authors. For example, the line-rupture model of Der Kiureghian and Ang [66] is obtained by setting $w_r = 0$, $\psi = 0$ and $z = h$, and the point-rupture model of Cornell [54 , 55] is obtained by additionally setting $l_r = 0$.

4.2.2. General Area Source

Area source models are necessary for seismically active regions where no specific seismic features are known. In this model, the earthquake source is also modeled by a rupture area. However, the rupture orientation is assumed to be random, except when a preferred orientation for the source area is known. Two simple shapes are considered in this general description of the area source; namely, annular and triangular areas. A general seismic area can be described by a synthesis of these simple area source models.

(1) **Annular Region.** This area is defined in polar coordinates as depicted in Fig. 4.2a. The radial and angular coordinates of the annular area are constrained by $\rho_a \leq \rho \leq \rho_b$ and $\theta_a \leq \theta \leq \theta_b$. The depth is measure along a z coordinate.

The site is assumed to be located at the origin of the coordinate system, i.e., $\rho = \theta = z = 0$. The location of the center of the rupture in the seismic source is random and defined by its coordinates, ρ, θ and z, with joint PDF $f_{P\Theta Z}(\rho, \theta, z)$. The horizontal distance between the vertical projection of the site on the horizontal plane $Z = z$ and the center of the rupture is $d = \rho$.

The total area of this region is given by

$$A_{an} = \frac{1}{2}(\rho_a{}^2 - \rho_b{}^2)(\theta_a - \theta_b) \tag{4.16}$$

This value is used when contribution of the seismicity of each subarea, $A_{an,i}$, to the seismicity of the total area, $A_{tot} = \sum_i A_{an,i}$, is to be evaluated,

When the center of rupture is equally likely to occur anywhere within the area source, ρ and θ are independent and uniformly distributed random variables with the joint PDF

$$f_{P\Theta}(\rho, \theta) = \frac{\rho}{A_{an}} \qquad \rho_a \le \rho \le \rho_b \;,\; \theta_a \le \theta \le \theta_b \tag{4.17}$$

However, one can specify any joint distribution $f_{P\Theta Z}(\rho, \theta, z)$ that represents the likelihood of earthquake occurrences within the seismic area.

(2) **Triangular Region**. This shape is selected for its versatility and simplicity. A general triangle is defined by the coordinates of its vertices, as shown in Fig. 4.2b, the only condition being that the three vertices not be aligned. The area of the triangular region is

$$A_{tr} = \left[s \prod_{i=1}^{3} (s - l_i) \right]^{\frac{1}{2}} \tag{4.18}$$

where $s = (l_1 + l_2 + l_3)/2$, and l_1, l_2 and l_3 are the lengths of its sides. These lengths can be obtained from the coordinates of the vertices as

$$l_j = \sqrt{(x_j - x_{j+1})^2 + (y_j - y_{j+1})^2} \qquad j = 1,2 \text{ or } 3 \tag{4.19}$$

where $x_4 \equiv x_1$ and $y_4 \equiv y_1$. As for the previous case, this value of the area is used when the contribution of the seismicity of each subarea, $A_{tr,i}$, to that of the total area, $A_{tot} = \sum_i A_{tr,i}$, is to be evaluated.

The deterministic coordinates $(x_s, y_s, 0)$ specify the location of the site. The location of the center of the earthquake rupture is randomly distributed over the entire seismic source. Its coordinates (x, y, z) are assumed random variables characterized by their joint PDF $f_{XYZ}(x, y, z)$. When the likelihood of earthquake occurrences is uniform within the seismic area, then the joint PDF of the coordinates of the center of the rupture is $f_{XYZ}(x, y, z) = f_{XY}(x, y) f_Z(z)$, where

$$f_{XY}(x, y) = \frac{1}{A_{tr}} \qquad (x, y) \in \Omega \tag{4.20}$$

where Ω represents the triangular seismic region, and $f_Z(z)$, the distribution in depth of earthquake occurrences, can be any suitable PDF. When the seismic area is composed of several of these subareas, A_{tr} should be replaced by A_{tot} in Eq. 4.20, and Ω represents the total seismic region considered.

The horizontal distance between the vertical projection of the site on the horizontal plane $Z = z$ and the center of the rupture, is given in this model by

$$d = \sqrt{(x_s - x)^2 + (y_s - y)^2} \tag{4.21}$$

Once the position in space of the center of the rupture is located, its size and orientation remain to be defined. The size is defined in an analogous manner to the previous case, by means of Eqs. 4.4 and 4.5, since the rupture is modeled as rectangular. The orientation of the earthquake rupture is defined by its strike and dip, which are considered random variables with their associated PDF's as in the preceding general fault model. For simplicity, the rake or plunge of the rupture is assumed to have a deterministic value $\psi = 0$. If information about distribution of the plunge of ruptures is available, it can be easily incorporated in the analysis.

For a given location of the center of the earthquake rupture (x, y, z), in Cartesian coordinates, the characteristics of the rupture and associated distances to the site are shown in Fig. 4.3. Expressions for these quantities are summarized below

$$\tilde{d}_p = |(x - x_s)\sin\alpha - (y - y_s)\cos\alpha| \tag{4.22a}$$
$$\tilde{d}_l = |(x - x_s)\cos\alpha + (y - y_s)\sin\alpha| \tag{4.22b}$$
$$d_1 = |z\cos\phi + \tilde{d}_p \sin\phi| \tag{4.22c}$$
$$d_2 = |z\sin\phi - \tilde{d}_p \cos\phi| \tag{4.22d}$$

$$d_3 = \tilde{d}_l \tag{4.22e}$$

where the orientation of the rupture is defined by the strike α, and dip, ϕ, angles. The different measures of distance are presented below for this type of source model.

(a) Shortest distance to the rupture:

$$R_f = \sqrt{d_1^2 + [\max\{0; d_2 - w_r/2\}]^2 + [\max\{0; d_3 - l_r/2\}]^2} \tag{4.23}$$

(b) Shortest distance to the projection of the rupture on the fault trace:

$$R_y = \sqrt{[d_1 \operatorname{cosec}\phi]^2 + [\max\{0; d_3 - l_r/2\}]^2} \tag{4.24}$$

(c) Distance to the center of rupture:

$$R_h = \sqrt{(x_s - x)^2 + (y_s - y)^2 + z^2} \tag{4.25}$$

(d) Distance to surface projection of the center of rupture:

$$R_e = d = \sqrt{(x_s - x)^2 + (y_s - y)^2} \tag{4.26}$$

When the rupture is not horizontal but with a plunge, ψ, d_2 and d_3 in the above formulas should be replaced with $d_2 \cos\psi + d_3 \sin\psi$ and $d_3 \cos\psi - d_2 \sin\psi$, respectively.

The particular area source models shown in Fig. 2.2 can be obtained from the above general area source modeled as follows: (a) the model for area with preferred fault orientation is obtained with deterministic depth $z = h$, strike $\alpha = \alpha_o$, dip $\phi = 0$, and rupture width $w_r = 0$; (b) the model for area with unknown faults is the same as (a) but with random strike uniformly distributed between 0 and 2π; and (c) the model for uniform seismicity is obtained with an annular region having $\rho_a = 0$, $\rho_b = r$, $\theta_a = 0$, $\theta_b = 2\pi$, and with deterministic depth $z = h$, dip angle $\phi = 0$, and rupture width $w_r = 0$.

4.3. Improved Modeling of the Attenuation Law

In the current practice, models of earthquake intensity attenuation are restricted to functional forms of the type given by Eq. 2.27, that include only two independent random variables. Such models are clearly crude representations of the actual attenuation of seismic waves. The independent variables are a measure of distance, R, and a measure of the earthquake size, generally the magni-

tude M. However, no consensus has yet been reached on the precise definition of either variable. Several measures of distance have been proposed, which were discussed earlier. For sites located several source dimensions away from the source, there is little difference between the various distance measures. On the other hand, for shorter distances, the difference between the various distance measures becomes significant.

The earthquake magnitude also has its limitations. There are a variety of magnitude scales and that often leads to confusion. Most of them, except moment magnitude, saturate as the size of the earthquake increases. Bolt [25] argues that the magnitude is not a robust scaling factor for ground motion intensity attenuation. He favors stress drop, among the presently defined source parameters, as the most satisfactory to describe the local intensity of shaking.

To overcome these and other difficulties, a general formulation of the attenuation law is considered. Let **X** be a vector containing all random variables that affect the intensity attenuation in a region of interest. The elements of **X** may include source parameters, e.g., stress drop, fault slip, corner frequency, cut-off frequency; rupture propagation parameters, e.g., duration, velocity, direction of propagation; barriers (or asperities) characteristics; properties of the ground medium, e.g., rigidity, shear wave velocity, density; etc. Also let **P** denote a vector of parameters that influence the ground motion and are predictable in advance. Examples for the components of this vector are parameters that define the type of faulting or mechanism, the type and depth of soil or rock and topographic features on which the site is located, and the type and size of the structure that will experience the shaking. In most cases, the components of this vector are indicator variables, taking the values one or zero, depending on whether a specified condition is satisfied or not. Finally, let **C** denote a vector of the constants defining the attenuation model, which are obtained from regression analysis of recorded data. A general representation of the attenuation law is

$$\mathbf{Y} = \mathbf{Y}(\mathbf{X}, \mathbf{P}, \mathbf{C}) \tag{4.27}$$

Simple versions of this representation are the attenuation relationships reported in recent years by Cambpell [43], Joyner and Boore [97], Bolt and Abrahamson [28], Brillinger and Preisler [37 , 38] and others (See Table 4.1). An enhanced example of this representation is developed below.

4.3.1. Model with Source Directivity Effect

Focusing effects of ground motion intensity due to propagating ruptures have been recognized for quite some time. The ground motion felt within a small azimuth from the direction of rupture is considerably larger in amplitudes and with higher frequency content than that observed in other directions. Theoretical seismologists were the first to develop interest in the problem of azimuthal variation of the characteristics of a seismic signal due to the movement of the emitting source. Later, due primarily to observed patterns of damage in earthquakes, the engineering profession became aware of the importance of such phenomenon. Discussions and references on the problem can be found for example in Ref. 27.

Although this phenomenon has been known for some time now, it is only recently that the influence of the directivity effect on seismic hazard has been investigated [10]. In that study it was concluded that the directivity effect is significant, particularly at high acceleration levels (low hazard levels), which are of engineering interest. At such levels, the effect of the directivity is an increase in the hazard by a factor of around 10 to 20 for an example case. The corresponding acceleration level for a fixed hazard is increased by a factor of two to three. These results are consistent with a rule of thumb proposed by McGuire [127]: "A change in assumptions that results in a factor X change in the annual probability of exceedance at a given ground motion level, will result in cube-root of X change in the ground motion for a target annual probability".

The effect of the moving rupture is incorporated in the attenuation law by means of a directivity factor that modulates the intensity

$$a_{rms} = \frac{M_0}{4\pi\rho {v_s}^3} \frac{\exp[-q\,R]}{R} \frac{1}{(K_t^{-1})^3} \left[\frac{K_t^{-1}}{T_r}\right]^{\frac{1}{2}} D(\gamma, Mc) \tag{4.28}$$

in which a_{rms} is the root-mean-square acceleration, M_0 is the seismic moment, v_s is the shear-wave velocity, R is the distance from the source to the site, ρ is the density of the medium of propagation of waves, K_t^{-1} is the correlation time of the stochastic rupture model, q is an inelastic attenuation parameter, T_r is the duration of the rupture also called faulting duration, and $D(\gamma, Mc)$ is a directivity factor given by

$$D(\gamma, Mc) = \frac{1}{2 - Mc\cos\gamma}\left[\frac{3 - Mc\cos\gamma}{1 - Mc\cos\gamma}\right]^{\frac{1}{2}} \tag{4.29}$$

in which $m = v_r/v_s$, the ratio of the rupture velocity, v_r, to the shear wave velocity, v_s, is the seismic Mach number and γ is the angle between the direction of the rupture propagation and the radius vector from the reference point on the rupture to the site. This attenuation law was proposed by Faccioli [78] based on the theoretical model of the rupture mechanism developed by Haskell [86]. This attenuation relationship was tested for a number of earthquake records (49 records from 11 earthquakes worldwide), ranging from local magnitude $M_L = 4.7$ to surface wave magnitude $M_s = 7.7$, from a variety of tectonic settings and at hypocentral distances of 5 to 100 km. Predicted values are reported to be within $\pm 50\%$ of the observed ones in 42 of the records, including the Pacoima Dam record.

There is theoretical and empirical evidence of correlation between K_i^{-1} and M_o. Faccioli [78], using records from earthquakes in Italy and Yugoslavia found the relationship

$$\ln K_i^{-1} = (0.26 \pm 0.02)\ln M_o - (16.08 \pm 0.99) \tag{4.30}$$

This equation has good agreement with the relation $K_i^{-1} \propto M_o^{0.27}$ obtained on purely seismological grounds [86]. For the value of T_r, the faulting duration, a relation of the form $T_r = b_1 M_o^{b2}$ was fitted [78] to a set of observations (15 in total) corresponding to earthquakes from the Western US, Friuli, Montenegro and Japan. The prediction equation is

$$T_r = 7.05 \times 10^{-6} M_o^{0.23} \tag{4.31}$$

with a standard deviation of 1.9 sec. Based on observational evidence, an approximate relation between seismic moment, M_o, and seismic magnitude, M, is given by [102]

$$\log M_o = 1.5M + 16 \tag{4.32}$$

Replacing the functional relations for K_i^{-1} and T_r in terms of M_o, and the latter in terms of the preceding equation, Eq. 4.28 may be written in the familiar form

$$a_{rms} = \frac{c_1 e^{c_2 M - c_3 R}}{(R + c_4)} D(\gamma, Mc) \tag{4.33}$$

where c_1, c_2, c_3 and c_4 are regional constants that must be obtained through regression analysis.

The addition of c_4 to R in the denominator is done primarily to extend the applicability of the present model to the near-field, thus avoiding divergence of Eq. 4.33 when R approaches zero. Also, the distance term R is interpreted here as the nearest distance from the recording site to the rupture trace to account for the rupture dimension and to be consistent with the rupture model used in the analysis. In that model, the intensity of ground motion is assumed to depend mainly on the portion of the rupture that runs closest to the site. Although this definition is generally regarded as better than the epicentral or hypocentral distance, it has its own shortcomings. In particular, the directivity effect on the seismic intensity at a site is produced by the contribution of all ruptures occurring along the entire segment that breaks during the earthquake. Therefore, a measure of significant distance that is a sort of average between the distance from the point where the rupture starts and that where it stops, seems more consistent with the physics of the problem. (In all this discussion it is assumed that the rupture is unilateral, i.e, it propagates in only one direction). The definition of elliptical distance by Bureau [42], as the average of the distances from the site to the ends of the fault surface rupture, satisfies this condition.

The angle γ in the directivity function is defined in the present study as the angle formed by the trace of the rupture and the horizontal line joining the epicenter and the site. This selection is made to simplify the solution procedure since it is not yet clear which angle influences directivity. The use of this angle or that defined previously, will make little difference in the analysis, since directivity effects are observed mainly in the near-field where the differences between such angles is small. On the other hand, greater uncertainties are involved due to factors that often mask focusing effects like scattering, attenuation, and source asperities.

Similarly to an average measure of distance, one can define an average measure of the angle γ to be used in the directivity function. This can be particularly meaningful when long ruptures run close to the site. Consistent with the use of the elliptical distance, γ can be defined as the half angle formed by the lines joining the site and the end points of the fault. For sites located in the forward or backward direction of the rupture propagation, this definition makes no significant changes in the directivity function with respect to the previous definitions. The differences arise when the length of

the rupture is large compared to the distance from the site to the rupture. To compare the results, consider the following example: the site is located at a perpendicular distance of 10 km from the middle of a rupture with length of 100 km. The value of the angle formed by the trace of the rupture and the horizontal line joining the epicenter and the site is $\gamma_1 = 0.1974$ rad. The value of the half angle formed by the lines joining the site and the end points of the fault is $\gamma_2 = 1.3734$ rad. The ratio $r_D = D(\gamma_1, Mc)/D(\gamma_2, Mc)$ depends also on the value of the seismic Mach number Mc. For this example, r_D varies from 1.93 to 5.02 when Mc varies from 0.65 to 0.95. This is a significant difference and the validity of either definition of γ, as well as the definition of the measure of distance, should be examined with data from future well instrumented earthquakes.

The directivity effect is largely influenced by the seismic Mach number. This influence is more dramatic for seismic Mach numbers close to unity. It has been reported (Refs. 32 and 33, for example) that this parameter has a striking effect on the normal component of the near-fault motions, but a small effect on the radial motion.

At the present time, Eq. 4.33 should be regarded merely as a plausible model for the attenuation law. Recordings showing this effect are presently scarce. The model should be tested against data collected from future earthquakes. It was recently brought to the author's attention that Campbell [45] is in the process of including directivity as a parameter in regression analysis of earthquake data. He applied it to only 3 recordings out of a total of 134, acknowledging that other recordings in the data set might also be "affected to some degree" by directivity. This seems to be the first attempt to empirically incorporate source directivity effects in attenuation relations and is a clear evidence of the paucity of data.

The model for seismic intensity attenuation incorporating the source directivity effect is one example of an improved attenuation model that can be used with the seismic hazard formulation developed in this study.

4.3.2. Band Limited White Noise Model

Physical models of the energy release and of the attenuation of energy with distance recently have been gaining interest in ground motion estimation. One of these, presented as an example, is

the model developed by Hanks and McGuire [85]. Using an operation of Parseval's theorem on the Brune source model [39 , 40], the RMSA for far-field shear waves in the presence of anelastic attenuation is expressed as

$$a_{rms} = 0.85 \frac{(2\pi)^2}{106} \frac{\Delta\sigma}{\rho R} \left[\frac{f_{max}}{f_o} \right]^{\frac{1}{2}} \tag{4.34}$$

where a_{rms} is given in cm/sec^2, $\Delta\sigma$ is the earthquake stress drop in bars, ρ is the crustal density in gm/cm^3, R is hypocentral distance in kilometers, f_{max} is the highest frequency passed by the accelerograph or the Earth's attenuation, and f_o is the spectral corner frequency for the far-field shear radiation, both in hertz.

The factor 0.85 in Eq. 4.34 accounts for the average S-wave radiation pattern, free surface amplification and the assumption that the energy is equally partioned into two horizontal components. The corner frequency is related to the seismic moment, M_o, by the expression [39 , 40]

$$f_o = \left[\frac{\Delta\sigma \, v_s^{\,3}}{8.47 M_o} \right]^{1/3} \tag{4.35}$$

where v_s is shear-wave velocity in km/sec, and M_o is measured in dyne-cm. Any of the quantities involved in Eq. 4.34 can be regarded as random variables; however, only an analysis of sensitivities can assess the relative importance of each variable on the estimated seismic hazard.

Although there are different opinions on what values of stress drop should be used, Hanks and McGuire report a relatively stable value of 100 bars (within a factor of 2) for most earthquakes they analyzed. The observed spread in the values can be modeled with a probability distribution for $\Delta\sigma$.

From the RMSA, peak acceleration values and ordinates of linear response spectra can be obtained using results from random vibration theory. Thus, the Band Limited White Noise (BLWN) model provides a comprehensive, physically based method of estimating earthquake ground motions, which can have a particular advantage over empirical methods when data is scarce. It is likely that ground motion models of this type will have wide use in the future. Additional studies on this topic can be found in Refs. 129 , 31 , 128 , 12 and 162, for example.

4.3.3. Hazard-Consistent Earthquake Motion Model

Kameda and Nojima [100] present a novel formulation to determine hazard-consistent earthquake motion, that combines hazard analysis and stochastic models of ground motion. In their analysis, the stochastic model for the ground motion is specified in terms of a number of parameters which are all expressed as functions of the earthquake magnitude and distance. Attenuation laws relating each parameter to the earthquake magnitude, M, and epicentral distance, R_e, are developed by regression analysis. Following Kameda and Nojima [100], let the ground acceleration process be represented by

$$\ddot{u}_r(t) = \sum_{k=1}^{m} \sqrt{2 G_r(t, \omega_k)\, \Delta\omega} \cos(\omega_k t + \phi_k) \tag{4.36}$$

in which $G_r(t, \omega_k)$ is the Evolutionary Power Spectral Density (EPSD) at time t and angular frequency ω_k; ϕ_k are independent random phase angles uniformly distributed between 0 and 2π, and m is the number of superposed harmonic components. The EPSD is modeled by

$$G_r(t, 2\pi f) = \alpha_f(t) \frac{2\zeta_r}{\pi^2 f_p} \frac{(f/f_p)^2}{[1-(f/f_p)^2]^2 + 4\zeta_r^2 (f/f_p)^2} \tag{4.37}$$

where f_p is the stationary predominant frequency, ζ_r is the spectral shape parameter, and $\alpha_f(t)$ is a modulating intensity function described by

$$\alpha_f(t) = \delta^2 (t/t_m)^2 \exp[2(1 - t/t_m)] \tag{4.38}$$

in which t_m is the time to the maximum of $\alpha_f(t)$ and $\delta = \sqrt{\alpha_f(t_m)}$ is the peak mean-square acceleration. Regression equations were developed for the model parameters δ, t_m, f_p and ζ_r in terms of magnitude and epicentral distance. These relationships can be expressed in a vector form as in Eq. 3.1, where $\mathbf{Y} = (\delta, t_m, f_p, \zeta_r)$ and $\mathbf{X} = (M, R_e)$. They are,[100]:

$$\delta = \frac{89.125\, e^{1.237M}}{(R_e + 30)^{1.991}} \tag{4.39}$$

$$t_m = 19.77 - 7.35M + 0.7196M^2 + 0.0023(M-1)R_e \tag{4.40}$$

$$f_p = 4.124 + (0.0115 - 0.0048M + 0.000272M^2) R_e + 10^{-4} \times (-0.7959 + 0.2577M - 0.01743M^2) R_e^2 \tag{4.41}$$

$$\zeta_r = -0.2306 + 0.2967M - 0.0174M^2 + (-0.0193 + 0.0049M - 0.0003M^2) R_e \tag{4.42}$$

where R_e is expressed in km and M is the magnitude. The predominant frequency f_p has a lower

bound that depends on magnitude M such that

$$(f_p)_{\min} = 6.78 \exp[-0.23M] \tag{4.43}$$

These regression equations are valid only for epicentral distances $R_e \geq R_{e_o}$, where

$$R_{e_o} = 1.06 \exp[0.557M] - 30 \tag{4.44}$$

for $M > 6.0$. The ground motion for the near-field region ($R_e < R_{e_o}$) is assumed to have uniform intensity, whereby the earthquake parameters are determined with $R_e = R_{e_o}$.

Performing a conventional seismic hazard analysis, Kameda and Nojima [100] obtain the peak rms acceleration level, δ_o, for a specified level of the hazard, h_o. The parameters in the stochastic model for the given hazard are then determined as the conditional expectations given that the peak RMSA is equal to or greater than δ_o. They select this approach partly because of the limitations of conventional seismic hazard analysis techniques. Hazard-consistent time histories for the selected hazard level are simulated by use of Eq. 4.36 and the conditional means of the parameters.

The method to obtain the value of the variables needed for the simulation is slightly modified in the present study. The procedure adopted is as follows: (a) perform a seismic hazard analysis for the peak rms acceleration, δ, and obtain the threshold corresponding to the selected hazard level; (b) determine the most likely magnitude and distance associated with the selected hazard level; (c) obtain the remaining parameters by replacing in their attenuation relations the most likely values of the magnitude and epicentral distance. An earthquake ground motion generated based on such values of the parameters may be regarded as a sample history of the most likely stochastic ground motion model for the specified level of the seismic hazard.

In their analysis, Kameda and Nojima [100] included uncertainty only in the attenuation equation for the intensity parameter δ as an additional random variable Z_δ that multiplies such relation. This variable, when included in the analysis, is assumed to be lognormally distributed with median of 1.0 and coefficient of variation equal to 0.427. Uncertainty in the model parameters should be incorporated by means of random variables multiplying their respective attenuation relations and accounting for the dispersion in the regression. These random variables, denoted by $\mathbf{Z} = (Z_\delta, Z_{t_s}, Z_{f_p}, Z_\zeta)$, are correlated among themselves and are described by their joint PDF,

$f_Z(z)$.

Site Effects. The simulated ground motion obtained from Eq. 4.36 corresponds to the motion at the baserock level. An approximation of the movement at the surface level is obtained by applying conversion factors to the EPSD of the baserock motion. These factors account for the nonlinear effect of the overlaying soils on the intensity and frequency content of the transmitted motion. The transformation from baserock to soil surface motion is performed by

$$G_s(t, 2\pi f) = [H_r(f)]^2 G_r(t, 2\pi f) \tag{4.45}$$

where the conversion factor is represented by the filtering function

$$H_r(f) = \frac{1 + 2a^2(f/f_s)^2}{[1-(f/f_s)^2]^2 + 4h_s^2(f/f_s)^2} \tag{4.46}$$

Model parameters f_s, h_s and a are determined by an approximate procedure described by Kameda [99]. Three values, β_1, β_2 and β_3, of the "exact" filtering function, $\beta_\alpha(f)$, defined as the ratio between observed EPSD at surface and baserock levels are obtained for three selected frequencies f_1, f_2 and f_3. This filtering function is given in terms of the blow-count profile of the site, $N(z)$, the depth of soil surface to bedrock, z_r, and the rock motion EPSD, $G_r(t_m, 2\pi f)$. A system of three equations is established for the three model parameters by equating the values of the "exact" to the "approximate" filtering function given by Eq. 4.46. The solution of these three equations provides the values of the parameters in Eq. 4.46. The earthquake acceleration at the ground level is then represented by

$$\ddot{u}_s(t) = \sum_{k=1}^{m} \sqrt{2 G_s(t, \omega_k)\, \Delta\omega}\, \cos(\omega_k t + \phi_k) \tag{4.47}$$

which can be used to generate sample time histories. One interesting application with the above model is to select a more general intensity measure for the seismic hazard analysis that incorporates all variables involved in the description of the ground motion model. For this purpose, it is necessary that the intensity measure be in terms of the individual time history. A good choice is Arias' intensity defined by

$$I_A = \frac{\pi}{2g} \int_0^{t_*} [\ddot{u}_s(t)]^2\, dt \tag{4.48}$$

where $\ddot{u}_g(t)$ is given by Eq. 4.47 and t_o is the total duration of the earthquake ground motion. The vector of basic random variables includes $\mathbf{X} = (M, R_e, Z_\delta, Z_{t_m}, Z_{f_p}, Z_\zeta)$ and the vector of model parameters **Y** is obtained from Eqs. 4.39-4.42, where the variables Z multiply each attenuation relation. During the process of solution, the set of most likely values for the basic random variables, $\mathbf{x}^*$, is obtained. The set of most likely values for the model parameters, $\mathbf{y}^*$, is then obtained from this last vector. Samples of this most likely ground motion stochastic model for given probability of exceedance of I_A is obtained by replacing these parameters and variables in Eq. 4.47.

Table 4.1. Recent Examples of Strong-Motion Attenuation Relations

Y	X	$a_i(.)$	C	σ_{Z_y}	Reference
PHA_m	R_f $M \begin{cases} M_l\ (M<6) \\ M_s\ (M>6) \end{cases}$ Z_y	$Z_y \dfrac{c_1 e^{c_2 M}}{(R_f + c_4 e^{c_5 M})^{c_3}}$	$c_1 = 0.0159$ $c_2 = 0.868$ $c_3 = 1.09$ $c_4 = 0.0606$ $c_5 = 0.70$	0.37	Campbell [43]
PHA_l	R_s M Z_y	$Z_y \dfrac{c_1 e^{c_2 M}}{(R_s^2 + c_4^2)^{1/2}}$	$c_1 = 0.0955$ $c_2 = 0.573$ $c_3 = 1.0$ $c_4 = 7.3$	0.26	Joyner-Boore [97]
PHA_l	R_s M Z_y	$Z_y \dfrac{c_1 e^{c_2 M}}{[(R_s + c_4)^2 + 1]^{c_3}}$	$c_1 = 1.6$ $c_2 = -0.026$ $c_3 = 0.19$ $c_4 = 8.5$	0.09	Bolt [28]
PHA_l	R_s M Z_y	$\ln^3 \left[Z_y \dfrac{c_1 e^{c_2 M}}{(R_s^2 + c_4^2)^{c_3}} \right]$	$c_1 = 1.540$ $c_2 = 0.110$ $c_3 = 6.35$ $c_4 = 0.0947$	variable	Brillinger [37]

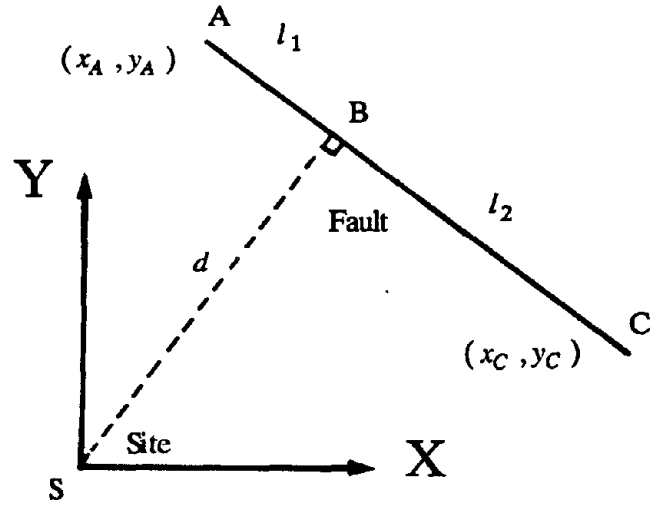

(a) Plan View

(b) Isometric View

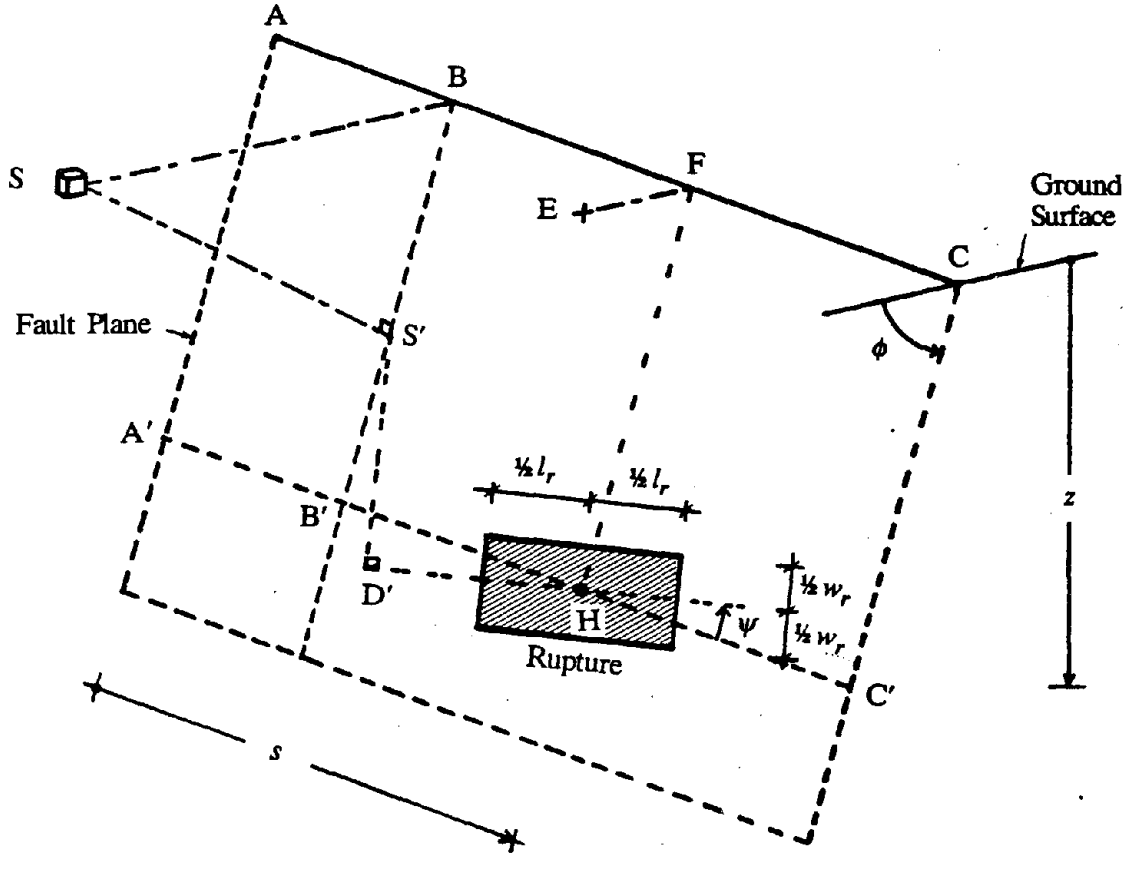

Fig. 4.1. Geometric Description of Earthquake Rupture on General Fault Source

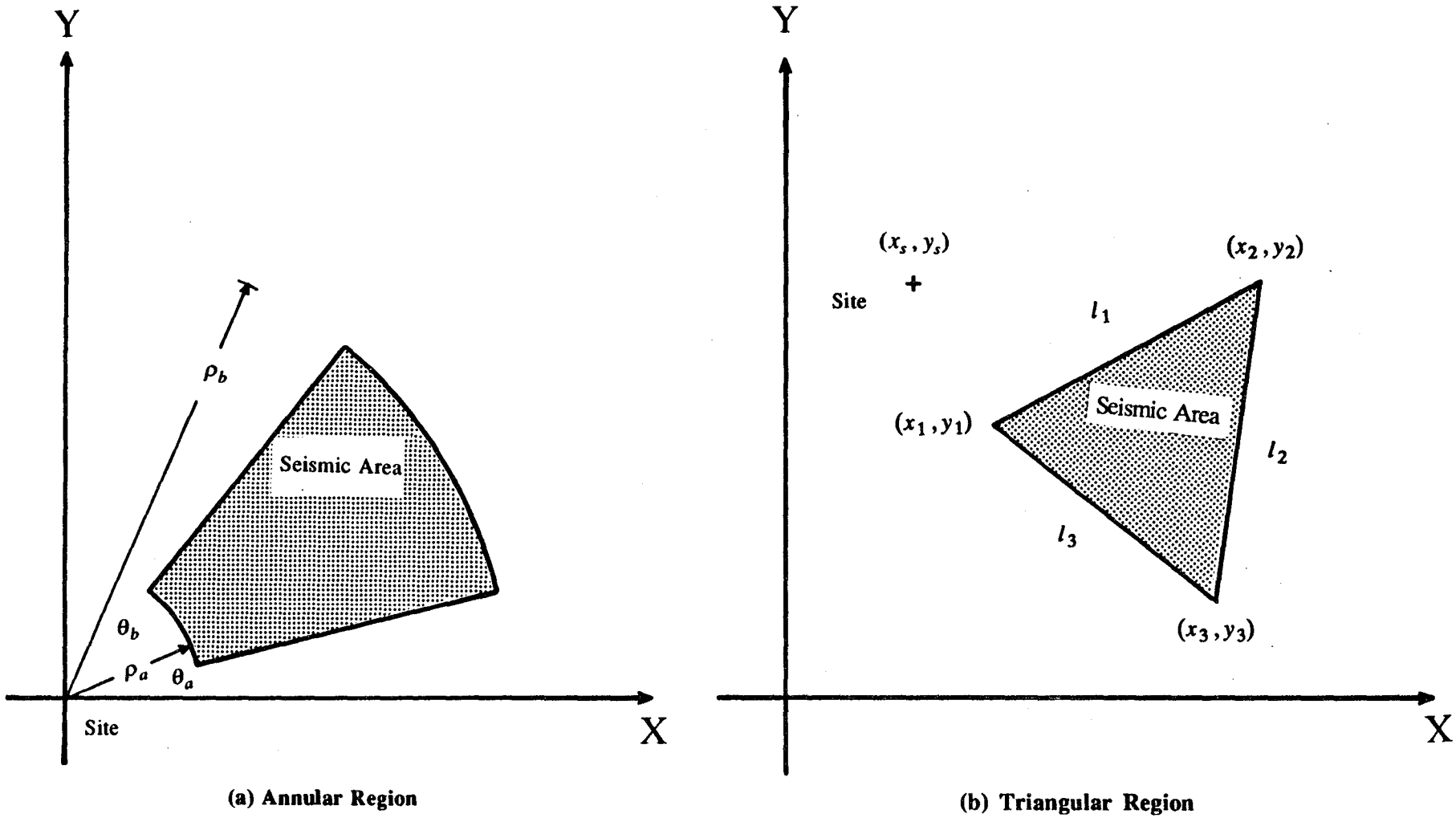

(a) Annular Region

(b) Triangular Region

Fig. 4.2. General Area Source Model

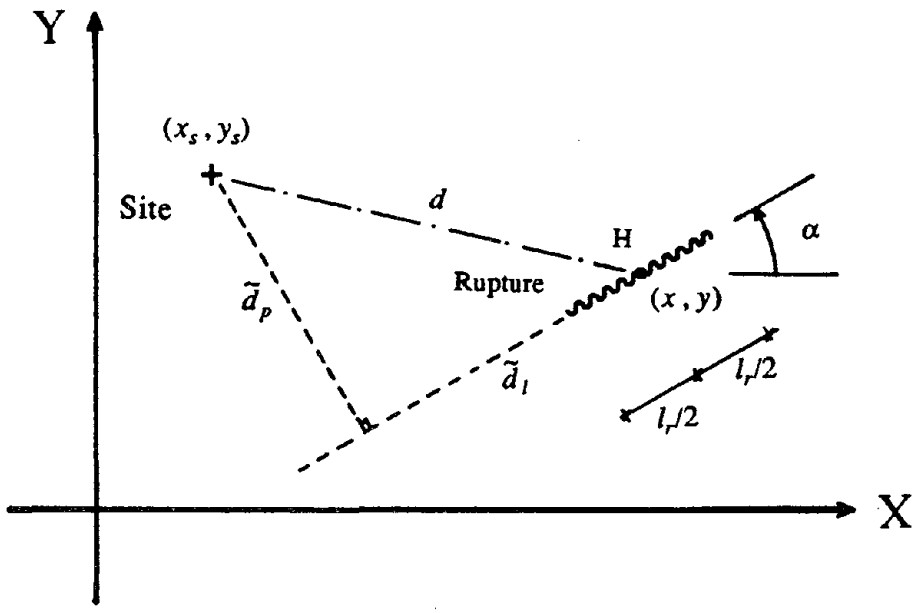

(a) Horizontal Plane Containing Center of Rupture

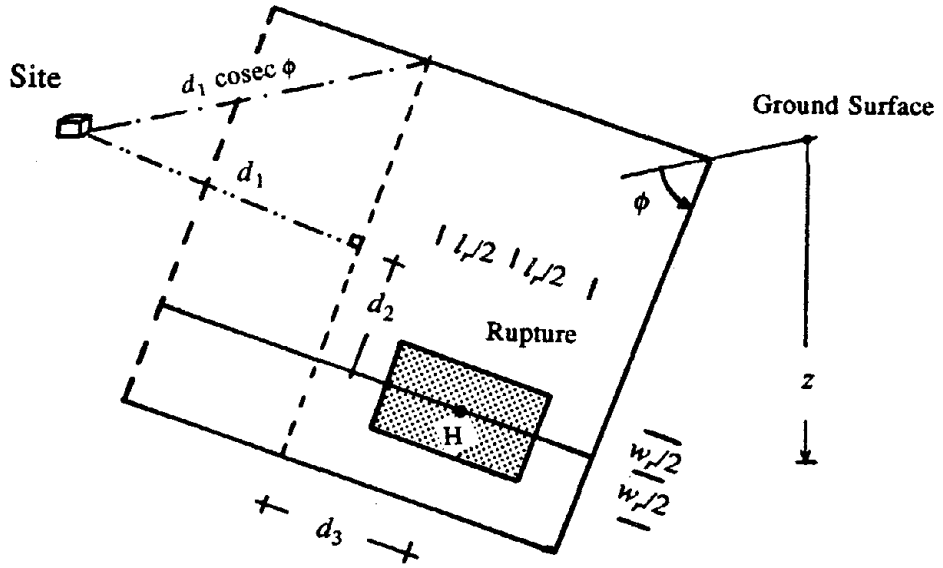

(b) Isometric View

Fig. 4.3. Geometric Description of Earthquake Rupture on General Area Source

Chapter 5

APPLICATIONS

5.1. Introduction

In order to test the accuracy of the proposed approximate methods of seismic hazard analysis, several example applications are examined in this chapter. The FORM and SORM results are compared with results obtained from direct numerical integration or from simulation procedures. In addition, several applications are presented to demonstrate the versatility of the proposed formulation. These include an application incorporating the source directivity effect and characteristics of the rupture process in the attenuation model and a procedure to define hazard-consistent earthquake acceleration time-histories. One objective of these applications is to demonstrate the advantages of the proposed methodology over existing procedures of seismic hazard analysis by direct numerical integration. Since solution by conventional methods is not feasible for several of these applications, simulation techniques are used to determine the "exact" value of the seismic hazard.

5.2. Accuracy of FORM and SORM for Seismic Hazard Analysis

Two examples are used to check the accuracy of the FORM, SORM-CF and SORM-PF methods presented in Chapter 3. These examples cannot provide a definitive measure of the accuracy, as the magnitude of the error depends on each particular case. However, they do provide estimates of the errors that can be expected in typical seismic hazard problems.

Example 1 – Seismic hazard for a site near a fault

The seismic hazard for peak ground acceleration at a site close to a long, linear fault is considered. The layout of the problem, shown in Fig. 5.1, is described by the general fault source model from Chapter 4 with deterministic values for the end coordinates, $x_A = -100$, $y_A = 10$, $x_C = 100$, and $y_C = 10$, where all distances are measured in kilometers. This definition implies that the strike is well known and, hence, deterministic. The dip angle is also assumed deterministic, with $\phi = \pi/2$.

The total length of the fault is l_f = 200 km and the perpendicular distance from the site to the fault trace, d = 10 km. Other basic assumptions and idealizations for this problem are:

1. Occurrences of earthquakes in time and space are statistically independent events. The occurrences in time constitute Poisson events with ν denoting the mean occurrence rate for the fault.

2. Earthquakes on the fault are modeled as line-ruptures whose total length, l_r, is given as a function of the earthquake magnitude by Eq. 4.4. The rupture may occur anywhere along the given fault with uniform likelihood.

3. Magnitudes of earthquake at successive occurrences are statistically independent and identically distributed variables with the probability density function given by Eq. 2.19.

4. The attenuation law model used is that given by Eq. 2.27 for peak ground acceleration. The significant distance used in the attenuation law is R_s, the shortest distance from the site to the surface projection of the rupture. This means that the level of ground motion intensity felt at the site is most influenced by the closest segment of the rupture trace to the site, which is the usual assumption for near-field ground motions.

5. The uncertainties in the attenuation law and the rupture-length relation are not considered in this analysis. Therefore, variables Z_y and Z_l in Eqs. 2.27 and 4.4 are considered to be deterministic with values equal to unity.

6. Two models of the earthquake rupture are considered: (a) the rupture can extend beyond the known ends of the fault; and (b) the rupture is "fault-contained", i.e., it cannot extend beyond the ends of the fault.

The values of the parameters selected are summarized in Table 5.1. For FORM and SORM analysis, the basic variables are the magnitude, M, and the distance from the left end of the fault to the center of the rupture, S. The truncated exponential distribution from Eq. 2.19 is selected for magnitude. The ruptures are assumed to be equally likely to occur along the fault and, accordingly, a uniform distribution for the random variable S is selected. For the first model of the rupture, the limits of this uniform PDF are $s = 0$ and $s = l_f$, since it is assumed that the rupture can extend

beyond the fault ends. For the second situation, however, the location of the center of the rupture is restricted between $s = l(m)/2$ and $s = l_f - l_r(m)/2$, such that the entire rupture is contained within the fault. For this case, a uniform PDF for S conditional on M is used

$$f_{S|M}(s|m) = \frac{1}{l_f - l_r(m)} \qquad \frac{l_r(m)}{2} \le s \le l_f - \frac{l_r(m)}{2} \tag{5.1}$$

Results from FORM and SORM approximations are compared with the "exact" values obtained from a direct numerical integration of Eq. 2.1. The results for this example are shown in Figs. 5.2 and 5.3 respectively, for the two rupture models described above. The FORM approximation greatly overestimates the probability of exceedance in this simple case, for all levels of the ground motion intensity. Results based on SORM-PF show great improvement, whereas the SORM-CF approximation does not improve the FORM result in this case, except for PGA's less than 0.10g. The reason for these results is explained below.

To examine the nature of errors of the results based on FORM and SORM, it is useful to plot the integration boundary in the standard normal space for various levels of the ground motion intensity. These are shown in Figs. 5.4 and 5.5. For this particular example, the curves are flat in the neighborhood of the design point and highly nonlinear away from it, especially for high levels of the intensity. Approximation of the boundary by a tangential plane at the design point is clearly not a good one and is the reason for the poor accuracy of the FORM result. Furthermore, since the curvatures of the true surface are zero at the design point, the SORM-CF procedure gives results which are identical to FORM, except for small acceleration levels for which the flat segment of the true surface is small and therefore, a nonzero curvature is obtained from the central-difference computation of the second derivatives. On the other hand, a good approximation is obtained with the SORM-PF procedure for all levels of intensity. This is because the approximating paraboloid in this method is obtained by fitting to points which are outside the flat portion of the surface. For this example, best results are achieved with $\gamma_r = 0.50$, as can be seen from the comparison shown in Figs. 5.2b and 5.3b. For larger γ_r, i.e., fitting points closer to the design point, the SORM-PF approximation deteriorates for higher levels of intensity. This is because for higher intensity levels, the flat zone in the vicinity of the design point is broader and, thus, with large γ_r fitting points come close to or

within the flat zones and predict zero curvature.

A comparison between the two methods for obtaining the fitting points in the SORM-PF, i.e., those originating from Eqs. 3.22 or 3.23, is presented in Figs. 5.2c and 5.3c. Both procedures give reasonable approximation, with the method from Eq. 3.22 yielding slightly better results. A comparison of Figs. 5.2a,b,c with the corresponding Figs. 5.3a,b,c reveals little differences between the hazard estimates and their accuracies for the two rupture models, i.e., the rupture contained or not contained within the ends of the fault. A more interesting comparison can be made in Figs. 5.4 and 5.5, which show the integration boundaries in the standard normal space for the two rupture models. Although the two sets of boundaries are considerably different, their differences occur at points with small densities in comparison to the design point, which explains why the hazard estimates are nearly the same. Two observations in Figs. 5.4 and 5.5 are noteworthy. One is the symmetry of the integration boundaries with respect to the u_2 axis. This is a consequence of the symmetry in the geometry of the fault with respect to the site (see Fig. 5.1). The second is the reason behind the flat segment on each boundary. This is due to the assumed rupture model, since for a fixed magnitude there are a multitude of rupture locations which pass through the nearest point on the fault (point B in Fig. 5.1) and, therefore, cause the same intensity at the site. Obviously, the symmetry and the flat segments on the integration boundaries are the reasons for the poor FORM and SORM-CF results. More generally, when symmetry does not exist, the design point may not be on the flat segment and better results are expected.

As an example, the seismic hazard for a site located close to one of the fault ends is computed. The geometric layout is similar to that shown in Fig. 5.1, but the coordinates of the fault ends are in this case $x_A = 0$, $y_A = 10$ and $x_C = 200$, $y_C = 10$, where all distances are measured in kilometers. The basic assumptions, idealizations and parameters selected are the same as in the previous example. Results from FORM, SORM and numerical integration are shown in Figs. 5.6 and 5.7, respectively, for the two rupture models considered. As expected, a significant improvement of the approximations, both first- and second-order, is obtained. Clearly, this is due to the lack of symmetry of the problem and to the fact that the design point is located outside the flat portion of the integration

boundary in the standard normal space, as can be seen from Figs. 5.8 and 5.9, respectively, for the two rupture models considered. These two conditions ensure that a good approximation of the integration boundary and, hence, of the seismic hazard, is obtained for this case.

Example 2 -- Seismic hazard analysis of a site including uncertainties

To demonstrate the versatility of the proposed methodology, an example taken from Ref. 134 is studied. In that study, only FORM estimates of the hazard were computed and no comparison with exact results was made. SORM estimates are included in the present study, which are compared with FORM and exact results. Because of the large number of random variables involved, a direct numerical integration is not feasible for this example. Thus, the exact results in this example are obtained by the directional simulation method.

The seismic hazard for peak ground acceleration at a site located near a fault is of interest. The fault geometry is a particular case of the general source model described in the previous chapter. For this example, the left end of the fault is defined by its deterministic coordinates $x_A = -50$ and $y_A = 40$ and the right end by $x_C = 200$ and $y_C = 40$, all measured in kilometers. Hence, the strike and length of the fault are well known, the latter being $l_f = 250$ km. The uncertainty in the dip angle is large; therefore ϕ is considered to be a random variable. The rupture is assumed to have zero plunge, i.e., $\psi = 0$.

The basic assumptions and idealizations employed are:

1. Earthquakes on the fault are modeled as rectangular area ruptures with dimensions given as functions of the earthquake magnitude, as expressed by Eqs. 4.4 and 4.5. The center of rupture is located on the fault plane with equal likelihood in the horizontal direction and at random depth Z. The rupture is assumed to be contained within the known ends of the fault. However, vertical restrictions, such as those in Eqs. 4.9-4.10, are not imposed.

2. The peak ground acceleration at the site is governed by the closest segment of the rupture to the site. Hence, the distance term in the attenuation law is R_f, the shortest distance from the site to the rupture. The attenuation law model is that given by Eq. 2.27.

3. All uncertainties are treated as inherent randomnesses and are incorporated in the formulation as random variables with specified probability distributions. Included in the analysis are the uncertainties in the relations for the dimensions of rupture (Eqs. 4.4 and 4.5), represented by random variables Z_l and Z_w, uncertainty in the seismicity parameter β, represented by random variable Z_β, uncertainty in the upper bound magnitude, M_1, and uncertainty in the attenuation law, represented by random variable Z_y.

In addition to the above, assumptions 1 and 3 of the previous example, regarding the occurrence model and the distribution of magnitudes are adopted for this example. Values of the model parameters for the attenuation law and the rupture dimension relations for this example are given in Table 5.2. Table 5.3 lists the basic random variables and their distributions. These values are the same as in Ref. 134, except for the random variable Z_w. For the latter, the parameters for Z_w were obtained in Ref. 134 by inverting the regression expression of M on the rupture area, A_r, and by dividing by the relation for the rupture length, l_r. As indicated before (see section 2.4), this procedure is inappropriate. Here, the mean regression expression is selected such as to give the same rupture width for a given magnitude as in Ref. 134. However, the random variable Z_w is defined as the ratio $Z_{w'}Z_A/Z_l$, where $Z_{w'}$ is a random variable used in Ref. 134 to describe the uncertainty in the rupture width relation obtained as a ratio of A_r/l_r. The distribution of Z_w (lognormal) is obtained by using the distributions assumed for $Z_{w'}$, Z_A, and Z_l in Ref. 134.

Results of the hazard analysis for this example are depicted in Figs. 5.10a-5.10c, where the exact estimates based on the directional simulation methods are also shown. The Monte Carlo simulation, even when the method of antithetic variates is used, is found to be far less efficient in terms of computing time than the directional simulation method, particularly for small values of the hazard. In the present analysis, the directional simulation procedure is halted when a specified level of dispersion in the estimated hazard, measured in term of the coefficient of variation (c.o.v.), is achieved. Simulation results plotted in Figs. 5.10a-5.10c are the mean and 95% confidence interval values obtained with a c.o.v. equal to 0.15.

In this example, SORM results greatly improve the approximation over FORM results. Best

results are obtained for the SORM-CF approximation and SORM-PF using the rule in Eq. 3.23 for finding the fitting points. When the fitting points are obtained for a fixed ratio of PDF's (Eq. 3.22) the results, although improved over the FORM approximation, are not as good as the other second-order approximations. The value $\gamma_r = 0.50$ for obtaining the fitting points with Eq. 3.22 was found to give the best results for this example.

The reason for the relatively poor approximation with the last SORM-PF method is not quite clear. Some of the transformations (Eqs. 3.9) involved in this example are highly nonlinear, thus, the integration boundary in the standard normal space may not be well approximated by the point-fitting method. A two-dimensional plot of the integration boundary in the standard normal space is shown in Fig. 5.11 to clarify this point. The selected axis, u_8 and u_9, have large α_i values and correspond to the transformed random variables describing the location of the center of rupture, X_c, and the earthquake magnitude, M, respectively (see Table 5.3). These two variables are the same as those plotted in Figs. 5.4 and 5.5 from the previous example.

The results of the previous two examples demonstrate that FORM does not provide a good approximation to the seismic hazard. SORM-CF provides reasonable results in most situations, except in cases of zero curvature at the design point, e.g., situations with symmetric geometry. The other method of second-order approximation presented, SORM-PF, is more stable and provides reasonably accurate results for the situations studied. Unfortunately, error bounds for the results provided by the different approximated procedures are not still available. Directional simulation, as an alternative method, is an effective tool for computing the seismic hazard.

5.3. Applications

The procedure for full probabilistic description of the seismic hazard problem is illustrated with several applications, including analysis of sensitivities and estimation of the standard error of the hazard estimate.

Example 3 – Seismic hazard analysis including directivity effect

In this example, taken from Ref. 10, the seismic hazard in terms of RMSA is examined for

five sites located near a fault with 400 km length. The five sites are located at 10 km perpendicular distance from the fault, where one is in the middle of the fault (site 1), two are at its ends (sites 3 and 5) and two are at intermediate positions (sites 2 and 4), see Fig. 5.12a. The RMSA attenuation law in Eq. 4.33, which includes the directivity effect by means of the factor $D(\gamma, Mc)$, is used for this example.

The earthquake rupture is assumed to start at a point on the fault (the epicenter) and to propagate in the direction from end A to end C with a total rupture length l_r, as shown in Fig. 5.12b. Further improvement in the model can be obtained by assuming that the rupture can break in any direction, i.e., from end A to end C or from end C to end A, with associated probabilities p and (1-p), respectively. In this latter case, the results can be obtained from those obtained for the first situation by a weighted average scheme. For example, results for site 1 can be computed from those for the first case as p times those for site 1 plus (1-p) times those for site 5.

The rupture is contained within the two ends of the fault, and its length is given in terms of the moment magnitude by a relation similar to Eq. 4.4. This implies that the rupture can start only at points located between the end A and a distance $l_r(M)$ from the end C of the fault. The location of the epicenter is random along this segment of the fault and it is assumed that all points in that segment are equally likely to initiate the rupture, i.e., epicenters are uniformly distributed in that segment of the fault.

As stated in Eq. 4.24, the significant distance that influences the measure of earthquake intensity is taken to be R_s, the shortest distance from the site to the projection of the rupture on the fault zone. To clearly demonstrate the effect of the rupture directivity, only three basic random variables are included in the analysis: the seismic Mach number, Mc, the moment magnitude of the earthquake, M, and the position of the epicenter on the fault, S. A uniform PDF is assumed for Mc between 0.60 and 0.95; a truncated, shifted exponential PDF (Eq. 2.19) is selected for M; and, as discussed before, the PDF of S is

$$f_{S|M}(s|m) = \frac{1}{l_f - l_r(m)} \qquad 0 \le s \le l_f - l_r(m) \tag{5.2}$$

Since this is a conditional distribution, the transformation from Eq. 3.14 is required in the analysis. No account for the uncertainties in the attenuation or rupture-length relations is made. For other variables, deterministic values are assumed: $\phi = 90°$, $\psi = 0°$, $w_r = 0$. A summary of selected parameters is given in Table 5.4.

The g-function from Eq. 3.5 for this example is

$$g(\mathbf{X}) = (a_{rms})_0 - \frac{c_1 e^{c_2 M - c_3 R_s}}{(R_s + c_4)} D(\gamma, Mc) \tag{5.3}$$

where $D(\gamma, Mc)$ is given by Eq. 4.27,

$$\gamma = \tan^{-1}\left[\frac{y_s}{(x_s - S)}\right] \tag{5.4}$$

and

$$R_s = \sqrt{y_s{}^2 + [x_s - S - l_r(M)]^2} \tag{5.5}$$

where (x_s, y_s) are the coordinates of the site as shown in Fig. 5.12b. The seismic hazard curves for the five sites obtained by directional simulation are shown in Fig. 5.13.

Sensitivities of the FORM results with respect to the parameters in the probability distributions and in the limit-state function are computed in the analysis. These measures provide useful information on the relative importance of the parameters.

Seismic hazard sensitivities with respect to the seismicity parameter β, the upper bound magnitude, m_1, the upper bound Mach number, mc_1, and the parameters c_1, c_2 and c_3 of the attenuation law are plotted in Figs. 5.14-5.16. Note that the first three are distribution parameters, whereas the last three are parameters in the limit-state function. These measures are scaled by estimated standard deviations of the parameters to make them dimensionless. This scaling also has the effect of making the parameter variations equally likely in a statistical sense. The parameter standard deviations, which are measures of uncertainty in their estimates, are assumed to be: $\sigma_\beta = 0.15$, $\sigma_{m_1} = 0.25$, $\sigma_{mc_1} = 0.03$, $\sigma_{c_1} = 0.0006$, $\sigma_{c_2} = 0.08$, and $\sigma_{c_3} = 0.001$.

The results presented in Fig. 5.14a indicate that the seismic hazard for site 1 is more sensitive to the parameters c_2 and c_1 in the attenuation law and to parameters mc_1 and β in the probability

distributions. The sensitivity of the seismic hazard to the parameter β is of negative sign, which means that reductions of this parameter will cause a marginal increase in the hazard. Such result is reasonable since a smaller β in the magnitude recurrence relation means that earthquakes of larger magnitude are more likely to occur. The sensitivity of the seismic hazard with respect to each parameter examined is enhanced at intensity levels around a_{rms} = 0.10g, especially for sites close to site 1.

Figs. 5.15a and 5.15b illustrate the sensitivity of the computed seismic hazard to parameters mc_1 and β, respectively, for different locations of the site along the fault and for different levels of earthquake intensity. The sensitivity of the hazard to both parameters is largest for sites located near the center of the fault, where contributions to the earthquake intensity at the site arise from ruptures occurring over an extended portion of the fault. This effect is decreased as the position of the site moves towards the ends of the fault, where the portion of the seismic feature with ruptures contributing to the earthquake intensity is largely reduced. Also, the higher the level of intensity, the larger the sensitivity of the seismic hazard to the specific parameter. This is also evident from Fig. 5.16 where the dimensionless sensitivities to the hazard for all parameters at a_{rms} = 0.10g are plotted against x_s, the abscissa of the site location.

From the results of this example it can be concluded that improvements in the determination of parameter β from the earthquake recurrence relationship and the upper bound seismic Mach number mc_1 will produce greater impact in the accuracy of the seismic hazard estimate. This example served two purposes: (1) to demonstrate that complex earthquake intensity modeling can be easily handled with the new formulation presented in Chapter 3; and (2) to illustrate the benefits from the direct sensitivity analysis that the solution procedure provides. Definitive conclusions on the effect of directivity in seismic hazard estimates cannot be drawn at this stage. Further validation of the attenuation relation used and of the appropriate definition of the distance R and angle γ need to be made. However, from the preliminary results shown in Fig. 5.13, it can be observed that the seismic hazard is significantly affected by the directivity effect, especially for sites close to the fault ends. This is observed by comparing the hazard curves for sites 2 and 4, and for sites 3 and 5, especially.

In the latter case, the hazard is increased approximately by an order of magnitude for low levels of intensity and slightly more for high levels of intensities.

Example 4 – Seismic hazard analysis with estimation of dispersion

A simple example is presented to illustrate the procedure for obtaining the standard error of the hazard estimate. The hazard curve for RMSA for a site near a fault is considered. The fault is modeled according to the general fault model described in Chapter 4. The end C of the fault is assumed to be deterministically known with coordinates, $x_C = 270$ km and $y_C = 15$ km. The end A is assumed to be on the arc of a circle centered at end C and a radius (length of fault) $l_f = 300$ km, see Fig. 5.17. Assuming a uniform distribution of the angle α shown in Fig. 5.17, the PDF of the coordinate X_A is

$$f_{X_A}(x_A) = \frac{10}{\pi\sqrt{17100 + 540x_A - x_A^2}} \qquad -30 \le x_A \le -15.32 \tag{5.6}$$

The y_A coordinate is given by the relation $y_A = 15 - [17100 + 540x_A - x_A^2]^{\frac{1}{2}}$. For this example, the attenuation law in Eq. 4.34 by Hanks and McGuire [85] is used. After rearranging the constants and replacing Eqs. 4.32 and 4.35 in Eq. 4.34, the Hanks-McGuire attenuation for RMSA can be expressed as

$$a_{rms} = \frac{c_1}{\rho}\left[\frac{c_2 Q}{\pi}\right]^{\frac{1}{2}} \frac{\Delta\sigma^{5/6}\, e^{0.25M + 2.67}}{R_h^{3/2}} \tag{5.7}$$

where a_{rms} is given in cm/sec^2, $c_1 = 0.85(2\pi)^2/106 = 0.3166$, $\rho = 2.7$ gm/cm^3, $c_2 = 8.47$, and $Q = 300$.

The distance measure used in the Hanks-McGuire attenuation model is the hypocentral distance and, therefore, no account of the rupture dimensions is necessary. Magnitudes of earthquakes are measured by moment magnitude M and, at successive occurrences, are assumed to be statistically independent and identically distributed variables with PDF given by Eq. 2.19. Values of the parameters selected for this distribution are $\beta = 2.0$, $m_0 = 4.0$, and $m_1 = 7.0$.

Other random variables included in the analysis are the depth of the earthquake focus, Z, which is uniformly distributed between 5 and 30 km; the dip angle of the fault plane, Φ, with

uniform PDF between 0.3π and 0.4π radians; the location of the rupture on the fault trace, S, with uniform PDF between 0 and 300 km; and the earthquake stress drop, $\Delta\sigma$. To represent the observed values of stress drop reported by Hanks and McGuire [85], a lognormal distribution is selected for $\Delta\sigma$ with mean equal to 100 bars and c.o.v. equal to 200 percent.

It is assumed that some of the parameters included in the analysis are determined with uncertainty. This collection of parameters is represented by the vector $\boldsymbol{\Theta}$. Included among these parameters are ρ, Q, c_1, and c_2 from the attenuation relation (Eq. 5.7), the parameter β from the magnitude distribution (Eq. 2.19), and the mean value assigned to the PDF of the stress drop, $\mu_{\Delta\sigma}$. The standard deviation of the computed seismic hazard is estimated using Eq. 3.50. For this purpose, the following standard deviation and correlation coefficients values are assumed: $\sigma_\rho = 0.54$, $\sigma_Q = 90$, $\sigma_{c_1} = 0.05$, $\sigma_{c_2} = 1.23$, $\sigma_\beta = 0.24$, $\sigma_{\mu_{\Delta\sigma}} = 25$, $\rho_{\rho Q} = \rho_{Q\rho} = -0.3$, and $\rho_{\beta\mu_{\Delta\sigma}} = \rho_{\mu_{\Delta\sigma}\beta} = 0.15$ with all other correlation coefficients being zero.

The vector $\nabla_{\boldsymbol{\Theta}} H(\boldsymbol{\theta})$ of the partial derivatives of the seismic hazard with respect to the components of $\boldsymbol{\Theta}$ for each specified level of intensity, $(a_{rms})_o$, is computed for the mean values of $\boldsymbol{\Theta}$. The standard deviation, $(\hat{\sigma}_H)_{FO}$, for the FORM approximation of the seismic hazard is then obtained from Eq. 3.50 for each intensity level.

To obtain the standard deviation $(\hat{\sigma}_H)_{SO}$ of the SORM approximation, it is assumed that the coefficient of variation of the hazard estimate based on FORM and SORM approximations is the same. This leads to the approximation

$$(\hat{\sigma}_H)_{SO} \approx \frac{(H(\boldsymbol{\theta}))_{SO}}{(H(\boldsymbol{\theta}))_{FO}} (\hat{\sigma}_H)_{FO} \tag{5.8}$$

The mean and mean $\pm$ one standard deviation hazard estimates based on the above SORM analysis are shown in Fig. 5.18. Also presented in this figure are results from the FORM approximation and from a directional simulation, where these last results represent the 95% confidence interval of the mean hazard estimate as obtained with a simulation c.o.v. equal to 0.15.

Good agreement is obtained between SORM and "exact" results from directional simulation. For this example, FORM results are poor approximations of the "exact" seismic hazard results as can

be seen from Fig. 5.18. This simple example illustrates how an estimate of the dispersion in the seismic hazard, arising from uncertainties in the model parameters, is obtained by use of the sensitivity measures.

Example 5 -- Hazard-consistent earthquake ground motion for Tokyo

A case study taken from Ref. 100 is analyzed, where hazard-consistent earthquake motions for different subsoil conditions are determined for the city of Tokyo, Japan. The modified procedure suggested in Chapter 4 is used to obtain the parameters of the earthquake ground motion model.

The seismicity model for the area consists of five seismic subzones with different seismicity characteristics. Each subzone is composed of several annular subareas, as described in the general area source model in Chapter 4 (see Fig. 5.19). The parameters that define the seismic sources are summarized in Table 5.5. For all subzones, the lower bound magnitude m_0 (which defines the limit below which earthquakes have no engineering importance for the site) is set to $m_0 = 6.0$. Although this value is large for California sites, it is appropriate for Japanese earthquakes which occur in a subduction zone.

Occurrences of earthquakes in time are assumed to constitute Poisson events with the mean occurrence rate ν. The total annual rate of earthquake occurrences in the seismic region is, according to the values reported in Table 5.5, $\nu = \sum_{i=1}^{5} \nu_i = 2.882$. The seismic hazard is defined as the yearly probability of exceedance of the peak rms acceleration, δ, and computed according to the Poisson model (Eq. 2.31) as

$$H(\delta_o) = 1 - e^{-\nu P(\delta > \delta_o)} \tag{5.9}$$

The value $P(\delta > \delta_o)$ is computed by the approximate procedures (FORM and SORM) presented in Chapter 3. The attenuation law used is that in Eq. 4.39, which uses the epicentral distance and ignores the rupture dimensions.

Although the uncertainty in the attenuation relation for δ can be included in the present formulation, it was not considered in the study in Ref. 100, and to be consistent with that study this uncertainty is also ignored here. Thus, for this example only three random variables are considered:

the polar coordinates of the epicenter in the seismic source, ρ and θ, and the magnitude of the earthquake, M. The likelihood of occurrence of earthquakes is uniform within each subzone, i.e.,

$$f_{P\Theta}(\rho,\theta) = \frac{\nu_i}{\nu}\frac{\rho}{A_i} \qquad (\rho,\theta) \text{ in subzone } i \tag{5.10}$$

where ν_i is the annual earthquake occurrence rate in subzone i (Table 5.5), and A_i, its area. The magnitudes have a conditional truncated exponential PDF in each subzone,

$$f_{M|P,\Theta}(m\,|\rho,\theta) = \frac{\beta^i e^{-\beta^i(m-m_0)}}{1-e^{-\beta^i(m-m_1^i)}} \qquad (\rho,\theta) \text{ in subzone } i \tag{5.11}$$

where $m_0 = 6.0$ and β^i and m_1^i depend on ρ and θ according to Table 5.5.

The hazard curve obtained from the FORM approximation is almost identical to that reported in Ref. 100, as can be seen in Fig. 5.20. Therefore, there is no need for a second-order approximation. The value $\delta = 0.202$ g, obtained by interpolation of the seismic hazard curve, corresponds to the target yearly probability of exceedance of 0.005 (or return period of 200 years). The most likely values of magnitude, M, and epicentral distance, R_e, corresponding to this level of hazard are $M^* = 7.267$, and $R_e^* = 30.88$ km. These values correspond to the coordinates of the design point and, therefore, can be interpreted as the most likely set of the magnitude and distance that give rise to accelerations equal to or greater than $\delta = 0.202$ g. The values M^* and R_e^* are substituted in Eqs. 4.40-4.42 to obtain the set of most likely values of the parameters of the earthquake ground motion model, giving $t_m^* = 4.80$, $f_p^* = 3.85$, and $\zeta_r^* = 1.02$. These values are not considerably different from those obtained in Ref. 100 by the alternative procedure which are, $\delta_o = 0.202$, $(t_m)_o = 6.55$, $(f_p)_o = 3.72$, and $(\zeta_r)_o = 1.01$. The latter values were obtained in Ref. 100 as conditional expectations given that the peak RMSA is equal to or greater than δ_o.

Three site conditions are defined for the generation of artificial earthquake ground motions: (1) soft ground, defined by the soil softness $S_n = 0.80$ and $z_m = 80$ m.; (2) intermediate ground, with $S_n = 0.20$ and $z_m = 50$ m.; and (3) firm ground, with $S_n = -0.20$ and $z_m = 20$ m. The soil softness S_n is defined by [100]

$$S_n = 0.264\int_0^{z_n} \exp[\,-0.04N(z) - 0.14z\,]\,dz - 0.885 \tag{5.12}$$

where $N(z)$ is the SPT blow count at depth z (in meters), and z_n is the total depth of the blow count profile.

The simulated hazard-consistent ground motions for the city of Tokyo, corresponding to a return period of 200 years, are shown in Fig. 5.21 for the three soil conditions. A clear difference in the frequency content of the earthquake ground motion is apparent in these plots, where higher frequency content is observed for motions on firmer soils. Fig. 5.22 qualitatively show the nonlinear effect of the soil on the earthquake ground accelerations: the amplitudes are increased and the frequency content of the motion is filtered producing lower frequencies for softer soils. The PGA of the generated sample of the baserock motion is recorded at $t = 2.68$ sec. and measures 0.39 g. When this shaking is filtered by a deep layer of soft soil, the PGA of the shaking is increased to 0.445 g and the time where it is recorded is shifted to $t = 5.34$ sec. For the case of the motion recorded at a site with intermediate ground conditions, a PGA of 0.405 g at $t = 5.32$ sec. is recorded. The shallow layer of firm soil has the effect of increasing the amplitude level of the earthquake accelerations but has little effect on its frequency content. The ground motion at firm soil conditions shows a PGA of 0.46 g at $t = 2.68$ sec., the same time for which the maximum peak acceleration was recorded at the baserock level.

Table 5.1. Values of Coefficients used in Example 1

c_1	c_2	c_3	c_4	a_l	b_l	β	m_0	m_1
0.0159	0.868	1.09	4.0	1.948	-10.037	1.7	4.0	7.5
Eq. 2.27				Eq. 4.4		Eq. 2.19		

Table 5.2. Values of Coefficients used in Example 2

c_1	c_2	c_3	c_4	a_l	b_l	a_w	b_w
2.2	0.7	1.8	20.0	0.921	-2.763	1.623	-8.627
Eq. 2.27				Eq. 4.4		Eq. 4.5	

Table 5.3. Distributions of Random Variables Considered in Example 2

i	X_l	Distribution	Parameters	Mean	Standard Deviation
1	Θ	Lognormal	$\lambda = 0.440$ $\zeta = 0.149$	$\frac{\pi}{2}$	0.2356
2	Z	Lognormal	$\lambda = 3.247$ $\zeta = 0.555$	30.0	18.0
3	Z_y	Lognormal	$\lambda = -0.154$ $\zeta = 0.555$	1.0	0.60
4	Z_l	Lognormal	$\lambda = -0.030$ $\zeta = 0.246$	1.0	0.25
5	Z_w	Lognormal	$\lambda = -0.011$ $\zeta = 0.379$	1.06	0.417
6	Z_β	Normal	$\mu = 1.0$ $\sigma = 0.15$	1.0	0.15
7	M_1	Uniform	$a = 7.482$ $b = 8.018$	7.75	0.155
8	M	Conditional (1)	$\beta = 2.3$ $m_0 = 4.0$ z_β variable m_1 variable		
9	X_c	Conditional (2)	$a = \frac{1}{2} l_r(Z_l, M)$ (3) $b = l_f - \frac{1}{2} l_r(Z_l, M)$ (3)		

(1) The conditional PDF of M is given by

$$f_{M|Z_\beta, M_1}(m \mid z_\beta, m_1) = \frac{z_\beta \beta \exp[-z_\beta \beta (m - m_0)]}{1 - \exp[-z_\beta \beta (m_1 - m_0)]} \quad \text{for} \quad m_0 \le m \le m_1$$

(2) The conditional PDF of X_c, the location of the center of the rupture, is given by

$$f_{X_c|Z_l, M}(x_c \mid z_l, m) = \frac{x_c - \frac{1}{2} l_r}{l_f - l_r} \quad \text{for} \quad \frac{1}{2} l_r \le x_c \le l_f - \frac{1}{2} l_r$$

(3) The expression of l_r in terms of the random variables Z_l and M is given by Eq. 4.4.

Table 5.4. Values of Coefficients used in Example 3

c_1	c_2	c_3	c_4	a_l	b_l	β	m_0	m_1
0.00567	0.8065	0.0135	0.0	0.896	-1.778	1.7	5.0	8.5
Eq. 2.27				Eq. 4.4		Eq. 2.19		

Table 5.5. Parameters of the Seismic Source Model for Example 5

Subzone i	annular element	ρ_a (km)	ρ_b (km)	θ_a (°)	θ_b (°)	ν_i	m_1	β
I	1	0	100	0	360	2.253	8.0	2.28
	2	100	150	0	69			
	3	100	150	303	360			
	4	150	200	0	65			
	5	150	200	314	360			
	6	200	250	0	64			
	7	200	250	320	360			
	8	250	300	0	64			
	9	250	300	323	360			
II	1	100	150	216	303	0.284	8.5	2.28
	2	150	200	216	314			
	3	200	250	212	320			
	4	250	300	210	323			
III	1	100	150	69	216	0.179	7.25	3.02
	2	150	200	65	102			
	3	150	200	162	216			
	4	200	250	64	90			
	5	200	250	183	212			
	6	250	300	64	84			
	7	250	300	187	210			
IV	1	150	200	102	162	0.093	7.5	4.61
	2	200	250	90	168			
	3	250	300	84	158			
V	1	200	250	168	183	0.073	8.0	1.54
	2	250	300	158	187			

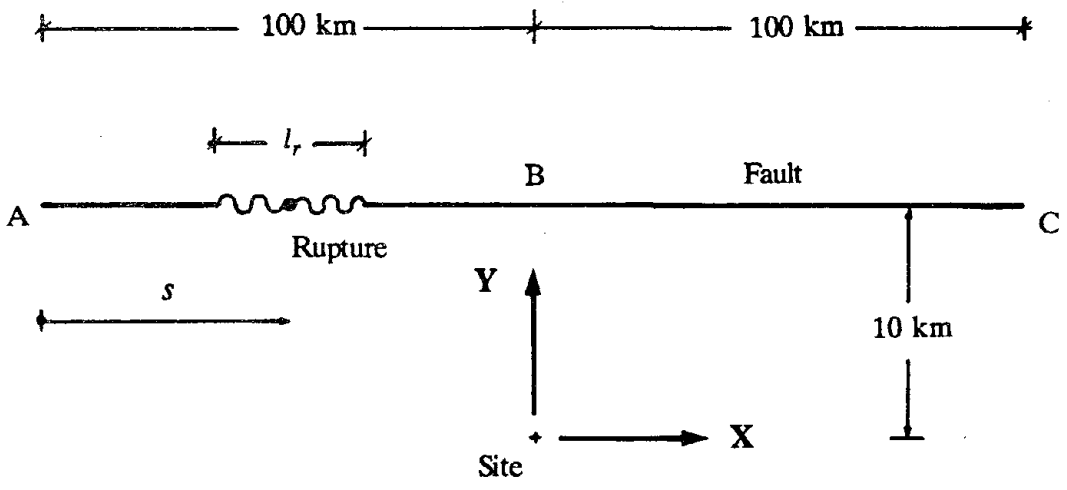

Fig. 5.1. Geometric Description of Example 1

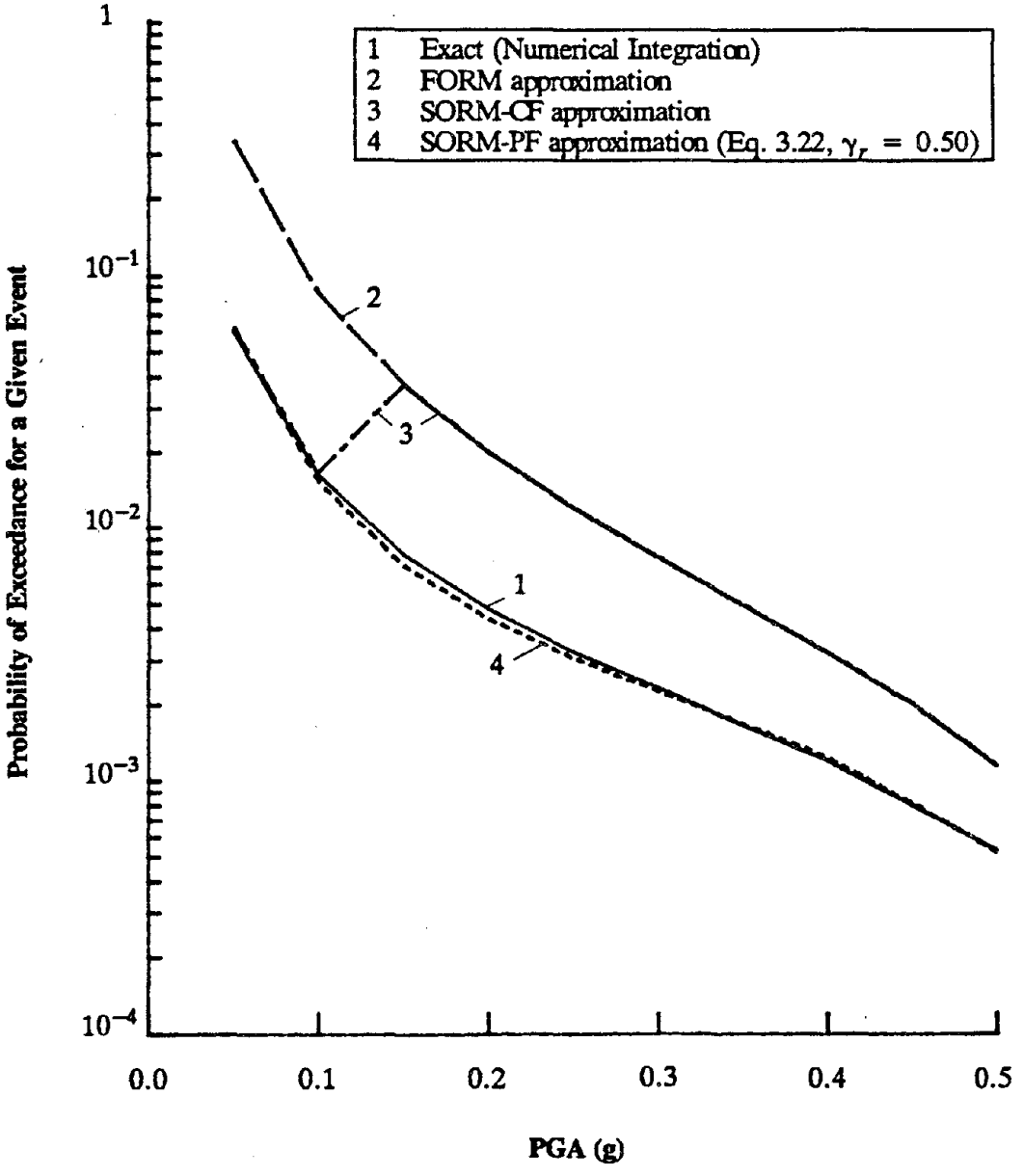

Fig. 5.2a. Probability of Exceedance of PGA (Example 1a, Fault with Extendable Ends)

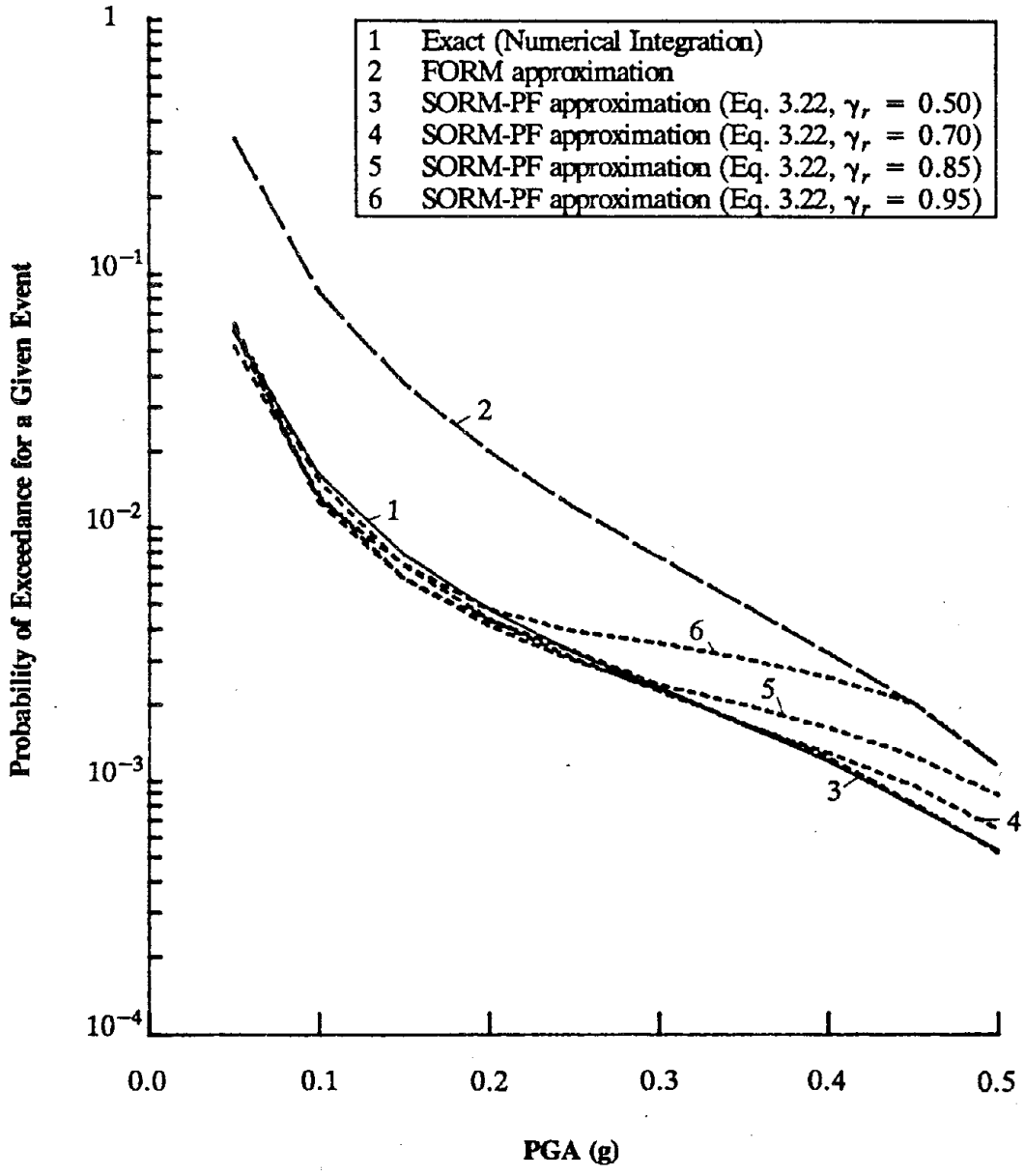

Fig. 5.2b. Probability of Exceedance of PGA (Example 1a, Fault with Extendable Ends)

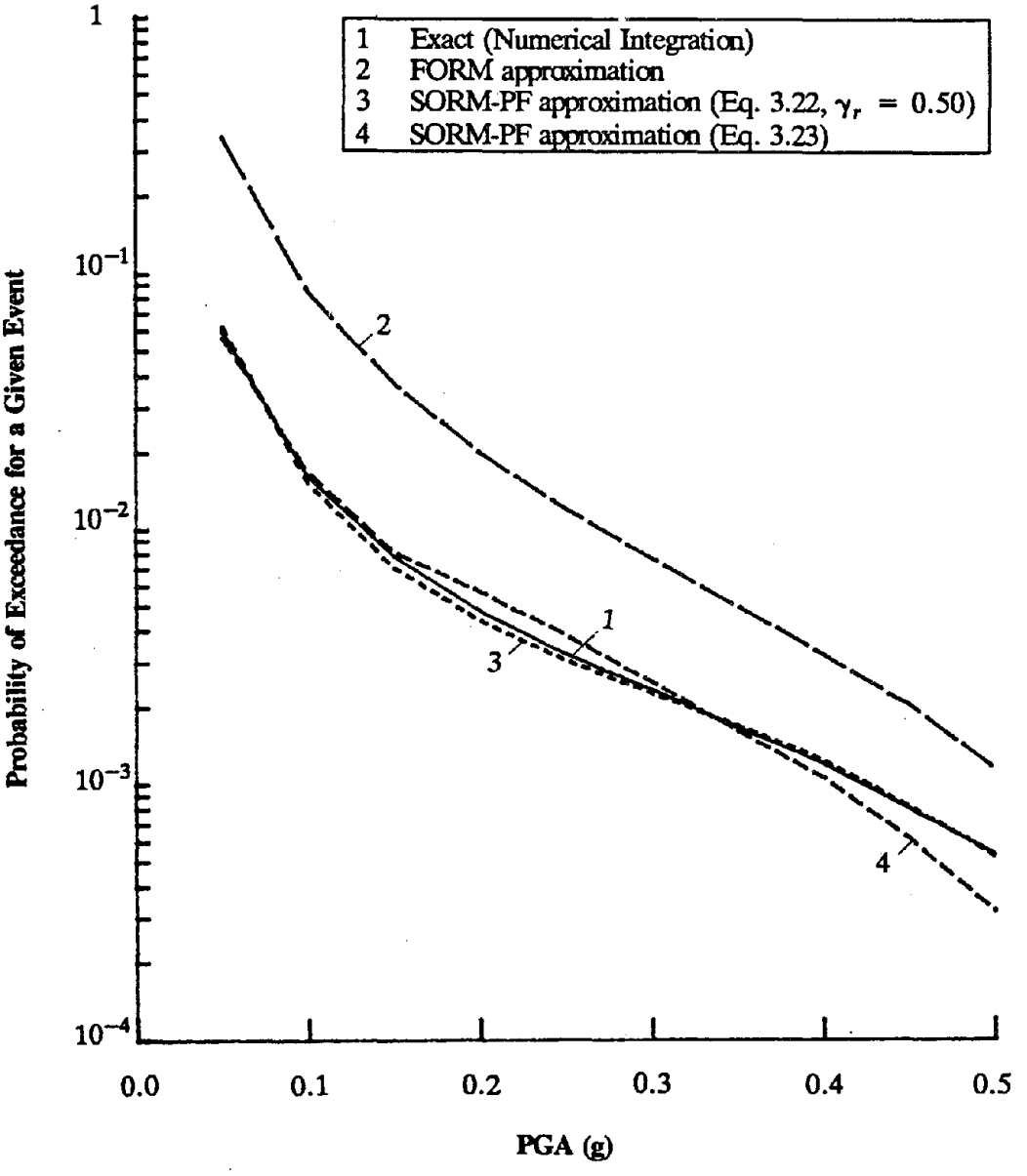

Fig. 5.2c. Probability of Exceedance of PGA (Example 1a, Fault with Extendable Ends)

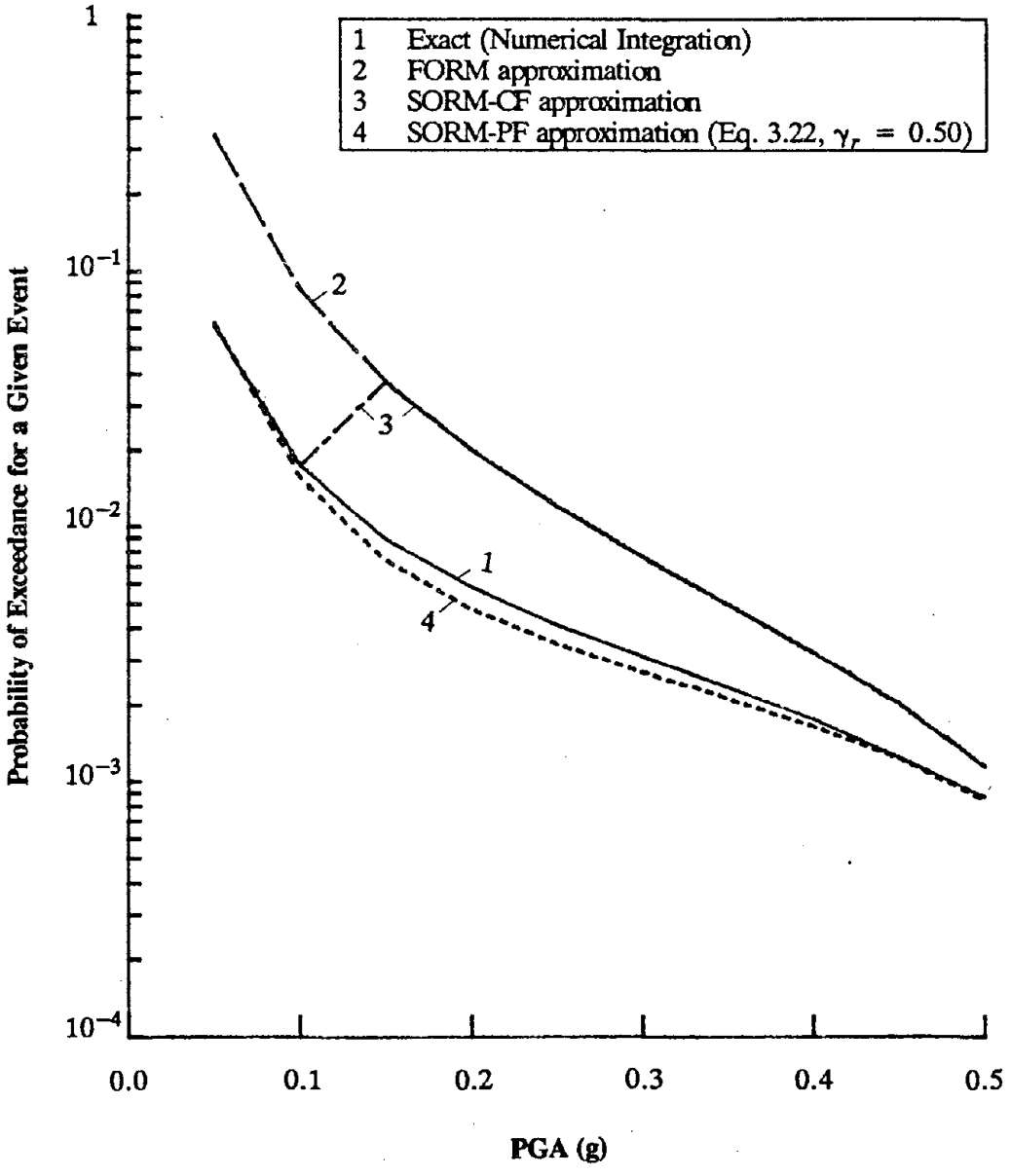

Fig. 5.3a. Probability of Exceedance of PGA (Example 1b, Fault with Non-Extendable Ends)

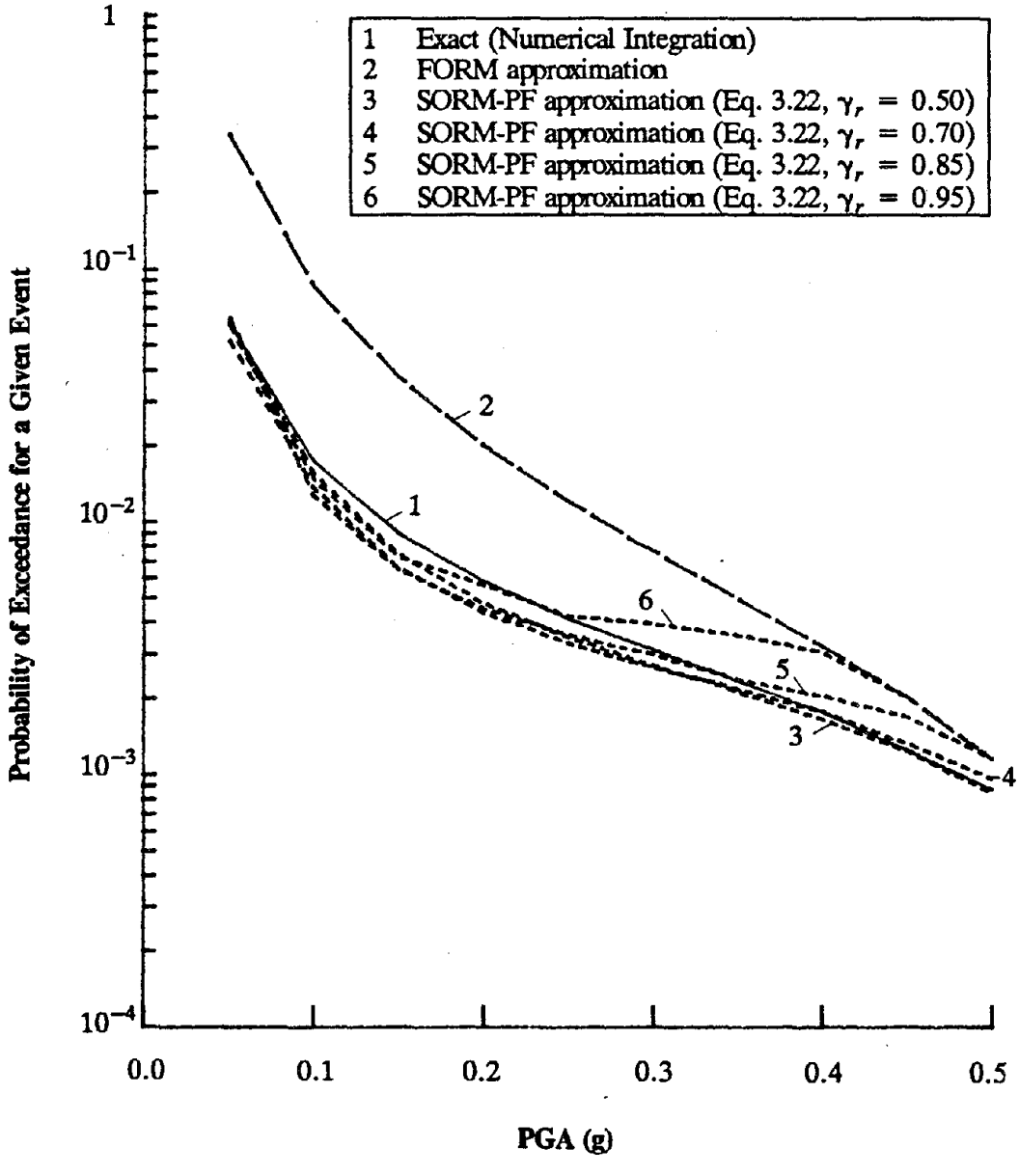

Fig. 5.3b. Probability of Exceedance of PGA (Example 1b, Fault with Non-Extendable Ends)

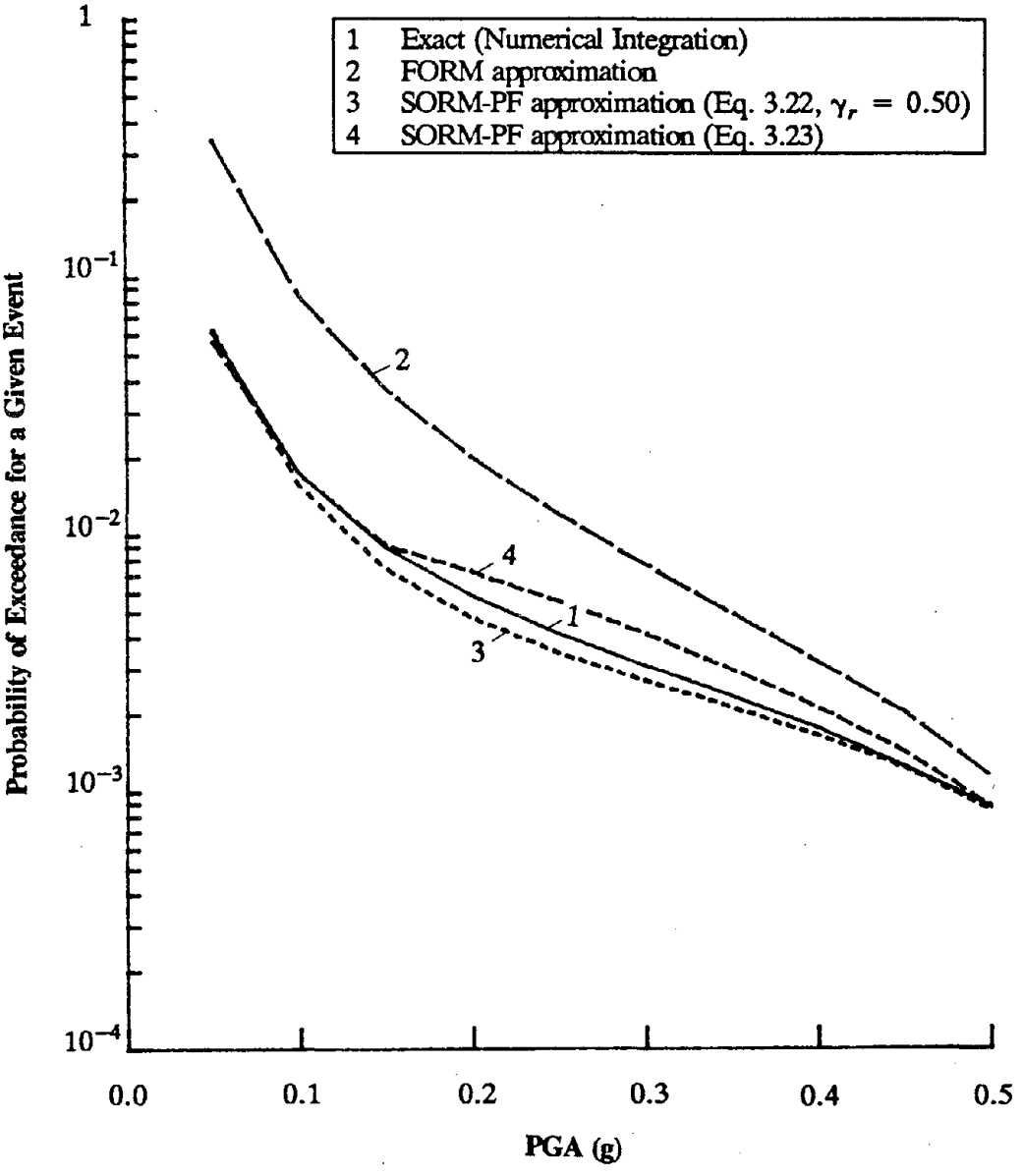

Fig. 5.3c. Probability of Exceedance of PGA (Example 1b, Fault with Non-Extendable Ends)

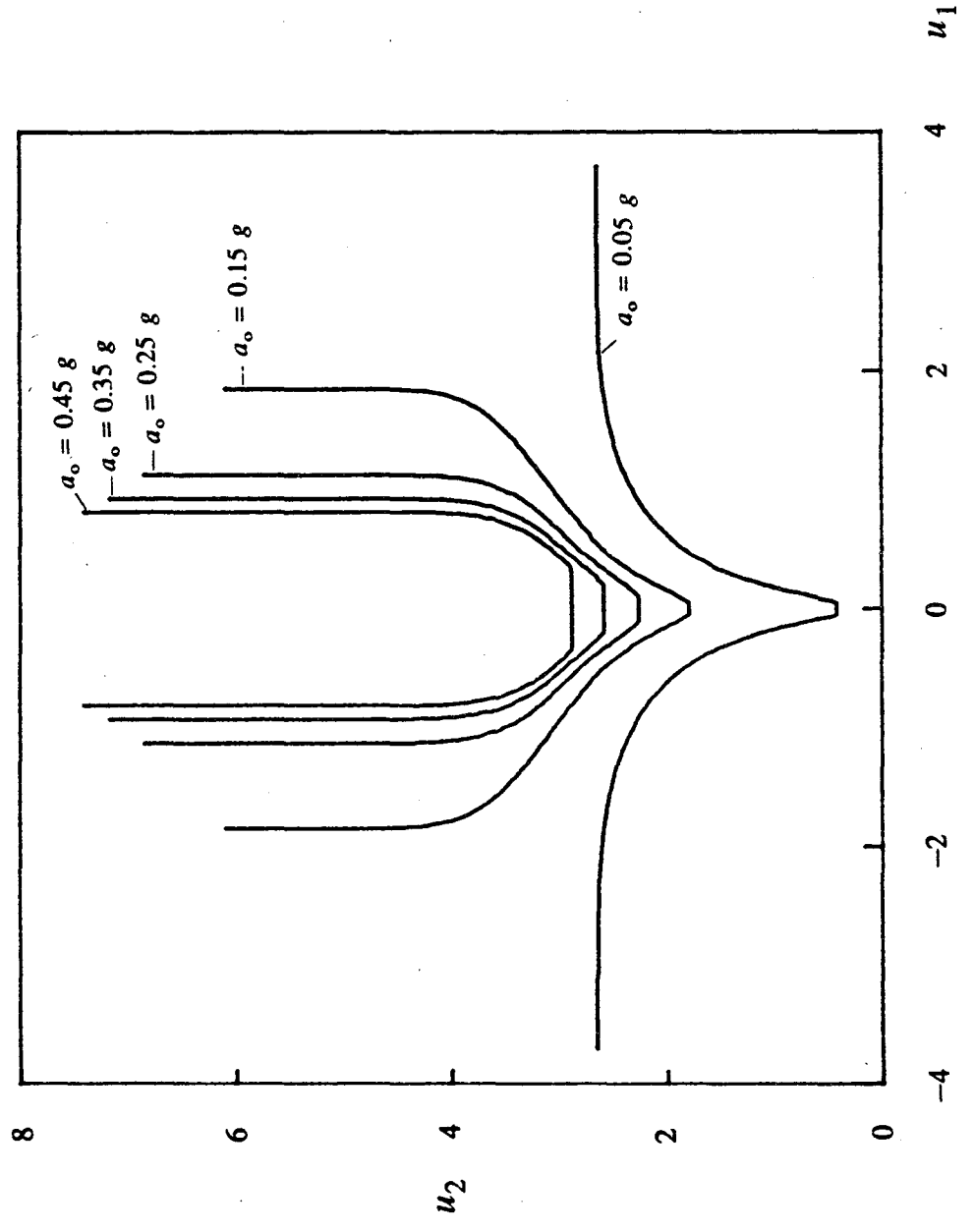

Fig. 5.4. Limit-State Functions in Standard Space (Example 1a)

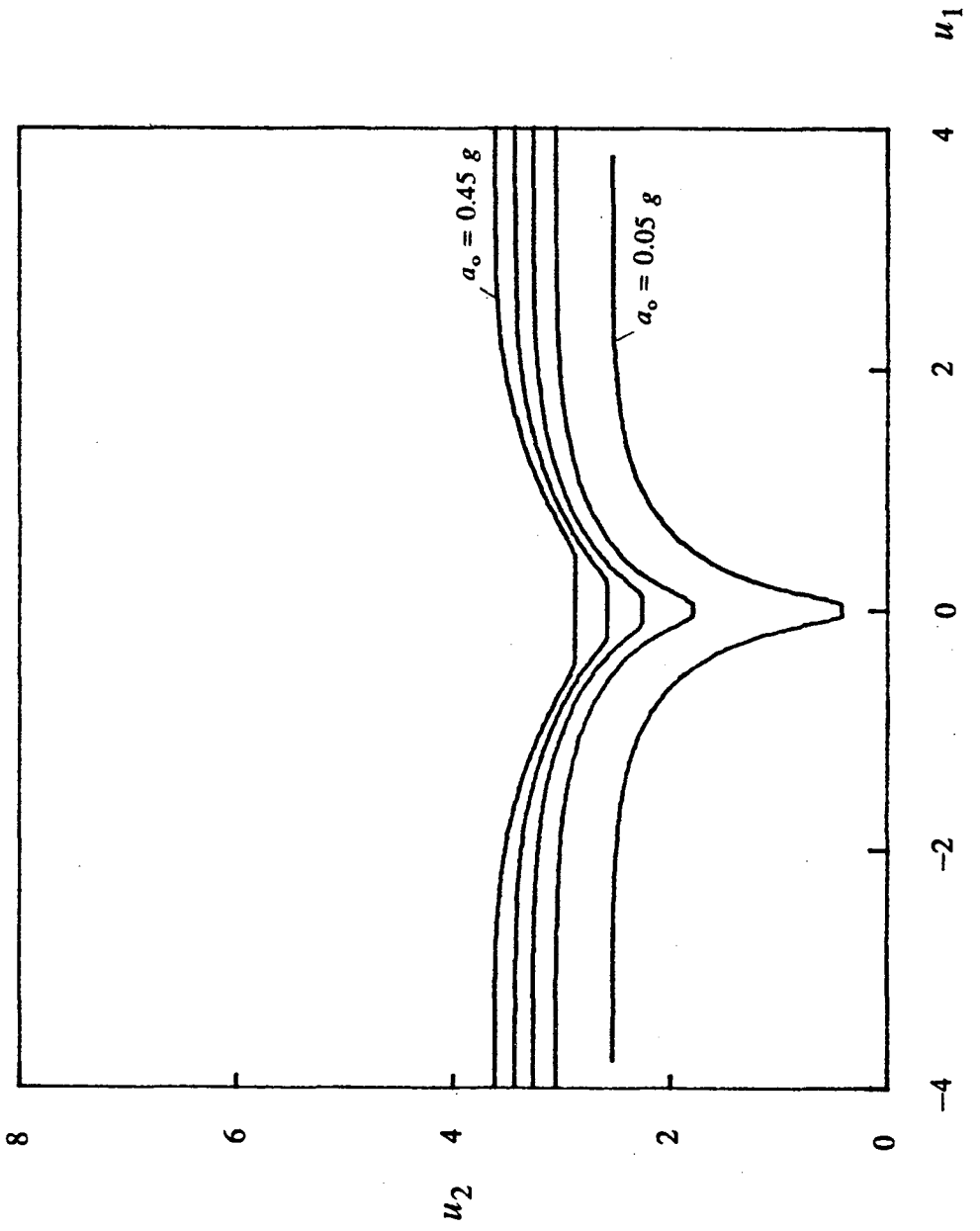

Fig. 5.5. Limit-State Functions in Standard Space (Example 1b)

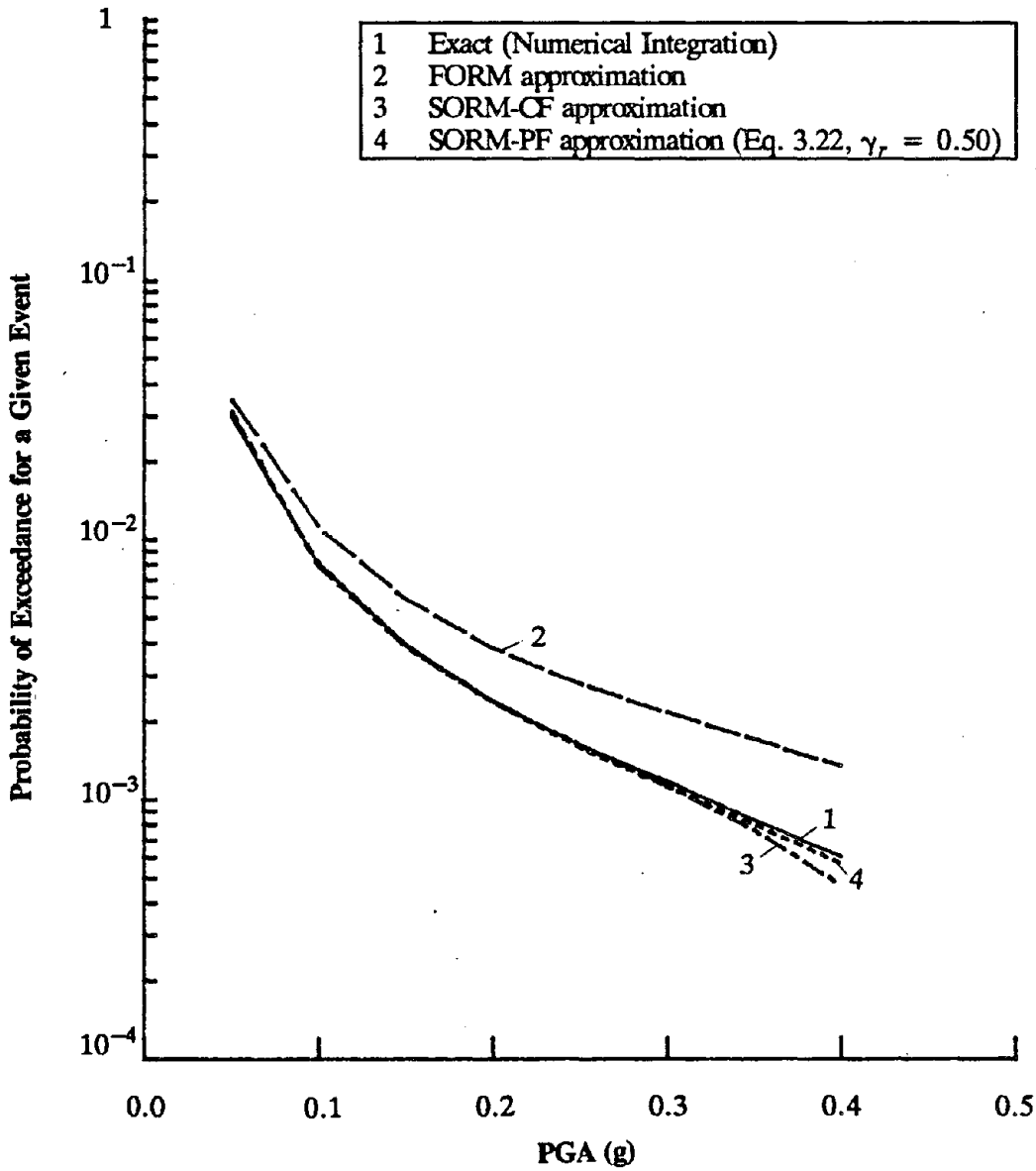

Fig. 5.6. Probability of Exceedance of PGA for Site close to the Fault End (Fault with Extendable Ends)

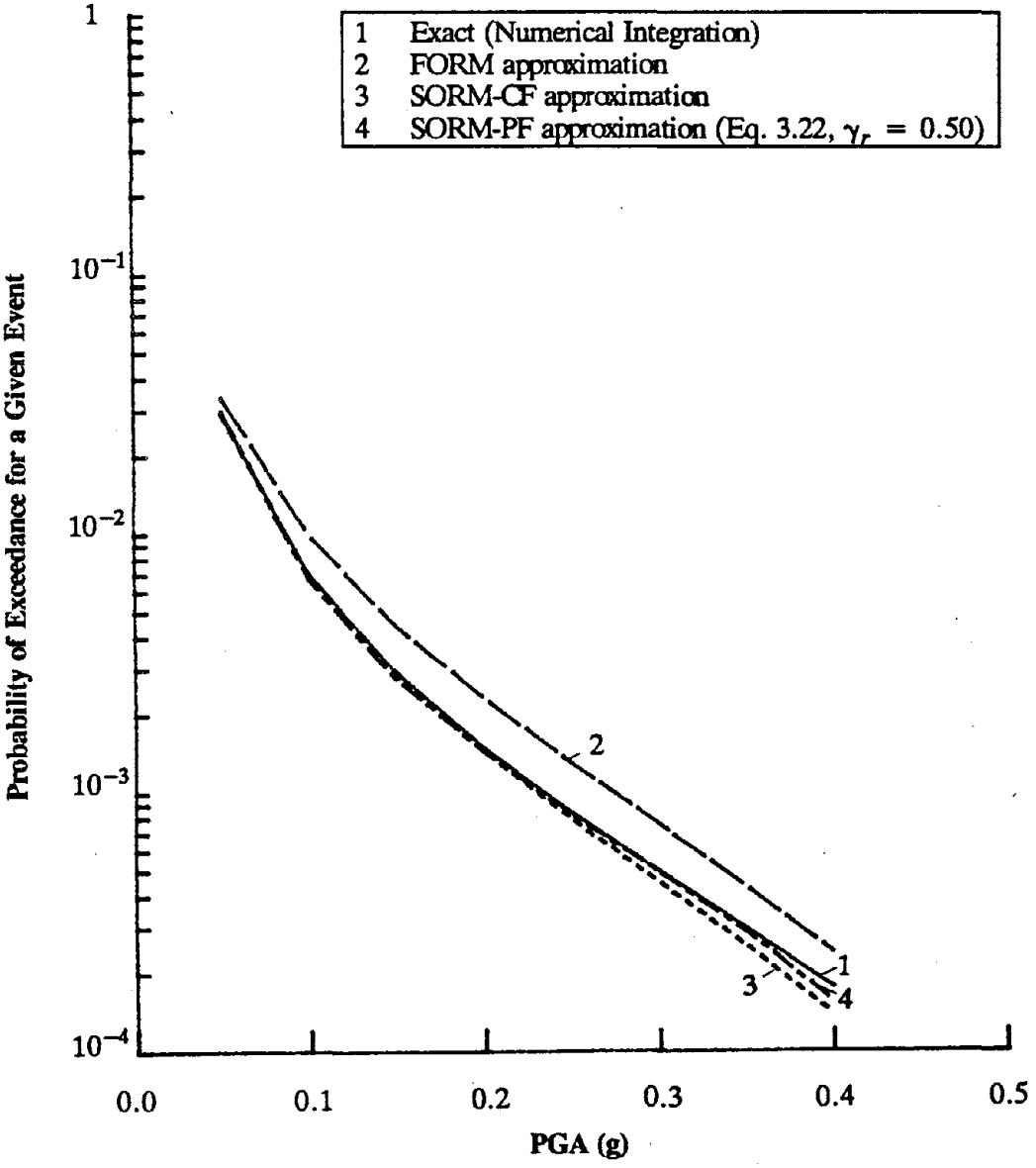

Fig. 5.7. Probability of Exceedance of PGA for Site close to the Fault End (Fault with Non-Extendable Ends)

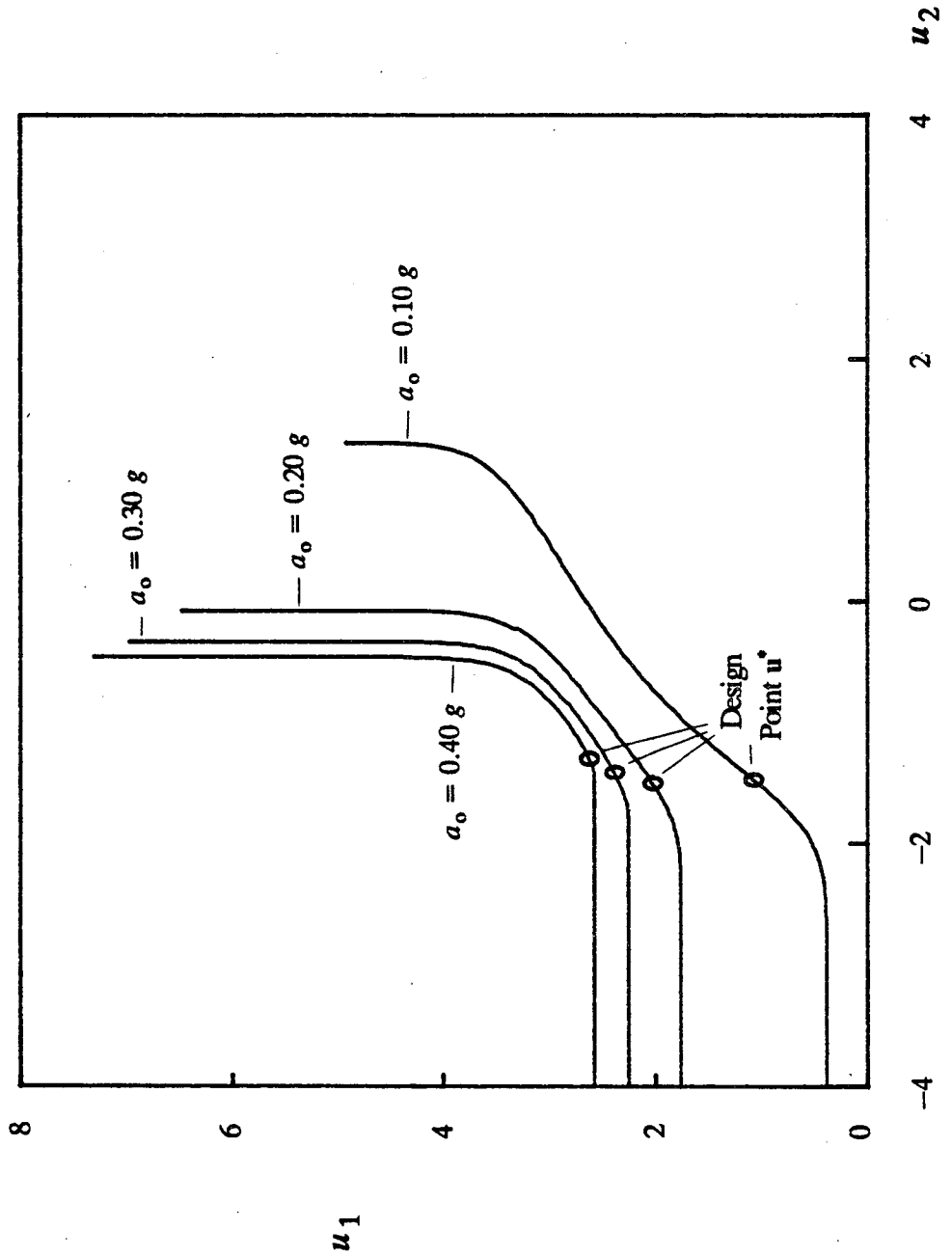

Fig. 5.8. Limit-State Functions in Standard Space (Example of Site close to the Fault End)

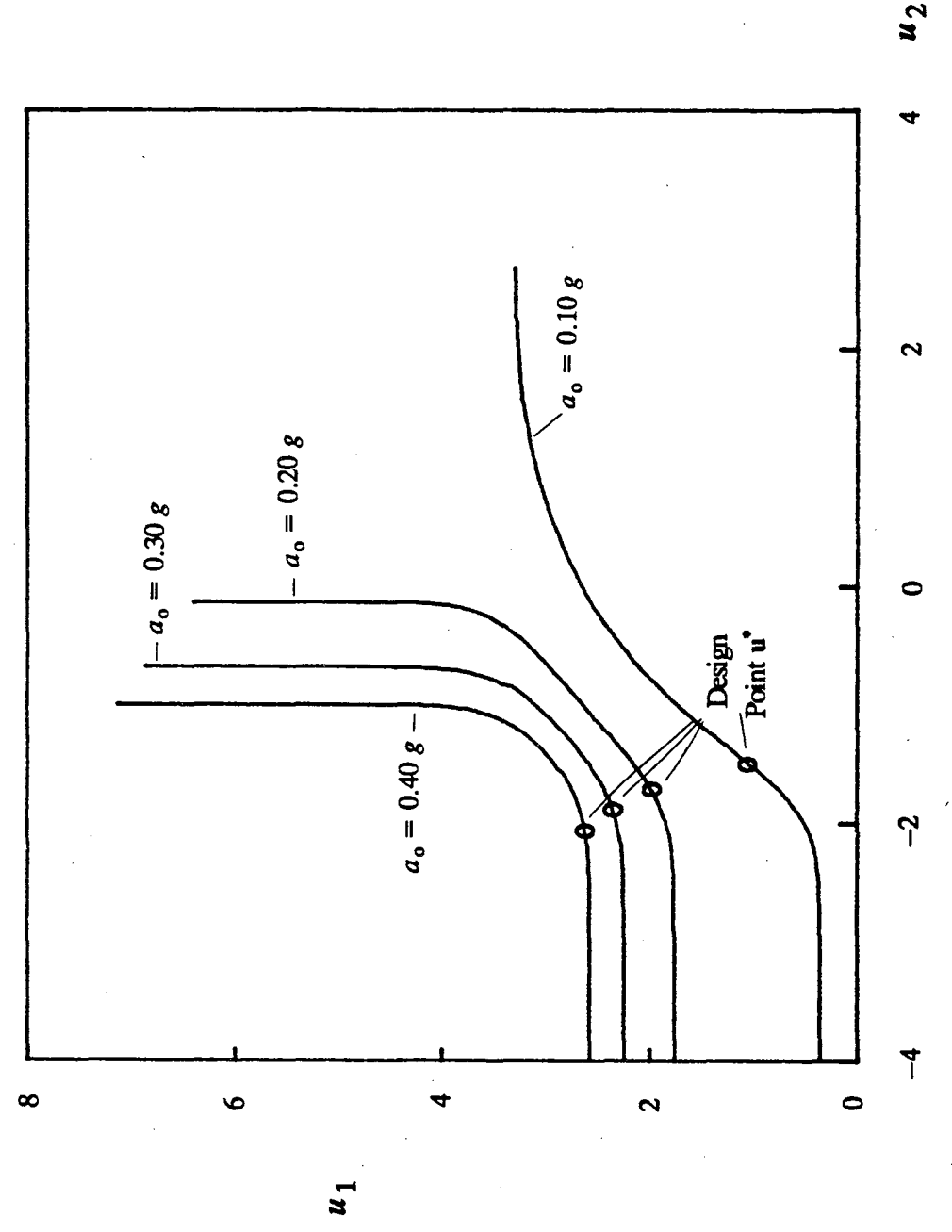

Fig. 5.9. Limit-State Functions in Standard Space (Example of Site close to the Fault End)

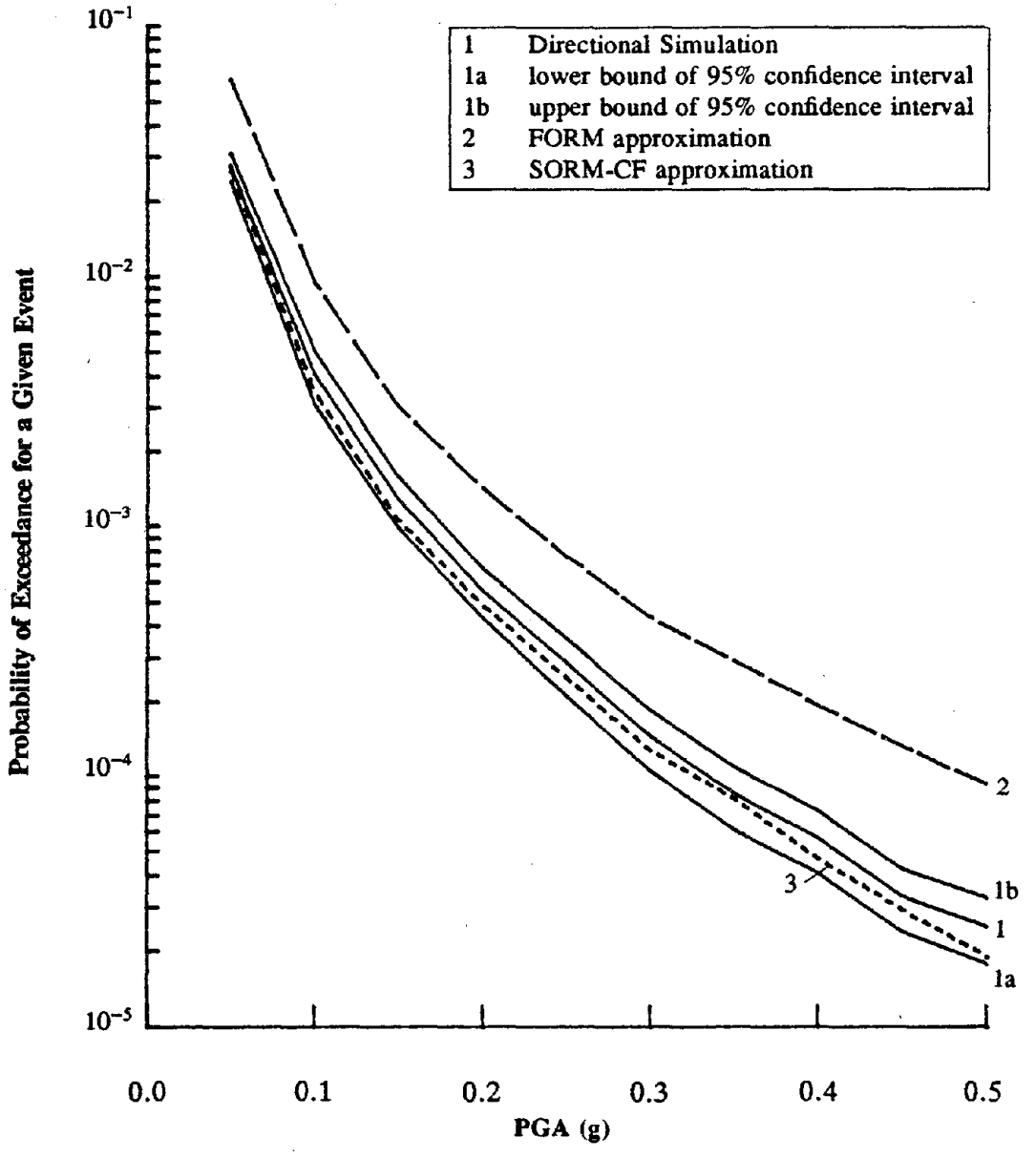

Fig. 5.10a. Probability of Exceedance of PGA (Example 2)

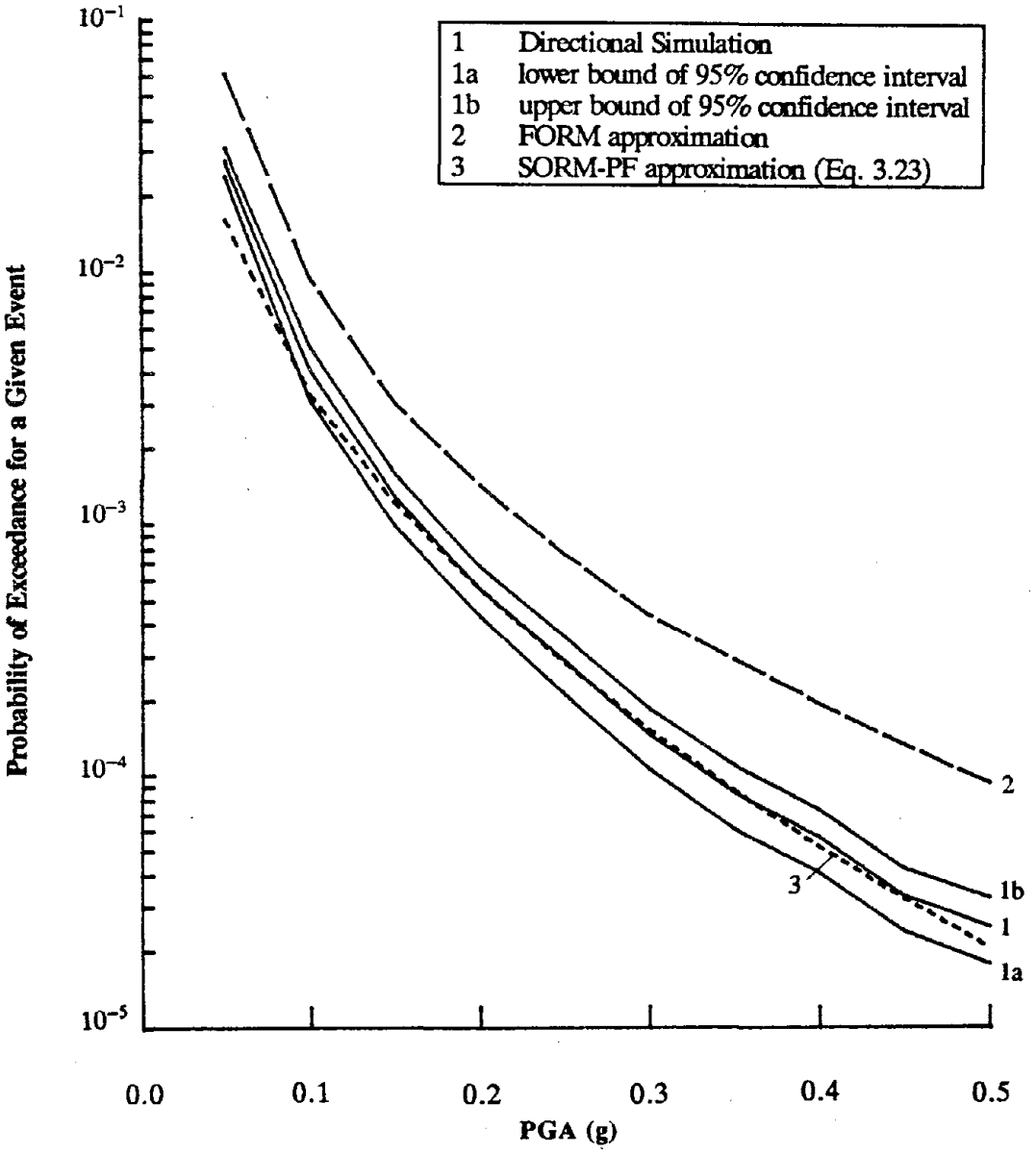

Fig. 5.10b. Probability of Exceedance of PGA (Example 2)

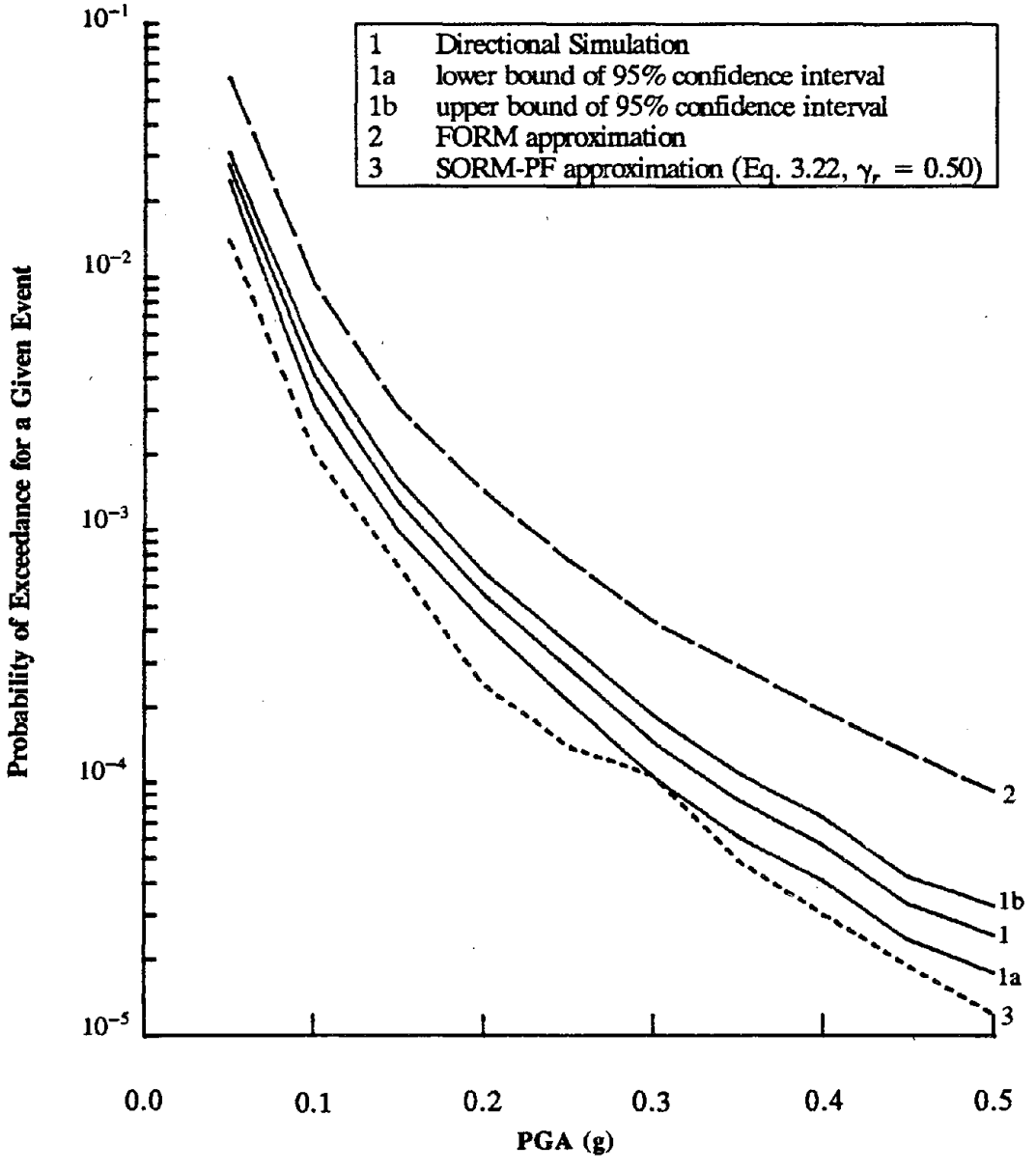

Fig. 5.10c. Probability of Exceedance of PGA (Example 2)

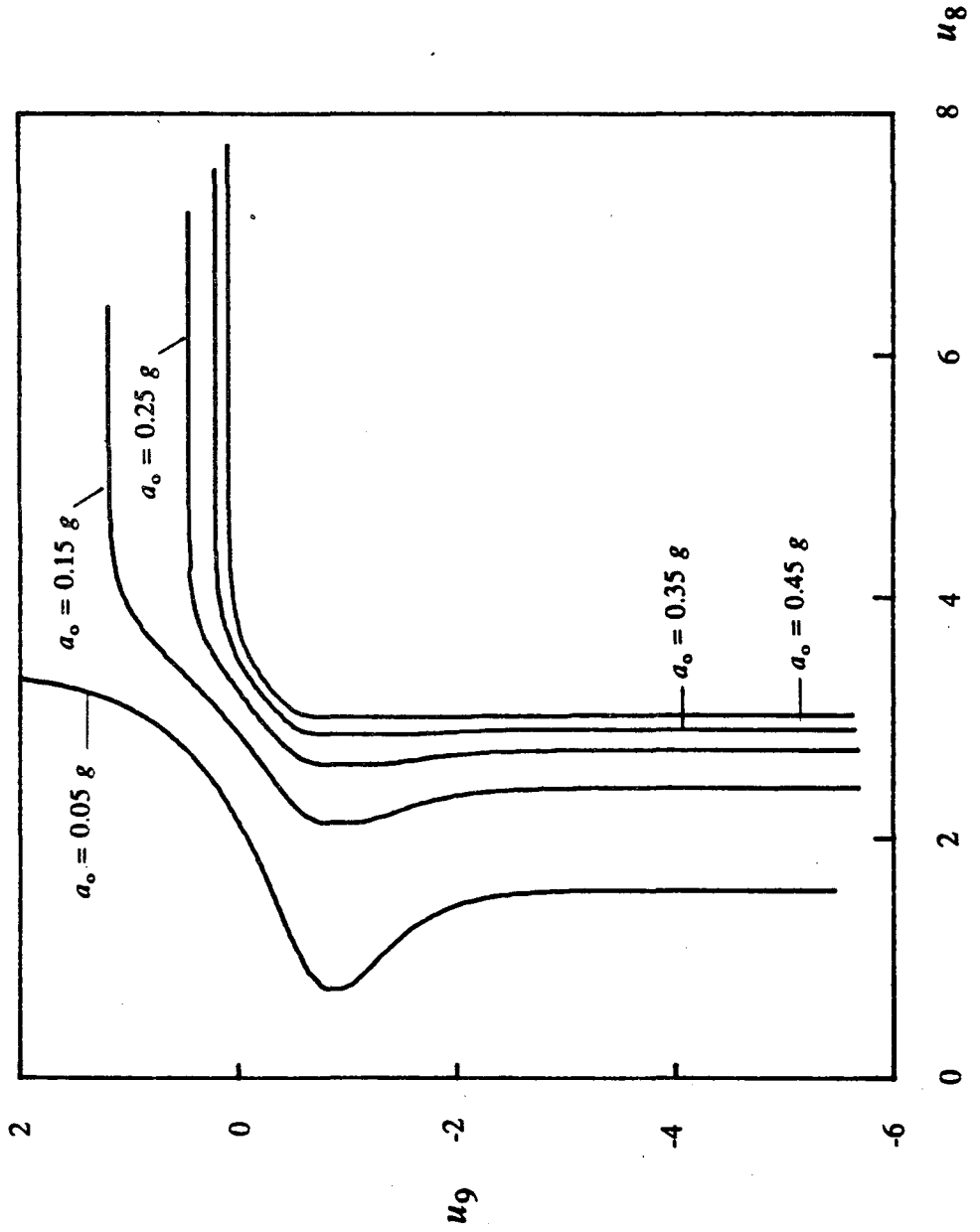

Fig. 5.11. Limit-State Function in Standard Space (Example 2)

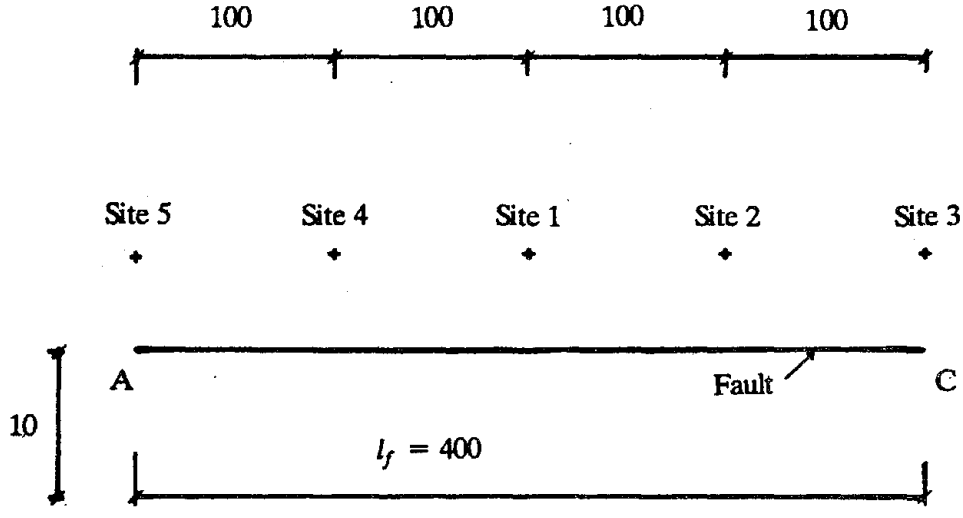

(a) Geometry and Location of Sites in Plan

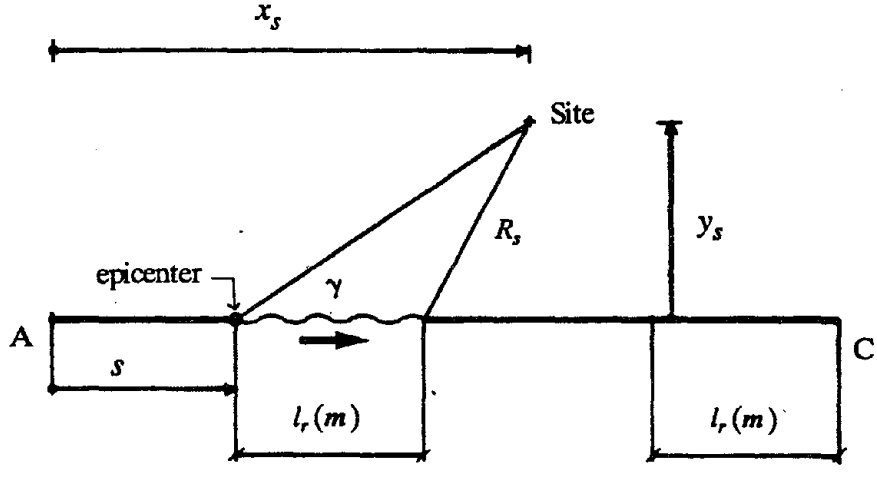

(b) Earthquake Rupture Description

Fig. 5.12. Geometric Description of Example 3

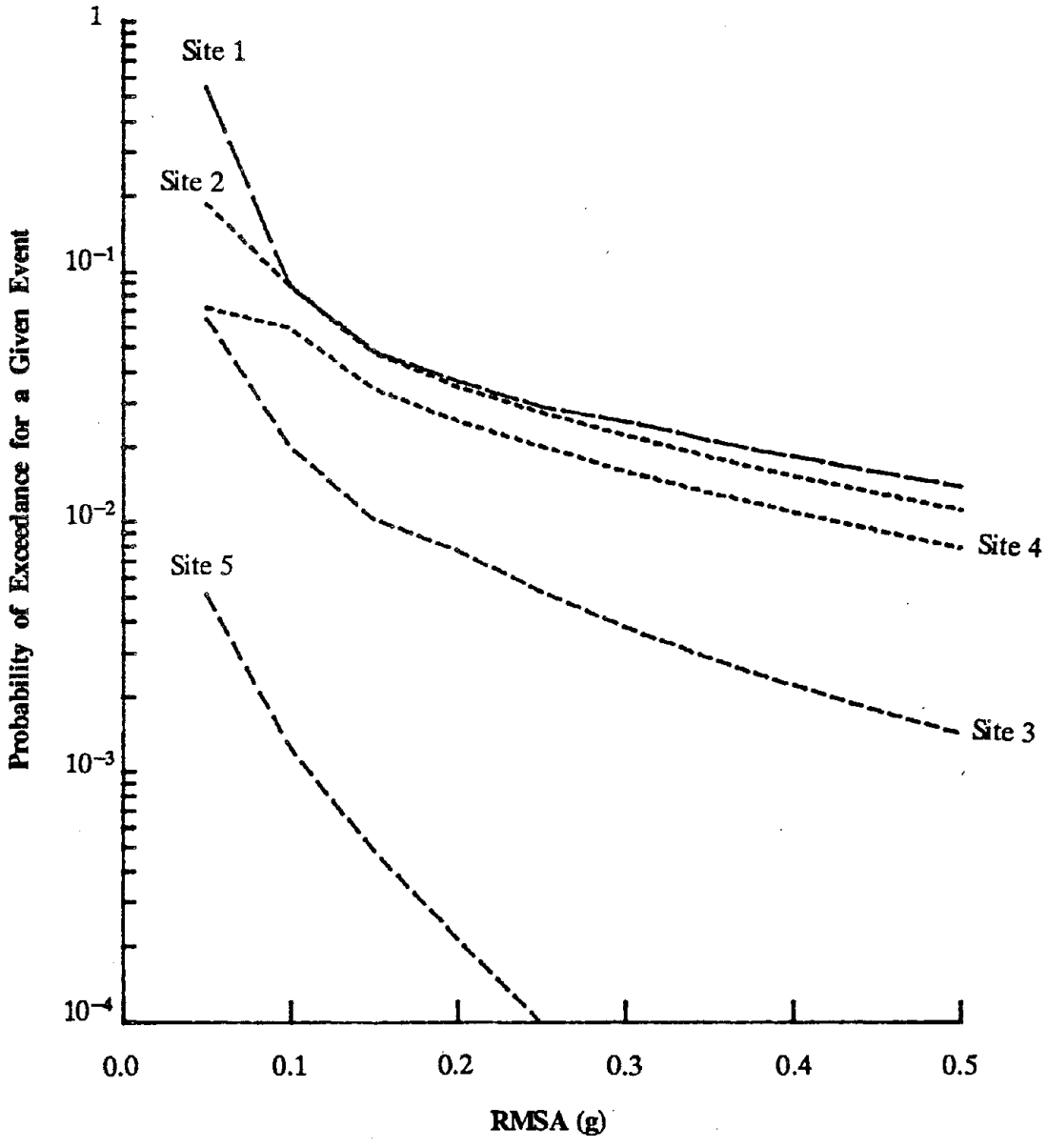

Fig. 5.13. Probability of Exceedance of RMSA including the Directivity Effect

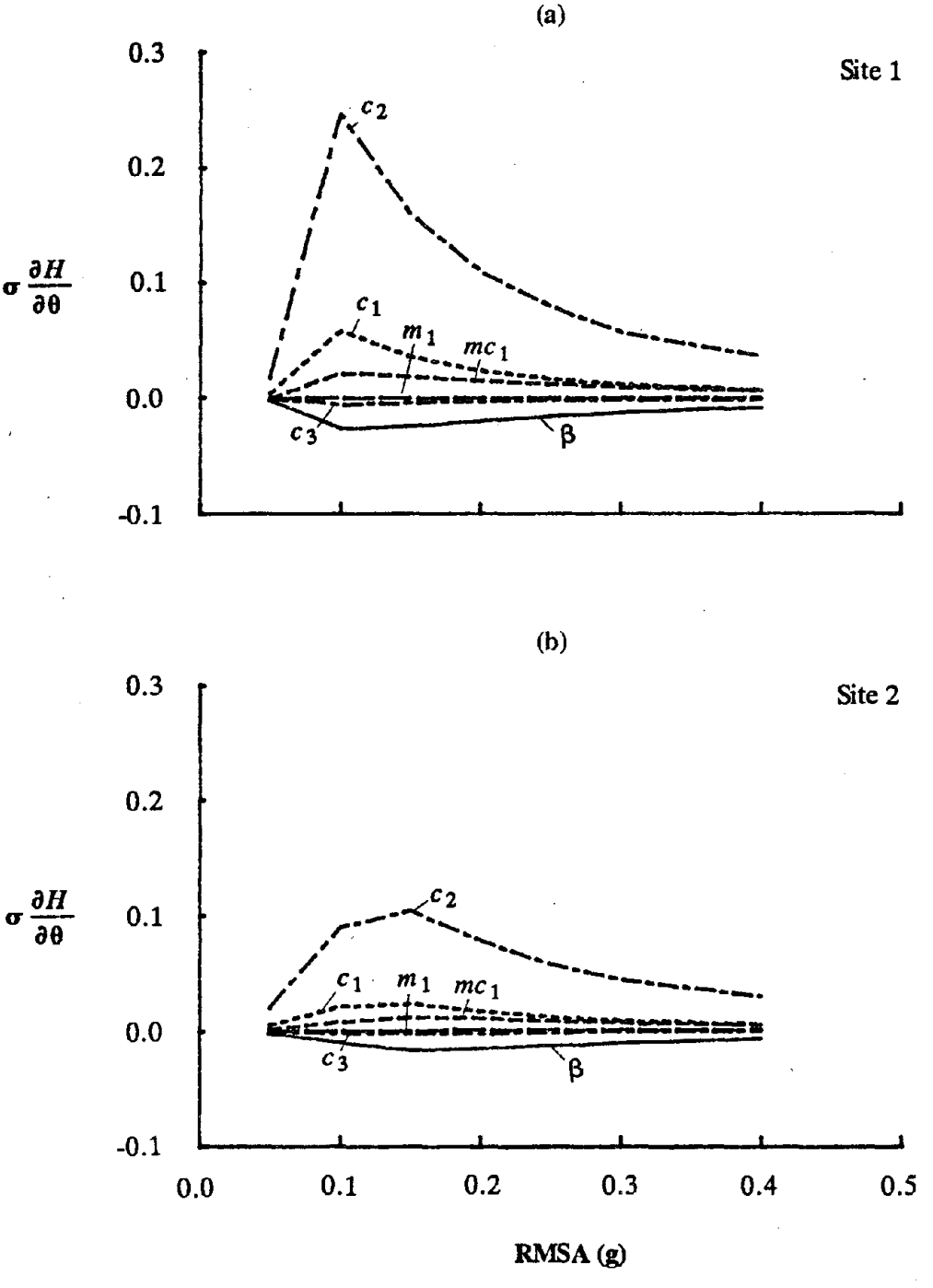

Fig. 5.14. Sensitivity Measures with Respect to Deterministic Parameters

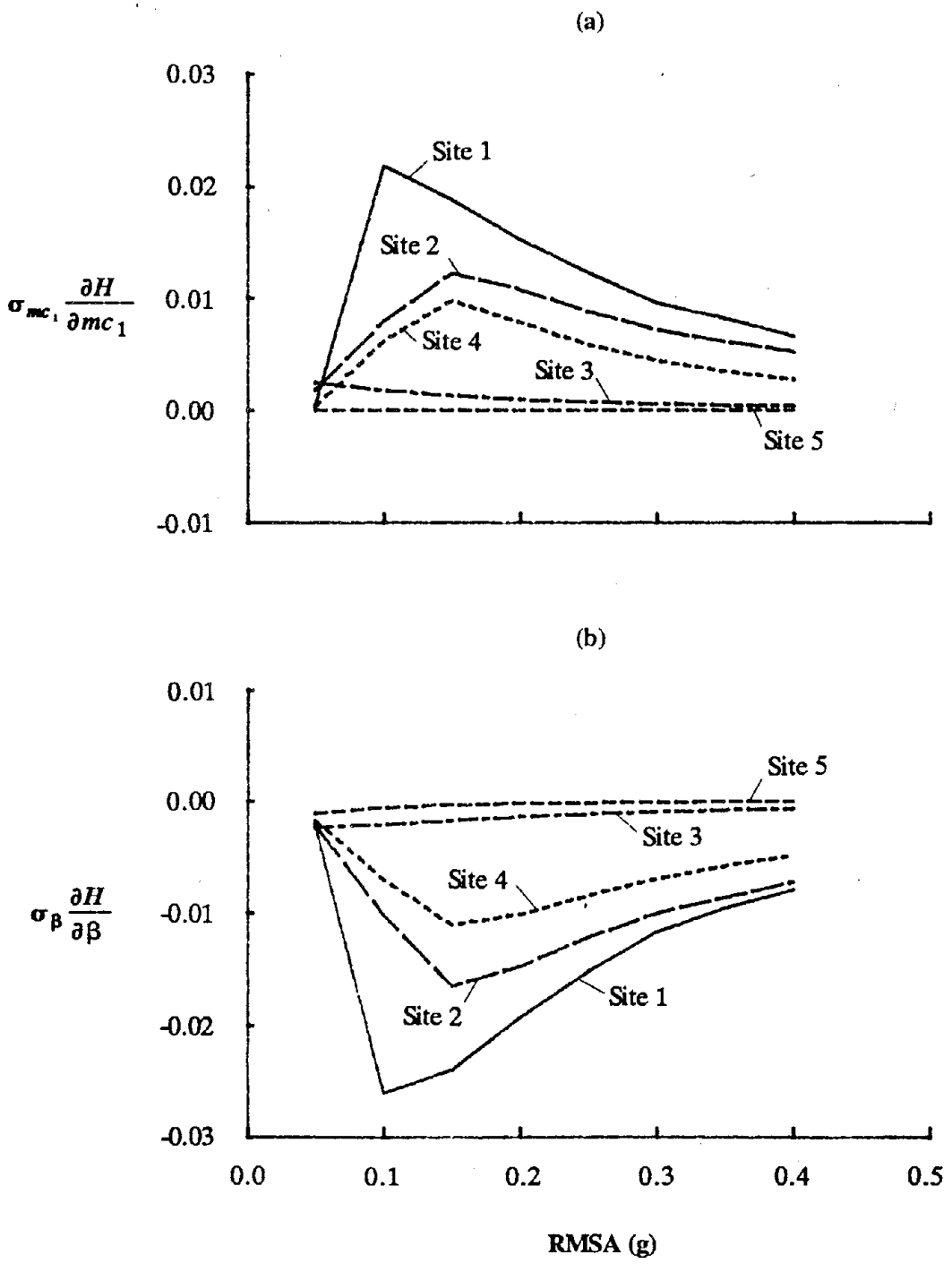

Fig. 5.15. Influence of Site Location on Seismic Hazard Sensitivities

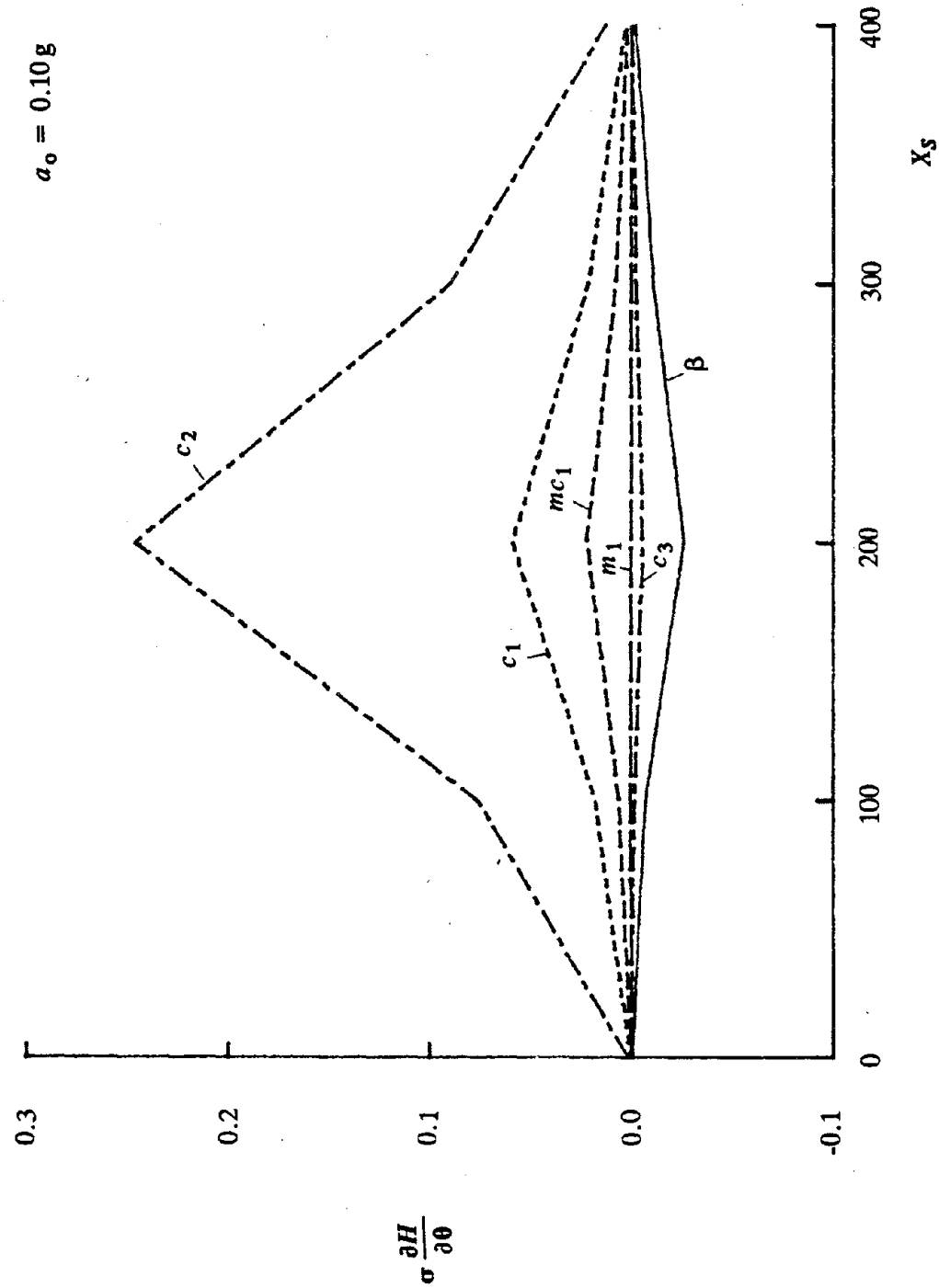

Fig. 5.16. Influence of RMSA on Seismic Hazard Sensitivities

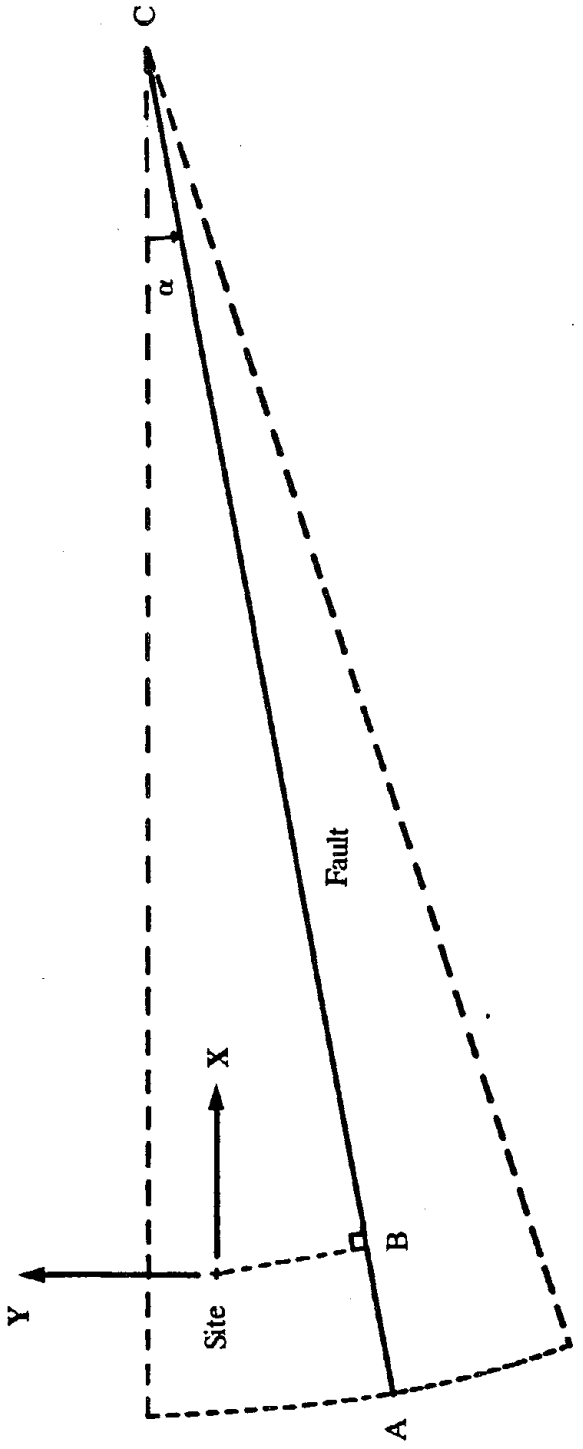

Fig. 5.17. Geometric Description of Example 4

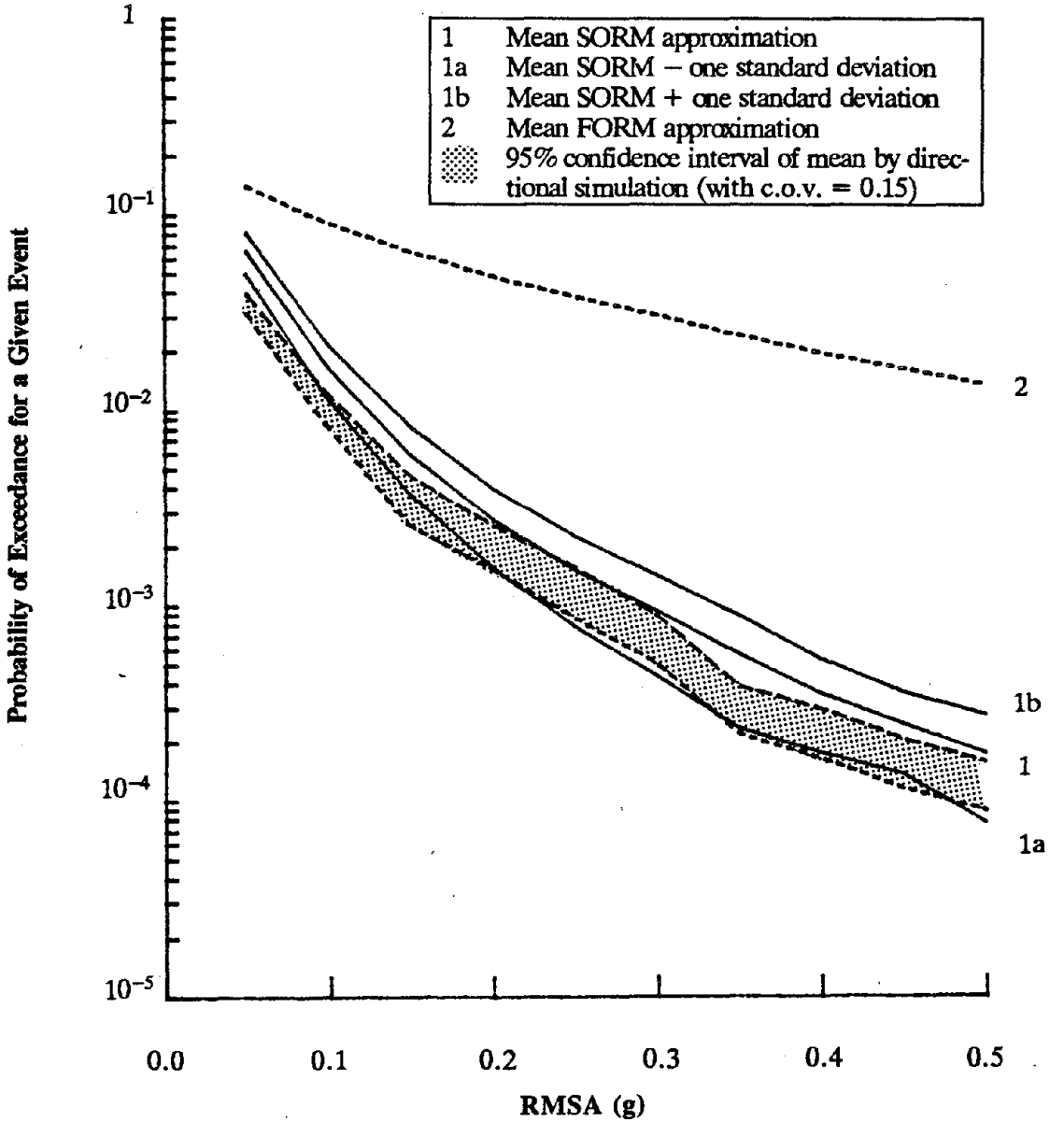

Fig. 5.18. Dispersion Estimate on Seismic Hazard Curve

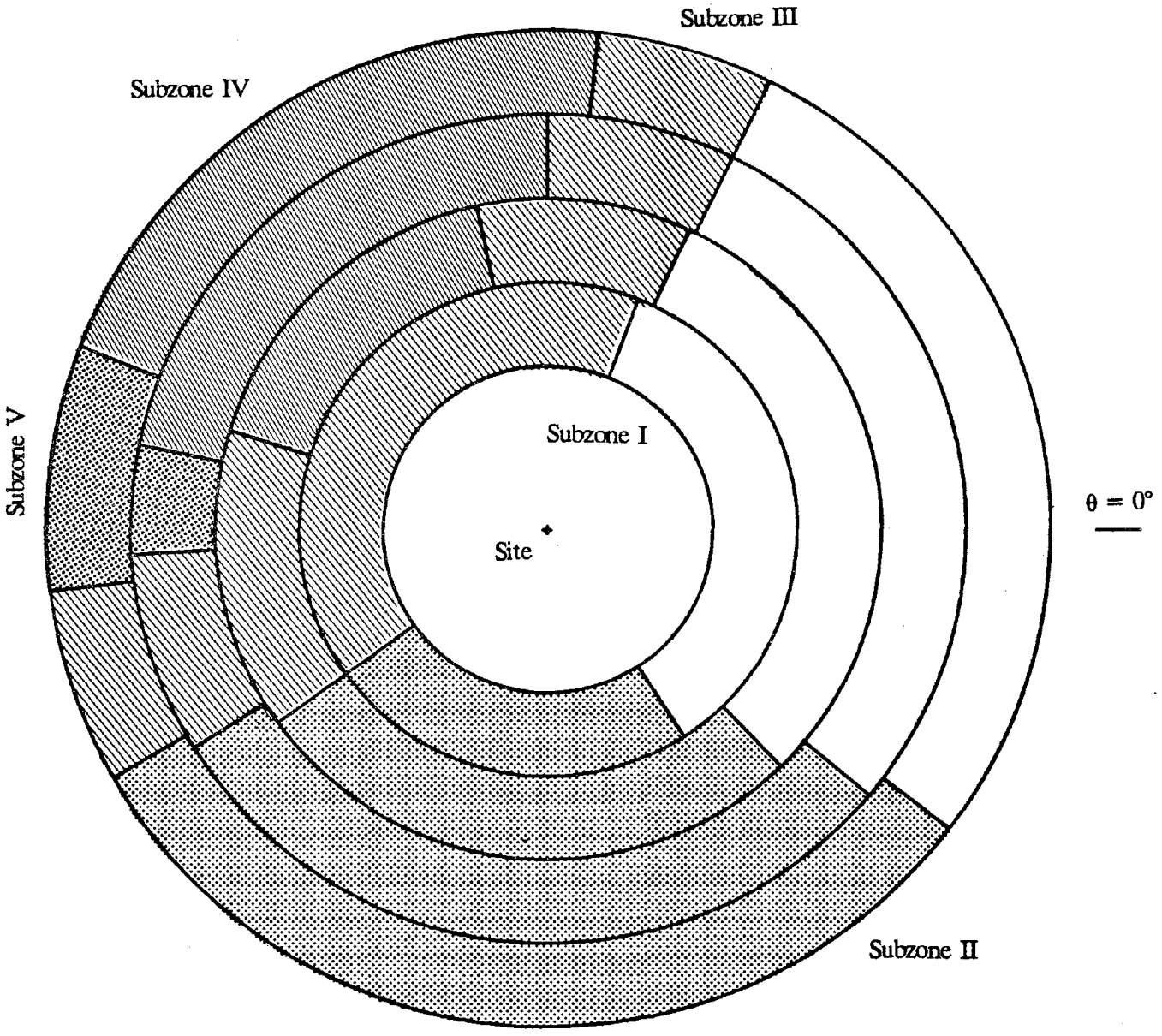

Fig. 5.19. Seismic Source Model for Tokyo

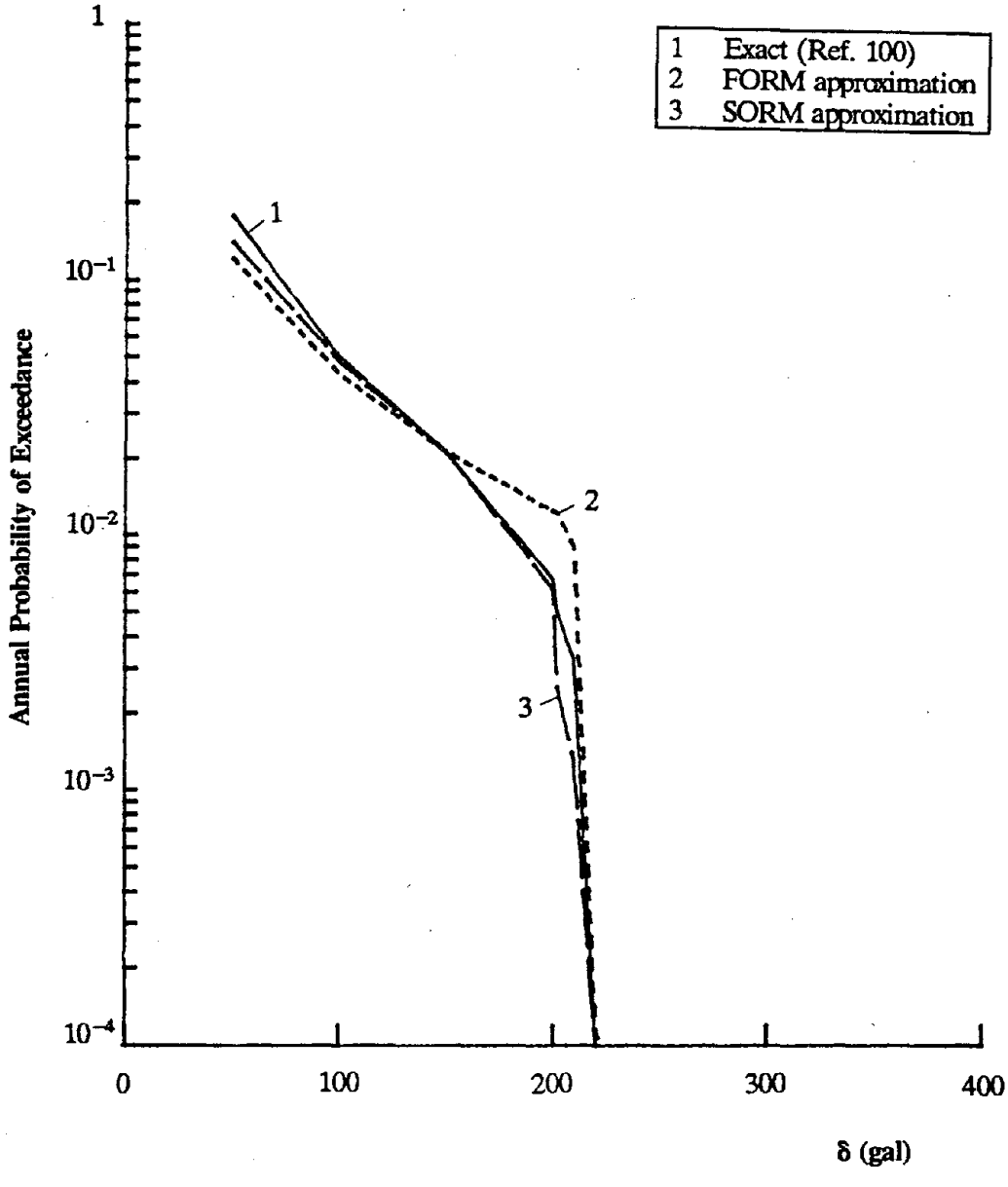

Fig. 5.20. Hazard Curves for Tokyo

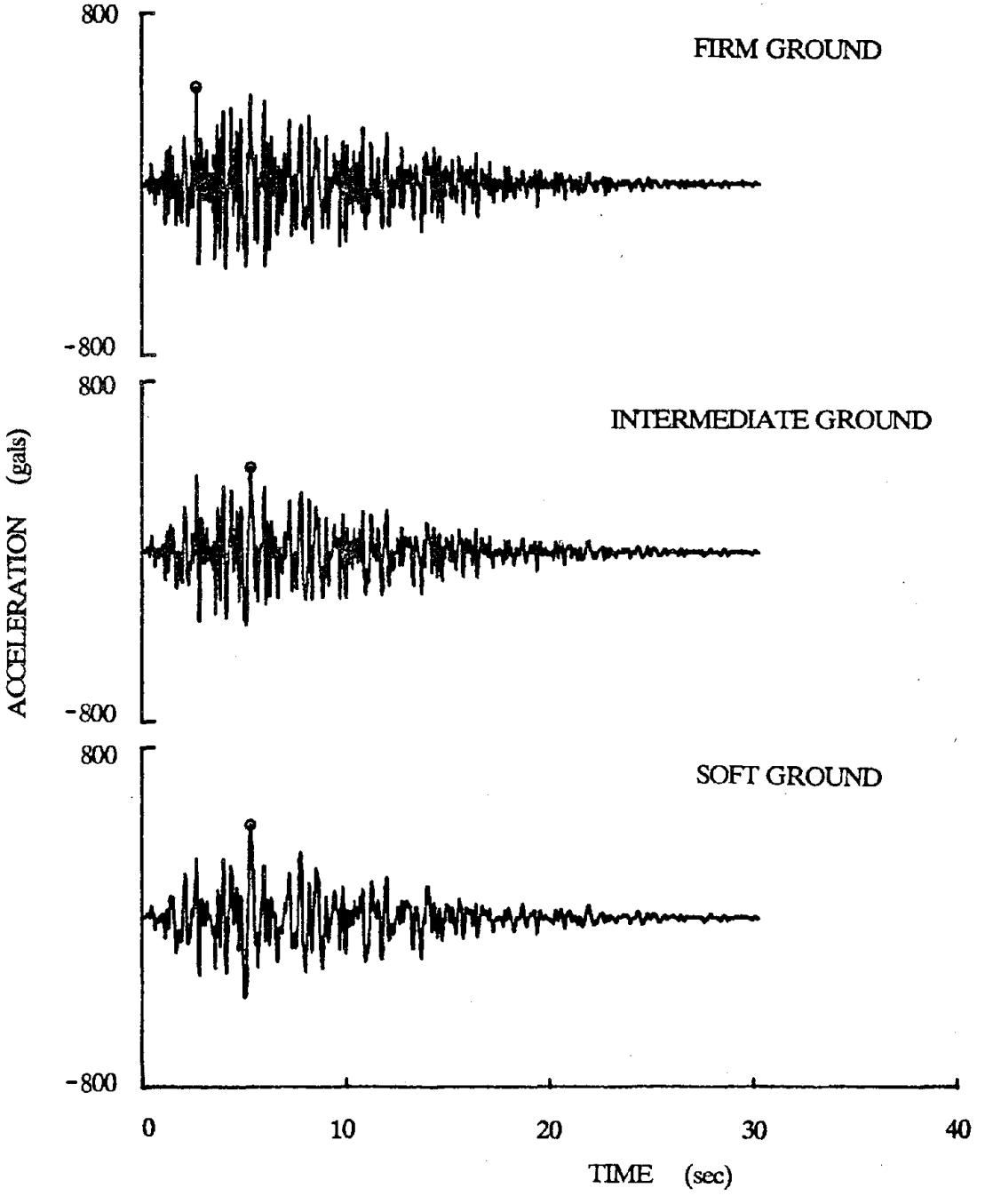

Fig. 5.21. Simulated Earthquake Ground Motions for Tokyo

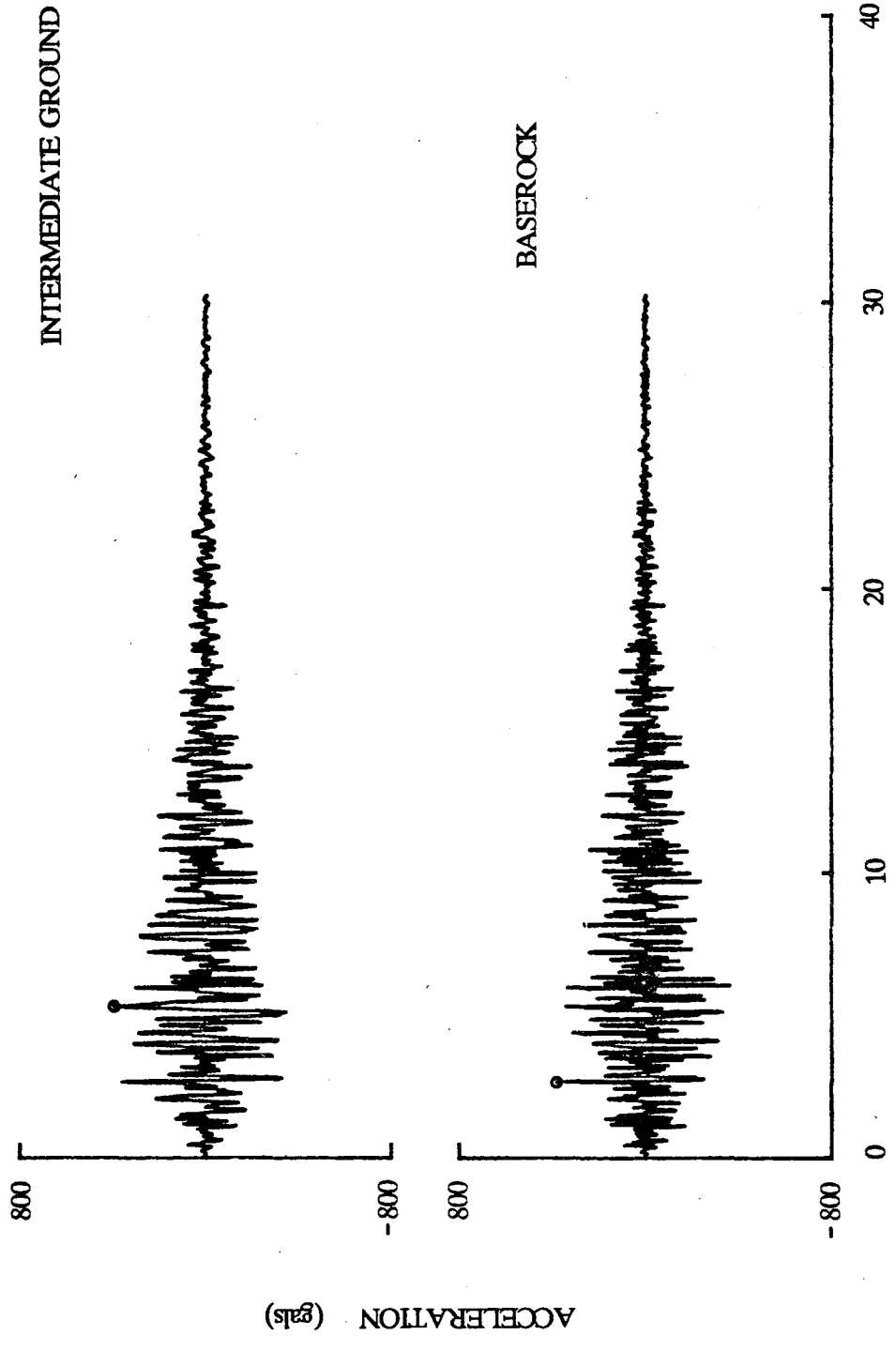

Fig. 5.22. Simulated Earthquake Motion on Baserock and Intermediate Ground

Chapter 6

SUMMARY AND CONCLUSIONS

In this study, a new methodology for the probabilistic assessment of seismic hazard is developed. It incorporates fast and efficient techniques of integration available from the field of structural reliability in the computation of the hazard, enabling a full probabilistic description of the earthquake process. A comprehensive review of the elements that integrate a probabilistic seismic hazard analysis is carried out.

The analogy between seismic hazard and structural reliability formulations is established and it is shown how the computation of the earthquake hazard can be done using approximate methods currently available from structural reliability theory. A number of methods to compute the probability of exceedance of a ground motion intensity level are examined. They include the first-order reliability method (FORM) and two second-order reliability methods, i.e., the curvature-fitting (SORM-CF) method and the point-fitting (SORM-PF) method. Several simulation methods are also discussed, including the directional simulation method.

With the new, improved formulation, the analysis of sensitivities and the treatment of uncertainties is greatly simplified. Sensitivities to the computed seismic hazard with respect to the basic random variables involved in the analysis, and with respect to deterministic parameters of the distributions and of the various models involved in the formulation are directly obtained during the process of solution. This is a clear advantage over the traditional procedures of seismic hazard analysis which require extensive repeated computations prior to the analysis of sensitivities. The analysis of uncertainties is carried out in a simple manner, which allows separate treatment of uncertainties arising from inherent variabilities from those arising from model and estimation errors. An estimate of the standard error in the computed hazard due to the latter source of uncertainties is obtained with little extra effort.

An important advantage provided by the new procedure is the ability to accommodate very general earthquake modeling. Two general seismic source models are developed and discussed:

a known fault model, and an area source model. Applications using various intensity attenuation models are presented to illustrate the use of sophisticated earthquake models and the versatility of the methodology.

From the examination of the results presented in this study, it is concluded that the proposed approximate solution techniques yield satisfactory results, especially when second-order reliability methods are used. The FORM approximation under certain conditions may lead to large errors and is not appropriate for the computation of the seismic hazard. The point-fitting procedure to obtain a second-order surface to approximate the boundary of integration (SORM-PF) is more stable and computationally less expensive than the curvature-fitting procedure (SORM-CF), giving an adequate approximation to the computed seismic hazard in most cases studied. Directional simulation is also found to be an effective tool for the computation of the seismic hazard.

The methodology presented in this study is a significant improvement over current methods of seismic hazard analysis. It not only permits a more comprehensive formulation of the problem, by incorporating earth science information relevant to seismic hazard that allows complex modeling of the earthquake generation mechanism and a general representation of the attenuation of seismic intensity, but also it provides direct information on sensitivities and a straightforward procedure for the analysis of uncertainties.

A complex model of attenuation of earthquake intensity incorporating the directivity effect is examined. In one example studied, the effect of directivity on the computed seismic hazard amounts to an increase of up to about one order of magnitude, depending on the relative position of the site of interest with respect to the orientation of the fault. The attenuation model including the directivity effect presented in this study should be validated against data from earthquake events as this information becomes available.

Future studies should assess which method, either SORM or directional simulation, presents more advantages for the estimation of the seismic hazard, the analysis of sensitivities and the treatment of uncertainties. Directional simulation is a procedure which holds promise for the

analysis of seismic hazard and should be thoroughly compared with the rest of the methods presented. A comprehensive analysis of sensitivities in real seismic hazard situations should be carried out to determine areas where further refinements and data are needed.

REFERENCES

1. Algermissen, S. T. and D. M. Perkins, "A Probabilistic Estimate of Maximum Acceleration in Rock in the Contiguous United States," U. S. Geological Survey, Open-File Report 74-416, 1976.
2. Algermissen, S. T., D. M. Perkins, W. Isherwood, D. Gordon, B. G. Reagor, and C. Howard, "Seismic Risk Evaluation of the Balkan Region," in *Proceedings of the Seminar on Seismic Zoning Maps*, vol. 2, pp. 172-240, Skopje, Yugoslavia, 1976.
3. Algermissen, S. T., D. M. Perkins, P. C. Thenhaus, S. L. Hanson, and B. L. Bender, "Probabilistic Estimates of Maximum Acceleration and Velocity in Rock in the Contiguous United States," U.S. Geological Survey, Open-File Report 82-1033, 1982.
4. Ambraseys, N. N. and J. Tchalenko, "Documentation of Faulting Associated with Earthquakes," Part I, Dept. of Civil Eng., Imperial College of Science, London, S.W.7, 1968.
5. Anagnos, T. and A. S. Kiremidjian, "Stochastic Time-Predictable Model for Earthquake Occurrences," *Bulletin of the Seismological Society of America*, vol. 74, no. 6, pp. 2593-2611, December 1984.
6. Anderson, J. G., "Program EQRISK: A Computer Program for Finding Uniform Risk Spectra of Strong Earthquake Ground Motion," Report, University of Southern California, Dept. of Civil Engineering, August 1978.
7. Anderson, J. G. and M. D. Trifunac, "Uniform Risk Functionals for Characterization of Strong Earthquake Ground Motion," *Bulletin of the Seismological Society of America*, vol. 68, no. 1, pp. 205-218, February 1978.
8. Ang, A. H.-S., "Probability Concepts in Earthquake Engineering," in *Applied Mechanics in Earthquake Engineering*, ed. W. D. Iwan, pp. 225-259, ASME, AMD 8, 1974.
9. Ang, A. H-S. and W. H. Tang, *Probability Concepts in Engineering Planning and Design - Volume II: Decision, Risk and Reliability,* John Wiley & Sons, Inc., New York, N. Y., 1984.
10. Araya, R. and A. Der Kiureghian, "Seismic Hazard Analysis Including Source Directivity Effect," in *Proceedings, Third U.S. National Conference on Earthquake Engineering*, vol. I, pp. 269-275, Charleston, South Carolina, 1986.
11. Araya, R. and G. R. Saragoni, "Earthquake Accelerogram Destructiveness Potential Factor," in *Proceedings, Eighth World Conference on Earthquake Engineering*, vol. II, pp. 835-843, San Francisco, California, July 1984.
12. Atkinson, G. M., "Attenuation of Strong Ground Motion in Canada from a Random Vibration Approach," *Bulletin of the Seismological Society of America*, vol. 74, no. 6, pp. 2629-2653, December 1984.
13. Atkinson, G. M. and R. G. Charlwood, "Uncertainties in Probabilistic Seismic Hazard Assessment as a Function of Probability Level: A Case History for Vancouver, British Columbia," *Bulletin of the Seismological Society of America*, vol. 73, no. 4, pp. 1225-1241, August 1983.
14. Barlow, R. E., "The Bayesian Approach in Risk Analysis," ASCE Specialty Conference on Probabilistic Mechanics and Structural Reliability, Berkeley, California, January 11-13, 1984.
15. Bender, B., "Maximum Likelihood Estimation of *b* Values for Magnitude Grouped Data," *Bulletin of the Seismological Society of America*, vol. 73, no. 3, pp. 831-851, June 1983.
16. Bender, B., "Seismic Hazard Estimation Using a Finite-Fault Rupture Model," *Bulletin of the Seismological Society of America*, vol. 74, no. 5, pp. 1899-1923, October 1984.
17. Bender, B., "Incorporating Acceleration Variability into Seismic Hazard Analysis," *Bulletin of the Seismological Society of America*, vol. 74, no. 4, pp. 1451-1462, August 1984.

18. Bender, B., "Modeling Source Zone Boundary Uncertainty in Seismic Hazard Analysis," *Bulletin of the Seismological Society of America*, vol. 76, no. 2, pp. 329-341, August 1986.

19. Bender, B. and D. Perkins, "SEISRISK II, A Computer Program for Seismic Hazard Estimation," U.S. Geological Survey, Open-File Report 82-293, 1982.

20. Bender, B. and D. Perkins, "SEISRISK III: A Computer Program for Seismic Hazard Estimation," U.S.G.S. Bulletin 1772, 1987.

21. Bernreuter, D. L., J. B. Savy, R. W. Mensing, H. C. Chen, and B. C. Davis, "Seismic Hazard Characterization of the Eastern United States: Vols. 1 & 2," LLNL Report UCID 20421, April 1985.

22. Berrill, J. B. and R. O. Davis, "Maximum Entropy and the Magnitude Distribution," *Bulletin of the Seismological Society of America*, vol. 70, no. 5, pp. 1823-1831, October 1980.

23. Bjerager, P., "Probability Integration by Directional Simulation," *Journal of the Engineering Mechanics Division.* submitted for publication

24. Bjerager, P. and S. Krenk, "Sensitivity Measures in Structural Reliability Analysis," 1st IFIP Working Conference on *Reliability and Optimization of Structural Systems*, University of Aalborg, Aalborg, Denmarck, May 6-8, 1987.

25. Bolt, B. A., "Fallacies in Current Ground Motion Prediction," in *Proceedings of the Second International Conference on Microzonation for Safer Construction - Research and Application*, vol. II, pp. 617-633, San Francisco, California, 1978.

26. Bolt, B. A., "Incomplete Formulations of the Regression of Earthquake Magnitude with Surface Fault Rupture Length," *Geology*, vol. 6, pp. 233-235, 1978.

27. Bolt, B. A., "The Contribution of Directivity Focusing to Earthquake Intensities. - State of the Art for Assessing Earthquake Hazards in the United States," Report 20, U.S. Army Engineer Waterways Experiment Station, Vicksburg, Mississippi, August 1983.

28. Bolt, B. A. and N. A. Abrahamson, "New Attenuation Relations for Peak and Expected Accelerations of Strong Ground Motion," *Bulletin of the Seismological Society of America*, vol. 72, no. 6, pp. 2301-2321, December 1982.

29. Bonilla, M. G. and J. M. Buchanan, "Interim Report on Worldwide Historic Surface Faulting," U. S. Geological Survey, Open-File Report, 1970.

30. Bonilla, M. G., R. K. Mark, and J. J. Lienkaemper, "Statistical Relations Among Earthquake Magnitude, Surface Rupture Length, and Surface Fault Displacement," *Bulletin of the Seismological Society of America*, vol. 74, no. 6, pp. 2379-2411, December 1984.

31. Boore, D. M., "Stochastic Simulation of High-Frequency Ground Motions Based on Seismological Models of the Radiated Spectra," *Bulletin of the Seismological Society of America*, vol. 73, no. 6, pp. 1865-1894, December 1983.

32. Boore, D. M., K. Aki, and T. Todd, "A Two-Dimensional Moving Dislocation Model for a Strike-Slip Fault," *Bulletin of the Seismological Society of America*, vol. 61, no. 1, pp. 177-194, February 1971.

33. Boore, D. M. and M. D. Zoback, "Near-Field Motions from Kinematic Models of Propagating Faults," *Bulletin of the Seismological Society of America*, vol. 64, no. 2, pp. 321-342, April 1974.

34. Breitung, K., "Asymptotic Approximations for Multinormal Integrals," *Journal of the Engineering Mechanics Division*, vol. 110, no. EM3, pp. 357-366, ASCE, March 1984.

35. Brillinger, D. R., "Some Bounds for Seismic Risk," *Bulletin of the Seismological Society of America*, vol. 72, no. 4, pp. 1403-1410, August 1982.

36. Brillinger, D. R., "Seismic Risk Assessment: Some Statistical Aspects," *Earthquake Prediction Research*, vol. 1, pp. 183-195, 1982.

37. Brillinger, D. R. and H. K. Preisler, "An Exploratory Analysis of the Joyner-Boore Attenuation Data," *Bulletin of the Seismological Society of America*, vol. 74, no. 4, pp. 1441-1450, August 1984.

38. Brillinger, D. R. and H. K. Preisler, "Further Analysis of the Joyner-Boore Attenuation Data," *Bulletin of the Seismological Society of America*, vol. 75, no. 2, pp. 611-614, April 1985.

39. Brune, J. N., "Tectonic Stress and the Spectra of Seismic Shear Waves from Earthquakes," *Journal of Geophysics Research*, vol. 75, no. 26, pp. 4997-5009, 1970.

40. Brune, J. N., "Correction," *Journal of Geophysics Research*, vol. 76, no. 20, p. 5002, 1971.

41. Bufe, C. G., P. W. Harsh, and R. O. Burford, "Steady-State Seismic Slip -- A Precise Recurrence Model," *Geophys. Res. Letters*, vol. 4, no. 2, pp. 91-94, February 1977.

42. Bureau, G. J., "Influence of Faulting on Earthquake Attenuation," in *Proceedings of ASCE Specialty Conference on Earthquake Engineering and Soil Dynamics*, vol. I, pp. 290-307, Pasadena, California, 1978.

43. Campbell, K. W., "Near-Source Attenuation of Peak Horizontal Acceleration," *Bulletin of the Seismological Society of America*, vol. 71, no. 6, pp. 2039-2070, December 1981.

44. Campbell, K. W., "Strong Motion Attenuation Relations: A Ten-Year Perspective," *Earthquake Spectra*, vol. 1, no. 4, pp. 759-804, August 1985.

45. Campbell, K. W., "Predicting Strong Ground Motion in Utah," in *Evaluation of Regional and Urban Earthquake Hazard and Risk in Utah*, ed. W. W. Hays and P. L. Gori, 1987. U. S. Geological Survey Professional Paper (in preparation).

46. Chiang, W-L., G. A. Guidi, C. P. Mortgat, C. C. Schoof, and H. C. Shah, "Computer Programs for Seismic Hazard Analysis. A User Manual (STAnford Seismic Hazard Analysis -- STASHA)," Report No. 62, The J. A. Blume Earthquake Engineering Center, Stanford University, January 1984.

47. Chinnery, M. A., "Earthquake Magnitude and Source Parameters," *Bulletin of the Seismological Society of America*, vol. 59, no. 5, pp. 1969-1982, October 1969.

48. Cluff, L. S., "Geologic Considerations for Seismic Microzonation," in *Proceedings of the Second International Conference on Microzonation for Safer Construction - Research and Application*, vol. I, pp. 135-152, San Francisco, California, 1978.

49. Cluff, L. S., A. S. Patwardhan, and K. J. Coppersmith, "Estimating the Probability of Occurrences of Surface Faulting Earthquakes on the Wasatch Fault Zone, Utah," *Bulletin of the Seismological Society of America*, vol. 70, no. 5, pp. 1463-1478, October 1980.

50. Coppersmith, K. J., "Probabilities of Earthquake Occurrences on the San Andreas Fault Based on Geologic Risk," *EOS*, vol. 62, no. 17, p. 322, 1981.

51. Coppersmith, K. J., "Application of Earth Science Information in Seismic Studies in the Eastern United States," in *Proceedings of Conference XXXIV--A Workshop on "Probabilistic Earthquake Hazards Assessments"*, ed. Walter W. Hays, U. S. Geological Survey, Open-File Report 86-185, pp. 158-171, Reston, Virginia, 1986.

52. Coppersmith, K. J. and R. R. Youngs, "Capturing Uncertainty in Probabilistic Seismic Hazard Assessments Within Intraplate Tectonic Environments," in *Proceedings, Third U.S. National Conference on Earthquake Engineering*, vol. I, pp. 301-312, Charleston, South Carolina, 1986.

53. Cornell, C. A., "Bounds on the Reliability of Structural Systems," *Journal of the Structural Division*, vol. 93, no. ST1, pp. 171-200, ASCE, February 1967.

54. Cornell, C. A., "Engineering Seismic Risk Analysis," *Bulletin of the Seismological Society of America*, vol. 58, no. 5, pp. 1583-1606, October 1968.

55. Cornell, C. A., "Probabilistic Analysis of Damage to Structures under Seismic Loads," in *Dynamic Waves in Civil Engineering*, ed. D. A. Howells, I. P. Haigh and C. Taylor, J. Wiley, London, 1971.

56. Cornell, C. A. and H. A. Merz, "Seismic Risk Analysis of Boston," *J. Struct. Div., ASCE*, vol. 101, no. ST10, pp. 2027-2043, October 1975.

57. Cornell, C. A. and E. H. Vanmarcke, "The Major Influences on Seismic Risk," in *Proceedings, Fourth World Conference on Earthquake Engineering*, vol. I, pp. 69-83, Santiago, Chile, 1969.

58. Cornell, C. A. and S. R. Winterstein, "Applicability of the Poisson Earthquake-Occurrence Model," Seismic Hazard Methodology for the Central and Eastern United States, Vol. 1: Probabilistic Seismic Hazard Methodology, EPRI Research Report, Project P101-38, May 1986.

59. Cosentino, P., V. Ficarra, and D. Luzio, "Truncated Exponential Frequency-Magnitude Relationship in Earthquake Statistics," *Bulletin of the Seismological Society of America*, vol. 67, no. 6, pp. 1615-1623, December 1977.

60. Çinlar, E., *Introduction to Stochastic Processes*, Prentice-Hall,, New Jersey, 1975.

61. Dalal, J. S., "Probabilistic Seismic Exposure and Structural Risk Evaluation," Ph. D. Thesis, Stanford University, 1972.

62. Deàk, I., "Three Digit Accurate Multiple Normal Probabilities," *Numerische Mathematik*, vol. 35, pp. 369-380, 1980.

63. Der Kiureghian, A., "Seismic Risk Analysis Including Attenuation Uncertainty," in *Proceedings, U.S.-Southeast Asia Symposium on Engineering for Natural Hazards Protection*, ed. A. H-S. Ang, Manila, Philippines, September, 1977.

64. Der Kiureghian, A., "SRAP - Seismic Risk Analysis Program," Agbabian Associates, El Segundo, California, October 1978.

65. Der Kiureghian, A., "Seismic Risk Analysis of Structural Systems," *Journal of the Engineering Mechanics Division*, vol. 107, no. EM6, pp. 1133-1153, ASCE, December 1981.

66. Der Kiureghian, A. and A. H-S. Ang, "A Fault-Rupture Model for Seismic Risk Analysis," *Bulletin of the Seismological Society of America*, vol. 67, no. 4, pp. 1173-1194, August 1977.

67. Der Kiureghian, A. and R. Araya, "Source Models and Analysis of Uncertainties in Earthquake Hazard Assessment," in *Proceedings of Conference XXXIV--A Workshop on "Probabilistic Earthquake Hazards Assessments"*, ed. Walter W. Hays, U. S. Geological Survey, Open-File Report 86-185, pp. 142-157, Reston, Virginia, 1986.

68. Der Kiureghian, A., H-Z. Lin, and S-J. Hwang, "Second-Order Reliability Approximations," *Journal of the Engineering Mechanics Division*, vol. 113, no. EM8, pp. 1208-1225, ASCE, August 1987.

69. Der Kiureghian, A. and P-L. Liu, "Structural Reliability Under Incomplete Probability Information," *Journal of the Engineering Mechanics Division*, vol. 112, no. EM1, pp. 85-104, January 1986.

70. Ditlevsen, O., "Narrow Reliability Bounds for Structural Systems," *Journal of Structural Mechanics*, vol. 7, no. 4, pp. 453-472, December 1979.

71. Donovan, N. C., "Strong Motion Equations - A Critique," in *Proceedings of the Third International Conference on Microzonation*, vol. I, pp. 377-388, Seattle, Washington, 1982.

72. Donovan, N. C. and A. E. Bornstein, "Uncertainties in Seismic Risk Procedures," *Journal of the Geotechnical Engineering Division*, vol. 104, no. GT7, pp. 869-887, ASCE, July, 1978.

73. Douglas, B. M. and A. Ryall, "Return Periods for Rock Acceleration in Western Nevada," *Bulletin of the Seismological Society of America*, vol. 65, no. 6, pp. 1599-1611, December 1975.

74. Electric Power Research Institute,, "Seismic Hazard Methodology for Nuclear Facilities in the Eastern United States," EPRI Research Project No. P101-29, 1985.

75. Esteva, L., "Seismicity Prediction: A Bayesian Approach," in *Proceedings, Fourth World Conference on Earthquake Engineering*, vol. I, pp. 172-184, Santiago, Chile, 1969.

76. Esteva, L., "Seismic Risk and Seismic Design Decisions," in *Seismic Design for Nuclear Power Plants*, ed. R. J. Hansen, M.I.T. Press, Cambridge, Mass., 1970.

77. Esteva, L., "Seismicity," in *Seismic Risk and Engineering Decisions*, ed. C. Lomnitz and E. Rosenblueth, pp. 179-224, Elsevier Science Publication Company, New York, N. Y., 1976.

78. Faccioli, E., "Measures of Strong Ground Motion derived from a Stochastic Source Model," *Soil Dynamics and Earthquake Engineering*, vol. 2, no. 3, pp. 135-149, 1983.

79. Ferraes, S. G., "Test of Poisson Process for Earthquakes in Mexico City," *Journal of Geophysical Research*, vol. 72, no. 14, pp. 3741-3742, July 15, 1967.

80. Gardner, J. K. and L. Knopoff, "Is the Sequence of Earthquakes in Southern California, with Aftershocks Removed, Poissonian?," *Bulletin of the Seismological Society of America*, vol. 64, no. 5, pp. 1363-1367, October 1974.

81. Guarnieri Botti, L., V. Pasquale, and M. Anghinolfi, "A New General Frequency-Magnitude Relationship," *Pure and Applied Geophysics*, vol. 119, pp. 196-206, 1980/81.

82. Gutenberg, B. and C. F. Richter, "Frequency of Earthquakes in California," *Bulletin of the Seismological Society of America*, vol. 34, no. 4, pp. 185-188, October 1944.

83. Hagiwara, Y., "Probability of Earthquake Occurrence as Obtained from a Weibull Distribution Analysis of Crustal Strain," *Tectonophysics*, vol. 23, no. 3, pp. 313-318, August 1974.

84. Hammersley, J. M. and K. W. Morton, "A New Monte Carlo Technique Antithetic Variates," *Proc. Cambridge Phil. Soc*, vol. 52, pp. 449-474, 1956.

85. Hanks, T. C. and R. K. McGuire, "The Character of High-Frequency Strong Ground Motion," *Bulletin of the Seismological Society of America*, vol. 71, no. 6, pp. 2071-2095, December 1981.

86. Haskell, N. A., "Total Energy and Energy Spectral Density of Elastic Wave Radiation from Propagating Faults. Part II. A Statistical Source Model," *Bulletin of the Seismological Society of America*, vol. 56, no. 1, pp. 125-140, February 1966.

87. Hawkes, A. G. and L. Adamopoulos, "Cluster Models for Earthquakes-Regional Comparisons," *Bull. Int. Stat. Inst.*, vol. 45, no. 3, pp. 454-461, 1973.

88. Hohenbichler, M., "An Asymptotic Formula for the Probability of Intersections," Berichte zur Zuverlässigkeitstheorie der Bauwerke, Heft 69, pp. 21-48, Technical University of München, 1984.

89. Hohenbichler, M., S. Gollwitzer, W. Kruse, and R. Rackwitz, "New Light on First- and Second-Order Reliability Methods," *Structural Safety*, vol. 4, pp. 267-284, 1987.

90. Hohenbichler, M. and R. Rackwitz, "Non-Normal Dependent Vectors in Structural Safety," *Journal of the Engineering Mechanics Division*, vol. 107, no. EM6, pp. 1227-1238, ASCE, December 1981.

91. Idriss, I. M., "Characteristics of Earthquake Ground Motions," in *Proceedings of ASCE Specialty Conference on Earthquake Engineering and Soil Dynamics*, vol. III, pp. 1151-1265, Pasadena, California, 1978.

92. Idriss, I. M., "Evaluating Seismic Risk in Engineering Practice," in *Proceedings, Eleventh International Conference on Soil Mechanics and Foundation Engineering*, vol. 1, pp. 255-320, San Francisco, California, August 1985.

93. Iida, K., "Earthquake Energy and Earthquake Fault," *J. Earth. Sci., Nagoya Univ.*, vol. 7, no. 2, pp. 98-107, December 1959.

94. Iida, K., "Earthquake Magnitude, Earthquake Fault and Source Dimensions," *J. Earth. Sci., Nagoya Univ.*, vol. 13, no. 2, pp. 115-132, December 1965.

95. Ishimoto, M. and K. Iida, "Observations sur les séismes enregistrés par le microseismographe construit dernièrment," *Bull. Earthquake Res. Inst., Univ. Tokyo*, vol. 17, pp. 443-478, 1939.

96. Johnson, N. L. and S. Kotz, *Distributions in Statistics - Continuous Multivariate Distributions*, John Wiley & Sons, Inc., New York, N. Y., 1976.

97. Joyner, W. B. and D. M. Boore, "Peak Horizontal Acceleration and Velocity from Strong-Motion Records Including Records from the 1979 Imperial Valley, California, Earthquake," *Bulletin of the Seismological Society of America*, vol. 71, no. 6, pp. 2011-2038, December 1981.

98. Kallberg, K. T. and C. A. Cornell, "Seismic Risk in Southern California," Research Report, M.I.T., Department of Civil Engineering, June, 1969.

99. Kameda, H., "Engineering Application of Stochastic Earthquake Motion Models with Non-linear Soil Amplification," in *Proceedings, 9th International Conference on Structural*

Mechanics in Reactor Technology, vol. A, pp. 321-336, Lausanne, Switzerland, 1987.

100. Kameda, H. and N. Nojima, "Simulation of Risk-Consistent Earthquake Motion," submitted for possible publication in the *International Journal of Earthquake Engineering and Structural Dynamics*.
101. Kameda, H. and Y. Ozaki, "A Renewal Process Model for Use in Seismic Risk Analysis," *Memoirs of the Faculty of Engineering, Kyoto University*, vol. 41, pp. 11-35, 1979.
102. Kanamori, H. and D. L. Anderson, "Theoretical Basis for some Empirical Relations in Seismology," *Bulletin of the Seismological Society of America*, vol. 65, no. 5, pp. 1073-1095, October 1975.
103. Kennedy, R. P., S. A. Short, K. L. Merz, F. J. Tokarz, I. M. Idriss, M. S. Power, and K. Sadigh, "Engineering Characterization of Ground Motion - Task I: Effects of Characteristics of Free-Field Motion on Structural Response," U.S. Nuclear Regulatory Commission Rept. NUREG/CR-3805, 1984.
104. King, C.-Y. and L. Knopoff, "Stress Drop in Earthquakes," *Bulletin of the Seismological Society of America*, vol. 58, no. 1, pp. 249-257, February 1968.
105. King, G. and J. Nábělek, "Role of Fault Bends in the Initiation and Termination of Earthquake Rupture," *Science*, vol. 228, pp. 984-987, 24 May 1985.
106. Kiremidjian, A. S. and T. Anagnos, "Stochastic Models for Earthquake Occurrence," Report, The John A. Blume Earthquake Engineeering Center, Stanford University, May 1983.
107. Kiremidjian, A. S. and T. Anagnos, "Stochastic Slip-Predictable Model for Earthquake Occurrences," *Bulletin of the Seismological Society of America*, vol. 74, no. 2, pp. 739-755, April 1984.
108. Kiremidjian, A. S. and H. C. Shah, "Seismic Hazard Mapping of California," Report No. 21, The John A. Blume Earthquake Engineering Center, Stanford University, November 1975.
109. Kiremidjian, A. S. and H. C. Shah, "Seismic Hazard Analysis of Honduras," Report No. 38, The John A. Blume Earthquake Engineering Center, Stanford University, August 1979.
110. Kiremidjian, A. S., H. C. Shah, and L. Lubetkin, "Seismic Hazard Mapping for Guatemala," Report No. 26, The John A. Blume Earthquake Engineering Center, Stanford University, May 1977.
111. Klimkiewicz, G. C., G. Leblanc, R. J. Holt, and T. R. Thiruvengadam, "Relative Seismic Hazard Assessment for the North Central United States," in *Proceedings, Eighth World Conference on Earthquake Engineering*, vol. I, pp. 149-156, San Francisco, California, 1984.
112. Krinitzsky, E. L., "Fault Assessment in Earthquake Engineering. - State of the Art for Assessing Earthquake Hazards in the United States," Report 2, U.S. Army Engineer Waterways Experiment Station, Vicksburg, Mississippi, May 1974.
113. Kulkarni, R. B., K. Sadigh, and I. M. Idriss, "Probabilistic Evaluation of Seismic Exposure," in *Proceedings of the 2nd U. S. National Conference on Earthquake Engineering*, pp. 90-98, Stanford, California, 1979.
114. Kulkarni, R. B., R. R. Youngs, and K. J. Coppersmith, "Assessment of Confidence Intervals for Results of Seismic Hazard Analysis," in *Proceedings, Eighth World Conference on Earthquake Engineering*, vol. I, pp. 263-270, San Francisco, California, 1984.
115. Lin, H-Z. and A. Der Kiureghian, "Second-Order System Reliability Using Directional Simulation," in *Reliability and Risk Analysis in Civil Engineering, ICASP5*, ed. N. C. Lind, vol. 2, pp. 930-937, Institute for Risk Research, University of Waterloo, Ontario, Canada, 1987.
116. Liu, P-L. and A. Der Kiureghian, "Multivariate Distribution Models with Prescribed Marginals and Covariances," *Probabilistic Engineering Mechanics*, vol. 1, no. 2, pp. 105-112, 1986.
117. Liu, P-L. and A. Der Kiureghian, "Optimization Algorithms for Structural Reliability Analysis," Report No. UCB/SESM-86/09, Dept. of Civil Engineering, University of California, Berkeley, July 1986.

118. Lomnitz-Adler, J. and C. Lomnitz, "A Modified Form of the Gutenberg-Richter Magnitude-Frequency Relation," *Bulletin of the Seismological Society of America*, vol. 69, no. 4, pp. 1209-1214, August 1979.

119. Lomnitz, C., "Poisson Processes in Earthquake Studies," *Bulletin of the Seismological Society of America*, vol. 63, no. 2, p. 735, April 1973.

120. Madsen, H. O., S. Krenk, and N. C. Lind, *Methods of Structural Safety,* Prentice-Hall, Inc., Englewood Cliffs, N.J., 1986.

121. Main, I. G. and P. W. Burton, "Information Theory and the Earthquake Frequency-Magnitude Distribution," *Bulletin of the Seismological Society of America*, vol. 74, no. 4, pp. 1409-1426, August 1984.

122. Mark, R. K., "Application of Linear Statistical Models of Earthquake Magnitude versus Fault Length in Estimating Maximum Expectable Earthquakes," *Geology*, no. 5, pp. 464-466, 1977.

123. Mark, R. K., "Comment on 'Incomplete Formulations of the Regression of Earthquake Magnitude with Surface Fault Rupture Length'," *Geology*, vol. 6, p. 6, 1978.

124. Mark, R. K. and M. G. Bonilla, "Regression Analysis of Earthquake Magnitude and Surface Fault Length using the 1970 data of Bonilla and Buchanan," U. S. Geological Survey, Open-File Report, 1977.

125. McGuire, R. K., "Fortran Computer Program for Seismic Risk Analysis," U.S. Geological Survey, Open-File Report 76-67, 1976.

126. McGuire, R. K., "FRISK: Computer Program for Seismic Risk Analysis Using Faults as Earthquake Sources," U.S. Geological Survey, Open-File Report 78-1007, 1978.

127. McGuire, R. K., "Seismic Hazard Analysis Methodology," in *Notes from course on Recent Advances in Earthquake-Resistant Design*, University of California, Berkeley, July 20-24, 1987.

128. McGuire, R. K., A. M. Becker, and N. C. Donovan, "Spectral Estimates of Seismic Shear Waves," *Bulletin of the Seismological Society of America*, vol. 74, no. 4, pp. 1427-1440, August 1984.

129. McGuire, R. K. and T. C. Hanks, "RMS Acceleration and Spectral Amplitudes of Strong Ground Motion during the San Fernando, California, Earthquake," *Bulletin of the Seismological Society of America*, vol. 70, no. 5, pp. 1907-1920, October 1980.

130. McGuire, R. K. and K. M. Shedlock, "Statistical Uncertainties in Seismic Hazard Evaluations in the United States," *Bulletin of the Seismological Society of America*, vol. 71, no. 4, pp. 1287-1308, August 1981.

131. Merz, H. A. and C. A. Cornell, "Seismic Risk Analysis Based on a Quadratic Magnitude-Frequency Law," *Bulletin of the Seismological Society of America*, vol. 63, no. 6, pp. 1999-2006, December 1973.

132. Mihailov, V., "Sensitivity Analysis of Uncertainty in Seismic Sources Modeling on Seismic Hazard Mapped Parameters," in *Proceedings of the 2nd U. S. National Conference on Earthquake Engineering*, pp. 783-792, Stanford, California, 1979.

133. Milne, W. G. and A. G. Davenport, "Distribution of Earthquake Risk in Canada," *Bulletin of the Seismological Society of America*, vol. 59, no. 2, pp. 729-754, April 1969.

134. Moghtaderi-Zadeh, M. and D. Diamantidis, "Full Probabilistic Seismic Risk Evaluation," in *Proceedings of the 8th European Conference on Earthquake Engineering*, pp. 2.5/25-2.5/32, Lisbon, Portugal, 1986.

135. Moghtaderi-Zadeh, M., R. K. Wood, A. Der Kiureghian, and R. E. Barlow, "Seismic Reliability of Lifeline Networks," *Journal of the Technical Councils*, vol. 108, no. TC1, pp. 60-78, ASCE, May 1982.

136. Monzón-Despang, H., "Seismic Performance Analysis of Spatially Distributed Systems," Report, The J. A. Blume Earthquake Engineering Center, Stanford University, June 1980.

137. Mortgart, C. P., T. C. Zsutty, H. C. Shah, and L. Lubetkin, "A Study of Seismic Risk for Costa Rica," Report No. 25, The John A. Blume Earthquake Engineering Center, Stanford

University, April 1977.

138. Mortgat, C. P. and H. C. Shah, *Seismic Hazard Analysis of Algeria*, The John A. Blume Earthquake Engineering Center, Stanford University, June 1978.
139. Nishioka, T. and H. C. Shah, "Application of the Markov Chain on Probability of Earthquake Occurrences," in *Proceedings of JSCE*, pp. 137-145, June 1980.
140. Oliveira, C. S., "Seismic Risk Analysis," Report No. EERC 74-1, University of California, Berkeley, 1974.
141. Oliveira, C. S., "Comparative Seismic Hazard Studies for the San Francisco Bay Region," in *Proceedings of the 2nd U. S. National Conference on Earthquake Engineering*, pp. 62-71, Stanford, California, 1979.
142. Patwardhan, A. S., R. B. Kulkarni, and D. Tocher, "A Semi-Markov Model for Characterizing Recurrence of Great Earthquakes," *Bulletin of the Seismological Society of America*, vol. 70, no. 1, pp. 323-347, February 1980.
143. Purcaru, G., "A New Magnitude-Frequency Relation for Earthquakes and a Classification of Relation Types," *Geophys. J. R. astr. Soc.*, vol. 42, pp. 61-79, 1975.
144. Rice, J., "Statistical Methods of Use in Analyzing Sequences of Earthquakes," *Geophys. J. R. astr. Soc.*, vol. 42, pp. 671-683, 1975.
145. Rosenblatt, M., "Remarks on a Multivariate Transformation," *The Annals of Mathematical Statistics*, vol. 23, pp. 470-472, 1952.
146. Rubinstein, R. Y., *Simulation and the Monte Carlo Method*, John Wiley & Sons, Inc., New York, N. Y., 1981.
147. Savy, J. B., H. C. Shah, and D. M. Boore, "Nonstationary Risk Model with Geophysical Input," *J. Struct. Div., ASCE*, vol. 106, no. ST1, pp. 145-164, January 1980.
148. Schwartz, D. P. and K. J. Coppersmith, "Fault Behavior and Characteristic Earthquakes: Examples from the Wasatch and San Andreas Fault Zones," *J. Geophys. Res.*, vol. 89, no. B7, pp. 5681-5698, 1984.
149. Shah, H. C., C. P. Mortgat, A. S. Kiremidjian, and T. C. Zsutty, "A Study of Seismic Risk for Nicaragua, Part I," Report No. 11, The John A. Blume Earthquake Engineering Center, Stanford University, January 1975.
150. Shimazaki, K. and T. Nakata, "Time Predictable Recurrence for Large Earthquakes," *Geophys. Res. Letters*, vol. 86, no. 4, pp. 279-282, April 1980.
151. Shlien, S. and M. N. Toksöz, "A Clustering Model for Earthquake Occurrences," *Bulletin of the Seismological Society of America*, vol. 60, no. 6, pp. 1765-1787, December 1970.
152. Shlien, S. and M. N. Toksöz, "Frequency-Magnitude Statistics of Earthquake Occurrences," *Earthquake Notes*, vol. 41, no. 1, pp. 5-18, March 1970.
153. Shlien, S. and M. N. Toksöz, "A Branching Poisson-Markov Model of Earthquake Occurrences," *Geophys. J. R. astr. Soc.*, vol. 42, pp. 49-59, 1975.
154. Silva, F. S., "Seismic Risk in Chile," Technical Report, Department of Civil Engineering, Stanford University, 1973.
155. Singh, S. K., E. Bazán, and L. Esteva, "Expected Earthquake Magnitude from a Fault," *Bulletin of the Seismological Society of America*, vol. 70, no. 3, pp. 903-914, June 1980.
156. Slemmons, D. B., "Faults and Earthquake Magnitude - State of the Art for Assessing Earthquake Hazards in the United States," Report 6, U.S. Army Engineer Waterways Experiment Station, Vicksburg, Mississippi, May 1977.
157. Slemmons, D. B., "Determination of Design Earthquake Magnitude for Microzonation," in *Proceedings of the Third International Conference on Microzonation*, vol. I, pp. 119-130, Seattle, Washington, 1982.
158. Thenhaus, P. C., "Seismic Source Zones in Probabilistic Estimation of the Earthquake Ground Motion Hazard: A Classification with Key Issues," in *Proceedings of Conference XXXIV--A*

Workshop on "Probabilistic Earthquake Hazards Assessments", ed. Walter W. Hays, U. S. Geological Survey, Open-File Report 86-185, pp. 53-71, Reston, Virginia, 1986.

159. Thenhaus, P. C., D. M. Perkins, J. I. Ziony, and S. T. Algermissen, "Probabilistic Estimates of Maximum Seismic Horizontal Ground Motion on Rock in Coastal California and the Adjacent Outer Continental Shelf," U.S. Geological Survey, Open-File Report 80-924, 1980.
160. Thenhaus, P. C., J. I. Ziony, W. H. Diment, M. G. Hopper, D. M. Perkins, S. L. Hanson, and S. T. Algermissen, "Probabilistic Estimates of Maximum Seismic Horizontal Ground Motion on Rock in Alaska and the Adjacent Outer Continental Shelf," in *U.S. Geological Survey in Alaska - Accomplishments During 1980*, ed. W. L. Coonrad, pp. 5-9, U.S. Geological Survey Circular 844, 1982.
161. Tocher, D., "Earthquake Energy and Ground Breakage," *Bulletin of the Seismological Society of America*, vol. 48, no. 2, pp. 147-153, April 1958.
162. Toro, G. R. and R. K. McGuire, "An Investigation into Earthquake Ground Motion Characteristics in Eastern North America," *Bulletin of the Seismological Society of America*, vol. 77, no. 2, pp. 468-489, April 1987.
163. Tvedt, L., "Two Second-Order Approximations to the Failure Probability," *Section on Structural Reliability*, A/S Veritas Research, Høvik, Norway, 1984.
164. Tvedt, L., "On the Probability Content of a Parabolic Failure Set in a Space of Independent Standard Normally Distributed Random Variables," *Section on Structural Reliability*, A/S Veritas Research, Høvik, Norway, 1985.
165. U. S. Nuclear Regulatory Commission,, "PRA Procedures Guide," NUREG/CR-2300, September 1981.
166. Utsu, T., "A Three-Parameter Formula for Magnitude Distribution of Earthquakes," *J. Phys. Earth*, vol. 22, pp. 71-85, 1974.
167. Utsu, T. and A. Seki, "A Relation Between the Area of Aftershock Region and the Energy of Main Shock," *J. Seism. Soc. Japan*, vol. 7, pp. 233-240, 1954. (in Japanese)
168. Vagliente, V. N., "Forecasting the Risk Inherent in Earthquake Resistant Design," Technical Report, Department of Civil Engineering, Stanford University, 1973.
169. Veneziano, D. and A. L. Pais, "Automatic Source Identification Based on Historical Seismicity," in *Proceedings of the 8th European Conference on Earthquake Engineering*, Lisbon, Portugal, 1986.
170. Veneziano, D. and J. Van Dick, "Models of Seismicity and use of Historical Data in Earthquake Hazard Analysis," in *Proceedings of Conference XXXIV--A Workshop on "Probabilistic Earthquake Hazards Assessments"*, ed. Walter W. Hays, U. S. Geological Survey, Open-File Report 86-185, pp. 116-141, Reston, Virginia, 1986.
171. Vere-Jones, D., "Stochastic Models for Earthquake Occurrence (with discussion)," *J. Roy. Statist. Soc.*, vol. B32, no. 1, pp. 1-62, 1970.
172. Vere-Jones, D., "Stochastic Models for Earthquake Sequences," *Geophys. J. R. astr. Soc.*, vol. 42, pp. 811-827, 1975.
173. Vere-Jones, D. and T. Ozaki, "Some Examples of Statistical Estimation Applied to Earthquake Data. I. Cyclic Poisson and Self-Exciting Models," *Ann. Inst. Statist. Math.*, vol. 34, Part B, pp. 189-207, 1982.
174. Vere-Jones, D. and E. G. C. Smith, "Statistics in Seismology," *Commun. Statis. Theor. Meth.*, vol. A10, no. 15, pp. 1559-1585, 1980.
175. Weichert, D. H., "Estimation of the Earthquake Parameters for Unequal Observation Period for Different Magnitudes," *Bulletin of the Seismological Society of America*, vol. 70, no. 4, pp. 1337-1346, August 1980.
176. Wyss, M., "Estimating Maximum Expectable Magnitude of Earthquakes from Fault Dimensions," *Geology*, vol. 7, pp. 336-340, July 1979.

177. Wyss, M. and J. N. Brune, "Seismic Moment, Stress and Source Dimensions for Earthquakes in the California-Nevada Region," *J. Geophys. Res.*, vol. 73, no. 14, pp. 4681-4694, 1968.

178. Yegian, M. K., "Probabilistic Seismic Hazard Analysis - State of the Art for Assessing Earthquake Hazards in the United States," Report 13, U.S. Army Engineer Waterways Experiment Station, Vicksburg, Mississippi, July 1979.

179. Youngs, R. R., "Advances in Seismic Source Definition for Seismic Hazard Analyses in the Eastern United States," in *Proceedings of Conference XXXIV--A Workshop on "Probabilistic Earthquake Hazards Assessments"*, ed. Walter W. Hays, U. S. Geological Survey, Open-File Report 86-185, pp. 172-180, Reston, Virginia, 1986.

180. Youngs, R. R. and K. J. Coppersmith, "Implications of Fault Slip Rates and Earthquake Recurrence Models to Probabilistic Seismic Hazard Estimates," *Bulletin of the Seismological Society of America*, vol. 75, no. 4, pp. 939-964, August 1985.

181. Zemell, S. H., "Imposed Upper Limit for Probabilistic Seismic Risk," in *Proceedings, Eighth World Conference on Earthquake Engineering*, vol. I, pp. 239-245, San Francisco, California, 1984.

EARTHQUAKE ENGINEERING RESEARCH CENTER REPORT SERIES

EERC reports are available from the National Information Service for Earthquake Engineering(NISEE) and from the National Technical Information Service(NTIS). Numbers in parentheses are Accession Numbers assigned by the National Technical Information Service; these are followed by a price code. Contact NTIS, 5285 Port Royal Road, Springfield Virginia, 22161 for more information. Reports without Accession Numbers were not available from NTIS at the time of printing. For a current complete list of EERC reports (from EERC 67-1) and availablity information, please contact University of California, EERC, NISEE, 1301 South 46th Street, Richmond, California 94804.

UCB/EERC-80/01 "Earthquake Response of Concrete Gravity Dams Including Hydrodynamic and Foundation Interaction Effects," by Chopra, A.K., Chakrabarti, P. and Gupta, S., January 1980, (AD-A087297)A10.

UCB/EERC-80/02 "Rocking Response of Rigid Blocks to Earthquakes," by Yim, C.S., Chopra, A.K. and Penzien, J., January 1980, (PB80 166 002)A04.

UCB/EERC-80/03 "Optimum Inelastic Design of Seismic-Resistant Reinforced Concrete Frame Structures," by Zagajeski, S.W. and Bertero, V.V., January 1980, (PB80 164 635)A06.

UCB/EERC-80/04 "Effects of Amount and Arrangement of Wall-Panel Reinforcement on Hysteretic Behavior of Reinforced Concrete Walls," by Iliya, R. and Bertero, V.V., February 1980, (PB81 122 525)A09.

UCB/EERC-80/05 "Shaking Table Research on Concrete Dam Models," by Niwa, A. and Clough, R.W., September 1980, (PB81 122 368)A06.

UCB/EERC-80/06 "The Design of Steel Energy-Absorbing Restrainers and their Incorporation into Nuclear Power Plants for Enhanced Safety (Vol 1a): Piping with Energy Absorbing Restrainers: Parameter Study on Small Systems," by Powell, G.H., Oughourlian, C. and Simons, J., June 1980.

UCB/EERC-80/07 "Inelastic Torsional Response of Structures Subjected to Earthquake Ground Motions," by Yamazaki, Y., April 1980, (PB81 122 327)A08.

UCB/EERC-80/08 "Study of X-Braced Steel Frame Structures under Earthquake Simulation," by Ghanaat, Y., April 1980, (PB81 122 335)A11.

UCB/EERC-80/09 "Hybrid Modelling of Soil-Structure Interaction," by Gupta, S., Lin, T.W. and Penzien, J., May 1980, (PB81 122 319)A07.

UCB/EERC-80/10 "General Applicability of a Nonlinear Model of a One Story Steel Frame," by Sveinsson, B.I. and McNiven, H.D., May 1980, (PB81 124 877)A06.

UCB/EERC-80/11 "A Green-Function Method for Wave Interaction with a Submerged Body," by Kioka, W., April 1980, (PB81 122 269)A07.

UCB/EERC-80/12 "Hydrodynamic Pressure and Added Mass for Axisymmetric Bodies.," by Nilrat, F., May 1980, (PB81 122 343)A08.

UCB/EERC-80/13 "Treatment of Non-Linear Drag Forces Acting on Offshore Platforms," by Dao, B.V. and Penzien, J., May 1980, (PB81 153 413)A07.

UCB/EERC-80/14 "2D Plane/Axisymmetric Solid Element (Type 3-Elastic or Elastic-Perfectly Plastic)for the ANSR-II Program," by Mondkar, D.P. and Powell, G.H., July 1980, (PB81 122 350)A03.

UCB/EERC-80/15 "A Response Spectrum Method for Random Vibrations," by Der Kiureghian, A., June 1981, (PB81 122 301)A03.

UCB/EERC-80/16 "Cyclic Inelastic Buckling of Tubular Steel Braces," by Zayas, V.A., Popov, E.P. and Mahin, S.A., June 1981, (PB81 124 885)A10.

UCB/EERC-80/17 "Dynamic Response of Simple Arch Dams Including Hydrodynamic Interaction," by Porter, C.S. and Chopra, A.K., July 1981, (PB81 124 000)A13.

UCB/EERC-80/18 "Experimental Testing of a Friction Damped Aseismic Base Isolation System with Fail-Safe Characteristics," by Kelly, J.M., Beucke, K.E. and Skinner, M.S., July 1980, (PB81 148 595)A04.

UCB/EERC-80/19 "The Design of Steel Energy-Absorbing Restrainers and their Incorporation into Nuclear Power Plants for Enhanced Safety (Vol.1B): Stochastic Seismic Analyses of Nuclear Power Plant Structures and Piping Systems Subjected to Multiple Supported Excitations," by Lee, M.C. and Penzien, J., June 1980, (PB82 201 872)A08.

UCB/EERC-80/20 "The Design of Steel Energy-Absorbing Restrainers and their Incorporation into Nuclear Power Plants for Enhanced Safety (Vol 1C): Numerical Method for Dynamic Substructure Analysis," by Dickens, J.M. and Wilson, E.L., June 1980.

UCB/EERC-80/21 "The Design of Steel Energy-Absorbing Restrainers and their Incorporation into Nuclear Power Plants for Enhanced Safety (Vol 2): Development and Testing of Restraints for Nuclear Piping Systems," by Kelly, J.M. and Skinner, M.S., June 1980.

UCB/EERC-80/22 "3D Solid Element (Type 4-Elastic or Elastic-Perfectly-Plastic) for the ANSR-II Program," by Mondkar, D.P. and Powell, G.H., July 1980, (PB81 123 242)A03.

UCB/EERC-80/23 "Gap-Friction Element (Type 5) for the Ansr-II Program," by Mondkar, D.P. and Powell, G.H., July 1980, (PB81 122 285)A03.

UCB/EERC-80/24 "U-Bar Restraint Element (Type 11) for the ANSR-II Program," by Oughourlian, C. and Powell, G.H., July 1980, (PB81 122 293)A03.

UCB/EERC-80/25 "Testing of a Natural Rubber Base Isolation System by an Explosively Simulated Earthquake," by Kelly, J.M., August 1980, (PB81 201 360)A04.

UCB/EERC-80/26 "Input Identification from Structural Vibrational Response," by Hu, Y., August 1980, (PB81 152 308)A05.

UCB/EERC-80/27 "Cyclic Inelastic Behavior of Steel Offshore Structures," by Zayas, V.A., Mahin, S.A. and Popov, E.P., August 1980, (PB81 196 180)A15.

UCB/EERC-80/28 "Shaking Table Testing of a Reinforced Concrete Frame with Biaxial Response," by Oliva, M.G., October 1980, (PB81 154 304)A10.

UCB/EERC-80/29 "Dynamic Properties of a Twelve-Story Prefabricated Panel Building," by Bouwkamp, J.G., Kollegger, J.P. and Stephen, R.M., October 1980, (PB82 138 777)A07.

UCB/EERC-80/30 "Dynamic Properties of an Eight-Story Prefabricated Panel Building," by Bouwkamp, J.G., Kollegger, J.P. and Stephen, R.M., October 1980, (PB81 200 313)A05.

UCB/EERC-80/31 "Predictive Dynamic Response of Panel Type Structures under Earthquakes," by Kollegger, J.P. and Bouwkamp, J.G., October 1980, (PB81 152 316)A04.

UCB/EERC-80/32 "The Design of Steel Energy-Absorbing Restrainers and their Incorporation into Nuclear Power Plants for Enhanced Safety (Vol 3): Testing of Commercial Steels in Low-Cycle Torsional Fatigue," by Spanner, P., Parker, E.R., Jongewaard, E. and Dory, M., 1980.

UCB/EERC-80/33 "The Design of Steel Energy-Absorbing Restrainers and their Incorporation into Nuclear Power Plants for Enhanced Safety (Vol 4): Shaking Table Tests of Piping Systems with Energy-Absorbing Restrainers," by Stiemer, S.F. and Godden, W.G., September 1980, (PB82 201 880)A05.

UCB/EERC-80/34 "The Design of Steel Energy-Absorbing Restrainers and their Incorporation into Nuclear Power Plants for Enhanced Safety (Vol 5): Summary Report," by Spencer, P., 1980.

UCB/EERC-80/35 "Experimental Testing of an Energy-Absorbing Base Isolation System," by Kelly, J.M., Skinner, M.S. and Beucke, K.E., October 1980, (PB81 154 072)A04.

UCB/EERC-80/36 "Simulating and Analyzing Artificial Non-Stationary Earth Ground Motions," by Nau, R.F., Oliver, R.M. and Pister, K.S., October 1980, (PB81 153 397)A04.

UCB/EERC-80/37 "Earthquake Engineering at Berkeley - 1980," by , September 1980, (PB81 205 674)A09.

UCB/EERC-80/38 "Inelastic Seismic Analysis of Large Panel Buildings," by Schricker, V. and Powell, G.H., September 1980, (PB81 154 338)A13.

UCB/EERC-80/39 "Dynamic Response of Embankment, Concrete-Gavity and Arch Dams Including Hydrodynamic Interation," by Hall, J.F. and Chopra, A.K., October 1980, (PB81 152 324)A11.

UCB/EERC-80/40 "Inelastic Buckling of Steel Struts under Cyclic Load Reversal.," by Black, R.G., Wenger, W.A. and Popov, E.P., October 1980, (PB81 154 312)A08.

UCB/EERC-80/41 "Influence of Site Characteristics on Buildings Damage during the October 3,1974 Lima Earthquake," by Repetto, P., Arango, I. and Seed, H.B., September 1980, (PB81 161 739)A05.

UCB/EERC-80/42 "Evaluation of a Shaking Table Test Program on Response Behavior of a Two Story Reinforced Concrete Frame," by Blondet, J.M., Clough, R.W. and Mahin, S.A., December 1980, (PB82 196 544)A11.

UCB/EERC-80/43 "Modelling of Soil-Structure Interaction by Finite and Infinite Elements," by Medina, F., December 1980, (PB81 229 270)A04.

UCB/EERC-81/01 "Control of Seismic Response of Piping Systems and Other Structures by Base Isolation," by Kelly, J.M., January 1981, (PB81 200 735)A05.

UCB/EERC-81/02 "OPTNSR- An Interactive Software System for Optimal Design of Statically and Dynamically Loaded Structures with Nonlinear Response," by Bhatti, M.A., Ciampi, V. and Pister, K.S., January 1981, (PB81 218 851)A09.

UCB/EERC-81/03 "Analysis of Local Variations in Free Field Seismic Ground Motions," by Chen, J.-C., Lysmer, J. and Seed, H.B., January 1981, (AD-A099508)A13.

UCB/EERC-81/04 "Inelastic Structural Modeling of Braced Offshore Platforms for Seismic Loading," by Zayas, V.A., Shing, P.-S.B., Mahin, S.A. and Popov, E.P., January 1981, (PB82 138 777)A07.

UCB/EERC-81/05 "Dynamic Response of Light Equipment in Structures," by Der Kiureghian, A., Sackman, J.L. and Nour-Omid, B., April 1981, (PB81 218 497)A04.

UCB/EERC-81/06 "Preliminary Experimental Investigation of a Broad Base Liquid Storage Tank," by Bouwkamp, J.G., Kollegger, J.P. and Stephen, R.M., May 1981, (PB82 140 385)A03.

UCB/EERC-81/07 "The Seismic Resistant Design of Reinforced Concrete Coupled Structural Walls," by Aktan, A.E. and Bertero, V.V., June 1981, (PB82 113 358)A11.

UCB/EERC-81/08 "Unassigned," by Unassigned, 1981.

UCB/EERC-81/09 "Experimental Behavior of a Spatial Piping System with Steel Energy Absorbers Subjected to a Simulated Differential Seismic Input," by Stiemer, S.F., Godden, W.G. and Kelly, J.M., July 1981, (PB82 201 898)A04.

UCB/EERC-81/10 "Evaluation of Seismic Design Provisions for Masonry in the United States," by Sveinsson, B.I., Mayes, R.L. and McNiven, H.D., August 1981, (PB82 166 075)A08.

UCB/EERC-81/11 "Two-Dimensional Hybrid Modelling of Soil-Structure Interaction," by Tzong, T.-J., Gupta, S. and Penzien, J., August 1981, (PB82 142 118)A04.

UCB/EERC-81/12 "Studies on Effects of Infills in Seismic Resistant R/C Construction," by Brokken, S. and Bertero, V.V., October 1981, (PB82 166 190)A09.

UCB/EERC-81/13 "Linear Models to Predict the Nonlinear Seismic Behavior of a One-Story Steel Frame," by Valdimarsson, H., Shah, A.H. and McNiven, H.D., September 1981, (PB82 138 793)A07.

UCB/EERC-81/14 "TLUSH: A Computer Program for the Three-Dimensional Dynamic Analysis of Earth Dams," by Kagawa, T., Mejia, L.H., Seed, H.B. and Lysmer, J., September 1981, (PB82 139 940)A06.

UCB/EERC-81/15 "Three Dimensional Dynamic Response Analysis of Earth Dams," by Mejia, L.H. and Seed, H.B., September 1981, (PB82 137 274)A12.

UCB/EERC-81/16 "Experimental Study of Lead and Elastomeric Dampers for Base Isolation Systems," by Kelly, J.M. and Hodder, S.B., October 1981, (PB82 166 182)A05.

UCB/EERC-81/17 "The Influence of Base Isolation on the Seismic Response of Light Secondary Equipment," by Kelly, J.M., April 1981, (PB82 255 266)A04.

UCB/EERC-81/18 "Studies on Evaluation of Shaking Table Response Analysis Procedures," by Blondet, J. M., November 1981, (PB82 197 278)A10.

UCB/EERC-81/19 "DELIGHT.STRUCT: A Computer-Aided Design Environment for Structural Engineering," by Balling, R.J., Pister, K.S. and Polak, E., December 1981, (PB82 218 496)A07.

UCB/EERC-81/20 "Optimal Design of Seismic-Resistant Planar Steel Frames," by Balling, R.J., Ciampi, V. and Pister, K.S., December 1981, (PB82 220 179)A07.

UCB/EERC-82/01 "Dynamic Behavior of Ground for Seismic Analysis of Lifeline Systems," by Sato, T. and Der Kiureghian, A., January 1982, (PB82 218 926)A05.

UCB/EERC-82/02 "Shaking Table Tests of a Tubular Steel Frame Model," by Ghanaat, Y. and Clough, R.W., January 1982, (PB82 220 161)A07.

UCB/EERC-82/03 "Behavior of a Piping System under Seismic Excitation: Experimental Investigations of a Spatial Piping System supported by Mechanical Shock Arrestors," by Schneider, S., Lee, H.-M. and Godden, W. G., May 1982, (PB83 172 544)A09.

UCB/EERC-82/04 "New Approaches for the Dynamic Analysis of Large Structural Systems," by Wilson, E.L., June 1982, (PB83 148 080)A05.

UCB/EERC-82/05 "Model Study of Effects of Damage on the Vibration Properties of Steel Offshore Platforms," by Shahrivar, F. and Bouwkamp, J.G., June 1982, (PB83 148 742)A10.

UCB/EERC-82/06 "States of the Art and Pratice in the Optimum Seismic Design and Analytical Response Prediction of R/C Frame Wall Structures," by Aktan, A.E. and Bertero, V.V., July 1982, (PB83 147 736)A05.

UCB/EERC-82/07 "Further Study of the Earthquake Response of a Broad Cylindrical Liquid-Storage Tank Model," by Manos, G.C. and Clough, R.W., July 1982, (PB83 147 744)A11.

UCB/EERC-82/08 "An Evaluation of the Design and Analytical Seismic Response of a Seven Story Reinforced Concrete Frame," by Charney, F.A. and Bertero, V.V., July 1982, (PB83 157 628)A09.

UCB/EERC-82/09 "Fluid-Structure Interactions: Added Mass Computations for Incompressible Fluid," by Kuo, J.S.-H., August 1982, (PB83 156 281)A07.

UCB/EERC-82/10 "Joint-Opening Nonlinear Mechanism: Interface Smeared Crack Model," by Kuo, J.S.-H., August 1982, (PB83 149 195)A05.

UCB/EERC-82/11 "Dynamic Response Analysis of Techi Dam," by Clough, R.W., Stephen, R.M. and Kuo, J.S.-H., August 1982, (PB83 147 496)A06.

UCB/EERC-82/12 "Prediction of the Seismic Response of R/C Frame-Coupled Wall Structures," by Aktan, A.E., Bertero, V.V. and Piazzo, M., August 1982, (PB83 149 203)A09.

UCB/EERC-82/13 "Preliminary Report on the Smart 1 Strong Motion Array in Taiwan," by Bolt, B.A., Loh, C.H., Penzien, J. and Tsai, Y.B., August 1982, (PB83 159 400)A10.

UCB/EERC-82/14 "Shaking-Table Studies of an Eccentrically X-Braced Steel Structure," by Yang, M.S., September 1982, (PB83 260 778)A12.

UCB/EERC-82/15 "The Performance of Stairways in Earthquakes," by Roha, C., Axley, J.W. and Bertero, V.V., September 1982, (PB83 157 693)A07.

UCB/EERC-82/16 "The Behavior of Submerged Multiple Bodies in Earthquakes," by Liao, W.-G., September 1982, (PB83 158 709)A07.

UCB/EERC-82/17 "Effects of Concrete Types and Loading Conditions on Local Bond-Slip Relationships," by Cowell, A.D., Popov, E.P. and Bertero, V.V., September 1982, (PB83 153 577)A04.

UCB/EERC-82/18 "Mechanical Behavior of Shear Wall Vertical Boundary Members: An Experimental Investigation," by Wagner, M.T. and Bertero, V.V., October 1982, (PB83 159 764)A05.

UCB/EERC-82/19 "Experimental Studies of Multi-support Seismic Loading on Piping Systems," by Kelly, J.M. and Cowell, A.D., November 1982.

UCB/EERC-82/20 "Generalized Plastic Hinge Concepts for 3D Beam-Column Elements," by Chen, P. F.-S. and Powell, G.H., November 1982, (PB83 247 981)A13.

UCB/EERC-82/21 "ANSR-II: General Computer Program for Nonlinear Structural Analysis," by Oughourlian, C.V. and Powell, G.H., November 1982, (PB83 251 330)A12.

UCB/EERC-82/22 "Solution Strategies for Statically Loaded Nonlinear Structures," by Simons, J.W. and Powell, G.H., November 1982, (PB83 197 970)A06.

UCB/EERC-82/23 "Analytical Model of Deformed Bar Anchorages under Generalized Excitations," by Ciampi, V., Eligehausen, R., Bertero, V.V. and Popov, E.P., November 1982, (PB83 169 532)A06.

UCB/EERC-82/24 "A Mathematical Model for the Response of Masonry Walls to Dynamic Excitations," by Sucuoglu, H., Mengi, Y. and McNiven, H.D., November 1982, (PB83 169 011)A07.

UCB/EERC-82/25 "Earthquake Response Considerations of Broad Liquid Storage Tanks," by Cambra, F.J., November 1982, (PB83 251 215)A09.

UCB/EERC-82/26 "Computational Models for Cyclic Plasticity, Rate Dependence and Creep," by Mosaddad, B. and Powell, G.H., November 1982, (PB83 245 829)A08.

UCB/EERC-82/27 "Inelastic Analysis of Piping and Tubular Structures," by Mahasuverachai, M. and Powell, G.H., November 1982, (PB83 249 987)A07.

UCB/EERC-83/01 "The Economic Feasibility of Seismic Rehabilitation of Buildings by Base Isolation," by Kelly, J.M., January 1983, (PB83 197 988)A05.

UCB/EERC-83/02 "Seismic Moment Connections for Moment-Resisting Steel Frames.," by Popov, E.P., January 1983, (PB83 195 412)A04.

UCB/EERC-83/03 "Design of Links and Beam-to-Column Connections for Eccentrically Braced Steel Frames," by Popov, E.P. and Malley, J.O., January 1983, (PB83 194 811)A04.

UCB/EERC-83/04 "Numerical Techniques for the Evaluation of Soil-Structure Interaction Effects in the Time Domain," by Bayo, E. and Wilson, E.L., February 1983, (PB83 245 605)A09.

UCB/EERC-83/05 "A Transducer for Measuring the Internal Forces in the Columns of a Frame-Wall Reinforced Concrete Structure," by Sause, R. and Bertero, V.V., May 1983, (PB84 119 494)A06.

UCB/EERC-83/06 "Dynamic Interactions Between Floating Ice and Offshore Structures," by Croteau, P., May 1983, (PB84 119 486)A16.

UCB/EERC-83/07 "Dynamic Analysis of Multiply Tuned and Arbitrarily Supported Secondary Systems," by Igusa, T. and Der Kiureghian, A., July 1983, (PB84 118 272)A11.

UCB/EERC-83/08 "A Laboratory Study of Submerged Multi-body Systems in Earthquakes," by Ansari, G.R., June 1983, (PB83 261 842)A17.

UCB/EERC-83/09 "Effects of Transient Foundation Uplift on Earthquake Response of Structures," by Yim, C.-S. and Chopra, A.K., June 1983, (PB83 261 396)A07.

UCB/EERC-83/10 "Optimal Design of Friction-Braced Frames under Seismic Loading," by Austin, M.A. and Pister, K.S., June 1983, (PB84 119 288)A06.

UCB/EERC-83/11 "Shaking Table Study of Single-Story Masonry Houses: Dynamic Performance under Three Component Seismic Input and Recommendations," by Manos, G.C., Clough, R.W. and Mayes, R.L., July 1983, (UCB/EERC-83/11)A08.

UCB/EERC-83/12 "Experimental Error Propagation in Pseudodynamic Testing," by Shiing, P.B. and Mahin, S.A., June 1983, (PB84 119 270)A09.

UCB/EERC-83/13 "Experimental and Analytical Predictions of the Mechanical Characteristics of a 1/5-scale Model of a 7-story R/C Frame-Wall Building Structure," by Aktan, A.E., Bertero, V.V., Chowdhury, A.A. and Nagashima, T., June 1983, (PB84 119 213)A07.

UCB/EERC-83/14 "Shaking Table Tests of Large-Panel Precast Concrete Building System Assemblages," by Oliva, M.G. and Clough, R.W., June 1983, (PB86 110 210/AS)A11.

UCB/EERC-83/15 "Seismic Behavior of Active Beam Links in Eccentrically Braced Frames," by Hjelmstad, K.D. and Popov, E.P., July 1983, (PB84 119 676)A09.

UCB/EERC-83/16 "System Identification of Structures with Joint Rotation," by Dimsdale, J.S., July 1983, (PB84 192 210)A06.

UCB/EERC-83/17 "Construction of Inelastic Response Spectra for Single-Degree-of-Freedom Systems," by Mahin, S. and Lin, J., June 1983, (PB84 208 834)A05.

UCB/EERC-83/18 "Interactive Computer Analysis Methods for Predicting the Inelastic Cyclic Behaviour of Structural Sections," by Kaba, S. and Mahin, S., July 1983, (PB84 192 012)A06.

UCB/EERC-83/19 "Effects of Bond Deterioration on Hysteretic Behavior of Reinforced Concrete Joints," by Filippou, F.C., Popov, E.P. and Bertero, V.V., August 1983, (PB84 192 020)A10.

UCB/EERC-83/20 "Correlation of Analytical and Experimental Responses of Large-Panel Precast Building Systems," by Oliva, M.G., Clough, R.W., Velkov, M. and Gavrilovic, P., May 1988.

UCB/EERC-83/21 "Mechanical Characteristics of Materials Used in a 1/5 Scale Model of a 7-Story Reinforced Concrete Test Structure," by Bertero, V.V., Aktan, A.E., Harris, H.G. and Chowdhury, A.A., October 1983, (PB84 193 697)A05.

UCB/EERC-83/22 "Hybrid Modelling of Soil-Structure Interaction in Layered Media," by Tzong, T.-J. and Penzien, J., October 1983, (PB84 192 178)A08.

UCB/EERC-83/23 "Local Bond Stress-Slip Relationships of Deformed Bars under Generalized Excitations," by Eligehausen, R., Popov, E.P. and Bertero, V.V., October 1983, (PB84 192 848)A09.

UCB/EERC-83/24 "Design Considerations for Shear Links in Eccentrically Braced Frames," by Malley, J.O. and Popov, E.P., November 1983, (PB84 192 186)A07.

UCB/EERC-84/01 "Pseudodynamic Test Method for Seismic Performance Evaluation: Theory and Implementation," by Shing, P.-S.B. and Mahin, S.A., January 1984, (PB84 190 644)A08.

UCB/EERC-84/02 "Dynamic Response Behavior of Kiang Hong Dian Dam," by Clough, R.W., Chang, K.-T., Chen, H.-Q. and Stephen, R.M., April 1984, (PB84 209 402)A08.

UCB/EERC-84/03 "Refined Modelling of Reinforced Concrete Columns for Seismic Analysis," by Kaba, S.A. and Mahin, S.A., April 1984, (PB84 234 384)A06.

UCB/EERC-84/04 "A New Floor Response Spectrum Method for Seismic Analysis of Multiply Supported Secondary Systems," by Asfura, A. and Der Kiureghian, A., June 1984, (PB84 239 417)A06.

UCB/EERC-84/05 "Earthquake Simulation Tests and Associated Studies of a 1/5th-scale Model of a 7-Story R/C Frame-Wall Test Structure," by Bertero, V.V., Aktan, A.E., Charney, F.A. and Sause, R., June 1984, (PB84 239 409)A09.

UCB/EERC-84/06 "R/C Structural Walls: Seismic Design for Shear," by Aktan, A.E. and Bertero, V.V., 1984.

UCB/EERC-84/07 "Behavior of Interior and Exterior Flat-Plate Connections subjected to Inelastic Load Reversals," by Zee, H.L. and Moehle, J.P., August 1984, (PB86 117 629/AS)A07.

UCB/EERC-84/08 "Experimental Study of the Seismic Behavior of a Two-Story Flat-Plate Structure," by Moehle, J.P. and Diebold, J.W., August 1984, (PB86 122 553/AS)A12.

UCB/EERC-84/09 "Phenomenological Modeling of Steel Braces under Cyclic Loading," by Ikeda, K., Mahin, S.A. and Dermitzakis, S.N., May 1984, (PB86 132 198/AS)A08.

UCB/EERC-84/10 "Earthquake Analysis and Response of Concrete Gravity Dams," by Fenves, G. and Chopra, A.K., August 1984, (PB85 193 902/AS)A11.

UCB/EERC-84/11 "EAGD-84: A Computer Program for Earthquake Analysis of Concrete Gravity Dams," by Fenves, G. and Chopra, A.K., August 1984, (PB85 193 613/AS)A05.

UCB/EERC-84/12 "A Refined Physical Theory Model for Predicting the Seismic Behavior of Braced Steel Frames," by Ikeda, K. and Mahin, S.A., July 1984, (PB85 191 450/AS)A09.

UCB/EERC-84/13 "Earthquake Engineering Research at Berkeley - 1984," by , August 1984, (PB85 197 341/AS)A10.

UCB/EERC-84/14 "Moduli and Damping Factors for Dynamic Analyses of Cohesionless Soils," by Seed, H.B., Wong, R.T., Idriss, I.M. and Tokimatsu, K., September 1984, (PB85 191 468/AS)A04.

UCB/EERC-84/15 "The Influence of SPT Procedures in Soil Liquefaction Resistance Evaluations," by Seed, H.B., Tokimatsu, K., Harder, L.F. and Chung, R.M., October 1984, (PB85 191 732/AS)A04.

UCB/EERC-84/16 "Simplified Procedures for the Evaluation of Settlements in Sands Due to Earthquake Shaking," by Tokimatsu, K. and Seed, H.B., October 1984, (PB85 197 887/AS)A03.

UCB/EERC-84/17 "Evaluation of Energy Absorption Characteristics of Highway Bridges Under Seismic Conditions - Volume I and Volume II (Appendices)," by Imbsen, R.A. and Penzien, J., September 1986.

UCB/EERC-84/18 "Structure-Foundation Interactions under Dynamic Loads," by Liu, W.D. and Penzien, J., November 1984, (PB87 124 889/AS)A11.

UCB/EERC-84/19 "Seismic Modelling of Deep Foundations," by Chen, C.-H. and Penzien, J., November 1984, (PB87 124 798/AS)A07.

UCB/EERC-84/20 "Dynamic Response Behavior of Quan Shui Dam," by Clough, R.W., Chang, K.-T., Chen, H.-Q., Stephen, R.M., Ghanaat, Y. and Qi, J.-H., November 1984, (PB86 115177/AS)A07.

UCB/EERC-85/01 "Simplified Methods of Analysis for Earthquake Resistant Design of Buildings," by Cruz, E.F. and Chopra, A.K., February 1985, (PB86 112299/AS)A12.

UCB/EERC-85/02 "Estimation of Seismic Wave Coherency and Rupture Velocity using the SMART 1 Strong-Motion Array Recordings," by Abrahamson, N.A., March 1985, (PB86 214 343)A07.

UCB/EERC-85/03 "Dynamic Properties of a Thirty Story Condominium Tower Building," by Stephen, R.M., Wilson, E.L. and Stander, N., April 1985, (PB86 118965/AS)A06.

UCB/EERC-85/04 "Development of Substructuring Techniques for On-Line Computer Controlled Seismic Performance Testing," by Dermitzakis, S. and Mahin, S., February 1985, (PB86 132941/AS)A08.

UCB/EERC-85/05 "A Simple Model for Reinforcing Bar Anchorages under Cyclic Excitations," by Filippou, F.C., March 1985, (PB86 112 919/AS)A05.

UCB/EERC-85/06 "Racking Behavior of Wood-framed Gypsum Panels under Dynamic Load," by Oliva, M.G., June 1985.

UCB/EERC-85/07 "Earthquake Analysis and Response of Concrete Arch Dams," by Fok, K.-L. and Chopra, A.K., June 1985, (PB86 139672/AS)A10.

UCB/EERC-85/08 "Effect of Inelastic Behavior on the Analysis and Design of Earthquake Resistant Structures," by Lin, J.P. and Mahin, S.A., June 1985, (PB86 135340/AS)A08.

UCB/EERC-85/09 "Earthquake Simulator Testing of a Base-Isolated Bridge Deck," by Kelly, J.M., Buckle, I.G. and Tsai, H.-C., January 1986, (PB87 124 152/AS)A06.

UCB/EERC-85/10 "Simplified Analysis for Earthquake Resistant Design of Concrete Gravity Dams," by Fenves, G. and Chopra, A.K., June 1986, (PB87 124 160/AS)A08.

UCB/EERC-85/11 "Dynamic Interaction Effects in Arch Dams," by Clough, R.W., Chang, K.-T., Chen, H.-Q. and Ghanaat, Y., October 1985, (PB86 135027/AS)A05.

UCB/EERC-85/12 "Dynamic Response of Long Valley Dam in the Mammoth Lake Earthquake Series of May 25-27, 1980," by Lai, S. and Seed, H.B., November 1985, (PB86 142304/AS)A05.

UCB/EERC-85/13 "A Methodology for Computer-Aided Design of Earthquake-Resistant Steel Structures," by Austin, M.A., Pister, K.S. and Mahin, S.A., December 1985, (PB86 159480/AS)A10 .

UCB/EERC-85/14 "Response of Tension-Leg Platforms to Vertical Seismic Excitations," by Liou, G.-S., Penzien, J. and Yeung, R.W., December 1985, (PB87 124 871/AS)A08.

UCB/EERC-85/15 "Cyclic Loading Tests of Masonry Single Piers: Volume 4 - Additional Tests with Height to Width Ratio of 1," by Sveinsson, B., McNiven, H.D. and Sucuoglu, H., December 1985.

UCB/EERC-85/16 "An Experimental Program for Studying the Dynamic Response of a Steel Frame with a Variety of Infill Partitions," by Yanev, B. and McNiven, H.D., December 1985.

UCB/EERC-86/01 "A Study of Seismically Resistant Eccentrically Braced Steel Frame Systems," by Kasai, K. and Popov, E.P., January 1986, (PB87 124 178/AS)A14.

UCB/EERC-86/02 "Design Problems in Soil Liquefaction," by Seed, H.B., February 1986, (PB87 124 186/AS)A03.

UCB/EERC-86/03 "Implications of Recent Earthquakes and Research on Earthquake-Resistant Design and Construction of Buildings," by Bertero, V.V., March 1986, (PB87 124 194/AS)A05.

UCB/EERC-86/04 "The Use of Load Dependent Vectors for Dynamic and Earthquake Analyses," by Leger, P., Wilson, E.L. and Clough, R.W., March 1986, (PB87 124 202/AS)A12.

UCB/EERC-86/05 "Two Beam-To-Column Web Connections," by Tsai, K.-C. and Popov, E.P., April 1986, (PB87 124 301/AS)A04.

UCB/EERC-86/06 "Determination of Penetration Resistance for Coarse-Grained Soils using the Becker Hammer Drill," by Harder, L.F. and Seed, H.B., May 1986, (PB87 124 210/AS)A07.

UCB/EERC-86/07 "A Mathematical Model for Predicting the Nonlinear Response of Unreinforced Masonry Walls to In-Plane Earthquake Excitations," by Mengi, Y. and McNiven, H.D., May 1986, (PB87 124 780/AS)A06.

UCB/EERC-86/08 "The 19 September 1985 Mexico Earthquake: Building Behavior," by Bertero, V.V., July 1986.

UCB/EERC-86/09 "EACD-3D: A Computer Program for Three-Dimensional Earthquake Analysis of Concrete Dams," by Fok, K.-L., Hall, J.F. and Chopra, A.K., July 1986, (PB87 124 228/AS)A08.

UCB/EERC-86/10 "Earthquake Simulation Tests and Associated Studies of a 0.3-Scale Model of a Six-Story Concentrically Braced Steel Structure," by Uang, C.-M. and Bertero, V.V., December 1986, (PB87 163 564/AS)A17.

UCB/EERC-86/11 "Mechanical Characteristics of Base Isolation Bearings for a Bridge Deck Model Test," by Kelly, J.M., Buckle, I.G. and Koh, C.-G., November 1987.

UCB/EERC-86/12 "Effects of Axial Load on Elastomeric Isolation Bearings," by Koh, C.-G. and Kelly, J.M., November 1987.

UCB/EERC-87/01 "The FPS Earthquake Resisting System: Experimental Report," by Zayas, V.A., Low, S.S. and Mahin, S.A., June 1987.

UCB/EERC-87/02 "Earthquake Simulator Tests and Associated Studies of a 0.3-Scale Model of a Six-Story Eccentrically Braced Steel Structure," by Whittaker, A., Uang, C.-M. and Bertero, V.V., July 1987.

UCB/EERC-87/03 "A Displacement Control and Uplift Restraint Device for Base-Isolated Structures," by Kelly, J.M., Griffith, M.C. and Aiken, I.D., April 1987.

UCB/EERC-87/04 "Earthquake Simulator Testing of a Combined Sliding Bearing and Rubber Bearing Isolation System," by Kelly, J.M. and Chalhoub, M.S., 1987.

UCB/EERC-87/05 "Three-Dimensional Inelastic Analysis of Reinforced Concrete Frame-Wall Structures," by Moazzami, S. and Bertero, V.V., May 1987.

UCB/EERC-87/06 "Experiments on Eccentrically Braced Frames with Composite Floors," by Ricles, J. and Popov, E., June 1987.

UCB/EERC-87/07 "Dynamic Analysis of Seismically Resistant Eccentrically Braced Frames," by Ricles, J. and Popov, E., June 1987.

UCB/EERC-87/08 "Undrained Cyclic Triaxial Testing of Gravels-The Effect of Membrane Compliance," by Evans, M.D. and Seed, H.B., July 1987.

UCB/EERC-87/09 "Hybrid Solution Techniques for Generalized Pseudo-Dynamic Testing," by Thewalt, C. and Mahin, S.A., July 1987.

UCB/EERC-87/10 "Ultimate Behavior of Butt Welded Splices in Heavy Rolled Steel Sections," by Bruneau, M., Mahin, S.A. and Popov, E.P., July 1987.

UCB/EERC-87/11 "Residual Strength of Sand from Dam Failures in the Chilean Earthquake of March 3, 1985," by De Alba, P., Seed, H.B., Retamal, E. and Seed, R.B., September 1987.

UCB/EERC-87/12 "Inelastic Seismic Response of Structures with Mass or Stiffness Eccentricities in Plan," by Bruneau, M. and Mahin, S.A., September 1987.

UCB/EERC-87/13 "CSTRUCT: An Interactive Computer Environment for the Design and Analysis of Earthquake Resistant Steel Structures," by Austin, M.A., Mahin, S.A. and Pister, K.S., September 1987.

UCB/EERC-87/14 "Experimental Study of Reinforced Concrete Columns Subjected to Multi-Axial Loading," by Low, S.S. and Moehle, J.P., September 1987.

UCB/EERC-87/15 "Relationships between Soil Conditions and Earthquake Ground Motions in Mexico City in the Earthquake of Sept. 19, 1985," by Seed, H.B., Romo, M.P., Sun, J., Jaime, A. and Lysmer, J., October 1987.

UCB/EERC-87/16 "Experimental Study of Seismic Response of R. C. Setback Buildings," by Shahrooz, B.M. and Moehle, J.P., October 1987.

UCB/EERC-87/17 "The Effect of Slabs on the Flexural Behavior of Beams," by Pantazopoulou, S.J. and Moehle, J.P., October 1987.

UCB/EERC-87/18 "Design Procedure for R-FBI Bearings," by Mostaghel, N. and Kelly, J.M., November 1987.

UCB/EERC-87/19 "Analytical Models for Predicting the Lateral Response of R C Shear Walls: Evaluation of their Reliability," by Vulcano, A. and Bertero, V.V., November 1987.

UCB/EERC-87/20 "Earthquake Response of Torsionally-Coupled Buildings," by Hejal, R. and Chopra, A.K., December 1987.

UCB/EERC-87/21 "Dynamic Reservoir Interaction with Monticello Dam," by Clough, R.W., Ghanaat, Y. and Qiu, X-F., December 1987.

UCB/EERC-87/22 "Strength Evaluation of Coarse-Grained Soils," by Siddiqi, F.H., Seed, R.B., Chan, C.K., Seed, H.B. and Pyke, R.M., December 1987.

UCB/EERC-88/01 "Seismic Behavior of Concentrically Braced Steel Frames," by Khatib, I., Mahin, S.A. and Pister, K.S., January 1988.

UCB/EERC-88/02 "Experimental Evaluation of Seismic Isolation of Medium-Rise Structures Subject to Uplift," by Griffith, M.C., Kelly, J.M., Coveney, V.A. and Koh, C.G., January 1988.

UCB/EERC-88/03 "Cyclic Behavior of Steel Double Angle Connections," by Astaneh-Asl, A. and Nader, M.N., January 1988.

UCB/EERC-88/04 "Re-evaluation of the Slide in the Lower San Fernando Dam in the Earthquake of Feb. 9, 1971," by Seed, H.B., Seed, R.B., Harder, L.F. and Jong, H.-L., April 1988.

UCB/EERC-88/05 "Experimental Evaluation of Seismic Isolation of a Nine-Story Braced Steel Frame Subject to Uplift," by Griffith, M.C., Kelly, J.M. and Aiken, I.D., May 1988.

UCB/EERC-88/06 "DRAIN-2DX User Guide.," by Allahabadi, R. and Powell, G.H., March 1988.

UCB/EERC-88/07 "Cylindrical Fluid Containers in Base-Isolated Structures," by Chalhoub, M.S. and Kelly, J.M. , April 1988.

UCB/EERC-88/08 "Analysis of Near-Source Waves: Separation of Wave Types using Strong Motion Array Recordings," by Darragh, R.B., June 1988.

UCB/EERC-88/09 "Alternatives to Standard Mode Superposition for Analysis of Non-Classically Damped Systems," by Kusainov, A.A. and Clough, R.W., June 1988.

UCB/EERC-88/10 "The Landslide at the Port of Nice on October 16, 1979," by Seed, H.B., Seed, R.B., Schlosser, F., Blondeau, F. and Juran, I., June 1988.

UCB/EERC-88/11 "Liquefaction Potential of Sand Deposits Under Low Levels of Excitation," by Carter, D.P. and Seed, H.B., August 1988.

UCB/EERC-88/12 "Nonlinear Analysis of Reinforced Concrete Frames Under Cyclic Load Reversals," by Filippou, F.C. and Issa, A., September 1988.

UCB/EERC-88/13 "Implications of Recorded Earthquake Ground Motions on Seismic Design of Building Structures," by Uang, C.-M. and Bertero, V.V., November 1988.

UCB/EERC-88/14 "An Experimental Study of the Behavior of Dual Steel Systems," by Whittaker, A.S. , Uang, C.-M. and Bertero, V.V., September 1988.

UCB/EERC-88/15 "Dynamic Moduli and Damping Ratios for Cohesive Soils," by Sun, J.I., Golesorkhi, R. and Seed, H.B., August 1988.

UCB/EERC-88/16 "Reinforced Concrete Flat Plates Under Lateral Load: An Experimental Study Including Biaxial Effects," by Pan, A. and Moehle, J., October 1988.

UCB/EERC-88/17 "Earthquake Engineering Research at Berkeley - 1988," by EERC, November 1988.

UCB/EERC-88/18 "Use of Energy as a Design Criterion in Earthquake-Resistant Design," by Uang, C.-M. and Bertero, V.V., November 1988.

UCB/EERC-88/19 "Steel Beam-Column Joints in Seismic Moment Resisting Frames," by Tsai, K.-C. and Popov, E.P., November 1988.

UCB/EERC-88/20 "Base Isolation in Japan, 1988," by Kelly, J.M., December 1988.

UCB/EERC-89/01 "Behavior of Long Links in Eccentrically Braced Frames," by Engelhardt, M.D. and Popov, E.P., January 1989.

UCB/EERC-89/02 "Earthquake Simulator Testing of Steel Plate Added Damping and Stiffness Elements," by Whittaker, A., Bertero, V.V., Alonso, J. and Thompson, C., January 1989.

UCB/EERC-89/03 "Implications of Site Effects in the Mexico City Earthquake of Sept. 19, 1985 for Earthquake-Resistant Design Criteria in the San Francisco Bay Area of California," by Seed, H.B. and Sun, J.I., March 1989.

UCB/EERC-89/04 "Earthquake Analysis and Response of Intake-Outlet Towers," by Goyal, A. and Chopra, A.K., July 1989.

UCB/EERC-89/05 "The 1985 Chile Earthquake: An Evaluation of Structural Requirements for Bearing Wall Buildings," by Wallace, J.W. and Moehle, J.P., July 1989.

UCB/EERC-89/06 "Effects of Spatial Variation of Ground Motions on Large Multiply-Supported Structures," by Hao, H., July 1989.

UCB/EERC-89/07 "EADAP - Enhanced Arch Dam Analysis Program: User's Manual," by Ghanaat, Y. and Clough, R.W., August 1989.

UCB/EERC-89/08 "Seismic Performance of Steel Moment Frames Plastically Designed by Least Squares Stress Fields," by Ohi, K. and Mahin, S.A., August 1989.

UCB/EERC-89/09 "Feasibility and Performance Studies on Improving the Earthquake Resistance of New and Existing Buildings Using the Friction Pendulum System," by Zayas, V., Low, S., Mahin, S.A. and Bozzo, L., July 1989.

UCB/EERC-89/10 "Measurement and Elimination of Membrane Compliance Effects in Undrained Triaxial Testing," by Nicholson, P.G., Seed, R.B. and Anwar, H., September 1989.

UCB/EERC-89/11 "Static Tilt Behavior of Unanchored Cylindrical Tanks," by Lau, D.T. and Clough, R.W., September 1989.

UCB/EERC-89/12 "ADAP-88: A Computer Program for Nonlinear Earthquake Analysis of Concrete Arch Dams," by Fenves, G.L., Mojtahedi, S. and Reimer, R.B., September 1989.

UCB/EERC-89/13 "Mechanics of Low Shape Factor Elastomeric Seismic Isolation Bearings," by Aiken, I.D., Kelly, J.M. and Tajirian, F., December 1989.

UCB/EERC-89/14 "Preliminary Report on the Seismological and Engineering Aspects of the October 17, 1989 Santa Cruz (Loma Prieta) Earthquake," by EERC, October 1989.

UCB/EERC-89/15 "Experimental Studies of a Single Story Steel Structure Tested with Fixed, Semi-Rigid and Flexible Connections," by Nader, M.N. and Astaneh-Asl, A., August 1989.

UCB/EERC-89/16 "Collapse of the Cypress Street Viaduct as a Result of the Loma Prieta Earthquake," by Nims, D.K., Miranda, E., Aiken, I.D., Whittaker, A.S. and Bertero, V.V., November 1989.

UCB/EERC-90/01 "Mechanics of High-Shape Factor Elastomeric Seismic Isolation Bearings," by Kelly, J.M., Aiken, I.D. and Tajirian, F.F., March 1990.

UCB/EERC-90/02 "Javid's Paradox: The Influence of Preform on the Modes of Vibrating Beams," by Kelly, J.M., Sackman, J.L. and Javid, A., May 1990.

UCB/EERC-90/03 "Earthquake Simulator Tests of Viscoelastic Dampers for Medium Rise Structures," by Kelly, J.M. and Aiken, I.D., May 1990.

UCB/EERC-90/04 "Damage to the San Francisco-Oakland Bay Bridge During the October 17, 1989 Earthquake," by Astaneh, A., June 1990.

UCB/EERC-90/05 "Preliminary Report on the Principal Geotechnical Aspects of the October 17, 1989 Loma Prieta Earthquake," by Seed, R.B., Dickenson, S.E., Riemer, M.F., Bray, J.D., Sitar, N., Mitchell, J.K., Idriss, I.M., Kayen, R.E., Kroop, A., Harder, L.F., Jr. and Power, M.S., April 1990.

UCB/EERC-90/06 "Models of Critical Regions in Reinforced Concrete Frames Under Seismic Excitations," by Zulfiqar, N. and Filippou, F., May 1990.

UCB/EERC-90/07 "A Unified Earthquake-Resistant Design Method for Steel Frames Using ARMA Models," by Takewaki, I., Conte, J.P., Mahin, S.A. and Pister, K.S., June 1990.

UCB/EERC-90/08 "Soil Conditions and Earthquake Hazard Mitigation in the Marina District of San Francisco," by Mitchell, J.K., Masood, T., Kayen, R.E. and Seed, R.B., May 1990.

UCB/EERC-90/09 "Influence of the Earthquake Ground Motion Process and Structural Properties on Response Characteristics of Simple Structures," by Conte, J.P., Pister, K.S. and Mahin, S.A., July 1990.

UCB/EERC-90/10 "Experimental Testing of the Resilient-Friction Base Isolation Sytsem," by Clark, P.W. and Kelly, J.M., July 1990.

UCB/EERC-90/11 "Seismic Hazard Analysis: Improved Models, Uncertainties and Sensitivities," by Araya, R. and Der Kiureghian, A., March 1988.